Investigation of the interactions and aggregation mechanism of human insulin and bovine β-lactoglobulin in the presence of different chemical and physical modulators

Thesis submitted by

SHAHNAZ BEGUM

DOCTOR OF PHILOSOPHY (SCIENCE)

Department of Chemistry

Faculty Council of Science

Jadavpur University

Kolkata-700032, India

2024

JADAVPUR UNIVERSITY

KOLKATA-700032, INDIA

INDEX NO. 240/16/Chem./25

1. **Title of the thesis:** Investigation of the interactions and aggregation mechanism of human insulin and bovine β-lactoglobulin in the presence of different chemical and physical modulators

2. **Name, Designation, and institution of supervisor:**

Professor (Dr.) Umesh Chandra Halder

Professor,

Department of Chemistry,

Jadavpur University,

Kolkata-700032, India.

3. **List of publications (related to thesis):**

(i) **Shahnaz Begum,** Swarnali Paul, Hasan Parvej, Falguni Mondal, Ramkrishna Dalui, Anirban Pradhan, Nayim Sepay, and Umesh Chandra Halder. Anion–Induced Amyloid Fibrillation of Human Insulin In vitro. ChemistrySelect, 9(13), p.e202303699

(ii) **Shahnaz Begum,** Hasan Parvej, Ramkrishna Dalui, Swarnali Paul, Sanhita Maity, Nayim Sepay, Mohd Afzal, Umesh Chandra Halder. Structural modulation of insulin by hydrophobic and hydrophilic molecules. RSC advances, 13(48), pp.34097-34106.

Other Publications

(iii) Swarnali Paul, **Shahnaz Begum**, Hasan Parvej, Ramkrishna Dalui, Subrata Sardar, Falguni Mondal, Nayim Sepay, Umesh Chandra Halder. In vitro retardation and modulation of human insulin amyloid fibrillation by Fe^{3+} and Cu^{2+} ions. New Journal of Chemistry, 48(7), pp.3120-3135.

(iv) Hasan Parvej, **Shahnaz Begum**, Ramkrishna Dalui, Swarnali Paul, Barun Mondal, Subrata Sardar, Nayim Sepay, Gourhari Maiti and Umesh Chandra Halder. Coumarin derivatives inhibit the aggregation of β-lactoglobulin. RSC advances, 12(27), pp.17020-17028.

(v) Sampa Pal, Sanhita Maity, Subrata Sardar, **Shahnaz Begum**, Ramkrishna Dalui, Hasan Parvej, Kaushik Bera, Anirban Pradhan, Nayim Sepay, Swarnali Paul and Umesh Chandra Halder. Antioxidant ferulic acid prevents the aggregation of bovine β-lactoglobulin *in vitro*. Journal of Chemical Sciences, 132, pp.1-13.

(vi) Subrata Sardar, Md. Anas, Sanhita Maity, Sampa Pal, Hasan Parvej, **Shahnaz Begum**, Ramkrishna Dalui, Nayim Sepay, Umesh Chandra Halder. Silver nanoparticle modulates the aggregation of beta-lactoglobulin and induces to form rod-like aggregates. International journal of biological macromolecules, 125, pp.596-604.

(vii) Sanhita Maity, Sampa Pal, Subrata Sardar, Nayim Sepay, Hasan Parvej, **Shahnaz Begum**, Ramkrishna Dalui, Niloy Das, Anirban Pradhan and Umesh Chandra Halder. Inhibition of amyloid fibril formation of b-lactoglobulin by natural and synthetic curcuminoids. New Journal of Chemistry, 42(23), pp.19260-19271.

4. List of Presentations in National/ International/ Conferences/Workshops:

Participated in the National Seminar on Current Developments in Chemical Sciences (CDCS-2018) On 7th March 2018, Organized by the Department of Chemistry, Jadavpur University.

Poster presentation at International Conference on Chemistry for Human Development (ICCHD-2018) from 8-10th January 2018 held at Heritage Institute of Technology, Kolkata.

Poster presentation at National Conference on 'Recent Advances in Chemistry 2019' Department of Chemistry, NIT Meghalaya.

Poster Presentation at the National Seminar on Emerging Trends in Chemical Sciences on 7th January 2020, Organized by the Department of Chemistry, Jadavpur University.

Poster Presentation at National Seminar on Chemical Sciences: Today and Tomorrow (CSTT-2019) on 14th March 2019. Organized by the Department of Chemistry, Jadavpur University.

National Workshop on Electron Microscopy and its Applications in Material Science and Biological Science from 29-30th January 2018, Organized by the Department of Instrumentation Science, Jadavpur University.

"Statement of Originality"

I, **Shahnaz Begum**, registered myself on 6th December 2016. I hereby declare that this thesis titled **"Investigation of the interactions and aggregation mechanism of human insulin and bovine β-lactoglobulin in the presence of different chemical and physical modulators"** is a combination of literature survey and original research work completed by me as part of my Doctoral studies. All information presented in this thesis has been obtained and compiled in accordance with existing academic regulations and ethical conduct. As per these regulations, I declare that I have properly cited and referred all materials and results that are not original to this work.

Shahnaz Begum

Signatures of Candidate

Date: 26/04/2024

যাদবপুর বিশ্ববিদ্যালয়
কলকাতা-৭০০ ০৩২, ভারত

JADAVPUR UNIVERSITY
KOLKATA-700 032, INDIA

FACULTY OF SCIENCE DEPARTMENT OF CHEMISTRY ORGANIC CHEMISTRY SECTION

CERTIFICATE FROM THE SUPERVISOR

This is to certify that the thesis entitled **"Investigation of the interactions and aggregation mechanism of human insulin and bovine β-lactoglobulin in the presence of different chemical and physical modulators."**, submitted by **Shahnaz Begum** who got her name registered on **06.12.2016** in the Department of Chemistry under the Faculty council of Science for the award of Ph.D. (Science) degree of Jadavpur University is absolutely based upon her own work and neither the thesis nor any part of the thesis has been submitted for any degree/diploma or any other academic award anywhere before.

Umesh Chandra Halder 22/04/2024

Signature of the Supervisor

DR. UMESH CHANDRA HALDER
Professor of Chemistry
Department of Chemistry
Jadavpur University
Kolkata-700032

Telephone : 91-033-2414-6223 Internet : http:// www.jadavpur.edu Fax : 91-033-2414-6484

ACKNOWLEDGEMENTS

As I take a moment to reflect on my journey so far, I am filled with an overwhelming sense of gratitude for the blessings and opportunities that have led me to this point. First and foremost, I would like to thank God, the Almighty, for giving me the strength, knowledge, ability, and opportunity to undertake my PhD work and to persevere and complete it satisfactorily. It has been an incredible experience, and I remain hopeful that my hard work and dedication will pave the way for greater success in the future.

When I look back, I feel a deep sense of fulfillment and indebtedness to the many individuals who have supported and encouraged me along the way. However, there is one person in particular who has played an especially significant role in my journey: ***Prof. (Dr.) Umesh Chandra Halder.***

Prof. (Dr.) Umesh Chandra Halder *has been an unwavering source of guidance and mentorship throughout my PhD journey. His support, advice, and attention to detail have been absolutely invaluable to me. He has always been there to answer my questions, provide me with feedback, and encourage me to push the boundaries of my research. His erudite suggestions and unwavering support have allowed me to grow and develop as a researcher in ways that I never thought possible. Working under Prof. Halder's guidance has been a true honor. His untiring support and encouragement have been a constant source of inspiration for me, and I am incredibly grateful for the opportunity to learn from him. I am confident that the knowledge and skills that I have gained under his tutelage will serve me well in my future endeavors.*

I would like to express my heartfelt appreciation to the esteemed ***Indian Council of Medical Research (ICMR)****, Government of India, for graciously providing me with financial assistance from 24th July 2019 to 23rd July 2022. It is with great honor that I acknowledge the invaluable contribution of* ***ICMR*** *towards my academic pursuits. I would also like to thank the* ***JU-RUSA 2.0*** *doctoral scholarship scheme for providing fellowship from February to July 2019.*

I am extremely grateful to ***Prof. K. K. Rajak****, HOD (Chemistry), Jadavpur University, for providing me with all kinds of departmental facilities and moral support during this period. I am highly obliged to* ***Prof. A. Saha****,* ***Prof. P. Roy, and Prof. A. Gayen, former Heads of the Department of Chemistry, Jadavpur University, Kolkata, for providing me with*** *support, encouragement, and facility to conduct my research smoothly. I must not forget to acknowledge all their scientific, academic, and administrative help.*

I also want to thank ***Prof. A. K. Sarkar****, Dean, Faculty of Science, Jadavpur University, Kolkata, for his kind administrative help, advice, and encouragement.*

I would like to convey my sincere thanks to ***Prof. S. Bhar****,* ***Prof. G. Maiti****,* ***Dr. U. Jana****,* ***Dr. S. Haldar****,* ***Dr. T. Bhowmik****,* ***Dr. S Guha****,* ***Dr. A. Thakur****,* ***Dr. M. A. Mondal****,* ***Dr. A. Saha****,* ***Dr.***

T. Ghosh, ***Dr. S. Waiba*** *and all the faculty members of the Department of Chemistry, Jadavpur University, Kolkata, for their cordial advice and encouragement as and when I approached them.*

I would like to express my profound gratitude to my esteemed lab mates and seniors, ***Dr. Hasan Parvej, Ramkrishna Dalui, Dr. Sanhita Maity, Swarnali Paul, Dr. Subrata Sardar, Dr. Barun Mondal, Falguni Mondal, Dr. Sampa pal,*** *for their invaluable friendship, motivation, and knowledge-sharing throughout my academic journey.*

I am particularly indebted to ***Dr. Nayim Sepay,*** *Assistant Professor, Department of Chemistry, Lady Brabourne College, Kolkata, for his unwavering technical assistance and moral support during my research study.*

I am grateful to ***Dr. Md. Maidul Islam*** *and* ***Dr. Hedayetullah Mir****, Assistant Professor, Aliah University, Kolkata, for their valuable scientific advice and enormous encouragement.*

I extend my special thanks to ***Mrs. Sraboni Halder (Madam)*** *and* ***Ishani Halder*** *for their moral support, love, and motivation.*

I also want to thank my beloved friend ***Busrat Zehan*** *for her constant support and encouragement.*

I would like to express my deepest gratitude to my beloved husband, ***Mr. Ashique Al Hoque,*** *for the unwavering and unconditional support he has always provided me. His love and care have been a constant support of strength and motivation throughout my PhD journey.*

I express my profound gratitude to my parents, ***Mr. Jan Mohammad and Mrs. Sultanara Begum****, and younger brother,* ***Md. Shahbaz****, for their love, support, and encouragement throughout my academic journey. Their selfless sacrifices, unflinching belief in my abilities, and ceaseless encouragement have been a constant source of strength and inspiration. Their guidance, sagacity, and affection have enabled me to surmount the challenges of doctoral research and have helped shape the person I am today. Additionally, I want to thank the rest of my family members for their love and blessings. With the deepest love and gratitude, I also dedicate this work to them.*

Date: 26/04/2024

Place: Jadavpur University, Kolkata.

Shahnaz Begum

Shahnaz Begum

I dedicate this thesis to

My Parents and family

For their constant support and encouragement

PREFACE

The research related to the thesis for the Doctor of Philosophy (Science) degree has been carried out under the supervision of Prof. (Dr.) Umesh Chandra Halder, Department of Chemistry, Jadavpur University, Kolkata, India.

Proteins are ubiquitous bio-molecules that play a fundamental role in virtually all biological processes. Proteins are the backbone of living cells, consisting of a linear sequence of amino acids that are synthesized on ribosomes. They exhibit remarkable versatility in their ability to operate independently or in complex with other proteins or cellular components. Biological processes encompass a diverse range of phenomena, spanning from the intricate processes of development and differentiation to the catalysis of enzymatic reactions, modulation of gene expression, signal transduction, transport and storage of molecules, neurological activity, cell death, and apoptosis. Proteins are known to perform a diverse range of functions, which can be attributed to the intricate manner in which their polypeptide chains are folded into highly ordered structures. The folds are optimized to minimize the energy conformations of individual amino acid residues while maximizing the number of hydrogen bonds formed between polar groups. The outcome of this process is a compact, three-dimensional atomic structure that bears hydrophobic residues strategically hidden from the surrounding aqueous environment.

Protein misfolding is a common occurrence that can happen in cells due to various reasons, such as genetic mutations, errors in protein synthesis, abnormal modifications of proteins, exposure to high temperatures or oxidative stress, and incomplete protein complex formation. When a protein misfolds, it exposes its hydrophobic regions, leading to the formation of protein aggregates. These protein aggregates can disrupt normal cellular functions by trapping functional proteins and initiating a series of malfunctions.

Protein instability poses a formidable obstacle to biopharmaceutical formulations, and its resolution necessitates a thorough comprehension of the underlying physical mechanisms and the methods available to safeguard proteins. Misfolding of proteins results in the conversion of native states to non-native structures, which further transform into organized fibrils. Over 35 human diseases, including Alzheimer's disease, Parkinson's disease, Huntington's disease, and sickle cell anemia, have been linked to protein aggregation and misfolding, thereby imposing significant challenges to medical technology and industries. Moreover, the possibility of the formation of intermediates such as protofibrils and oligomers cannot be

disregarded. It is noteworthy that there exist 20 homologous proteins and a few associated proteins, including Aβ1–40, β-lactoglobulin, lysozymes, and insulin, which have been identified to form amyloid fibrils that are known to instigate incurable ailments, such as Parkinson’s disease, type-2-diabetes, Alzheimer's disease.

This thesis uses a multi-disciplinary approach to understand the interaction and aggregation process of two chosen proteins, insulin and beta-lactoglobulin, with different small modulator interfaces.

In my research, I've chosen human insulin as a model protein. It's an excellent example of studying oligomers in a native state. Under reversible aggregation conditions, it forms amyloid fibrils in a non-physiological state. Human insulin is a widely researched protein that serves as an essential model for understanding the underlying mechanisms of amyloid formation. The fibrillar structure of insulin closely resembles that of other amyloid-prone proteins, such as amyloid precursor protein (Aβ peptides), which are linked to Alzheimer's disease, atrial natriuretic factor (amyloid ANF), contributing to atrial amyloidosis, and prion protein, causing spongiform encephalopathies. However, the production of insulin can lead to amyloidogenesis, posing a significant challenge to its bioavailability. This is of particular concern in the case of continuous insulin delivery via insulin pumps, where fibrillation can cause inconsistent supply and further complications. To prevent unwanted and harmful aggregate formation, it is imperative to gain insight into the protein's specific structural transformation from its native state and to trace the mechanism of disruption of preformed aggregates with probable interacting molecules.

My first work (Chapter 2) involves the interaction of human insulin with hydrophobic and hydrophilic molecules. In this study, we have synthesized one hydrophobic Schiff's base (E)-2-((tert-butylimino) methyl)-6-methoxyphenol (compound 3a) and one hydrophilic Schiff's base (E)-2-((2-hydroxy-3-methoxybenzylidene) amino)-2-(hydroxymethyl)propane-1,3-diol (compound 3b). Insulin is known to bind with glucose, a polar poly-hydroxy compound. Thus, in our study, we designed a poly-hydroxy compound to investigate its interaction with insulin. To compare the effects of a hydrophobic molecule on insulin binding, we also designed a similar molecule without the hydroxyl group. Our findings reveal that hydrophilic molecules exhibit a slightly higher binding affinity for insulin than hydrophobic molecules. This indicates that insulin can bind with hydrophilic molecules in a similar manner as it does with glucose. However, the high insulin binding affinity of a hydrophobic molecule indicates

its dual nature. At a temperature of 283 K, the binding constant was found to be 6.64×10^4 M^{-1} for hydrophilic molecules and 4.99×10^4 M^{-1} for hydrophobic molecules. While the hydrophobic molecule binds to the hydrophobic pocket of the insulin surface, hydrophilic molecules interact with the polar surface of insulin. It is important to note that binding with the hydrophobic molecule significantly alters the secondary structure of insulin in comparison to hydrophilic molecules. Consequently, the stability of insulin decreases in the presence of hydrophobic molecules.

My second research work (Chapter 3) demonstrates the effect of three selected salt anions on the fibrillation of human insulin. For this study, we have chosen three biologically important salt anions, I^-, NO_3^-, and OAC^-, as they are present in our biological system at very low concentrations or physiological concentrations. Protein aggregation in salt solutions can create significant challenges during the separation, storage, and therapeutic use of proteins. This study seeks to explore the mechanism of fibrillation of human insulin, a crucial peptide hormone responsible for glucose metabolism. The experiments were conducted in an acidic environment, with low salt concentrations of the anions I^-, NO_3^-, and OAc- within the physiological range. To understand the fibrillation mechanism and fibril morphology, various spectroscopic and microscopic approaches, including ANS and Thioflavin T (ThT) fluorescence, circular dichroism (CD), dynamic light scattering (DLS), and transmission electron microscopy (TEM), were utilized. These findings could aid in the development of techniques for managing protein fibrillation in therapeutic applications.

After conducting a comprehensive investigation, it was discovered that insulin's structure experiences perturbations in an acidic environment when anions selectively bind to its positively charged residues. These interactions induce salt-induced aggregation and the formation of amyloid-like oligomeric products. These three anions, I^-, CH_3COO^-, and NO_3^-, differ markedly in their charge density, size, and shape. Among the three, the iodide ion is the smallest, spherical in shape, and carries the largest negative charge density. Consequently, it moves more quickly towards the positively charged side chain of insulin. Nitrate anion, on the other hand, has the lowest charge density, a larger size, and a planar geometry compared to iodide. Due to its slow approach towards insulin's positively charged residues, it takes a longer time for insulin fibril formation than iodide and acetate ions.

The findings of this study suggest that hydrophobic and electrostatic interactions play a predominant role in insulin's nucleation kinetics following heat incubation and subsequent fibril elongation in an acidic environment.

In my third research work (Chapter 4), I investigated the impact of Ultraviolet (UV) light exposure on human insulin. Ultraviolet radiation lies between visible light and X-rays in the electromagnetic spectrum, with wavelengths ranging from 10 nanometers to 400 nanometers. For comparison, the wavelength of violet light is roughly 400 nanometers (or 4,000 Å). The frequency of UV radiation ranges from 800 terahertz to 30,000 terahertz. UV light can cause damage to biological structures by interacting with protein molecules, leading to molecular alteration and structural rearrangement through photoionization.

In our research, we exposed monomeric insulin samples to UV light for different durations - 1 minute, 3 minutes, 7 minutes, and 15 minutes - at an excitation of 276 nm. Using the multi-spectroscopic method, we found that UV exposure causes aggregation of Human Insulin, which becomes more pronounced with longer exposure times. The exposure modifies the protein's structure by altering its secondary structure and exposing hydrophobic sites on the surface of the protein, resulting in protein aggregation. This effect is most significant for native Human Insulin under UV light exposure for 15 minutes, followed by 7 minutes, 3 minutes, 1 minute, and human insulin monomer.

In my fourth research work, which is Chapter 5 of my study, I have focused on studying the impact of the polarity of coumarin molecules on their binding with beta-lactoglobulin. For this purpose, I have selected β-lactoglobulin as the model protein. β-lactoglobulin is a whey protein that is found in cow's milk and other dairy products in large quantities. It is also the primary allergen in cow's milk and has the ability to interact with various molecules such as lipids, vitamins, minerals, drugs, toxins, and allergens. Coumarin is a secondary metabolite found in plants and is a member of the organic compounds' benzopyrone class. It is essential to study the protein interactions of coumarin as they play a crucial role in understanding its biological effects and its potential applications in healthcare. By studying these interactions, we can gain insights into the mechanisms by which coumarin interacts with proteins and understand its effects on various biological processes such as cell division, inflammation, and clotting.

This investigation entails the designing of two derivatives of coumarin-3-carbamide that contain both chloride and electron-donating groups in a singular molecule (C3A2). Literature

reports have demonstrated that the chloride groups in the coumarin moiety possess a strong binding affinity to β-lg. In our study, two molecules were synthesized, one with OMe and Cl groups (C3A2) and the other with only the Cl group, and both molecules had Cl groups attached to the aromatic ring at amide nitrogen. The protein interactions were studied with β-lg, and the results revealed that C3A2 has a greater binding ability in comparison to C3A1. Both compounds bind to β-lg through an endothermic process driven by entropy. During binding, C3A1 exhibits a preference for the hydrophobic surface of the protein, while C3A2 interacts with the calyx of the protein. This binding leads to conformational changes in the protein. Therefore, the presence of Cl and OMe groups in coumarin-3-carbamide introduces a polar nature in the molecule, which enhances the β-lg binding process.

LIST OF ABBREVIATIONS

°C	Celsius
Abs	Absorbance
APRs	Aggregation-prone regions
AA	Ascorbic acid
ATP	Adenosine triphosphate
Arg	Arginine
Aβ	Amyloid-beta
AD	Alzheimer's disease
ALS	Amyotrophic lateral sclerosis
AUC	Analytical ultracentrifugation
AFM	Atomic force microscopy
ANS	1-Anilino-8- naphthalenesulphonate
BSA	Bovine serum albumin
CD	Circular dichroism
CJD	Creutzfeldt-Jakob disea
CFTR	Cystic fibrosis transmembrane conductance regulator
CR	Congo red
cAMP	Cyclic adenosine monophosphate
Cys	Cysteine
CF	Caffeine
DLS	Dynamic light scattering
DMSO	Dimethyl Sulfoxide
DNA	Deoxyribonucleic Acid
DCM	Dichloromethane
DTT	Dithioerythritol
DTNB	5,5‟-dithiobis (2-nitrobenzoic acid)
DTAC	Dodecyltrimethylammonium chloride
DFT	Density functional theory
ER	Endoplasmic reticulum
EGCG	Epigallocatechin gallate
FA	Ferulic acid

FI	Fluorescence intensity
FESEM	Field emission scanning electron microscopy
FTIR	Fourier Transform Infrared Spectroscopy
FRET	Fluorescence resonance energy transfer
GSH	Glutathione
Gdn.HCl	Guanidinium chloride
Gdn.SCN	Guanidinum thiocyanate
g	Gram
GA	Gallic acid
HI	Human insulin
HAS	Human serum albumin
HIV-1	Human immunodeficiency virus 1
HHP	High hydrostatic pressure
His	Histidine
HRTEM	High-resolution transmission electron microscopy
IDPs	Intrinsically disordered proteins
IAPP	Islet amyloid polypeptide
IEX	Ion-exchange chromatography
IgG	Immunoglobulin G
IBA	Insulin-binding aptamer
IA	Insulin aggregates
IDE	Insulin-degrading enzyme
K_D	Dissociation constant
k_q	Quencher rate coefficient
K_{SV}	Stern-Volmer constant
K	Kelvin
kDa	Kilo Dalton
LSC	Lauryl succinyl chitosan
L-CPL	Left-handed circularly polarized light
mRNA	Messenger ribonucleic acid
MALS	Multiple-angle light scattering
MRE	Mean residence ellipticity
mg	milligram

Met	Methionine
M	Molar
MBL	Mannose-binding lectins
MCE	2-mercaptoethanol
MHCs	Major histocompatibility complexes
mV	Millivolt
mM	Milimolar
µM	Micromolar
MEP	Molecular electrostatic potential map
nM	Nanomolar
nm	Nanometer
NMR	Nuclear magnetic resonance
NPs	Nanoparticles
Phe	Phenylalanine
PEF	Pulsed electric field
PHL	Phloretin
PBS	Phosphate buffer saline
PrP	Prion protein
polyQ	Polyglutamine
PDI	Polydispersity index
PEG	Poly(ethylene glycol)
PAGE	Polyacrylamide gel electrophoresis
LC	L-cysteine
RI	Refractive index
ROS	Reactive oxygen species
R-CPL	Right-handed circularly polarized light
R_h	Hydrodynamic radii
SEC	Size exclusion chromatography
SDS	Sodium dodecyl sulfate
SOD1	Superoxide dismutase 1
SAXS	Small angle X-ray scattering
SAR	Structure-activity relationship
Trp	Tryptophan

Tyr	Tyrosine
T2DM	Type 2 diabetes mellitus
TMAO	Trimethylamine N-oxide
TFE	2,2,2-trifluoroethanol
tBHP	t-butyl hydroperoxide
TG	Transglutaminase
TLC	Thin layer chromatography
TDP-43	TAR DNA-binding protein 43
TEM	Transmission Electron Microscopy
Th T	Thioflavin T
UV/vis	Ultraviolet-visible spectroscopy
λ_{max}	Wavelength of maximum absorbance
µg	microgram
µl	Microliter
β	Beta
α	Alpha
α-lg	Alpha lactoglobulin
β –lg	Beta-lactoglobulin

CONTENTS

CHAPTER 1

INTRODUCTION

Introduction

1.1. General overview of proteins

Proteins are a vital and versatile class of macromolecules that are essential for life. Composed of amino acids arranged in precise sequences, they display remarkable structural and functional diversity. The primary sequence of amino acids, encoded by an organism's genetic information, serves as the blueprint for the protein's three-dimensional conformation, which is indispensable for its function.

Protein folding, a remarkable process governed by the primary structure, leads to the formation of various structural elements, culminating in the protein's native, functional structure (Matthews, 1993). In living organisms, proteins play numerous critical roles. They act primarily as enzymes, catalyzing chemical reactions within cells. For example, digestive enzymes like amylase and protease break down complex carbohydrates and proteins into simpler molecules for absorption (MacFarlane, 2018). Structural proteins like collagen and actin provide the framework and support necessary for maintaining cellular and tissue integrity. Collagen, the most abundant protein in the human body, imparts strength to connective tissues, skin, and bones. Actin and myosin, conversely, power muscle contractions, enabling movement.

Proteins are an essential component for the proper transportation of molecules within the body. Hemoglobin, for instance, is a protein found in red blood cells that binds with oxygen in the lungs and transports it to tissues and organs. This ensures that metabolic processes have the necessary oxygen supply. Various transport proteins, including those that assist in moving ions and molecules across cell membranes, are also crucial for nutrient uptake and waste removal.

Hormonal proteins, such as insulin, act as messengers between cells and tissues, regulating physiological processes. Insulin helps control blood glucose levels by facilitating glucose uptake into cells, ensuring energy production and storage (Newsholme et al., 2014). Proteins are also instrumental in cell signaling, where cell surface receptors bind to specific molecules and trigger intracellular signaling pathways that regulate cellular functions. Genetic regulation is another function of proteins, where transcription factors control gene expression by binding to specific DNA sequences, influencing protein synthesis and cellular activities. Beyond these critical functions, proteins contribute to growth, development, and overall health.

1.2. Structure of proteins

Proteins are vital biomolecules composed of amino acids via a complex folding process to achieve a unique and intricate structure. The functionality of a protein is intricately linked to its structure, with various roles such as structural, regulatory, contractile, and protective within the biological system.

1.2.1. Amino acids

Amino acids are the fundamental constituents that makeup proteins, and their structure consists of three main groups: the amino group or N terminus, the carboxyl group or C terminus, and the R group, which harbors the functional component of the amino acid. Notably, the R group confers specific features to the amino acid based on its polarity and charge, thereby influencing the chemical and biological properties of the protein. The diversity of amino acids is dictated by the nature of their R groups, which varies among the 20 amino acids. Of these, 11 can be endogenously synthesized, while the remaining 9 are classified as essential amino acids, necessitating their exogenous intake via dietary sources.

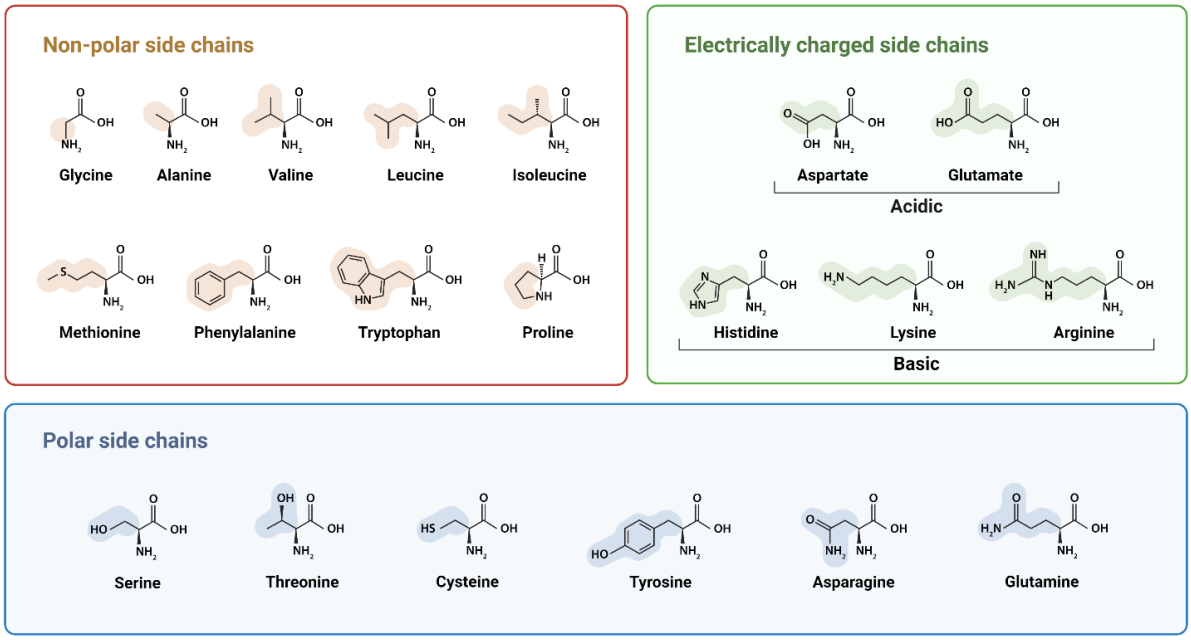

Figure 1: The 20 standard amino acids with their side chains that make the proteins.

The structure of a protein can be divided into four main types depending on the level of complexity.

1.2.2 Primary structure of protein

The primary structure of a protein refers to the fundamental arrangement of amino acids that are covalently bound together by peptide bonds, creating a polypeptide chain. These bonds take place between the amino group (N-terminal) of one amino acid and the carboxyl group (C-terminal) of the adjacent amino acid. These bonds are highly stable and can withstand both chemical and thermal denaturation. However, even minor changes to the amino acid sequence can disrupt the protein folding process, ultimately impacting its functionality. As a result, the precise organization of amino acids in the primary structure of proteins is crucial for ensuring proper folding and biological activity.

1.2.3. Secondary protein structure

The secondary structure of proteins is a vital aspect of their functionality, and it refers to the repetitive folding of polypeptide chains through hydrogen bonds between the hydroxyl (OH) group and the hydrogen molecule of the adjacent amino acid. This folding process is responsible for giving each protein its unique shape, which is critical to its overall function. The two most commonly known examples of secondary protein structures are the alpha-helix and beta-pleated sheets.

The alpha-helix is a structure formed by strong hydrogen bonds between the carbonyl and amino groups of different amino acids. This particular structure boasts strong tensile strength, which allows it to maintain its shape. It is commonly found in DNA and has been a subject of interest in the study of protein structures.

Conversely, hydrogen bonds between the hydrogen molecule of one amino acid on one sheet and the carboxyl group of another amino acid on another sheet generate the beta-pleated sheet structure. Different protein architectures result from the orientation of these sheets, which might be parallel or antiparallel. The beta-pleated sheet structure is well-known for its role in the formation of fibrous proteins, which are important components of connective tissues.

1.2.4. Tertiary structure

The overall 3D arrangement of a protein, known as its tertiary structure, involves the folding of secondary structure elements and the positioning of side chains. The main driving force behind this formation is the hydrophobic effect, which allows the protein to energetically favor folding and conceal its hydrophobic amino acid residues within its core, away from surrounding water. Along with this effect, various other bonds and interactions contribute to

the correct folding of the protein into its tertiary structure, including covalent disulfide bonds between sulfur atoms of two cysteine residues, electrostatic salt bridges between negatively and positively charged side chains, and hydrogen bonds and van der Waals interactions between hydrophobic residues.

1.2.5. Quaternary structure

When it comes to forming a quaternary structure, it takes more than one polypeptide chain. These chains can either be identical or have varying amino acid sequences. The weak interactions, including hydrogen bonding and London dispersion forces, play a vital role in binding the multiple polypeptides together to create the quaternary structure. Hemoglobin is a prime example of this, responsible for transporting oxygen in the bloodstream. It's composed of four peptide chains, two alpha and two beta chains, joining forces to form a tetramer.

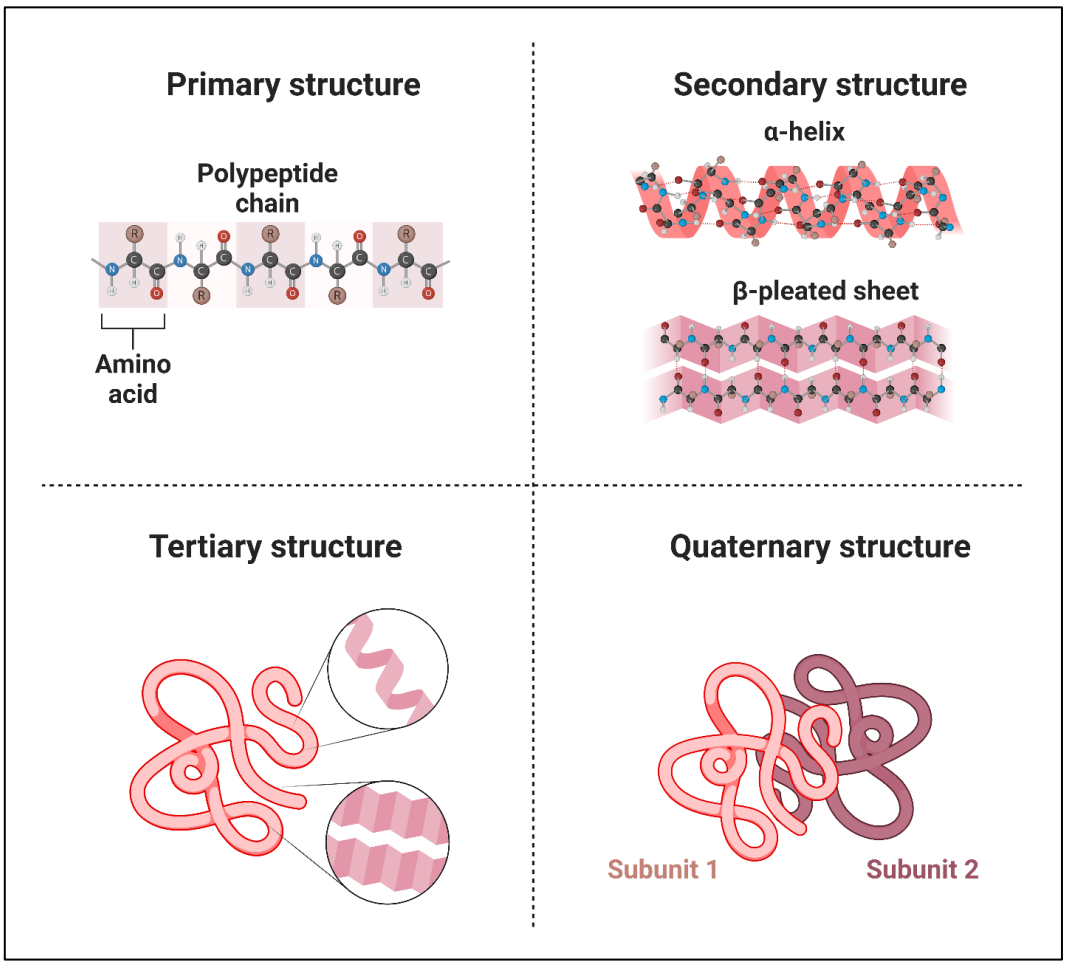

Figure 2: Proteins have four structures - primary, secondary, tertiary, and quaternary. The primary structure is the sequence of amino acids, while the secondary structure is the formation of regular substructures. The tertiary structure is the 3D arrangement of the protein, and the quaternary structure describes interactions between multiple polypeptide chains.

1.3. Protein misfolding and aggregation

The four main macromolecules that make up living systems are lipids, proteins, carbohydrates, and nucleic acids. Approximately 100,000 different types of proteins are involved in chemical interactions that support life; these proteins are identified by the distinct sequence of amino acids that make up their structures. As a result, proteins are essential to the operation of living things. Proteins are made by ribosomes in the cell; certain proteins fold instantly while still connected to the ribosomes (a process known as cotranslational folding), whereas other proteins follow a folding pathway in the endoplasmic reticulum following translation (Waudby, 2019). Organisms have developed several strategies to control the folding of proteins, including the use of chaperones and folding catalysts (Fink, 1999). Under unfavorable conditions, including stress, mutation, and aging, proteins may begin to misfold and lose their capacity to fold correctly. According to Sweeney et al. (2017), misfolded proteins typically cause a complicated biological reaction that includes heat shock and protein unfolding, both of which help in protein folding and destruction (Sweeney et al., 2017). Proteins that fold incorrectly can aggregate or be broken down by the cell's proteasome machinery, which can result in a number of harmful situations.

Protein misfolding can be a complex process with various factors contributing to its development, such as a loss of cellular protein quality control systems, inefficient molecular chaperone machinery, and destabilizing mutations (Wankhede et al., 2022). These factors can lead to the accumulation of misfolded proteins, forming amyloids - ordered structures that can be deposited intracellularly and extracellularly. Amyloids are linked to over 20 human diseases, including Alzheimer’s disease, Parkinson’s disease, type II diabetes, and systemic amyloidosis. It's important to note that amyloid formation can occur with any protein, but the amino acid sequence of polypeptides influences the likelihood of forming amyloids. Fibrils formed during amyloid formation can be toxic to cells and contribute to debilitating pathological conditions (Chaturvedi et al., 2016).

The formation of amyloid fibrils, which are associated with several incurable diseases like Parkinson's, is a complex process triggered by the aggregation of homologous proteins along with a few associated proteins like αβ1–40, lysozymes and insulin (Araki et al., 2019; Findeis et al., 1999; Cao et al., 2004; Sulatskaya et al., 2014). The fibrils are made up of 3-6 filaments that convert unfolded monomers into oligomers, followed by the metastable β-sheet conformation and, finally, the β-sheet-rich structures (Sacchettini and Kelly, 2002). The

nucleation-dependent process of fibril formation depends on the size of the nucleus and reaction kinetics. The formation of protein clusters that lead to the loss of biological activity and other effects is caused by several factors, including covalent and non-covalent interactions (Wang et al., 2010). Protein aggregation can occur when hydrophobic patches on proteins interact, causing them to fold into a flexible state and become insoluble. This self-aggregation is caused by non-covalent interactions like van der Waals forces and electrostatic interactions (Zhou and Pang, 2018; Mahadevi and Sastry, 2016). Insulin is often used to study oligomers in their natural state, and it can form amyloid fibrils when subjected to non-physiological conditions. Protein aggregates can be reversible or irreversible, covalent or non-covalent, and either small or soluble. Covalent aggregates can form through disulfide linkages via free thiol groups, while disulfide-bonded proteins aggregate through interchange via β-elimination (Trivedi et al., 2009). Protein aggregation can be induced through covalent interactions like dityrosine formation, oxidation, and the Maillard reaction, among others. Although only a few types of aggregates have been studied so far, research in this area is ongoing (Rajan et al., 2021).

The stability and solubility of proteins are crucial for their proper function. This can lead to the formation of large, insoluble aggregates. To maintain protein stability and prevent aggregation, it is essential to balance the presence of aggregation-prone regions (APRs) (Baets et al., 2014). APRs are usually short (5-15 residues), hydrophobic, have a low net charge, and have a high tendency to form beta-sheet structures. Every protein domain has at least one APR, which can interact with identical or homologous APRs to drive protein aggregation. APRs can be classified into two categories: buried and surface-exposed. Buried APRs are located inside the hydrophobic core of globular proteins and contribute to protein stability, while surface-exposed APRs are found outside (Louros et al., 2020). High temperatures can cause protein unfolding and lead to aggregation in most proteins.

Amyloidogenic polypeptides can be categorized into two groups. The first group comprises a vast array of amyloidogenic polypeptide regions (APRs) with no correlation to functional sites in proteins. The second, smaller group includes APRs associated with functional sites such as active sites in enzymes and protein-protein interaction sites. This association may enhance the propensity of aggregation of native states and intrinsically disordered proteins (IDPs), which are often related to pathological protein aggregation (Brylinski and Skolnick, 2011). An early lag (nucleation) phase, a fast exponential (growth) phase, and a final plateau phase are the three phases that commonly makeup polypeptide aggregation kinetics (Figure 3B). APRs of

monomeric species are exposed during the first lag phase as a result of unfolding or misfolding proteins. The oligomers that these APRs create by self-interaction can be categorized as fibrous, cylindrin-like, or domain-swapped beta-structures. By attracting monomers that have homologous or identical APRs, the freshly created oligomers function as seeds or seeding intermediates during the exponential phase, driving the formation of amyloid. According to Hausmans et al. (2023), these oligomers are thought to be the most cytotoxic species in a variety of diseases. They can overload the proteostasis machinery, disrupt biological membranes, and cause the aggregation of homologous or identical proteins. (Housmans et al., 2023).

To gain insight into the mechanics of protein aggregation and its connection to related illnesses, it is essential to identify various aggregate species, investigate aggregation kinetics, and uncover secondary structural changes. It is worth noting that proteins can either polymerize into highly ordered fibrils or amorphous aggregates, both of which are associated with protein misfolding diseases (Chiti and Dobson, 2017). Among these, amyloid fibrils are more commonly observed than amorphous aggregates. These fibrils contain β-sheet structures that are stabilized by the formation of a steric zipper structure (Shiraki et al., 2020). This structure locks APRs in a cross-β-sheet conformation, forming the core of the protofibrils (Figure 3). Amyloid polymorphisms can occur due to alternative tertiary zipper packing in amyloids. In contrast, amorphous aggregates lack the specific zipper packing of β-sheets (Taylor and Staniforth, 2022). However, they often have a high percentage of β-sheet structures, implying an amyloid-like assembly mechanism that fails to organize into higher-order assemblies (Low et al., 2022) (Figure 3A). Nonetheless, not all amorphous aggregates follow this trend. The same protein can polymerize into either linear amyloid fibrils or amorphous aggregates, depending on external conditions such as ionic strength, temperature, and the presence of molecular crowders.

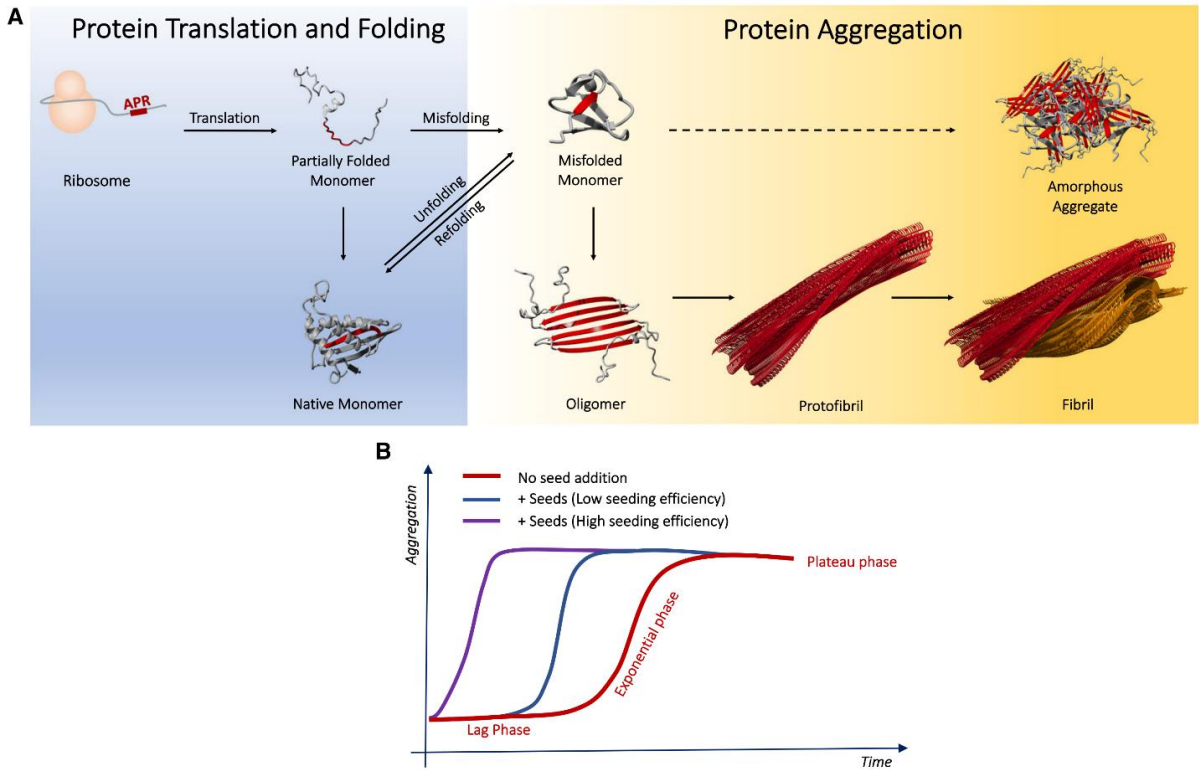

Figure 3: The process of protein translation and fibrillation/aggregation. (A) After being synthesized on the ribosome, polypeptides are folded into their native structure, which involves burying the APR (shown in red on the left, blue). However, protein aggregation can occur if misfolded monomers are present, which can arise during protein folding or if native monomers unfold or misfold. These misfolded monomers can then join together to form either amorphous aggregates (top) or linear fibrils (bottom). To assemble fibrils, the misfolded monomers undergo structural changes and form oligomers that contain b-sheets. These oligomers grow into protofibrils during an exponential phase, which in turn interact with each other to form a mature fibril. (B) The process of aggregation kinetics consists of a slow lag phase, an exponential phase, and a plateau phase. To shorten the lag phase, preformed seeds can be added. (Adapted from Housmans et al., 2023)

1.4. Consequences of protein aggregation

The process of protein aggregation involves changes in the structure of proteins, which eventually lead to the formation of oligomers (Invernizzi et al., 2012). These oligomers then grow into linear aggregates that ultimately form visible particles with low solubility. As far back as 1931, Hsien Wu recognized the protein instability issue and proposed a protein denaturation theory (Wu, 1995). Protein aggregation is not only linked to neurodegenerative diseases but also presents challenges for biotechnology product development and

commercialization. This phenomenon can occur at any stage of protein product development and manufacturing processes, including protein expression, formulation, purification, product filling, lyophilization, and storage. To solubilize insoluble particles or aggregates during protein purification, additional steps must be taken, which can lead to a reduction in the final yield of proteins and may not be cost-effective (Rajan et al., 2021).

It's important to be aware that protein aggregation can arise from several techniques, such as vial filtration, inactivation, and chromatography. Protein instability can also be induced by factors like high protein concentrations, shear stress, pH changes, and ionic strength. Chromatography, a widely used purification method, employs stationary and mobile phases, necessitating the use of protein stabilizers to avoid aggregation. To prevent the generation of reactive oxygen species that can encourage aggregation, additives like glutathione and ascorbic acid are commonly utilized (Len et al., 2019).

Proteins exhibit a propensity to adhere to the stationary phase in chromatography, which may result in protein denaturation and heightened aggregation (Fekete et al., 2014). Additionally, chromatography may necessitate a low pH, which might lead to conformational or colloidal instability of the protein and induce aggregation. Protein samples are prepared by subjecting them to centrifugation and filtration, which results in the proteins being exposed to shear stress. In addition, proteins located at the boundary between air and liquid can clump, forming either soluble or insoluble aggregates (Leiske et al., 2016). Hence, addressing factors contributing to protein aggregation throughout the purifying process is crucial.

Commercially available protein-based products play a vital role in curing multiple disorders such as myocardial infarction, diabetes, and cancer. After production, the pharmaceutical protein must be stabilized and have a shelf life of 1.5-2 years (Cleland et al., 1993). However, proteins are susceptible to aggregation, leading to their chemical and physical degradation and subsequent loss of activity (Zapadka et al., 2017). Under stress or favorable conditions, protein aggregation can occur. Small aggregates are reversible, but denatured protein aggregation or non-native b-sheet structures are not. Protein drugs currently available encounter challenges with aggregation. Insulin, for instance, has a tendency to precipitate and cause obstructions in implantable and portable delivery systems.

1.5. Diseases associated with protein misfolding

Protein misfolding and aggregation are at the heart of a diverse range of devastating disorders, collectively known as proteinopathies or protein misfolding diseases (Table 1). In these conditions, normally well-folded proteins undergo conformational changes, misfold, and aggregate into insoluble structures that can disrupt essential cellular processes and lead to tissue degeneration.

One of the most extensively studied proteinopathies is Alzheimer's disease (AD). In AD, the hallmark pathological features are the accumulation of extracellular amyloid-beta (Aβ) plaques and intracellular neurofibrillary tangles composed of the microtubule-associated protein tau. The misfolding and aggregation of Aβ into oligomeric and fibrillar forms is thought to be a key initiating event in the pathogenesis of AD, leading to synaptic dysfunction and neuronal death (Hardy et al., 2002). Concurrently, tau undergoes hyperphosphorylation and conformational changes, causing it to misfold and aggregate into insoluble neurofibrillary tangles, further contributing to neurodegeneration (Goedert et al., 2006). The progressive spreading of these misfolded protein aggregates through the brain is believed to underlie the relentless cognitive decline observed in AD patients.

Another prominent neurodegenerative disorder associated with protein misfolding is Parkinson's disease (PD). In PD, the presynaptic protein alpha-synuclein misfolds and aggregates into Lewy bodies and Lewy neurites within affected neurons, particularly in the substantia nigra (Recasens et al., 2014). The presence of these Lewy body inclusions is a hallmark pathological feature of PD and is thought to contribute to the selective degeneration of dopaminergic neurons, leading to the characteristic motor symptoms of the disease. Like in AD, the propagation of misfolded alpha-synuclein through the brain is believed to drive the progressive nature of PD (Goedert, 2001).

Huntington's disease (HD) is another neurodegenerative disorder caused by the misfolding of a specific protein. In HD, an abnormal expansion of the polyglutamine (polyQ) repeat in the huntingtin protein leads to its misfolding and aggregation into intranuclear inclusions within affected neurons (Walker et al., 2007). These huntingtin aggregates are thought to disrupt essential cellular processes, ultimately leading to the selective degeneration of medium spiny neurons in the striatum and the characteristic motor, cognitive, and psychiatric symptoms of HD.

Amyotrophic lateral sclerosis (ALS) is a fatal neurodegenerative disease characterized by the selective degeneration of motor neurons. In a subset of ALS cases, the misfolding and aggregation of proteins such as superoxide dismutase 1 (SOD1), TAR DNA-binding protein 43 (TDP-43), and fused in sarcoma (FUS) have been implicated in the pathogenesis of the disease (Taylor et al., 2006). The presence of these misfolded protein aggregates within motor neurons is thought to disrupt essential cellular processes and contribute to their degeneration.

Prion diseases, such as Creutzfeldt-Jakob disease (CJD), are a group of rare, fatal neurodegenerative disorders caused by the misfolding of the prion protein (PrP). In these diseases, the normal cellular form of PrP (PrPC) undergoes a conformational change, transforming into a pathogenic, misfolded isoform (PrPSc) (Prusiner, 1998). This misfolded PrPSc can then act as a template, inducing the misfolding of additional PrPC molecules, leading to the propagation of the disease-associated prion particles. The accumulation of these infectious prion aggregates within the brain ultimately leads to widespread neurodegeneration and the characteristic symptoms of prion diseases.

Protein misfolding and aggregation are not limited to neurodegenerative disorders. In cystic fibrosis, mutations in the CFTR gene can lead to the misfolding and degradation of the CFTR protein, which is responsible for regulating chloride channels in epithelial cells (Amaral et al., 2007). This misfolding and loss of functional CFTR contributes to the characteristic respiratory and digestive symptoms of the disease. Similarly, in sickle cell anemia, a single amino acid substitution in the hemoglobin protein can cause it to misfold and aggregate, leading to the deformation of red blood cells and the associated clinical manifestations (Eaton et al., 2017). In type II diabetes, the misfolding and aggregation of the islet amyloid polypeptide (IAPP) within the pancreatic islets are thought to contribute to the dysfunction and death of insulin-producing beta cells, ultimately leading to the development of the disease (Cao et al., 2013).

Across this diverse range of diseases, the common thread plays a central role in the misfolding and aggregation of specific proteins. Understanding the molecular mechanisms driving these pathological protein transformations, as well as developing effective strategies to prevent or reverse them, is an area of intense research in the biomedical sciences. The development of therapies targeting protein misfolding and aggregation holds great promise for the treatment of these debilitating and often fatal disorders.

Table 1: Protein misfolding diseases and their associated organs.

Name of Disease	Target Protein	Fibril Component	Organs Affected
Type II Diabetes	Islet amyloid polypeptide (IAPP)	Fragment of IAPP	Pancreatic islets
Parkinson's Disease	α-Synuclein	Lewy bodies	Basal ganglia, substantia nigra
Alzheimer's Disease	β-Amyloid	β-Peptide 1-40/1-42	Cortex, hippocampus
Huntington's Disease	Huntingtin	CAG-repeat extension	Striatum, other basal ganglia
Cystic fibrosis	Cystic fibrosis transmembrane regulator	Mutated CFTR	Lungs, pancreas, intestines
Sickle-cell anemia	Haemoglobin	HbS	Kidney, GI tract, liver, heart
Amyotrophic Lateral Sclerosis (ALS)	Superoxide dismutase (SOD1)	Mutated SOD1 proteins	Spinal motor neurons and motor cortex
Scrapie Creutzfeldt-Jakob Disease	Prion protein	PrP and non-protein components	Cortex, thalamus, brain stem, cerebellum
Injection-localized amyloidoses	Insulin	Insulin	Injection site (subcutaneous)
Primary systemic amyloidoses	Immunoglobulin light chain	Intact light chains or fragments	Heart, kidneys, liver, peripheral and autonomic nervous system, GI tract
Secondary systemic amyloidoses	Serum amyloid A	Amyloid A (76 residue fragment)	Kidneys, GI tract, heart

1.6. Factors affecting protein aggregation

Proteins are known to undergo aggregation under diverse environmental conditions, and the extent of aggregation observed is influenced by intrinsic (indirect) and extrinsic (direct) factors. Extrinsic factors encompass environmental factors, genetic factors, metal ions, pH, ionic strength, the role of temperature salt type and concentration, co-solutes, ligands, and oxidative substances that promote aggregation.

1.6.1. Role of temperature on protein aggregation

The influence of temperature on protein aggregation is of paramount importance as it operates through various mechanisms that affect protein-protein interactions, protein diffusion rate in different states, conformational stability, protein solubility, and chemical degradation. The thermodynamic stability of a protein in its native conformation ranges from 5-20 kcal mol^{-1} in free energy (Abramovich et al., 1998; Sumi et al., 2019). It is commonly observed that in physiological conditions, a protein's native state exhibits greater stability than its unfolded and biologically inactive states. The free energy of a protein's folding state is influenced by multiple factors, which include electrostatic forces, hydrophobic interactions, hydrogen bonding, van der Waals forces, and local peptide interactions (Dill et al., 1990). The unfolding of a protein is driven by the conformational entropy, which is sensitive to changes in salt concentration, solution pH, and temperature. The thermodynamic stability of a protein's native state varies with temperature and exhibits a parabolic profile (Franks et al., 1988). An increase in temperature is likely to accelerate the aggregation process as it amplifies the rate of protein diffusion and partially unfolded states for various proteins, as reported in the literature (Andrews et al., 2007).

According to Gibbs free energy ($\Delta G = \Delta H - T\Delta S$), the transition from a folded to an unfolded protein state is affected by temperature. As the temperature rises, the free energy (ΔG) of the unfolded state becomes lower than that of the folded state, making protein unfolding thermodynamically favorable at elevated temperatures. (Dill et al., 1990; Privalov et al., 1988). However, exposing proteins to high temperatures results in irreversible denaturation or physical degradation, leading to aggregation. This phenomenon has been observed in proteins such as recombinant human Flt2 ligand (Remmele et al., 1999), streptokinase (Azuaga et al., 2002), ribonuclease A (Tsai et al., 1998), and recombinant human keratinocyte growth factor (Chen et al., 1994). In contrast, completely folded protein molecules do not form aggregates because aggregation occurs at temperatures below the equilibrium melting temperature of proteins when the amounts of native and denatured proteins are at equilibrium. On the other hand, lowering the temperature of a protein can cause it to cold-fold, which leads to aggregation.

The impact of temperature on reaction kinetics is a crucial consideration. Higher temperatures cause reactions to occur at a faster rate due to increased molecular mobility and energy. This also means that the likelihood of collisions with enough energy to overcome activation barriers

increases (Atkins et al., 2009). Furthermore, higher temperatures can accelerate monomer diffusion, further speeding up the reaction. It's important to note that not all proteins behave the same way when exposed to a range of temperatures. While some proteins, like bevacizumab, follow the traditional Arrhenius relationship within a specific temperature range, most proteins do not (Oliva et al., 2016). Therefore, the rate of protein aggregation can vary significantly between temperatures, influenced by factors such as protein aggregate solubility, various aggregation mechanisms, conformational stability, and the reversibility of protein aggregation (Andrews et al., 2007; Ramakrishna et al., 2012).

1.6.2. Effect of pH on protein aggregation

A solution's pH level significantly impacts the charge and overall charge of proteins, which in turn affects their electrostatic interactions (Chiti et al., 2009). Proteins can only maintain their stability within a very narrow pH range, and any deviation from this range can cause them to aggregate. When proteins carry a high charge level, the repulsive forces between them help maintain their colloidally stable state, making the aggregation process energetically unfavorable. However, when a protein has both positively and negatively charged groups, creating an anisotropic charge distribution close to the pH value of its isoelectric point, it leads to dipoles. Under such conditions, protein-protein interactions can occur, resulting in favorable aggregation.

1.6.3. Effect of ionic strength on protein aggregation

Ionic strength plays a significant role in the behavior of proteins in a solution, particularly in conjunction with pH. The impact of ionic strength on protein aggregation varies depending on the specific protein. When salt facilitates charge neutralization, it can aid in protein folding and increase stability, thereby preventing aggregation at low ionic strength (Han et al., 2022). However, a high salt content might cause the protein to become unstable, which encourages aggregation. Ionic strength also has an impact on fibril structure. Thin and elongated fibrils are the result of low ionic strength, which promotes the addition of monomers exclusively at the ends of protofibrils, inhibiting interaction between axial sides due to electrostatic repulsion. High ionic strength, on the other hand, stimulates hydrophobic contacts, which bind monomers along the axial sides as well as at the ends of the fibrils, forming thick and short fibrils (Marek et al., 2012).

1.6.4. Cosolutes and ligands

Maintaining the physical stability of proteins requires strong binding ligands. According to the Wyman linkage function, the state with greater binding always prevails during a two-state equilibrium. The acidic fibroblast growth factor illustrates this as polyanions bind and shift the equilibrium towards the native state, while zinc ions bind to human growth hormone and increase the free energy of unfolding. Ammonium sulfate, sugars, and polyols stabilize native protein states, while guanidine hydrochloride and urea lead to denaturation. Stabilizing solutes prefer the native state, while denaturants prefer the unfolded state. Co-solutes such as sugars and polyols prevent aggregation and provide physiological osmolality in drug formulations (Rajan et al., 2021). They are excluded from protein surfaces, which increases with protein unfolding, indicating a preference for the native state. Sorbitol delays the depletion of monomers corresponding to protein unfolding when added to glycosylated IgG1 without a polyol sugar. Weakly binding solutes negatively impact the rate of protein aggregation (Nicoud et al., 2014).

1.6.5. Influence of pressure

Pioneering research conducted by Bridgman and his colleagues has shed light on how pressure impacts the behavior of proteins (Bridgman et al., 1964). It is widely recognized that proteins in solution exhibit only marginal stability when subjected to high pressure. This destabilization of the protein's native state disrupts the hydrophobic interactions necessary for stability, creating partially unfolded segments susceptible to aggregation. As a result, numerous researchers have explored the impact of pressure on protein aggregation to better understand the role of hydrophobic cavities and hydration (Heremans et al., 2005).

1.6.6. Effect of protein concentration on protein aggregation

Protein molecules can interact with each other, leading to a process known as protein aggregation. The likelihood of this happening depends on the protein concentration, where higher concentrations increase the formation of protein aggregates. (Mahler et al., 2009) This is due to the macromolecular crowding effect that encourages self-assembly and promotes aggregation (Berg et al., 1999). As protein concentration increases, the size and number of protein aggregates also increase. For instance, β-lactoglobulin has been found to increase in both aggregate size and number with increasing protein concentration. Conversely, diluting the protein concentration can affect the formation of protein aggregates. This is because the aggregates form through weak, reversible interactions that may dissociate as protein

concentration decreases. Furthermore, storing highly concentrated protein formulations in a quiescent state can accelerate the formation of protein aggregates (Hawe et al., 2012).

1.6.7. Effect of salt ions

The presence of salts has a notable influence on protein stability and solubility, as they affect the physical stability and rate of formation of non-native aggregates. Salts modulate electrostatic interactions between charged groups within the protein and between proteins (Zhou et al., 2018). A low salt concentration leads to charge shielding, whereas a high salt concentration causes ions to preferentially bind to the protein surface, ultimately reducing the thermodynamic instability of the native protein and promoting aggregation.

1.6.8. Effect of surfactants

Surfactants are unique molecules with both hydrophobic and hydrophilic properties. As they interact with aqueous solutions, they tend to arrange themselves to minimize exposure of their hydrophobic parts. In proteins, the presence of surfactants can have a significant effect by either stabilizing the protein, destabilizing it, or inducing protein aggregation. When cationic and anionic surfactants interact with protein charge centers or the hydrophobic tail, it can result in protein destabilization and ultimately lead to protein aggregation (Chaturvedi et al., 2016).

1.6.9. Effect of agitation

Protein aggregation may be triggered by agitation stresses, such as stirring and shaking (Torisu et al., 2017). Agitation can cause various effects, including shearing, interfacial disruption, cavitation, and localized thermal changes. It can also induce cavitation, which is the rapid formation and collapse of voids within the liquid, resulting in shock waves, extreme pressure, and temperature. Such conditions promote the generation of free radicals and, subsequently, protein aggregation.

1.6.10. Effect of mutation on protein aggregation

The scientific community widely acknowledges that the crucial information necessary for a polypeptide to properly fold into its 3D native structure is contained within its amino acid sequence. Any changes to this sequence can result in the polypeptide folding incorrectly or even misfolding, leading to the formation of protein aggregates. Such mutations have been linked to the development of diseases like Huntington's disease and type II diabetes (Powers et al., 2009). It is worth noting that mutations in the polypeptide sequence and in the components

of the protein quality control system can promote protein aggregation. For instance, a mutated version of the α-crystallin gene, a small HSP, is associated with cataract formation (Andley et al., 2006). Additionally, mutations in presenilin-1 and presenilin-2 proteases can increase the cellular level of β-peptides and contribute to the onset of Alzheimer's disease.

1.7. Analytical techniques to study protein fibrillation/aggregation

The characterization of protein aggregates is a crucial aspect of drug development, particularly when designing potential treatments for amyloid-associated pathogenesis. Comprehensive analysis of protein structure, biological integrity, and product-related impurities is essential during the manufacturing and storage of biopharmaceuticals. To achieve this, a combination of analytical methods, including amyloid fibrils, is employed to understand protein aggregation comprehensively. In the following sections, we will delve into the salient features of commonly used methods, underlying principles, and the detailed methodology for protein aggregate characterization.

1.7.1. Particle size and mass determination

Particle size or molecular weight measurement is the most direct method for determining a protein's aggregation state. Dynamic light scattering (DLS) is a widely used method for describing changes in particle size during protein aggregation. By detecting fluctuations in light intensity that are scattered by particles in solution as a result of Brownian motion, DLS measures particle size distributions in the nanometer to micrometer range. The digital autocorrelator makes it possible to determine the particle diffusion coefficient Dt by correlating the variation in light intensity over time (on the scale of nanoseconds to microseconds). Large particles diffuse more slowly, resulting in a correlation decay that lasts for a longer period of time, whereas small particles diffuse at a faster rate, causing a rapid correlation decay. The Strokes–Einstein equation can be used to calculate the particle size or hydrodynamic radius Rh, which is related to the diffusion coefficient Dt (Carvalho et al., 2018; Stetefeld et al., 2016). It is essential to remember that variables like temperature, solvent viscosity, and particle shape can impact how particles move. For accurate DLS measurements, therefore, it is essential to control these variables and comprehend solvent properties. However, DLS has some drawbacks, one of which is that it only provides a population average size that is most accurate for monodisperse samples. Deconvolution, on the other hand, can be error-prone for complex samples. Size exclusion chromatography (SEC) can be combined with multiple-angle light scattering (MALS) in a method known as SEC-MALS to overcome this limitation. This makes

it possible to determine the molecular weight of various protein species in a sample. According to Sahin and Roberts (2012), SEC separates particles based on their size, with larger species eluting more quickly than smaller ones (Sahin and Roberts, 2012). Using a MALS detector, MALS measures the light intensity that is scattered by particles at multiple angles to determine the absolute molecular weight of each eluted species simultaneously. After the concentration has been precisely determined using a UV or differential refractive index (RI) detector, the eluting particle's molecular weight can be calculated because the function of the scattered light intensity with the scattering angle is proportional to the particle's molecular weight and concentration. SEC-MALS's absolute molecular weight determination is more reliable than SEC alone because it does not require a size/mass calibration (Li et al., 2009). On the other hand, SEC-MALS is insufficient to identify mutants and variants of the same or similar mass, making it unsuitable for samples that have not been purified. Ion-exchange chromatography (IEX), which has a higher resolution than SEC and permits precise analysis of particles of comparable sizes, can be combined with MALS for analytes that cannot be eluted on SEC.

1.7.2. Rayleigh scattering (RLS) measurements

The way a solution interacts with light is determined by its optical properties, which are affected by the solution's ability to absorb or scatter light based on the properties of its molecules or particles. According to Rayleigh's theory, particles that are smaller than the wavelength of the light being used can scatter it. This means that particles should not be larger than one-tenth of the wavelength, and their shape is not a factor. Scientists have found light scattering to be a valuable tool in studying protein aggregation, and they can track it using a fluorescence spectrophotometer by setting identical excitation and emission wavelengths, typically at 350 nm. This technique has proven effective in detecting the formation of protein aggregates (Xu et al., 2001; Khurana et al., 2001)

1.7.3. Fluorescent dyes to identify the aggregates

In the field of protein aggregation studies, fluorescent dyes have emerged as a popular tool for identifying aggregates. These dyes manifest a spectral shift or an increase in fluorescence intensity upon binding to aggregated structures. However, it is worth noting that despite their ease of use, their application demands caution. Indeed, additional characterization methods are often employed in tandem with these dyes to investigate protein aggregation, as they can interfere with the aggregation process, thereby modifying the structure of the aggregate. Moreover, exogenous compounds can interfere with the fluorescent properties of the dye,

giving rise to artefactual results (Hudson et al., 2009). The binding affinity between the dyes and the aggregated protein is variable and depends on the binding mechanism and properties such as charge. In light of these considerations, the most commonly used groups of dyes based on the conjugated optical probe, with a particular focus on fluorescent molecular rotors, are shown in Table 2. These dyes do not emit fluorescent light upon excitation due to their rotational freedom; however, their fluorescence emission is observed upon rotational restriction by binding to aggregates. In light of the above, it is clear that caution should be exercised when using these dyes for protein aggregation studies (Housmans et al., 2023).

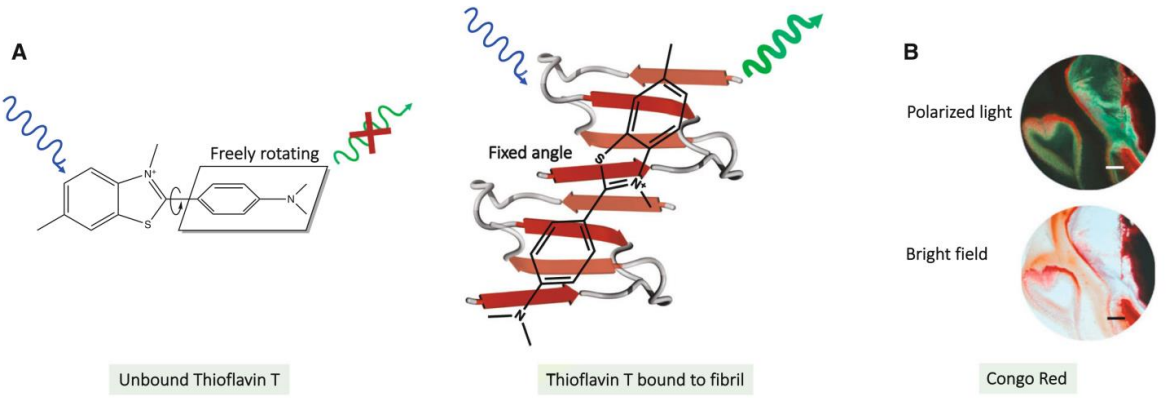

Figure 4: Example of amyloids dyed by Congo red and rotor-dye Thioflavin T. (A) Unbound Th T does not release fluorescent light upon stimulation due to its rotational freedom (left) upon attachment to fibrils; its rotational freedom is restrained, which results in fluorescence emission (Right). (B) Congo red staining of amyloid fibril suspension. Top, image acquired using polarized light and exhibiting the widely seen apple-green birefringence. Bottom, image captured with bright field microscopy revealing orange-red (scale bar: 500 nm). (Adapted from Housmans et al., 2023).

Table 2: Features of commonly used dyes to detect protein aggregation.

Class	Molecular name	Max. excitation wavelength (nm)	Max. emission wavelength (nm)	Binding species	Charge (physiological pH)	Used for measuring kinetics
Golden standards	Congo Red Th T	497 450	614 480	Fibrils Fibrils	Negative Positive	No Yes
LCP	PTAA tPTAA	488	600	Fibrils	Negative	Yes
LCO	pFTAA	450	530	Oligomers Fibrils Amorphous aggregates	Negative	Yes
ANS	ANS Bis-ANS	375	480	Oligomers Fibrils Amorphous aggregates	Negative	Yes

Since 1922, Congo red has been a dependable method for detecting amyloids in laboratory samples and tissue sections. This substance features a negatively charged sulfate group (Yakupova et al., 2019; Wu et al., 2012). When viewed under polarized light, Congo red-stained amyloids display anomalous colors, like the commonly observed apple-green birefringence and other colors. Additionally, when Congo red binds to amyloids, it significantly increases fluorescence at around 614 nm, which can be seen through fluorescence microscopy. These changes in color and fluorescence intensity are thought to be due to the binding of the dye to amyloid fibrils, which restricts the aromatic rings in its structure. Despite Congo red's continued use in laboratory settings, certain limitations should be taken into account, such as inconsistent staining results because of varying section thickness, insensitivity to minimal amyloid deposits, and false-positive results due to mounting medium (Bély et al., 2006).

One well-known dye that is used to detect and quantify amyloid fibrils in tissue sections and in vitro is thioflavin T (Th T). It is also frequently used in in vitro studies of aggregation kinetics (Naiki et al., 1989). A bond rotation in the middle of the molecule, connecting the dimethyl-anilino ring to the benzothiazole moiety, controls the intensity of Th T's fluorescence (Figure 4A). Th T increases the intensity of fluorescence at 480 nm by impeding aniline ring rotation when it binds to amyloid fibrils loaded with β-sheets (Fernandez-Flores, 2011). It is important to remember that rotation inhibition and a rise in fluorescence intensity can also result from an increase in solvent viscosity or non-specific binding to nonfibrillar proteins like albumin (Rovnyagina et al., 2018). Testing the specificity of thioflavin results is therefore crucial.

Because they can attach to exposed hydrophobic regions, positively charged fluorescent dyes ANS and its dimeric counterpart bis-ANS are frequently employed for investigations on protein folding and amyloid formation (Figure 5). These dyes generate a blue shift of the emission maxima from 520 nm to 480 nm and a substantial increase in fluorescence intensity around 480 nm upon binding to exposed hydrophobic areas and aggregated proteins (Guliyeva et al., 2020). For instance, ANS has been used to identify Aβ aggregation and Ca^{2+}-mediated changes in the hydrophobicity of SOD1 protein. Prefibrillar oligomers, protofibrils, fibrils, and amorphous aggregates can all be bound by ANS and bis-ANS; however, binding to fibrils results in a stronger fluorescence than binding to oligomers (Younan et al., 2015).

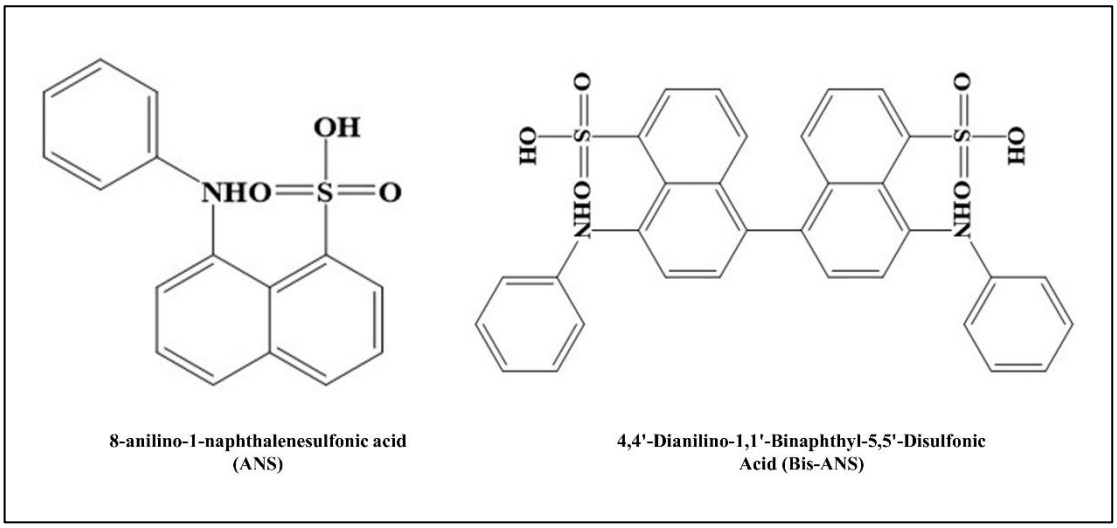

Figure 5: Chemical structure of extrinsic dyes used for the detection of aggregated proteins.

1.7.4. Intrinsic fluorescence measurements

Fluorescence characteristics, such as emission maxima (λmax) and fluorescence intensity (FI), are sensitive to modifications in the polarity and structural dynamics of protein chromophores, especially Trp and Tyr. According to Chakravedi et al. (2015), these factors are very useful in studying protein folding and assembly (Chaturvedi et al., 2015). Scientists have widely used the intrinsic fluorescence of aromatic residues to investigate the conformational dynamics and self-assembly of several amyloidogenic proteins, such as immunoglobulin G (IgG) light chains, prion, Aβ, IAPP, and α-synuclein. These factors have shown to be useful in the development of techniques for modifying protein function by describing changes in protein structure (Dusa et al., 2006; Serno et al., 2010).

1.7.5. Morphological features of aggregates

Aggregates can be found using a variety of techniques, such as dyes specific to amyloid, particle size, and molecular weight determination. On the other hand, direct visual information regarding the size, shape, aggregation extent, and classification of the aggregates at a nanoscale resolution is provided by atomic force microscopy (AFM) and transmission electron microscopy (TEM). TEM lacks additional information regarding aggregate topography and height; AFM does. TEM is a quick and accurate way to determine the existence of protein aggregates; however, in order to improve the contrast of biological samples for imaging, heavy metal staining with uranyl acetate or lead citrate is sometimes necessary. However, unstained samples in physiological solutions can also be imaged with AFM, which makes the imaging circumstances more representative of the in vivo setting. AFM imaging speed was once a constraint; however, current high-speed models are capable of capturing videos at 30–60 ms/frame-1 (Ando et al., 2008). Since not every species in a sample adheres to the support with the same affinity, it is challenging to determine if the images accurately depict the entire ensemble. Researchers have a solution to disperse nanodroplets throughout the grid, but this method is not yet commonly employed.

1.7.6. Monitoring the secondary structural changes

Various spectroscopic techniques, including CD, FTIR, and Raman spectroscopy, can be used to determine the proportion of different secondary structures in a protein. While each technique has its pros and cons, they complement each other in providing a more complete picture. FTIR and Raman spectroscopy are versatile and can be used with samples in both solution and solid state, while CD only works in solution (Tranter, 2017). However, when using FTIR and Raman spectroscopy, high concentrations are often required to overcome interference from water or inherent fluorescence. While these techniques are commonly used to determine the overall percentage of secondary structures within a protein, they are particularly informative when assessing structural changes under different conditions. These circumstances may involve modifications to the protein itself, such as mutations or post-translational modifications, or adjustments to the buffer, temperature, pH, and salt concentration used in the sample preparation. A particularly interesting structural analogy is the change of a protein from a monomeric to a fibrillar form. When fibrils form, the degree of other secondary structures usually decreases, and the percentage of β-strands often increases. Raman, FTIR, and CD

spectroscopy can also be used to compare the secondary structure ratios of various fibrillar proteins.

1.8. Introduction to human insulin

Insulin, a hormone produced by the beta cells of the islets of Langerhans in the pancreas, regulates glucose levels in the blood (Kulkarni et al., 2004; Ornellas et al., 2020). Upon an increase in blood glucose levels, insulin secretion occurs, typically after a meal. Conversely, insulin secretion ceases when blood glucose levels decrease, and the liver releases glucose into the bloodstream. The discovery of insulin can be traced back to 1921, when Canadian scientists Frederick G. Banting and Charles H. Best, along with Romanian physiologist Nicolas C. Paulescu, independently identified the substance in pancreatic extracts. A purified extract of insulin was successfully obtained through the assistance of Scottish physiologist J.J.R. Macleod and Canadian chemist James B. Collip. Banting and Macleod were jointly awarded the Nobel Prize for Physiology or Medicine in 1923 for their groundbreaking work.

Insulin is a peptide hormone that regulates glucose homeostasis in the human body. It is composed of two polypeptide chains, namely the A chain and the B chain. The A chain consists of 21 amino acids, while the B chain is made up of 30 amino acids. These chains are connected by disulfide bonds formed by sulfur atoms. Insulin is derived from a 74-amino-acid prohormone molecule known as proinsulin (Liu et al., 2021). Proinsulin is a relatively inactive insulin precursor secreted in small amounts under normal conditions. In beta cells' endoplasmic reticulum, proinsulin is cleaved into the A and B chains of insulin and an intervening C-peptide, which is biologically inactive. The A and B chains of insulin are linked by two disulfide bonds. Proinsulin, insulin, and C-peptide are stored in granules in the beta cells and released into the bloodstream in response to appropriate stimuli. The capillaries of the pancreatic islets drain into the portal vein, which carries blood from the digestive system to the liver. The pancreas of an average adult contains approximately 200 units of insulin, and the daily secretion of insulin in healthy individuals ranges from 30 to 50 units.

Insulin secretion is influenced by various factors, but the most significant among them is the concentration of glucose in the arterial blood that perfuses the islets (Komatsu et al., 2018). High glucose concentrations trigger beta cells to uptake and metabolize glucose, leading to an increase in insulin secretion. Conversely, low glucose concentrations result in a decrease in insulin secretion. Nonetheless, a small amount of insulin is secreted, even during periods of fasting. Besides glucose, insulin secretion can also be stimulated by amino acids, fatty acids,

keto acids, and hormones produced within the gastrointestinal tract (Torres et al., 2009; Keane et al., 2014). Conversely, the secretion of insulin is inhibited by somatostatin and by activation of the sympathetic nervous system.

Insulin is a hormone that is vital to the metabolism and storage of nutrients because it controls the uptake of glucose in adipose (fat), muscle, and liver tissues (Norton et al., 2022; Saltiel et al., 2001). Insulin initiates metabolic processes within target cells by binding to particular receptors on their outer membrane. In order to facilitate glucose absorption and utilization, insulin plays a crucial role in promoting the translocation of glucose transporters from within the cell to the cell membrane. Insulin is a key player in the uptake and utilization of glucose in adipose tissue. This results in increased circulation uptake of fatty acids, increased cellular fatty acid synthesis, and increased esterification of fatty acids with glycerol to form triglycerides, which are the storage form of fat. In order to preserve fatty acids and glycerol in fat cells for usage during exercise or fasting, insulin is also a strong inhibitor of lipolysis, the breakdown of triglycerides (Czech et al., 2013). In contrast, lipolysis and the release of fatty acids rise when serum insulin concentrations decline. Insulin promotes the uptake of glucose and amino acids into muscle cells, where glucose is stored as glycogen, a substance that can be broken down to provide energy for physical activity or fasting. The amino acids transported into muscle cells are utilized for the synthesis of protein, which is critical for muscle building and repair. In the absence of insulin, muscle protein is broken down to supply amino acids to the liver for transformation into glucose. Thus, insulin plays a vital role in regulating glucose uptake and utilization, lipid metabolism, and protein synthesis in various tissues, making it a crucial hormone for maintaining overall metabolic health.

Insulin plays a critical role in glucose metabolism in liver cells, stimulating glycogen synthesis while simultaneously inhibiting glycogenolysis and gluconeogenesis (Srivastava et al., 1998). The overall effect of insulin is to increase glucose storage while simultaneously decreasing glucose production and release by the liver. It is noteworthy that these actions of insulin are counteracted by glucagon, another pancreatic hormone produced by cells in the islets of Langerhans.

Insufficient insulin production is the underlying cause of diabetes mellitus, a metabolic disorder characterized by elevated blood glucose levels. Severe diabetics require periodic injections of insulin to maintain normal blood glucose levels. In the past, insulin injections were prepared from pig, sheep, and cattle hormone extracts. However, by the early 1980s, specific strains of

bacteria were genetically engineered to produce human insulin. Nowadays, the treatment of diabetes mellitus primarily relies on human insulin produced using recombinant DNA technology (Johnson et al., 1983).

1.9. Structure of insulin

Insulin, a hormone responsible for regulating glucose metabolism in the human body, exhibits a complex yet elegantly structured molecular architecture. Insulin's structure epitomizes biological sophistication at its finest, comprising two polypeptide chains, the A chain and the B chain. The A chain consists of 21 amino acids, while the B chain comprises 30 amino acids, and together, these intertwine to form the backbone of this vital hormone (Figure 6). Crucially, disulfide bonds link these chains, adding a layer of stability and integrity to insulin's structure.

The monomeric form of insulin is crucial for its functionality, as the A and B chains are arranged precisely, enabling insulin to bind seamlessly to its receptor sites on target cells, allowing for a cascade of molecular events that dictate cellular responses critical for glucose homeostasis. Under physiological conditions, insulin has a propensity to dimerize, where two insulin monomers join forces through a disulfide bond between their A chains, creating a dimeric structure, which enhances insulin's stability and bioactivity, ensuring its efficacy in orchestrating glucose uptake and storage within cells (De Meyts, 2016).

In the presence of zinc ions, insulin undergoes a remarkable transformation, transitioning from dimers to hexamers, where three insulin dimers assemble into a hexameric architecture. In this hexameric conformation, the B chains converge inwardly, forming a central core, while the A chains extend outwardly. This hexameric conformation serves as the cornerstone of insulin storage, allowing the hormone to be stored efficiently within the pancreas and pharmaceutical formulations. Furthermore, the hexameric assembly confers resilience upon insulin, shielding it from degradation and ensuring its longevity until it's called upon to fulfill its metabolic duties.

The interplay between insulin's monomeric, dimeric, and hexameric forms underscores the hormone's adaptive nature, finely tuned to meet the dynamic demands of glucose regulation. While the monomeric insulin serves as the functional unit, facilitating cellular signaling and glucose uptake, the dimeric and hexameric forms offer a reservoir of insulin, ready to be mobilized when needed. Insulin's structural intricacies are not limited to mere molecular configurations. They serve as a testament to the evolutionary pressures that have sculpted this vital hormone over millions of years. Insulin has evolved to optimize its functionality, ensuring

its efficacy in navigating the complexities of glucose metabolism across diverse species. In the realm of biomedical research and pharmaceutical development, the structural dynamics of insulin hold profound implications. Insights gleaned from studying insulin's structural intricacies pave the way for designing novel therapeutics to treat diabetes and related metabolic disorders. Understanding the nuances of insulin's architecture is paramount in the quest for improved treatments.

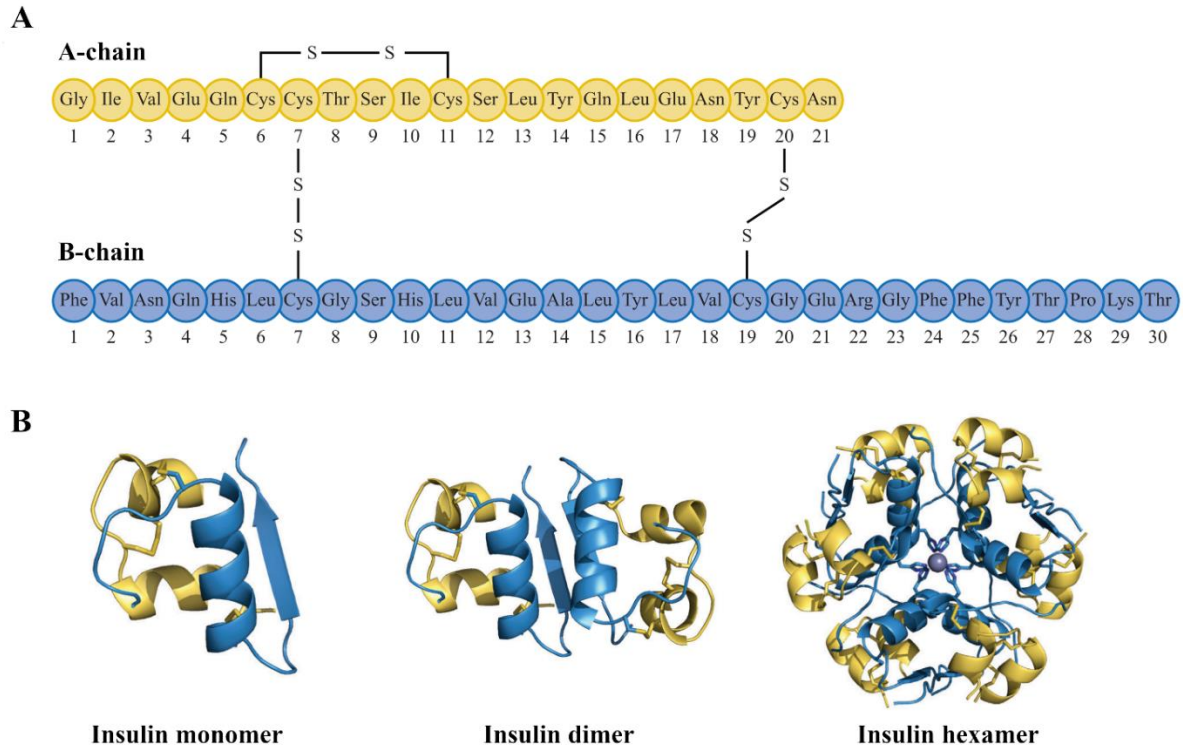

Figure 6: (A) Human insulin's amino acid composition and sequence. (B) The structure of insulin is in three dimensions. When insulin monomers are present in large quantities, they can self-associate to form dimers. Two dimers can then self-associate into hexamers, which can be stored efficiently prior to exocytosis. The blue arrows in the dimer and monomer represent beta-sheets, which are secondary structural elements in proteins that are made up of elongated amino acid arrangements. (Adapted from Rogol et al., 2022)

1.10. Insulin production pathway

The insulin manufacturing route is a complex biological mechanism that controls the synthesis, processing, and secretion of insulin, a critical hormone that regulates glucose metabolism in the body. It starts with the insulin gene's transcription in the pancreatic beta cells' nucleus, where regulatory proteins govern gene expression. The resultant mRNA is translated into

preproinsulin, a precursor molecule that goes through post-translational changes in the endoplasmic reticulum (ER) and Golgi apparatus. These alterations include signal peptide cleavage, folding, and the creation of disulfide bonds, which are essential for insulin's structural integrity. Proinsulin, the intermediate form, is then cleaved in the Golgi apparatus to produce mature insulin and C-peptide. Insulin molecules are bundled into secretory vesicles and transported to the cell membrane, where they are released into the bloodstream through exocytosis in reaction to high blood glucose levels. Once in circulation, insulin binds to receptors on target cells like muscle, liver, and adipose tissue, triggering signaling cascades that enhance glucose uptake and use. This carefully regulated system maintains glucose homeostasis, which is critical for metabolic health (Figure 7). Dysregulation of the insulin manufacturing pathway can result in metabolic diseases, including diabetes mellitus, highlighting its vital role in human physiology (Steiner et al., 2009; Lizcano et al., 2002; Boland et al., 2017).

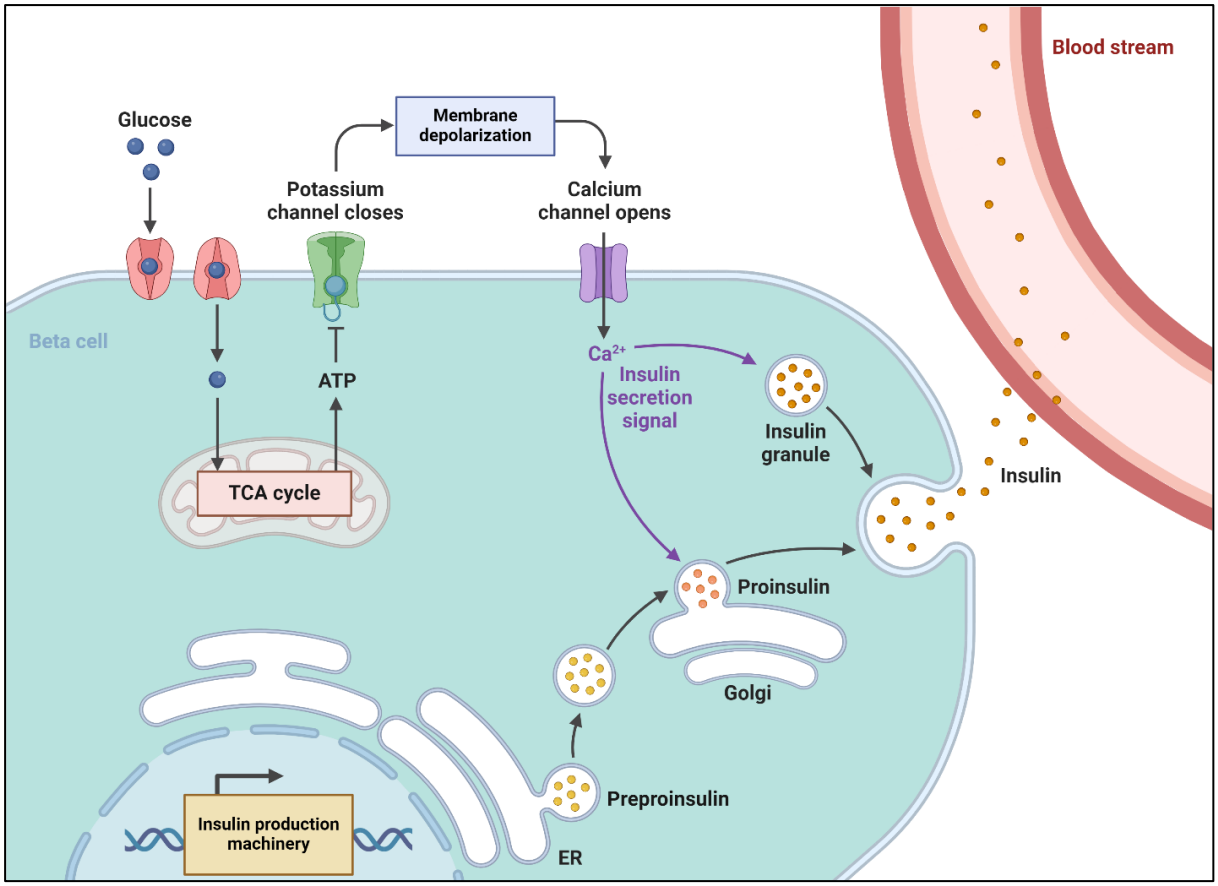

Figure 7: Schematic illustration of human insulin production pathway.

1.11. Insulin mechanism of action

The hormone insulin, which is generated by the pancreatic beta cells, has a significant impact on many different bodily tissues and is essential for controlling the metabolism of glucose. Insulin works by coordinating complex signaling channels that control how cells react to variations in blood glucose levels (Straub et al., 2002; Rutter et al., 2015).

Insulin binds to insulin receptors on the surface of target cells, such as muscle, liver, and adipose tissue, when it is released into the bloodstream. When insulin binds to the transmembrane insulin receptor, it can phosphorylate certain tyrosine residues due to its intrinsic tyrosine kinase activity. This sets off a series of intracellular signaling events that eventually alter the cellular mechanisms governing glucose intake, use, and storage. Insulin promotes the translocation of glucose transporter proteins, specifically GLUT4, from intracellular vesicles to the cell membrane, hence facilitating glucose absorption in muscle and adipose tissue (Watson et al., 2001; Watson et al., 2001). GLUT4 proteins function as molecular doors via which glucose can enter cells and be stored as triglycerides or glycogen or used for energy production. Important enzymes in the glycolysis process—which breaks down glucose to produce ATP, the main energy unit of cells—are also activated by insulin.

Insulin influences glucose metabolism directly and indirectly in the liver (Lewis et al., 2021). Insulin directly prevents the liver from producing glucose by inhibiting gluconeogenesis, which is the process by which glucose is made from precursors other than carbohydrates, like glycerol and amino acids. Furthermore, insulin facilitates the liver's production of glycogen, which allows extra glucose to be stored as glycogen for later use. By indirectly inhibiting lipolysis—the process by which triglycerides are broken down into fatty acids and glycerol—insulin lowers the amount of substrates that are available for gluconeogenesis. Moreover, insulin is essential for controlling the metabolism of proteins (Biolo et al., 1993). By encouraging the absorption of amino acids and triggering the translation of proteins important in development and repair, it stimulates protein synthesis in a variety of tissues, including muscle. In times of nutritional abundance, insulin also prevents the breakdown of proteins, preserving lean body mass.

Insulin affects many other physiological processes in the human body in addition to metabolism. It contributes to the preservation of tissue homeostasis and general health by controlling gene expression, cell division, and growth. Glucagon, leptin, and growth factors are

examples of other hormonal pathways with which insulin signaling interacts to coordinate metabolic responses to changing environmental conditions.

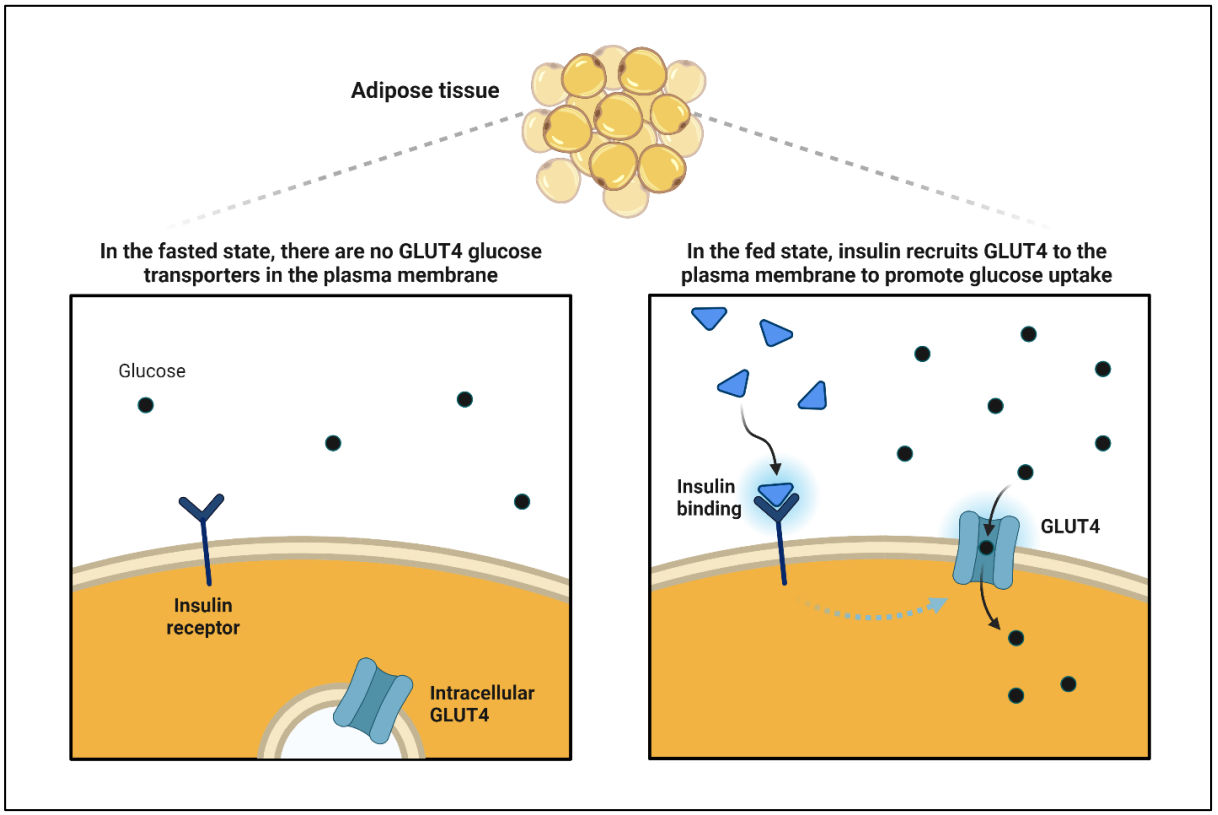

Figure 8: Mechanism of action of human insulin

1.12. Insulin fibrillation

Insulin fibrillation, often referred to as insulin aggregation, is the structural alteration of insulin molecules that produces fibrils or insoluble clumps (Brange et al., 1997). Insulin fibrillation can develop *in vivo* in some pathological circumstances, such as amyloidosis; however, it is primarily linked to the formulation and storage of therapeutic insulin formulations.

The 51 amino acids that make insulin are organized in two polypeptide chains (A and B) and connected by disulfide links. Insulin is a peptide hormone. Its main job is to control the metabolism of glucose by making it easier for cells to absorb glucose and encouraging the storage of glucose as fat or glycogen. On the other hand, insulin molecules have the ability to undergo conformational modifications that result in the conversion of their native soluble state into insoluble fibrillar forms. The B-chain residues, including GlyB8, SerB9, GluB13, ValB12, TyrB16, GlyB23, PheB24, PheB25, TyrB26, and ThrB27, play a crucial role in insulin self-assembly. These dimers work together to foster nucleus formation, with key residues such as

PheB1, ValB2, GluB13, GlnB4, AlaB14, LeuB17, ValB18, CysB19, and GlyB20 from the insulin B-chain and LeuA13, TyrA14, and GluA17 from the insulin A-chain being the most impactful drivers (Das et al., 2022). The process is driven by hydrogen bonding and hydrophobic interactions, and it's believed that a nucleus is comprised of three to four insulin monomers. However, it remains unclear whether the growth of mature fibrils occurs through the addition of monomeric or oligomeric species to the growing fibril.

Insulin fibrillation is a complicated process that is affected by a number of variables, such as pH, temperature, agitation, and the presence of metal ions (Sluzky et al., 1992). Insulin molecules are monomeric at physiological pH and temperature, where disulfide bonds and intramolecular interactions maintain them. These stabilizing factors, however, can be upset by environmental changes, which expose hydrophobic areas and create transitory oligomeric intermediates.

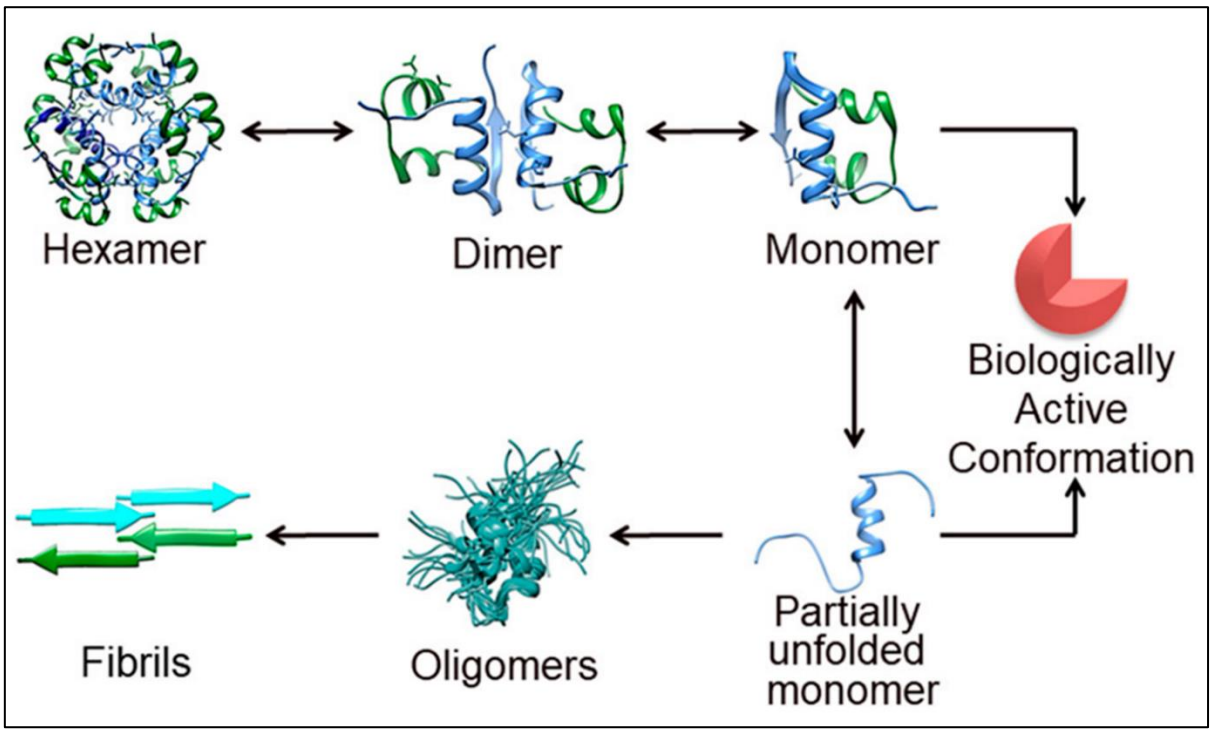

Figure 9: Pathway of insulin aggregation (Adapted from Das et al., 2022).

These oligomeric species function as sites of nucleation for further aggregation, starting a series of actions that eventually result in the creation of insoluble fibrils. Insulin molecules associate with each other by non-covalent interactions such as electrostatic, hydrogen bonding, and hydrophobic interactions, which define the aggregation process. As a result of these interactions, insulin molecules gradually assemble into fibrillar structures rich in β-sheets that are extremely durable and resistant to breaking down. Insulin fibrillation can have serious

repercussions, especially when it comes to medicinal insulin compositions. Insulin fibrillation can lower the stability, bioavailability, and pharmacokinetic profile of insulin products, hence compromising their safety and efficacy. Insulin preparations with fibrillation may show changed pharmacodynamic characteristics, which might cause irregular glucose regulation and raise the risk of hypo- or hyperglycemia in diabetic patients.

Additionally, insulin fibrillation can result in the development of amyloid-like aggregates, which have been linked to the etiology of a number of illnesses, including type 2 diabetes and neurological conditions (Blázquez et al., 2014; Ghulam et al., 2014). Tissue damage, inflammatory responses, and cellular malfunction can result from the accumulation of these aggregates in tissues and organs. It has been suggested that amyloid buildup in the pancreatic islets of diabetics causes β-cell malfunction and insulin resistance, which in turn accelerates the disease's course.

Numerous analytical methods, such as NMR, X-ray, and microscopy, have been used to investigate the structural characteristics of insulin and other amyloids. The structure of insulin amyloid protofilaments was studied using cryo-electron microscopy by Jimenez et al. (Jiménez et al., 2002). The results showed that the protofilaments were twisted around one another or grouped in pairs with a long-range twist around the constituent β-strand. The non-interacting portions on the protofilament surface were free to interact with other monomeric proteins without interfering with the packing due to the left-handed twists around the protofilaments. The disulfide connections inside and between chains were essential for the packing of fibrils and were preserved in the amyloid state. The strands ran parallel because of the interchain disulfide connections, while one of the sheets bulged because of the intrachain disulfide bond (Hong et al., 2012). Other proteins, such as lysozyme and Aβ (1–42), also created similar fibrils in which two to six protofilaments intertwined to form a mature fibril (Rambaran et al., 2008).

The structure of the oligomeric species of insulin was ascertained by Vestergaard et al. using small-angle X-ray scattering (SAXS) studies (Figure 10B) (Vestergaard et al., 2007). Their research showed that the oligomers were helical in nature and that the interwound helical oligomers formed a protofibril with an average diameter of 100 Å. According to their theory, the helical oligomer is prearranged so that it can connect with other oligomers and lengthen protofibrils into mature fibrils.

The core of insulin fibrils is formed by the B-chain residues LVEALYLV, as Ivanova et al. found (Ivanova et al., 2009). Together, these residues create parallel β-sheets along the whole

length of the fiber. The hydrophobic, highly complementary "steric zipper" interface is created when side chain residues L, E, L, and L from one sheet engage with identical residues from another sheet. There are two steric zippers that are the same and two internal dry sheets that are encircled by six water molecules. The β-sheet in the fibril structure replaces the α-helix in native insulin in the α-helix spanning region B11–B17 LVEALYL. Stacking SLYQLENY from the insulin A chain compacts the dry steric zipper surface of LVEALYLV together (Figure 10C). Along the fibril's moist surface, the Tyr residue and Tyr of LVEALYL engage to sustain the "kissing tyrosine" connection. Additionally, in accordance with Jimenez et al., X-ray diffraction investigations of insulin fibrils indicated that there are two insulin molecules per 4.7 Å layer of fibril. Using mass analysis, restricted proteolysis, and bioinformatics, Surin et al. identified the polypeptide sections that make up the spine of insulin fibrils (Surin et al., 2019; Surin et al., 2020). They found that the areas made up of A8–A15, B12–B19, and B23–B25 formed the spine of the fibrils for both human insulin and its analogues.

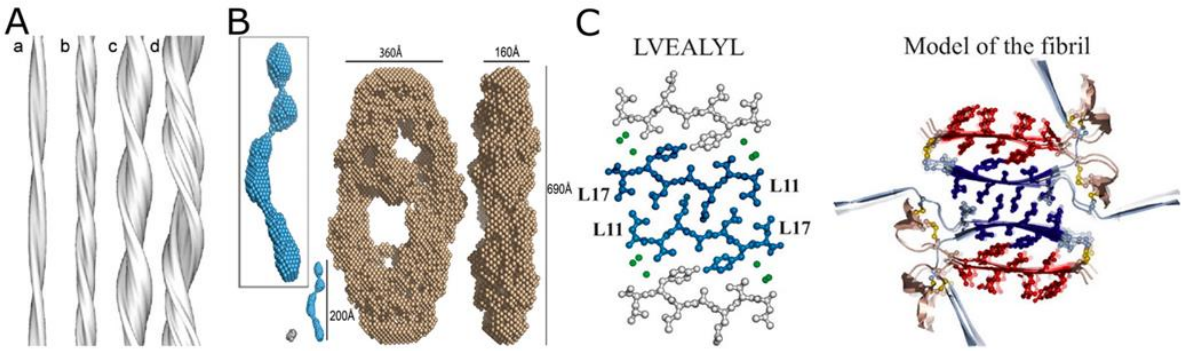

Figure 10: (A) The insulin fibril's cryo-EM structure, showing (a) two, (b) four, and (c) six protofilaments twisted around one another and (d) a ribbon twisted into a protofibril. (B) The ab initio helical oligomer is displayed in blue, the repeating helical unit of the fibril (front and side view) is displayed in brown, and the structure of the insulin monomer from SAXS analysis is displayed in the lower left corner (gray). The insulin oligomer is shown by the boxed upper left corner. (C) (Left) Four β-sheets made of B chain residues LVEALYL are shown in their X-ray crystal structure. The blue sheets are the two that make up the steric zipper interface. Water molecules are represented by the green spheres. The insulin A and B chain fibril model is shown on the right in pale red and pale blue, respectively. Dark blue represents the LVEALYL fragment, which makes up the fibril's spine. Dark red is the hue of the SLYQLENY region from the A chain, which produces auxiliary sheets to the fibril's spine. The yellow color represents the disulfide bonds. (Adapted from Das et al., 2022).

Extensive attempts have been made to comprehend the underlying mechanisms and create ways to prevent or decrease aggregation in order to reduce the hazards associated with insulin fibrillation. To stabilize insulin molecules and prevent aggregation, these tactics involve optimizing formulation parameters like pH, temperature, and excipient composition. Furthermore, the application of cutting-edge drug delivery techniques, like insulin analogs and nanoformulations, shows promise for improving the bioavailability and stability of insulin treatments while lowering the risk of problems connected to fibrillation.

1.13. Interactions of insulin with various molecules

The conversion of soluble proteins into insoluble fibrils, also known as amyloid fibrils, is a fascinating and complex area of research. These fibrils are often linked to various neurodegenerative diseases, including Alzheimer's, Parkinson's, and Type II diabetes. Amyloidogenic proteins and peptides, such as amyloid β-peptide (Aβ), alpha-synuclein, insulin, islet amyloid polypeptide, and transthyretin, have been identified as key components. While cross beta-sheets and elongated structures typically characterize amyloid fibrils, it's worth noting that non-disease-related proteins can also form fibrils *in vitro*. The process of fibrillation usually follows a nucleation-dependent polymerization mechanism, though the aggregation model can differ depending on the initial state of the proteins. For example, Aβ and alpha-synuclein aggregation start from folding, as they have an unfolded (disordered) structure before aggregation. Conversely, proteins such as insulin and transthyretin exist in the folded form in the native state before dissociating into a partially folded form (disordered structure) before aggregation. Even proteins with predominantly alpha-helical structures, like myoglobin and apo-cytochrome c, can form fibrils under certain conditions. One common property of any polypeptide chains or proteins associated with amyloid formation is that they tend to unfold from their native structure to partially folded intermediates before self-association. These fibrils are incredibly stable, resisting temperature, hydrolytic pressure, proteolytic enzymes, and denaturants.

Insulin is a complex protein composed of two polypeptide chains, the A-chain and the B-chain, which are connected by disulfide bonds. The B-chain's N- and C-terminal segments contribute to insulin's dynamic structure. In the 1940s, researchers discovered that insulin can fibrillate, resulting in a beta-sheet-rich structure that binds to Congo red and ThT, similar to other amyloid fibrils. Insulin fibrils have been found in arterial walls, membrane surfaces, and patients with type II diabetes. The aggregation and fibrillation of insulin can cause issues during

drug production, storage, and delivery. Inhibiting fibril formation is a primary therapeutic approach to treating insulin fibrillation-related diseases. Interestingly, the primary structure of proteins is not important in fibril formation, as proteins with no sequence homology can form fibrils. Therefore, an effective amyloid fibril inhibitor can target only the cross-beta-sheet secondary structure formation.

The inhibition of insulin amyloid fibrillation and disruption of pre-formed amyloid deposits have been identified as crucial therapeutic strategies. In this regard, several natural polyphenolic small molecule inhibitors, synthetic small molecules, nanoparticles, etc., have been reported to prevent insulin fibrillation effectively.

Jayamani et al. (2014) investigated the mechanism of fibrillation of insulin in the presence of ferulic acid (FA), a type of phenolic acid, by utilizing various biophysical techniques and discovered that FA has the ability to hinder insulin fibril formation *in vitro* (Jayamani et al., 2014). The concentration-dependent potency of FA's inhibitory activity decreases at lower concentrations and totally inhibits at higher values. The CD and FTIR analysis results provided evidence for the inhibitory effect of FA at elevated doses by demonstrating the inhibition of the usual conformational shift from an α-helix to a β-sheet during the production of insulin fibrils. Spectroscopic findings verified that FA preserves insulin's native structure, obstructing the conformational shift necessary for the in vitro development of amyloid fibrils. Based on previous and current research, it is advised that the phenyl, hydroxyl, and carboxylic moieties in FA contribute to its inhibitory activity against insulin amyloid fibrillation. These findings also imply that FA might be taken into account in treatments to slow the spread of amyloidosis.

Arora et al. (2004) found in another study that tiny stress molecules can stop the development of insulin amyloid, including ectoine, betaine, trehalose, and citrulline. Ectoine, trehalose, and citrulline completely prevented the development of insulin amyloid when they were present at a concentration of 300 mM, as seen by the lack of ThT fluorescence even after 40 hours of incubation. At the same dose, betaine also exhibited an inhibitory effect, bringing the stationary ThT fluorescence down to one-third of the control value. Nevertheless, amyloid production was not suppressed at the same concentration by the disaccharides maltose and sucrose despite their structural similarity to trehalose. AFM pictures were used for further research, and the results revealed that the control sample had a high density of unbranched insulin amyloid fibrils, but those containing trehalose, betaine, ectoine, and citrulline had very few fibrils. On the other hand, large fibril densities were seen when maltose was present, suggesting that the

inhibitor was inactive. In the meantime, natural insulin had two minima at 208 and 222 nm, according to CD analysis data, which were replaced by a single minimum at 216 nm after incubation at 50°C. A single minimum was seen in the CD spectra of the insulin solution, including trehalose and betaine, between 208 and 216 nm, suggesting that the presence of these solutes reduced the development of amyloid. Trehalose's CD spectrum was more similar to that of natural insulin, indicating a stronger inhibitory impact than betaine. As seen by larger values of negative ellipticity at 208 nm in the trehalose CD spectra, higher amounts of native insulin were present with increased trehalose concentrations (Arora et al., 2004).

A study by Patel et al. (2017) shown how well the naturally occurring small molecule morin hydrate works to stop human insulin from amyloid fibrillating in vitro. Through the use of transmission electron microscopy and spectroscopic experiments, their research demonstrated that morin hydrate suppresses insulin amyloid fibrillation in an efficient and dose-dependent way, exhibiting over 80% suppression at a 1:1 concentration. Studies using fluorescence spectroscopic titration demonstrate that insulin and morin hydrate have a significant affinity of -26.436 kJ mol−1. The structural alterations of insulin in the presence of Morin hydrate were also examined using circular dichroism (CD) spectroscopy, which showed that insulin may bind to amyloid fibrils, intermediate oligomeric species, and the native monomeric protein or its near-native state. According to Patel et al. (2017), computational docking and molecular dynamics investigations revealed that Morin hydrate binds to residues that have a higher tendency for aggregation, limiting structural and/or conformational alterations that cause amyloid fibrillation (Patel et al., 2017).

In 2017, Alam et al. conducted a study examining the formation of amyloid fibrils by human insulin (HI) and the impact of ascorbic acid (AA) on their formation through various techniques such as imaging, spectroscopy, and computation. The findings indicated that AA effectively inhibits the fibrillation of HI in a dose-dependent manner. Additionally, AA destabilizes pre-formed amyloid fibrils and protects the human neuroblastoma cell line (SH- SY5Y) from amyloid-induced cytotoxicity. This study suggests that AA has the potential to prevent human insulin aggregation and related pathophysiologies (Alam et al., 2017).

In a study conducted by Achari et al. (2017), it was discovered that the addition of L-cysteine (LC) to one's diet can raise Glutathione (GSH) levels and lower reactive oxygen species (ROS) levels, leading to improved insulin sensitivity (Figure 11). This is achieved by inducing adiponectin secretion in adipocytes that have been treated with high glucose (HG). The findings

of this study provide valuable insight into the cellular processes involved and suggest that LC may hold promise as a potential supplement for individuals with diabetes (Achari et al., 2017).

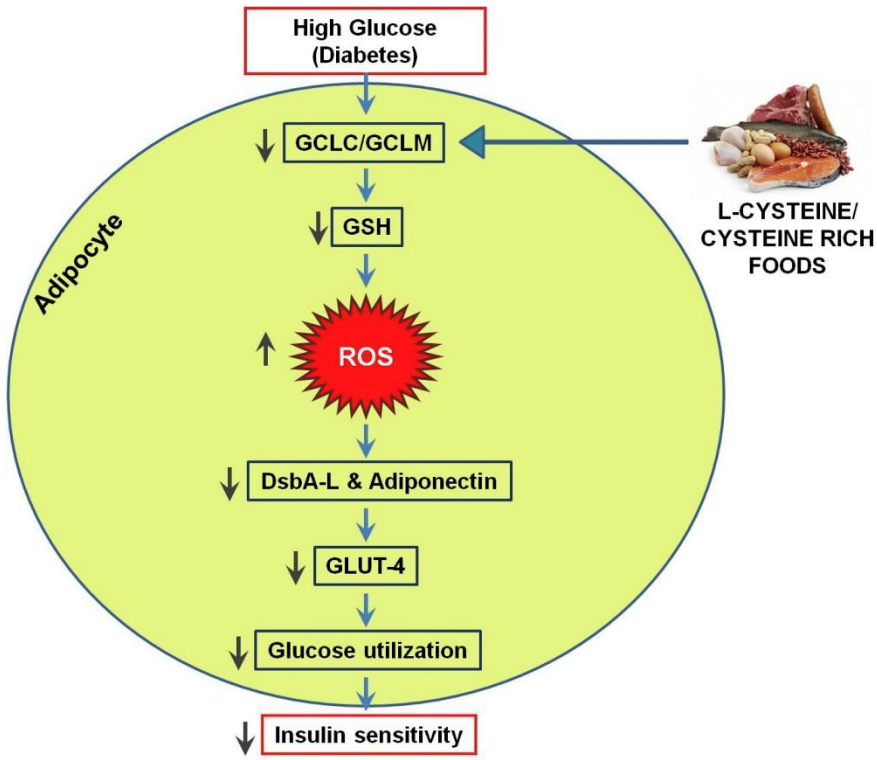

Figure 11: Diagrammatic representation of the possible interaction between insulin and LC on the production of adiponectin and the use of glucose. (Adapted from Achari et al., 2017)

In a recent study by Yanti et al. (2021), the interaction between phloretin (PHL) and insulin (INS) was investigated using various spectroscopic techniques. The team employed UV/Vis spectroscopy, fluorescence spectroscopy, and circular dichroism spectropolarimeter to analyze the interaction. The UV/Vis spectra indicated a strong absorption at a wavelength of 282 nm, indicating significant interaction between PHL and INS. The fluorescence analysis showed that excitation and emission occurred at 280 nm and 305 nm wavelengths, respectively. Interestingly, temperature changes did not impact INS emissions, but the PHL-INS interaction resulted in a shift towards longer wavelengths from 305 to 317 nm. The binding constant decreased with increasing temperature, but the binding site increased. PHL was found to stabilize the structure of insulin, leading to regional configuration changes in insulin. The interaction between phloretin and insulin resulted in the formation of a complex, which enhanced the α-helix structural configuration in insulin. This finding here in the study explains how phloretin improves insulin resistance (Yanti et al., 2021).

Samant et al. (2014) used fluorescence XRD and FTIR spectroscopy to investigate how insulin and Fe_3O_4 nanoparticles interact. The results showed that Fe_3O_4, Fe_3O_4-glutathione (GSH), and Fe_3O_4-GSH-polyamidoamine (Fe_3O_4-GSH-PAMAM G4) all strongly interacted with insulin and caused a decrease in its fluorescence intensity. The constants K_{sv} and K for fluorescence quenching and binding suggested that the interaction between Fe_3O_4 and insulin was stronger than its conjugates. Furthermore, the FTIR spectra indicated that the presence of nanoparticles could affect the secondary structure of insulin. This study can provide valuable insights into protein-nanoparticle interactions, which can help in the development of nano/micro delivery carriers for biology (Samant et al., 2014).

In 2015, Verdian-Doghaei and colleagues conducted a study exploring the interaction between insulin and the insulin-binding aptamer (IBA) using various spectroscopy techniques. These included UV/vis absorption, fluorescence, resonance light-scattering spectra (RLS), synchronous fluorescence, and three-dimensional fluorescence. The team also investigated the thermodynamic parameters (K_b, ΔH, ΔG, and ΔS) of the insulin-IBA complex by measuring temperature-dependent fluorescence between 25-37°C. Results demonstrated that the IBA caused a structural change in insulin, with the folding of the dual-labeled insulin-binding aptamer FL-IBA, resulting in contact quenching. This was due to the formation of a non-fluorescent complex between donor and acceptor. The researchers suggested that a significant fluorescent signal change when FL-IBA was bound to insulin was attributed to a conformational change in FL-IBA from a loose random coil to a compact G-quadruplex (Verdian-Doghaei et al., 2015).

In a study conducted by Gancar et al. (2020), the potential anti-amyloid activity of four green tea constituents was investigated. These included (-)-epigallocatechin gallate (EGCG), (-)-epicatechin (EC), gallic acid (GA), and caffeine (CF), both individually and in equimolar mixtures with exogenous insulin - a therapeutic agent for diabetes. The researchers discovered that only EGCG was effective in inhibiting the fibrillization process, while the individual EC, GA, and CF molecules were not. However, when EGCG was combined with GA, EC, or CF in equimolar concentrations, the mixtures showed inhibitory activity. Molecular docking studies demonstrated that EGCG interacts with a critical amyloidogenic region of insulin chain B (Figure 12). Interestingly, the inactive GA was found to enhance the inhibitory activity of EGCG, while EC and CF had a negative impact on the activity of the mixtures. The researchers also observed different types of amyloid aggregates formed in vitro in the presence of the

studied compounds and characterized their distinct morphology and amount (Gancar et al., 2020).

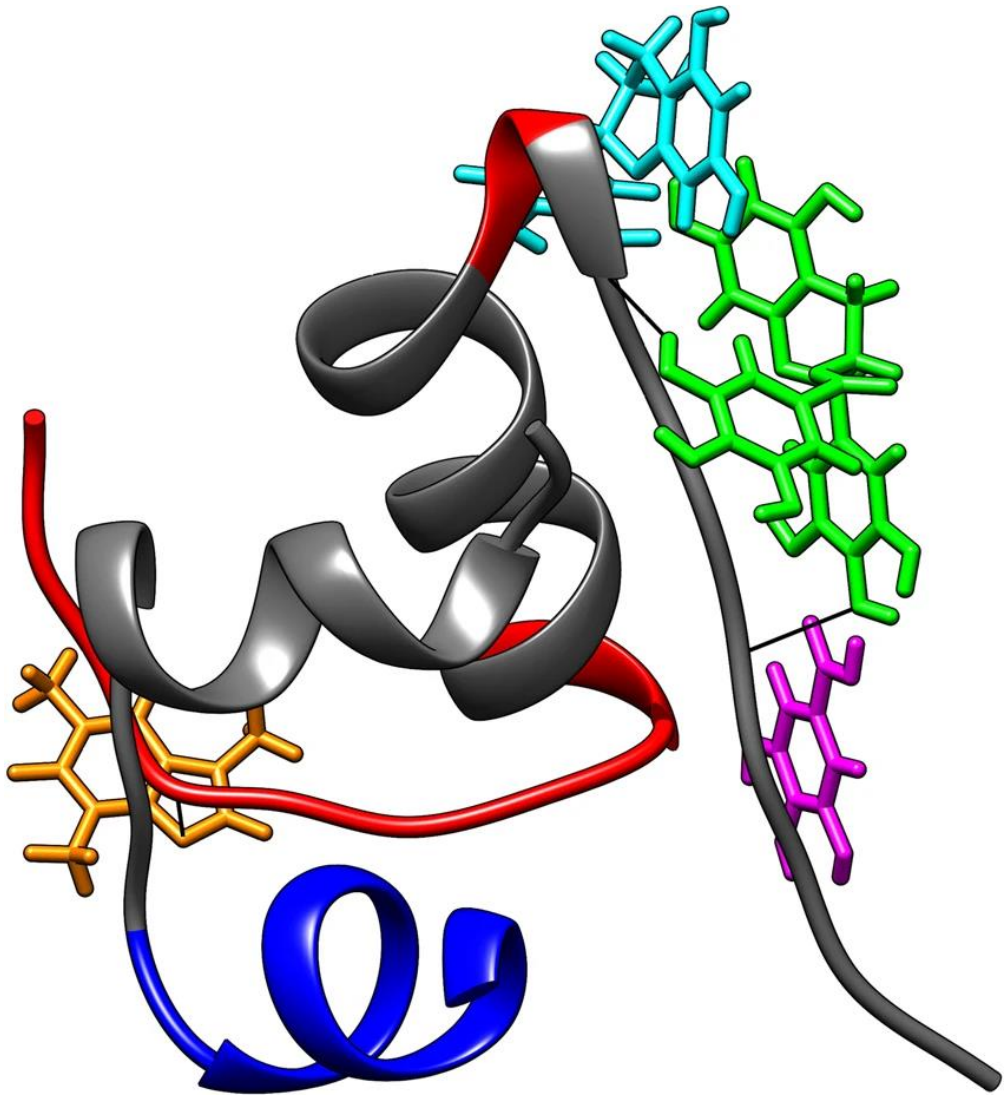

Figure 12: Human insulin structure at pH 1.9 (PDB ID: 2MVC) and the best docking poses for analyzed compounds (GA - magenta; EGCG - green; EC - turquoise; CF - ochre) Calculated amyloidogenic regions are colored in grey. (Adapted from Gancar et al., 2020)

The research conducted by Das and Bhattacharyya (2017) elucidated the destabilization of insulin aggregates by peptides derived from fruit bromelain. The study sheds light on the mechanisms governing the interactions between the peptides and insulin, providing valuable insights into the underlying biochemical pathways (Figure 13). This work provides further evidence of the potential impact of natural products, such as fruit bromelain, on biological systems and underscores the importance of understanding the molecular-level interactions that occur between such compounds and their targets (Das and Bhattacharyya, 2017).

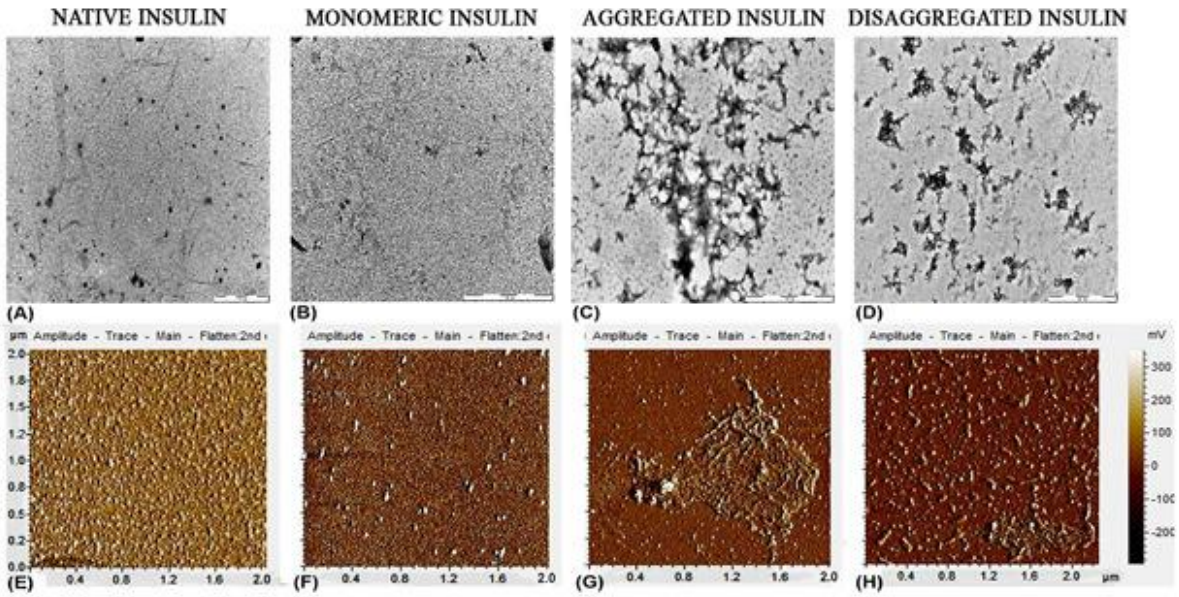

Figure 13: TEM images of native (hexameric) (A), monomeric (B), aggregated (C), and disaggregated (D) state of insulin. The scale bar of 1,000 nm is indicated. Corresponding AFM images are shown in (E–H). (Adapted from Das and Bhattacharyya, 2017)

In 2020, Sadrjavadi et al. conducted a study to assess the viability of using tragacanthic acid (TA) as a biocompatible polymer for insulin-delivery vehicles via poly-electrolytic complexes. The study revealed that insulin and TA had a natural affinity due to entropy, with hydrogen bonds being the primary enthalpic factor. The interaction between the two components was relatively weak, making it simpler for TA to efficiently capture and release insulin. These results indicate that TA-based systems could be employed for insulin storage and delivery (Sadrjavadi et

al., 2020).

In 2013, Chen et al. conducted a study affirming the potential of resveratrol and insulin to work synergistically in preventing and treating chronic diseases. Their research revealed that resveratrol could enhance insulin sensitivity, reduce oxidative stress, and activate the Akt pathway in type 2 diabetic patients by inhibiting insulin responses through a SirT1-independent pathway. Spectroscopy methods were employed to confirm the combined effect of resveratrol and insulin, with the researchers discovering that the two interacted to form a 1:1 complex through an exothermal and spontaneous reaction. As a result of this interaction, insulin underwent changes in conformation, leading to a decrease in polarity around the tyrosine residue and α-helical content, breakdown of the disulfide bridges, depolymerization of insulin

dimers into monomers, and alteration of the orientation of aromatic side chains in insulin. Furthermore, insulin was found to increase the stability of resveratrol (Chen et al., 2013).

In a study (2015) Dubey and colleagues, stable gold (AuNPsTyr, AuNPsTrp) and silver (AgNPsTyr) nanoparticles were synthesized and surface functionalized with tyrosine or tryptophan residues. The researchers investigated the nanoparticles' ability to inhibit amyloid aggregation of insulin. The presence of AuNPsTyr, AgNPsTyr, and AuNPsTrp nanoparticles effectively prevented both spontaneous and seed-induced aggregation of insulin and disassembled insulin amyloid fibrils (Figure 14). The study suggests that surface functionalization with amino acids is a crucial factor in the inhibition effect, as isolated tyrosine and tryptophan molecules did not have the same preventive effect on insulin aggregation (Dubey et al., 2015).

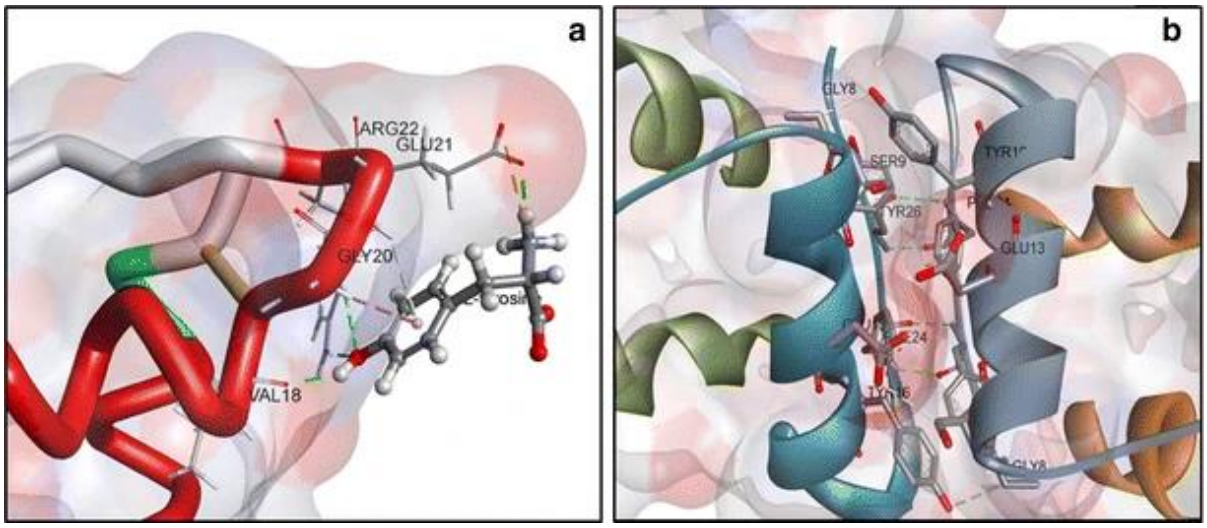

Figure 14: a) Tyrosine molecule and insulin molecular docking experiments. Seven interactions are seen in the complex, which includes two pi interactions (B:GLU21:HN—L-tyrosine, B:GLY20:HA1—L-tyrosine), one electrostatic bond (B:GLU21:OE2—L-tyrosine:N13), and four hydrogen bonds (B:ARG22:HE—L-tyrosine:O14, B:A RG22:HH21—L-tyrosine:O14, B:GLU21:OE1—L-tyrosine:H21, and B:VAL18:O—L-tyrosine:H24). b) Examining the crystal structure of the insulin dimer to see which functional groups at the interface of one insulin molecule attach to the tyrosine residue of another insulin molecule. (Adapted from Dubey et al., 2015)

1.14. Diseases associated with insulin

The process of protein misfolding, which leads to the formation of amyloids, plays a crucial role in the development of various diseases, including Alzheimer's disease, Parkinson's disease,

Huntington's disease, and type 2 diabetes. When proteins misfold into β-sheet-rich intermediates, they may form toxic aggregates that assemble into soluble oligomers and eventually linear mature fibrils. These aggregated species have the ability to attach to cell membranes, causing membrane permeabilization, cell dysfunction, and, ultimately, apoptosis (Oren et al.,1998). Scientists suggest interrupting amyloid aggregation could be a viable therapeutic strategy for treating protein-misfolding diseases.

Insulin, an essential hypoglycemic hormone, has been widely used as an anti-diabetic drug. However, repeated insulin injections in diabetic patients or clinical formulations can lead to the development of insulin amyloidosis (Okamura et al.,2013). Unlike other natively unstructured amyloidogenic proteins, such as islet amyloid polypeptide, amyloid-β, and α-synuclein, insulin belongs to the category of natively structured amyloidogenic proteins, including prion and lysozyme. Insulin amyloids possess a typical cross-β structure, similar to the mature fibrils of disease-relevant amyloids, making them an attractive model system to study the mechanisms of protein fibrillation. Additionally, insulin amyloids serve as a valuable tool to explore potential aggregation inhibitors for amyloid-related diseases (Gong et al., 2014)

The pancreas secretes the hormone insulin, essential for controlling the body's glucose metabolism. Many illnesses and conditions can develop from reduced or impaired insulin action, with the main ones centered on disruptions to glucose homeostasis. Here, we examine a number of illnesses linked to insulin dysfunction (Rahman et al., 2021; Mlinar et al., 2007).

1.14.1. Insulin resistance

Insulin aggregation can lead to insulin resistance. Insulin resistance is a medical condition where target tissues, such as the liver, muscle, and adipose tissue, have a reduced response to insulin stimulation. This results in a decrease in glucose disposal, leading to increased beta-cell insulin production and hyperinsulinemia. Insulin resistance has a range of metabolic consequences, including hyperglycemia, hypertension, dyslipidemia, hyperuricemia, elevated inflammatory markers, endothelial dysfunction, and a prothrombotic state. Consequently, insulin resistance is a major risk factor for developing a variety of metabolic disorders, including type 2 diabetes, cardiovascular disease, and metabolic syndrome (Wilcox, 2005).

1.14.2. Type 1 Diabetes Mellitus (T1DM)

Type 1 diabetes mellitus, or T1DM, is an autoimmune disease that results in complete insulin insufficiency by destroying the pancreatic beta cells that produce insulin (Katsarou et al., 2017;

Kaul et al., 2015). Hyperglycemia is the result of insufficient insulin, which prevents glucose from entering cells to be converted into energy. For the duration of their lives, people with type 1 diabetes need to take insulin replacement therapy in order to control their blood sugar levels and avoid acute consequences such as diabetic ketoacidosis (DKA).

1.14.3. Type 2 Diabetes Mellitus (T2DM)

Insulin resistance, or the cells' decreased sensitivity to the effects of insulin, is the hallmark of type 2 diabetes mellitus (T2DM), which results in poor glucose absorption and utilization (Goldstein, 2002; Hameed et al., 2015). At first, the pancreas makes up for this by manufacturing more insulin, but eventually, beta cell function deteriorates, and there is a relative insulin shortage. Genetic susceptibility, sedentary lifestyle, and obesity are all closely linked to type 2 diabetes. Treatment usually consists of dietary changes, oral anti-diabetic drugs, and insulin therapy in more severe situations.

1.14.4. Gestational Diabetes Mellitus (GDM)

Pregnancy-related glucose intolerance is known as gestational diabetes mellitus. Elevated blood glucose levels can result from pregnancy-related hormonal changes and insulin resistance, especially in women who have risk factors, including obesity or a family history of diabetes. Preeclampsia, neonatal hypoglycemia, macrosomia (high birth weight), and other problems are more common in women with GDM. Management includes changing one's diet, keeping an eye on blood sugar levels, and using insulin therapy as needed (Akbay et al., 2009; Langer et al., 1991).

1.14.5. Alzheimer's Disease (AD)

Alzheimer's disease is a neurological disorder that causes memory loss and cognitive decline due to the accumulation of abnormal amyloid-β in the brain. It is worth noting that, despite its lack of direct association with insulin, insulin-degrading enzyme (IDE) is accountable for the degradation of both insulin and amyloid-beta (Aβ) peptides, which are recognized as key players in the pathogenesis of Alzheimer's disease (AD) (Jha et al.,2015). It has been hypothesized that insulin aggregation may indirectly affect AD pathology via competitive binding with IDE, thereby influencing the clearance of Aβ peptides.

1.14.6. Insulinoma

Insulinoma is a rare neuroendocrine tumor of the pancreas that causes hypoglycemia by producing an excessive quantity of insulin (Shin et al., 2010; Grant et al., 2005). Although insulinomas are usually benign and tiny in size, they can induce hypoglycemia, which can lead to severe symptoms like palpitations, sweating, and confusion. Imaging investigations are often used to pinpoint the tumor, and biochemical tests are used to detect high insulin levels in the diagnosis. Surgical removal of the tumor or symptom management with medication are possible treatment options.

1.14.7. Metabolic syndrome

This group of disorders raises the risk of type 2 diabetes and cardiovascular disease. It includes insulin resistance, dyslipidemia, hypertension, and abdominal obesity. The pathophysiology of metabolic syndrome is largely influenced by insulin resistance, which also contributes to the development of dyslipidemia, chronic inflammation, and hyperglycemia. The mainstays of management are dietary changes, physical activity, and lifestyle interventions aimed at weight loss (Mikhail et al., 2009; Gluvic et al., 2017).

1.14.8. Polycystic Ovary Syndrome (PCOS)

PCOS, or polycystic ovary syndrome, is a prevalent endocrine illness marked by insulin resistance, ovarian dysfunction, and hormonal abnormalities (Maqbool et al., 2019; Ovalle et al., 2002). Menstrual abnormalities, infertility, and hirsutism are caused by the stimulation of androgen production by the ovaries caused by hyperinsulinemia resulting from insulin resistance in PCOS. The goals of management include reducing symptoms and treating underlying metabolic imbalances using drugs, hormone therapy, and lifestyle changes.

1.14.9. Amyloidosis

Insulin aggregates can group together to form insoluble protein aggregates called amyloid fibrils. When these fibrils deposit in various tissues throughout the body, they can cause damage and dysfunction to organs, leading to a condition called amyloidosis (Ashraf et al.,2014). Specifically, the deposition of amyloid fibrils in pancreatic islets is known as islet amyloidosis, which is linked to diabetes.

1.15. Introduction to beta-lactoglobulin (β-lg)

Many mammalian species, as well as the milk of ruminant animals such as sheep, buffaloes, and goats, contain the beta-lactoglobulin protein. It is not present in rodents, lagomorphs, or human milk. Beta-lactoglobulin (β-lg) from cows is a significant component of whey protein found in their milk. Bovine milk is a liquid diet with 87% water content, which has an average of 13% total solids and roughly 9% solids but no fat. Milk is a nutrient-dense food supplement that includes calcium, vitamin A, riboflavin, potassium, phosphorus, and B12. The two main components of milk are soluble whey proteins and insoluble caseins. Caseins make up almost 80% (w/w) of the total protein inventory. The main component of milk is whey. Whey, commonly known as cheese serum, is a yellow-green liquid that is produced when milk coagulates and separates the curd utilizing acids or proteolytic enzymes (Minj and Anand, 2020). It is a liquid milk by-product that has a lot of beneficial ingredients. Quantitatively, the main component of the whey protein portion of milk is β-lg, accounting for 55% (w/w). β-lg is involved in regulating phosphorus metabolism at the mammary gland and transferring passive immunity to the baby. The mammillary glands of ruminants manufacture β-lg, which is subsequently combined with milk. According to Kontopidis et al. (2002), β-lg can bind with tiny hydrophobic ligands such as calcium, retinol, fatty acids, protoporphyrin IX, triacylglycerols, alkanes, aliphatic ketones, aromatic chemicals, vitamin D, cholesterol, and palmitic acid (Kontopidis et al., 2002).

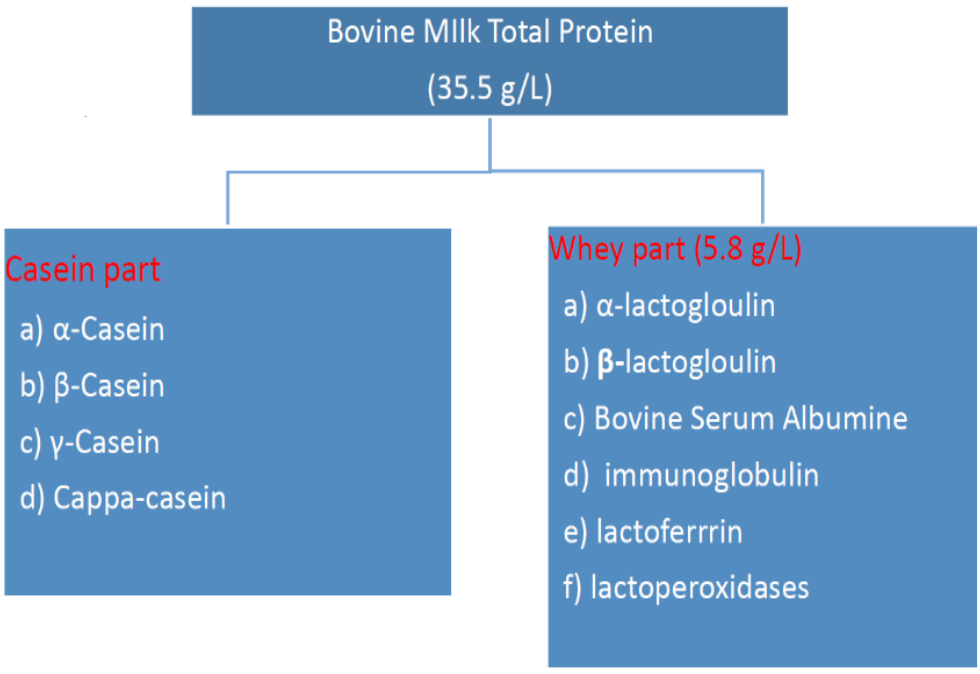

Figure 15: Schematic Representation of protein content of bovine milk

Encapsulation properties of liposomes and serve as a stable system for vitamin E delivery (Rovoli et al., 2014). It shows several other therapeutic applications. β-lg is well studied protein for its biological function, availability, and separation technique. We choose this single whey protein, β-lg, as one of our model proteins.

1.15.1. History and developments in isolation and purification of bovine β-lactoglobulin

β-lg was first discovered through a salt fraction of cow's milk by Palmer et al. in 1934 (Palmer, 1933). In 1936, Pedersen found a number of peaks in the sedimentation pattern during an ultrasound study of milk and whey (Pedersen, 1936). Pedersen denoted these peaks as α, β, γ, etc., and then identified β-peak as arising from the "Palmer's protein." The first X-ray crystallography of β-lg was obtained by Crowfoot in 1938 (Crowfoot and Riley, 1938). The term β-lactoglobulin was first introduced by Svedberg)1939((Svedberg, 1939). Two genetic variants of β-lg A and B were first introduced by Aschaffenburg and Drewry (1957(. They isolate β-lg by Na_2SO_4 precipitation at 40ºC followed by acidic precipitation at pH 2, dialysis, and crystallization (Aschaffenburg and Drewry, 1957). In 1959, Green et al. developed an X-ray diffraction study of derivatives of β-lactoglobulin (Green and Aschaffenburg, 1959). X-ray Crystallographic Study of β-lactoglobulin was carried out by Aschaffenburg et al. 1965 (Aschaffenburg et al., 1965). In 1967, Fox et al. and Armstrong et al. separated β-lactoglobulin by trichloroacetic acid through $(NH_4)_2SO_4$ precipitation at 20ºC, acidic precipitation at pH 2 followed by Na_2SO_4 precipitation at pH 6, dialysis, and crystallization (Fox et al., 1967; Armstrong et al., 1967). The crystal structure of orthorhombic lattice Y form was observed by Papiz et al. 1986 (Papiz et al., 1986). Large-scale separation of β-lactoglobulin was developed by Mate & Krochta, 1994 (MATÉ and KROCHTA, 1994). The most abundant variants are labelled b-Lg A and b-Lg B and differ by two amino acid substitutions, Asp64Gly and Val118Ala, respectively (Farrell et al., 2004). The β-lg exists both as dimer and monomer; in ruminants, it presents in the dimer, but in monogastric species, for example, dolphins, horses, and pigs, β-lg exists in a monomeric form of approximately M_r 18,300 Da (Sawyer, 2012). Quaternary structures occur in a variety of forms depending on the pH of the medium: a stable dimmer with a molecular weight of 36,700 kDa occurs at pH values between 7 and 5.2; an octamer with a molecular weight of 140,000 kDa occurs between pH values of 5.2 and 3.5; an octamer with two cysteine residues per monomer at pH 3.0-0.2 and above 8.0. The crystal structure of bovine β -lactoglobulin was observed by Rocha et al. 1996 (Rocha et al., 1996).

Table 3: Recent Past developments in isolation and purification of bovine β-lactoglobulin

Year	Isolation, Purification, and X-ray Crystallographic Study	References
1997	Centrifugation, acidic precipitation at pH 4.6, filtration, dialysis, and gel filtration.	Felipe and Law, 1997
	Acidic precipitation at pH 4.6, Centrifugation, and N-retinyl-celite affinity chromatography.	Heddleson et al., 1997
	Triclinic lattice X at 1.8 Aº resolution and lattice Y at 2.1 Aº resolution.	Brownlow et al., 1997
	Isolated by combining a precipitation process and a diafiltration process.	Caessens et al., 1997
1998	Crystallographic presentation of external ligand-binding sites.	Sawyer et al., 1998
1999	Crystallographic three-dimensional aspects of β-lactoglobulin and functional properties.	Sawyer et al., 1999
2001	Centrifugation, acidic precipitation at pH 4.4-4.5, base precipitation at pH 7.2, centrifugation followed by anion-exchange and gel filtration Chromatography	de Jongh et al., 2001
2008	10-90% $(NH_4)_2SO_4$ precipitation, cation-exchange chromatography, dialysis, and lyophilization.	Lozano et al., 2008
2010	Gel filtration Chromatography at low pH using a Bio-Gel P10 column.	Naqvi et al., 2010
2012	One-step method by anion exchange chromatography, high-performance liquid chromatography and mass spectroscopy.	Stojadinovic et al., 2012
2014	Combining ion exchange chromatography and gel filtration by adsorbed on DEAE-Sepharose FF packed column and Sephadex G-75 gel and SDS-PAGE.	Buyanbadrakh et al., 2014
2015	Gel filtration chromatography using Sephacryl S-200 at acidic pH 4.6	Aich et al., 2015
2019	The structure of bovine β-lactoglobulin in crystals grown at pH 3.8 exhibiting novel threefold twinning	Todd et al., 2019

1.15.2. Secretion of β-lg

Like the majority of milk proteins, β-lg is made by the mammary gland's secreting epithelial cells, and it is regulated by the prolactin hormone (Jawasreh et al., 2019). The mammary gland synthesizes messenger RNA coding for β-lg, which is then translated into pre-β-lg, a 180 amino acid molecule (Rytkönen, 2006). An 18-amino acid signal peptide that is highly conserved can be found in pre-β-lg. The mature protein itself has a molecular weight of 18400D and 162 amino acids. When lactose and milk protein-containing secretory vesicles fuse with the apical plasma membrane, milk is released from the bovine mammary gland (Broersen, 2020).

1.15.3. Molecular structure of bovine β-lactoglobulin

According to several studies, the monomer has a spherical shape with a block of electron density and a rod-like structure across one face (Green and Aschaffenburg, 1959). The secondary structure of β-lg was predicted to contain ∼50% β-sheet ∼, 15% α-helix, and 15–20% reverse turn (Wang et al., 2022). In 1986, the first medium-resolution structure of β-lg was published. β-lg has a predominantly β-sheet structure (Figure 16) with eight stranded anti-parallel (A-H) β-barrel, one small three turn α-helix on the outer surface, and a β-strand 'I' immediately before the C-terminal end (Papiz et al., 1986). In the crystal structure, it has been revealed that the typical lipocalin consists of an eight-strand anti-parallel barrel oriented in an anti-parallel ring structure, whereby the hydrophobic ligands/molecules are encapsulated in the hydrophobic calyx (Monaco et al., 1987; Brownlow et al., 1997). As far as its structure is concerned, it is quite globular in nature, having 162 amino acid residues and an estimated molecular mass of 18400. β-lg has a conserved three-dimensional structural domain (sequence motifs) and small hydrophobic molecule binding and transportation property for which it is typified to the lipocalin family (Sawyer and Kontopidis, 2000). β-lg has extensive sequence homology with the retinol-binding protein, and its function is thought to be the binding and transportation of retinol in mammals (Redl and Habeler, 2022). β-lg exists as a dimmer at physiological pH. Below pH 3.0 and above pH 7.0, it exists as a monomer. At pH 2.0, β-lg dissociates into its monomer form with a native conformation (Crowther, 2017). The x-ray crystallographic presentations of β-lg show that A—>D strands participate in the formation of one side of the β-barrel and strand E—>H are involved in the other side, whereas strand 'I' is projected outward the calyx acting as dimmer interface by ionic strength/ salt dependent or through hydrogen bonding (Qin et al., 1998; Sakurai and Goto, 2002). β-lg is resistant to acid hydrolysis as well as pepsin digestion (Rahaman et al., 2017). This pH-dependent monomer ←→ dimmer transformation is strictly attributed to non-covalent and hydrophobic interactions (Sakurai et al., 2001).

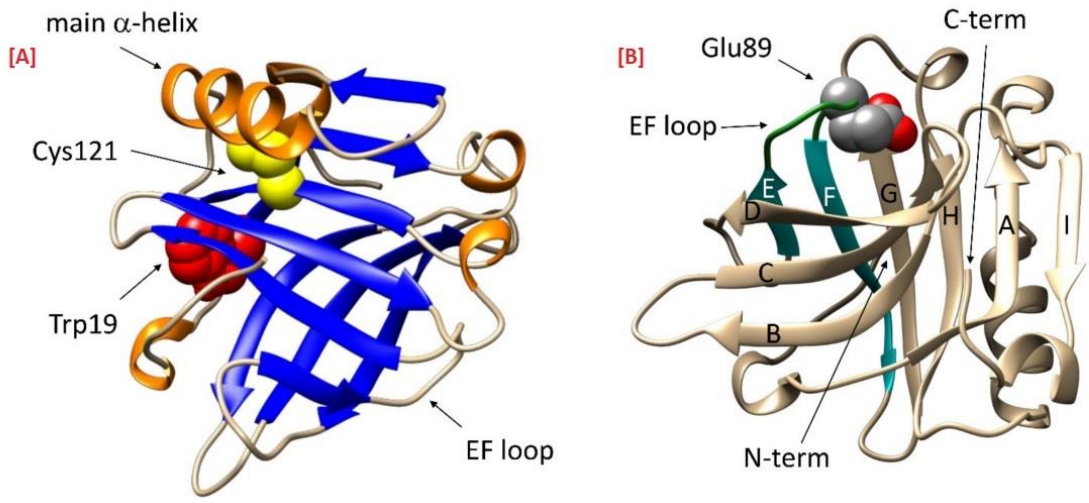

Figure 16: Properties of the native BLG structure that are pertinent to research on folding stability. (A): Trp19 (red) is at the base of the beta-barrelled calyx (blue); Cys121 (yellow) is concealed behind the major alpha-helix (orange). (B): The EF loop forms a "lid," which closes when Glu89, seen in CPK colors, is protonated (dark green). The free graphics program UCSF Chimera (version 1.14, University of California, San Francisco, CA, USA) was used to create the structures.

The presence of Aromatic residues such as two tryptophan, four tyrosine, and four phenylalanine residues make β-lg fluorescence active (Xu et al., 2019). These groups are also responsible for the near UV CD of β-lg spectra, which helps investigate site-specific conformational changes. β-lg has a high helical propensity despite being a predominantly β-sheet protein. During its refolding from the fully unfolded state, an intermediate with a non-native α-helical structure accumulates because the local interactions between neighbouring amino acid residues favour the α -helical structure (Hamada et al., 1996). In particular, the EF loop, consisting of amino acids 85-90, acts as a gate over the binding site. At low pH, it is in the “closed” position, and binding is inhibited or impossible, whereas, at high pH, it is open, allowing ligands to penetrate the hydrophobic binding site. In EF loop, the Glutamic acid (Glu89) plays a key role for the entry of the small hydrophobic molecule in the calyx of β-lg accompanied by the ‘lid-motion’ along with the Serine residue (Seri 16) via H-bond formation in pH-dependent manner (Qin et al., 1998; Tanford and Nozaki, 1959; Brownlow et al., 1997; Kontopidis et al., 2004). β-lg forms disulfide-linked covalent dimers or oligomers accompanied by the free thiol (Cysl21) group or disulfide exchange process during the unfolding/ refolding pathway under thermal stress (Hoffmann and van, 1997; QI et al., 1997; Oliveira et al., 2001). Cys106 and Cys119 residues form the disulfide bridge in the β-G and β-H strands, providing

the α-helix remains packed against the exterior of the calyx. However, this disulfide bridge is not solvent-accessible and is shielded from the thiol of Cys121 by the side chains of Phe136, Ala139, and Leu140. Cys66-Cys160 makes the second disulfide bridge fasten the C-terminal loop to the exterior of the calyx (Brownlow et al., 1997).

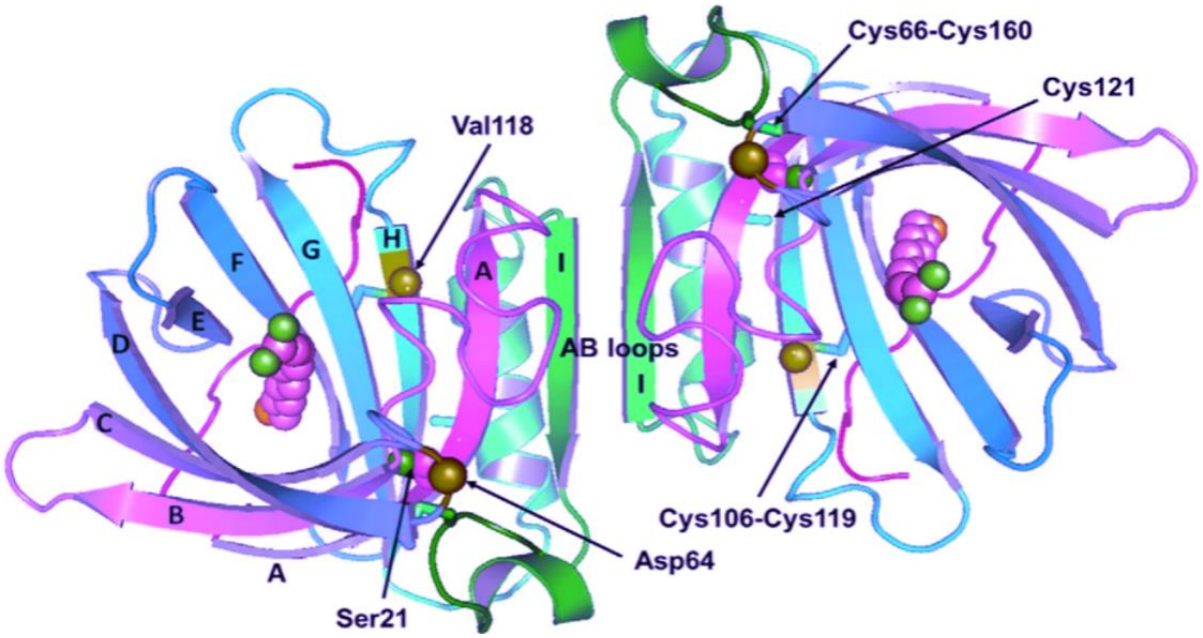

Figure 17: Diagram showing the two-fold axis orientation of the dimeric structure of bovine β-lg A. The trigonal Z lattice structure of β-lg A, which has 12-bromododecanoic acid attached, provides the coordinates (PDB code: 1bso). The β barrel is made up of strands that are designated A through H. At neutral pH, the dimer interface is formed by the I strand and a portion of the AB loop. Additionally displayed are the locations of the spots where the A and B variants differ from one another. Figure drawn with PyMOL (Delano, 2002).

1.15.4. Amino acid sequence of β-lg

β-lg have 4 tyrosine residues at positions 20, 41, 99, 102 in the amino acid sequence and have 15 lysine residues. The two genetic variants of β-lg differ in the position of Asp64→Gly64 and Val 118→Ala 118 (Sawyer et al., 1999), and the isoelectric points of β-lg A and β-lg B are 5.1 and 5.3 respectively. Both these variants contain two tryptophan residues (Trp 19 and Trp 61 residues). Trp19 residue remains hidden in the hydrophobic calyx of native β-lg, showing the major fluorescence property of β-lg (Saha et al., 2023).

The Val118Ala substitution causes no change to the structures, but the presence of bulky isopropyl substituent creates void space in the hydrophobic core of the B variant, which is less well-packed and exhibits less thermal stability under some measurement conditions. However,

the Asp64Gly substitution in these two genetic variants alters CD loop conformations (Qin et al., 1999).

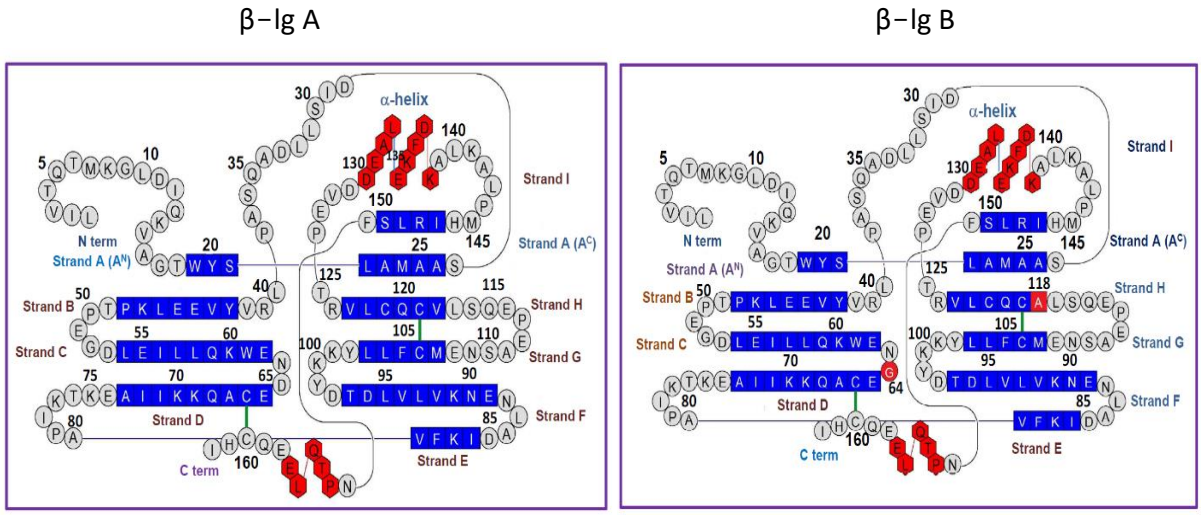

Figure 18: A schematic representation of the amino acid residues of the β-lg A and β-lg B sequence. Residues making up the α-helix, β-sheet, and loop are represented by hexagons in red, squares in blue, and circles in grey, respectively. Green lines indicate the positions of disulfide bonds. The substitutions Val118Ala (A→B) and Asp64Gly (A→B) are shown in red square and red circle, respectively. (Adapted from Qin et al., 1999)

1.15.5. Structure of bovine β-lactoglobulin in aqueous solution and monomer–dimer equilibrium of bovine β-lactoglobulin in aqueous solution

The three-dimensional structure of β-lg in aqueous solution has been accurately determined using various techniques such as X-ray crystallography and nuclear magnetic resonance (NMR) spectroscopy. The NMR technique is useful for monomeric proteins with molecular weights <∼25 kDa and usually requires recombinant singly (^{15}N) or doubly (^{15}N / ^{13}C) labelled material for protein molecules with molecular weights >∼8 kDa. The structure of β-lg consists of two main domains: an N-terminal domain (NTD) and a C-terminal domain (CTD). The N-terminal domain consists of a hydrophobic core that stabilizes the protein structure and prevents aggregation. This domain also contains several solvent-exposed regions, which facilitate the binding of β-lg to different ligands and antigens. The C-terminal domain is composed of an extended loop region responsible for binding and transporting other molecules. This domain also contains a disulfide bridge, which is essential for maintaining the structural integrity of β-lg. Using NMR spectroscopy, protein structures in the solution phase are developed (Cavanagh, 1996). Therefore, the NMR studies of bovine β-lg generally carried out at pH 2 to 3 and,

importantly, at very low ionic strength, where the molecule is in monomer form. Using NMR, Molinari's group confirmed the presence of the eight-stranded b-barrel in the wild-type-B variant (Fogolari et al., 1998).

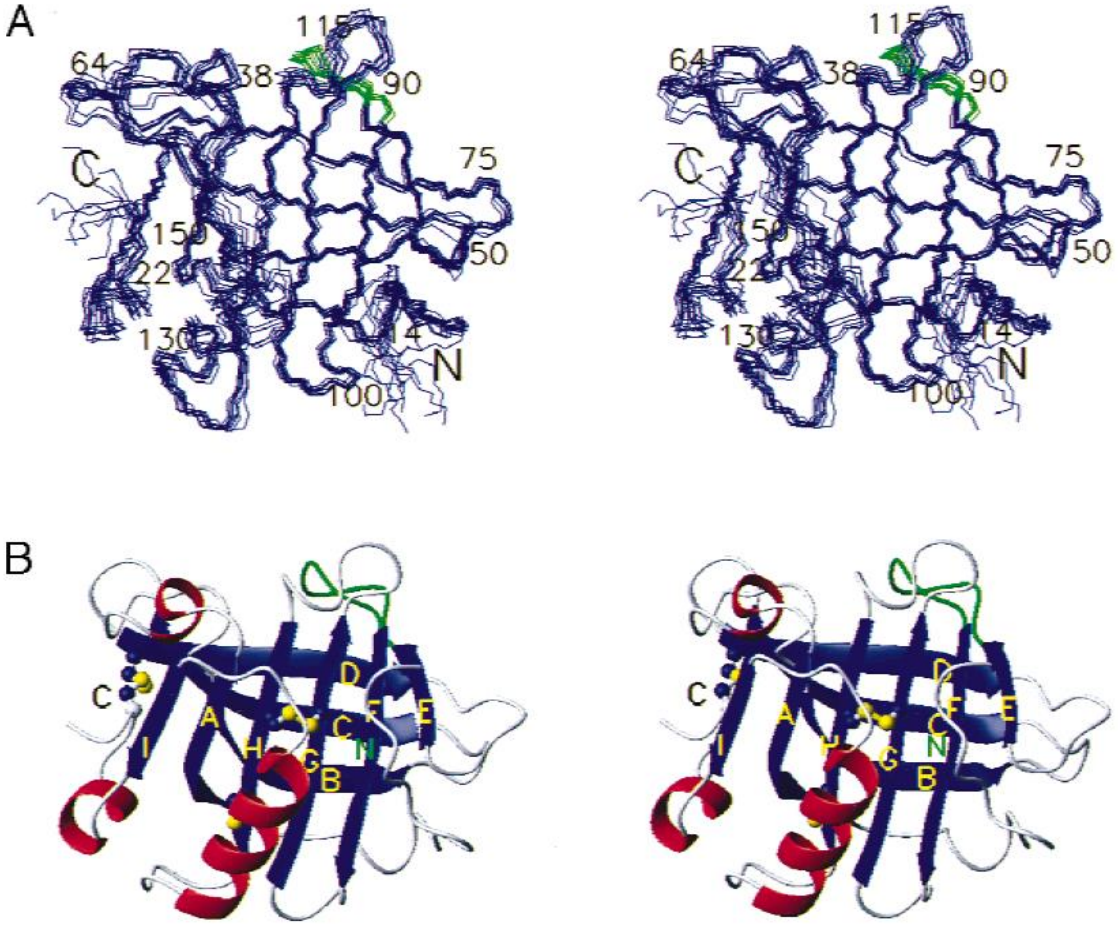

Figure 19: (A) NMR and (B) X-ray structures of bovine b-lactoglobulin. An X-ray coordinate (3blg) and secondary structure locations are available from the Brookhaven PDB. A diagram illustrating the superimposition of the 17 NMR structures was created using MOLMOL. Disulfide bonds (Cys66–Cys160 and Cys106–Cys119) and a free thiol group (Cys12) are shown in (B), helical regions are coloured red, and loop EF is a green colour. (Adapted from Koradi et al., 1996).

The β-lg structure in the solution phase was shown by both Kuwata et al. (1999) and Uhrínová et al. (2000) provided overall similarity to that established earlier structure by x-ray crystallography at pH 6.2 (Kuwata et al., 1999; Uhrínová et al., 2000). When β-lg is dissolved in aqueous solution, it undergoes conformational changes that can affect its stability and activity. These conformational changes can occur due to various factors, such as temperature, pH, and the presence of other molecules. At lower temperatures, β-lg tends to adopt a more

compact and rigid structure, while at high temperatures, it can unfold and unfold. The pH of the solution also influences the conformation of β-lg, with lower pH values favouring a more compact conformation and higher pH values promoting a more extended and unfolded state.

The structure of β-lg in aqueous solution provides valuable insights into the mechanisms involved in ligand binding. The hydrophobic nature of the NTD domain allows it to interact with hydrophobic residues on the ligands, while the CTD domain provides additional binding sites for hydrophilic molecules. It is quite evident that the protein's surface charge increased due to the decreased pH (which, in turn, caused the protein's pH to be lower) required to obtain usable NMR spectra from monomeric bovine β-lg. It is apparent from the X-ray structures that the side chains of the Glu89 'latch' are buried under the EF loop at pH 6.3, just as they are in the EF loop at pH 6.3. There is one major difference between the X-ray structure of the Z lattice structure at pH 6.2 and the structure of the three-turn a-helix at pH 6.2 (Qin et al., 1998), which is that the three-turn a-helix adopts a different position in relation to the b-barrel, perhaps as a result of the positive charge increased on the surface of the protein as a result of pH change. As a result, the lack of a dimer interface at low pH also makes it possible to free up some restraints involved in the AB loop's conformation, which constrains the position of the helices when in dimers but not in direct contact (Figure 19).

There was also a difference in the N- and C-termini; these differences may be explained because recombinant proteins with non-native N termini were synthesized for the NMR structure, while crystal packing effects may have affected the X-ray structure. Many of the residues from residues 152 to 162 in the C-terminus are either completely absent or poorly defined in electron density maps in some crystal forms.

Over a long period of time, several techniques have been used to study the monomer-dimer equilibrium of bovine β-lg, such as analytical ultracentrifugation (AUC), light scattering, SAXS, and isothermal dilution calorimetry. Although dimer dissociation is an essential step in the denaturation of bovine β-lg and its subsequent chemical processes, the rate constants associated with this phase have never been measured. Analytical centrifugation measurements confirmed earlier values for dimer dissociation equilibrium in an essentially constant ionic strength medium of 100 mM NaCl. According to Mercadante et al. (2012) (Mercadante et al., 2012). The association rate constant is well outside the diffusion-controlled limit, and the dissociation rate constant is also quite slow due to the considerable restructuring of counter-ions during dimerization. The counter-anions are restructured substantially at low pH, where

the β-lg is strongly positively charged, and when pH is >7, where it is mildly negatively charged, the counter-cations are restructured, and distance dependence is sharp for optimizing hydrophobic contacts. In isothermal dilution calorimetry at temperatures up to 35°C, variant B of β-lg dissociates at a slower rate than variant A. Dissociation constants measured by analytical ultracentrifugation are very similar to those determined by pH 7.0 phosphate buffer and 100 mM NaCl at 14.5(1) mM.

1.15.6. The lipocalins and β-lactoglobulin: structure and function

Lipocalin is the family of proteins that have the ability to bind with small, principally hydrophobic molecules, steroids, bilins, retinoids, lipids, and specific cell surface receptors and form macromolecular complexes. Small extracellular proteins that possess similar properties, such as binding hydrophobic molecules and ligands to specific cell surface receptors, are termed lipocalins. There are 160-180 amino acids in lipocalins, and they usually have a vastly preserved crystal structure (sequence motif) but a low degree of sequence similarity (Newcomer et al., 1984; Virtanen, 2001). Selectivity is determined by the overall size and conformation of the pocket and loop scaffold, as well as by the makeup of its amino acids. The lipocalin fold's structural elements—a sizable cup-shaped cavity inside the β-barrel and a loop scaffold at the entrance—are perfectly suited for the job of ligand binding. This antiparallel beta-barrel has eight strands and an internal ligand binding site. It has a repeating +1 topology. (Cowan et al., 1990).

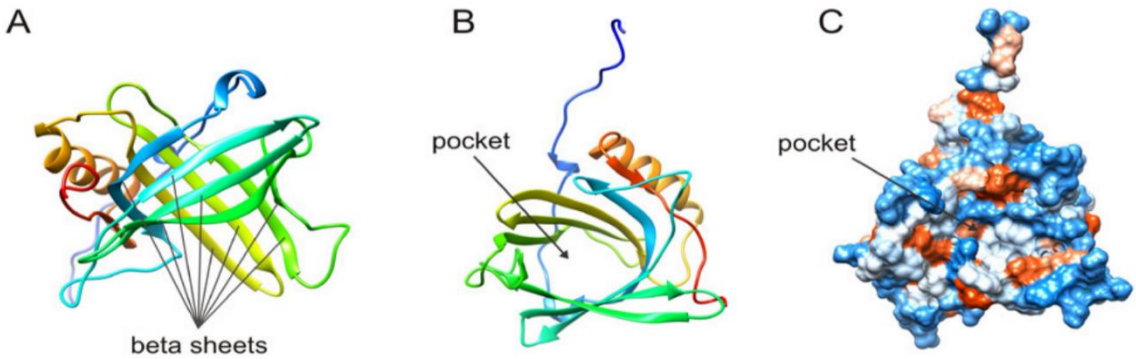

Figure 20: The crystal structures of lipocalin that are highly conserved are made up of an antiparallel β-barrel (A) that is constantly hydrogen-bonded and has eight strands. This barrel defines a calyx shape that indicates the internal ligand binding site (B) and the hydrophobicity surface (C). Using the UCSF Chimera software, which is provided by the University of California, San Francisco's Resource for Biocomputing, Visualization, and Informatics, images

were created from the RCSB PDB database (http://www.rcsb.org) (ID: 1NGL). (supported by NIGMS P41-GM103311) (Coles et al., 1999).

1.15.7. The bioavailability of β-lactoglobulin

Bovine β-lg is the most important protein found in milk's whey. It is commonly found in the milk of animals such as cows, dolphins, baboons, pigs, sheep, horses (Conti et al., 1984), goats, cats (Halliday et al., 1991), buffaloes (Aich et al., 2014), and bison among other species. There is no evidence that it is present in human milk (Sawyer et al., 1999). Normally, it can be found at a concentration of 3 gL^{-1} in milk (Kontopidis et al., 2004). When comparing the sequences of lipocalins, it was found that glycodelin, which is produced in the endometrium of pregnant women, shows the greatest similarity to β-lg (Koistinen et al., 1999; Halttunen et al., 2000). In 1972, Larson reported that only glycodelin was established in human sources. β-lg is produced and secreted from the epithelial cells of the mammary gland under the control of the prolactin hormone (Larson, 1972). This type of transcript is synthesized in the mammary gland, after which it is translated into a later form of mRNA coding for a globin with 180 amino acids (Yoshikawa et al., 1978). This is due to the signal peptide, a highly conserved peptide consisting of 18 amino acids, which precedes the 162 amino acids in the linear chains of β-lg. There are 162 amino acids in this linear peptide chain that are responsible for refolding to the native conformer for the linear peptide. Glycodelin has thus far not been revealed to have distinct functional aspects, but lipocalins are linked to β-lg.

1.16. Structural stability of bovine β-lactoglobulin

1.16.1. Impact of heat-processing on β-lactoglobulin structure

The conformation of bovine β-lactoglobulin changes upon change of pH or heat. The globular native noncovalently bound dimeric structure of β-lactoglobulin can be found to be the most thermodynamically stable structure in milk, and a small fraction of the protein can also be found in metastable partially unfolded monomeric states. As a result of the dissociation of hydrogen bonds in the hydrogen bond network, this relationship may be shifted by heating and other types of processing and conditions (Seo et al., 2010; Kuwata et al., 1999; Crowther et al., 2018). The monomer-dimer equilibrium of β-lactoglobulin is reached at pH 2.5 and 100 mM NaCl. Destabilization and partial unfolding of its globular shape cause residues of histidine, tyrosine, and tryptophan to become exposed to the solvent, increasing the reactivity of buried thiol groups, which causes its initial conformation shift following heating (Kella & Kinsella,

1988). Following these brief and reversible conformational changes, intramolecular interactions break down, and a partially unfolded state known as the "molten globule state" is occupied. This state is also populated when β-lactoglobulin refolds, exposing the protein's buried hydrophobic core and thiol group (Judy and Kishore, 2019; Bhattacharjee et al., 2005). Although temperatures as low as 40°C can cause initial conformational shifts, achieving fully denatured "β-lactoglobulin" requires temperatures higher than 130°C, indicating a multiple-step process. The midpoint of transition between patterns of abrupt large-scale loss of spiral structural elements occurs around 65°C, depending on environmental conditions (Qi et al., 1997).

The partially denatured β-lactoglobulin proteins are prone to thiol/disulfide exchange reactions, which result in covalent aggregation, with non-covalent interactions playing a minor role (Quevedo et al., 2019). It has been observed under low salt, neutral pH conditions a quantitative kinetic model that describes the irreversible aggregation of β-lactoglobulin as a function of thiol/disulfide exchange reactions at 60-75°C (Roefs and De Kruif, 1994) upon heating at that temperature and then with increasing salt levels. This is a result of radical polymerization reactions involving initiation, propagation, and termination steps. These steps correspond to the exposure of a free sulfhydryl group, the exchange of a thiol for a disulfide, and the reaction of two reactive intermediates. In test tube conditions, studies like these have influenced our understanding of how β-lactoglobulin is denatured and aggregated. However, in many cases, these conditions are very different from the complex environment in milk, containing lipids, lactose, and other proteins.

1.16.2. Effect of pH on bovine β-lactoglobulin

Bovine β-lg undergoes a variety of local and global structural changes induced by pH. At neutral pH (pH 7), it is present as a dimer but dissociates into monomeric species with a pH of 2. Between pH 2 and pH 1.5, the protein volume and compressibility increase but decrease sharply below pH 1.5. According to N. Taulier, this transition is difficult to explain as all ionizable groups should have been protonated by pH 2 (Taulier and Chalikian, 2001). So, this transition may be due to the protein undergoing some electrostatically driven structural changes in response to an increased concentration of Cl^- anions. The monomeric population at pH 2 is attributed to the residues of the conformer of β-lg sited in the AB loops.

Specifically, near pH 3, the protein dimerizes with minor alteration in structure, which can be confirmed by the monomer-dimer equilibrium about the dimeric interface (Sakurai and Goto,

2002). It is also found that between pH 4 and pH 5, β-lg undergo the dimer-to-octamer transition as suggested by a variety of biophysical methods, including optical rotation dispersion spectroscopy, ultracentrifugation, electrophoresis, light scattering, and NMR spectroscopy (Gołębiowski et al., 2020). Contrary to these reports, no significant octamerization of the protein was found by N. Taulier around pH 4.5 (Taulier and Chalikia, 2001).

1.16.3. Tanford transition

The protein undergoes multiple conformational changes between pH 6 and 8, which are referred to as the "Tanford transition" (Qin et al., 1998; Sakurai & Goto, 2006). This transition is characterized by the protein expanding. At the atomic level, the molecular underpinning of these conformational alterations in the wild type is still unknown. The Tanford transition, so named because it was initially discovered by Tanford and associates fifty years ago, is the pH-induced transition of β-lg between pH 6 and 8. Alterations in the EF loop shape are found at the protein cavity's open end. Unusual protonation of E89 (pKa = 7.5), which is accessible to solvent at neutral pH and is confined at the EF loop where it forms a hydrogen bond with S116 at acid pH (Qin et al., 1998).

Furthermore, as the EF loop probably controls access to the b-barrel, the Tanford transition is expected to control ligand binding to BLG (Qin et al., 1999). The energetic study indicated that when E89 is protonated and deprotonated, respectively, there are closed and open states present; nevertheless, the conformational transition of opening and closing of the EF loop was not seen by the researchers. Afterwards, Goto et al. used the dimeric BLG mutant A34C to conduct NMR studies at neutral pH in order to study the conformational change from an open to a closed EF loop. Because the monomer-dimer equilibrium of wild-type BLG caused substantial signal widening due to the timescale being comparable (micro- to milliseconds) to that of the NMR studies, preventing NMR measurements, a covalent dimeric A34C mutant was utilized (Sakurai & Goto, 2006). They discovered that the Tanford transition can only take place via a conformational shift between the EF and GH loops before the open to closed BLG state transition, using the dimeric BLG mutant A34C. The EF loop was seen to move in two different ways: slowly in milliseconds or on a slower timeline and quite quickly in the micro-to-millisecond range. These earlier investigations offer important information since they suggest that the dimeric state is a useful paradigm for examining this structural phenomenon. Nonetheless, the primary structural alteration of the protein is the opening of the calyx's interior

above pH 7.5, which is explained by the displacement of the EF loop (Qin et al., 1998). The Tanford transition is believed to be initiated by the protonation of this residue. Tanford transition and the opening of the EF loop, which is closed below pH 6.2 and opens above pH 7.1, cause the protein molecule's volume to expand. As a result, the carboxyl group of Glu89, which has been buried and has an unusually high pKa value up until this point, becomes accessible to the solvent (Kontopidis et al., 2004).

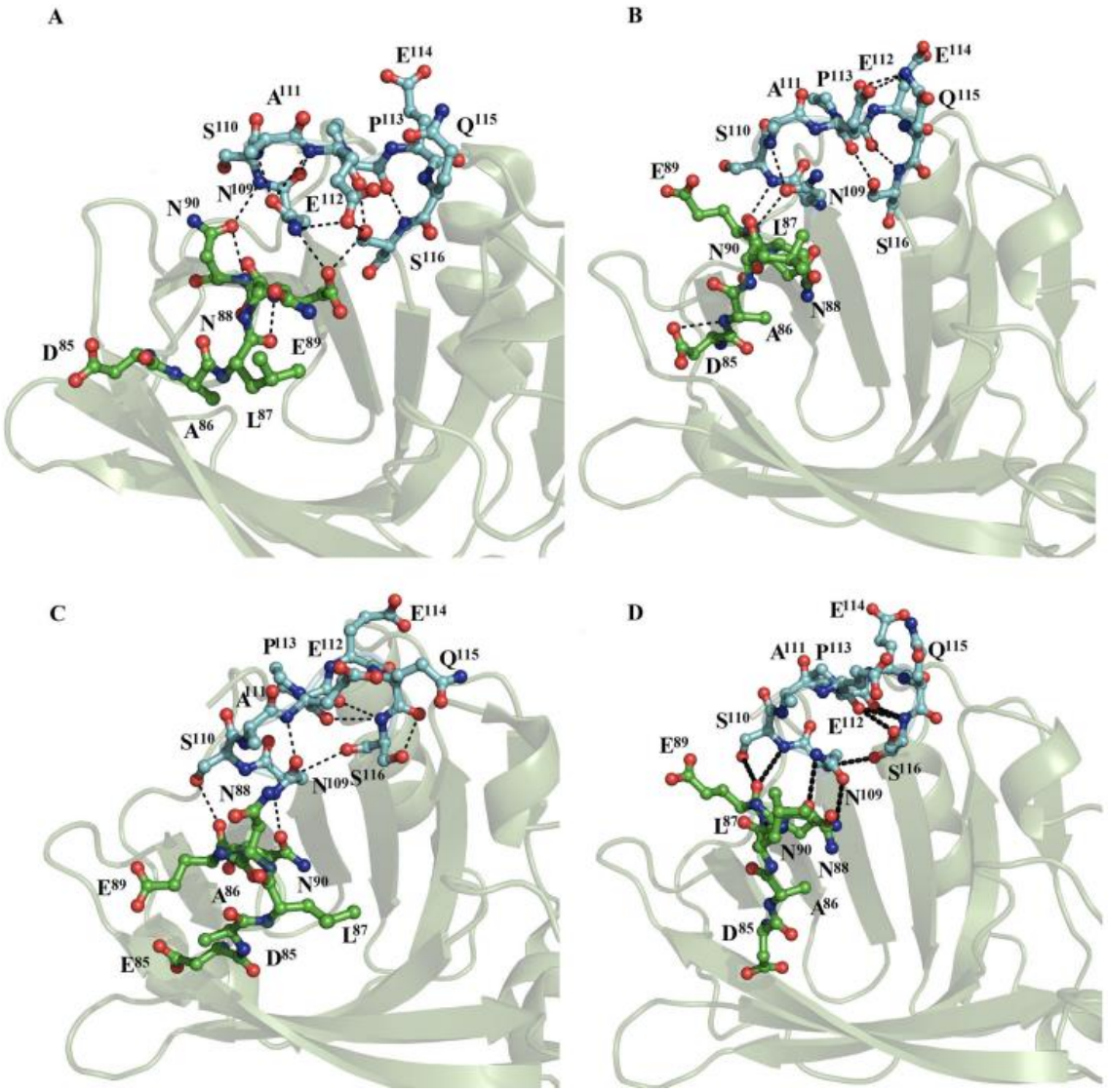

Figure 21: BLG crystal structures solved at pH values of 6.2, 7.1, 7.5, and 8.2. Structure of crystals at pH values of 6.2 (A), 7.1 (B), 7.5 (C), and 8.2 (D). The Tanford transition between the EF (green ball-and-stick representations) and GH loops (green ball-and-stick representations) is explained by structural differences.

At low pH, loop EF serves as a door or lid to block access to the calyx. Tanford transition involves the alterations in the secondary and in the local microenvironment of aromatic

residues of β-lg, with these alterations being rather local and causing no global change in protein conformation global change in protein conformation.

1.16.4. Effect of osmolytes

The majority of osmotically active solutes, known as osmolytes (or osmoprotectants), are small organic molecules that are accumulated by many cells and organisms to protect against internal or external osmotic stresses, such as high concentrations of protein denaturants, freezing, dehydration, temperature fluctuations, variable pH, and high salinity (Yancey et al., 1979). These osmolytes are classified as follows: free amino acids and their derivatives (proline, taurine, and b-alanine); polyhydric alcohols (polyols), such as trehalose, glycerol, and sucrose; and By stabilizing macromolecules, organic osmolytes like sugar and polyols are known to play a significant role in stress prevention. Because of their effect on proteins' thermodynamic stability in the face of chemical or thermal denaturation, osmolytes function as protein stabilizers (Sharma et al., 2021). Natural osmolytes actively participate in the folding of proteins in addition to serving as Osmo protectants. Comparing osmolytes to denaturants, it has been demonstrated that glycine, N-methylglycine (sarcosine), N trimethylglycine (betaine), trimethylamine N-oxide (TMAO), and myo-inositol double protein stability (Rabbani and Choi, 2018). Sarcosine, betaine, and TMAO interact negatively with the unfolded state as protective osmolytes, giving the folded state some relative stability.

1.16.5. Effect of chemical denaturants on bovine β-lactoglobulin

Alcohols, particularly 2,2,2-trifluoroethanol (TFE), Urea, 1,3- dimethylurea, 1,3-diethylurea, guanidinum thiocyanate (Gdn. SCN) and Guanidinium chloride (Gdn.HCl) are commonly used as denaturants to denature the β-lg by increasing amount of a-helical secondary structure than native β-lg. Alcohols that impair hydrophobic contacts and improve the helical propensity, like TFE, may disturb this equilibrium (Vincenzi et al., 2019). At both acidic and neutral pH levels, TFE at greater protein concentrations (5% v/v and 8% v/w, respectively) can cause fibrillar aggregation and gel formation of bovine β-lg.

In addition, urea combines with proteins to generate hydrogen bonds with their backbone. The unfolding of the protein results from a decrease in the strength of the hydrophobic effect (Su and Dias, 2017). First described as a two-stage process, urea accelerates the unfolding of bovine β-lg at acidic pH (Báez et al., 2011). A two-state transition between a folded protein and an unfolded state was also brought about by urea at pH 2.1 through the coordinated unfolding of the main α-helix's C-terminus and b-barrel. Because they attach inside the calyx, anionic

amphiphiles, sodium dodecyl sulfate (SDS), or palmitate prevent β-lg from unfolding when exposed to urea.

Guanidinium chloride is a commonly used denaturant in protein studies. Often, guanidinium chloride is used instead of urea in protein stability studies. Typically, GdmCl is fully dissociated at neutral pH or acidic pH. At low concentrations of GdmCl (<~1 M), chloride ions screen electrostatic repulsion between positively charged protein groups. Because GdmCl has extra electrostatic interactions compared to neutral urea, it can stabilize and destabilize protein structure depending on its concentration (Hagihara et al., 1993). It disrupts proteins' secondary and tertiary structures, leading to their unfolding and aggregation. The impact of guanidinium chloride on the β-Lactoglobulin structure has been extensively studied. When β-Lactoglobulin is exposed to guanidinium chloride, the hydrogen bonds and hydrophobic interactions that stabilize its native structure are disrupted. As a result, the protein undergoes a conformational transition, unfolding and exposing its hydrophobic regions. The unfolding process leads to the formation of non-native structures, such as aggregates. D'Alfonso et al. have compared the denaturation of bovine β-lg B with both GdmCl and urea between pH 2 and pH 8, as monitored by CD, UV differential absorption, and fluorescence measurements (D'Alfonso et al., 2002).

The GdmCl-induced unfolding intermediate of bovine β-lg A at pH 2 has been reported to have increased α-helical structure (Dar et al., 2007). The exposure of hydrophobic regions due to the unfolding of β-Lactoglobulin upon guanidinium chloride treatment leads to significant changes in its surface properties. The protein's surface becomes more hydrophilic, resulting in increased affinity for water molecules and hydrogen bonds with water. These changes in the surface properties can affect interactions with other molecules, such as antibodies or enzymes.

Hattori et al. reported unfolding/refolding studies on bovine β-lg with monoclonal antibodies as Probes and concluded that renatured β-lg molecules as a stable form unfolded in specific regions (Hattori et al., 1993). The two-step thermal denaturation process of β-lg was further investigated by J. A. Seo et al. in 20-100 °C temperature range by Raman Spectroscopy. According to Seo et al. (2011), there are two distinct steps in the process: the first involves the dissociation of dimers, which is linked to an increase in tertiary structure flexibility. In the second step, significant conformational changes are observed in the secondary structure, which are characterized by the loss of α-helix structures and the concurrent formation of β-sheets. (Seo et al., 2011).

1.16.6. Effect of surfactant

Surfactants help to solubilize insoluble proteins in water; they are also used to determine the molecular weight of proteins (SDS-polyacrylamide gel electrophoresis). Surfactants also denature native proteins. Kerstens et al. investigated the binding of cetyltrimethyl ammonium bromide (CTAB) with β-lg. The binding occurs in two or three distinct stages, depending on the overall structure of the β-lg molecules. Perfluorooctanoate (PFOA), a perfluorinated surfactant, upon interaction with β-lg, decreases its thermal stability in aqueous solutions and denature the native protein (Kerstens et al., 2006). The neutron reflectivity of β-lg films adsorbed at the air-water interface in the presence of nonionic surfactant hexaoxyethy lene dodecylether (C12E6) in a concentration-dependent manner is measured by Horne et al. (Horne et al., 1998) The anionic sodium n-alkyl sulfate, sodium dodecanoate (SDD), cationic n-alkyl trimethyl ammonium chloride, non-ionic n-alkyl maltopyranoside (alkyl length n differs from C8 to C14) surfactants interact with bovine β-lg and modulate the conformational propensity in a concentration dependant manner. This may be attributed to the length of the alkyl chain, which greatly affects the strength of interactions between surfactants and proteins. The effect of model anionic surfactants such as sodium dodecyl sulfate (SDS) on the conformational changes of β-lactoglobulin is discussed in terms of the ionic charge arising for protein pH ranging from 2.0 to 5.8 at high temperature (Viseu et al., 2007).

1.16.7. Effect of pressure on bovine β-lactoglobulin

β-lg is the most susceptible to pressure-induced change than other major whey proteins. Perhaps this is due to the relatively inefficient packing caused by the large solvent-exposed hydrophobic pocket and the lower number of disulfide bonds (two versus four in, for example, the similar-sized a-lactalbumin). It has been reported that bovine β-lg has a reduced molar volume at pressures as low as 10 MPa, possibly because the calyx has contracted (Hinnenkamp, 2020). According to several studies, β-lg becomes more susceptible to enzymatic cleavage when under pressure, possibly due to pressure-induced conformational changes (Carullo et al., 2020). β-lg's tertiary and quaternary structure is irreversibly altered by pressures greater than 300 MPa. When β-Lg was exposed to pressures as high as 900 MPa at neutral pH, CD and fluorescence spectroscopy showed that pressure causes monomer formation with subsequent aggregation but only small irreversible effects on its tertiary structure (Edwards and Jameson, 2020).

During enzymatic proteolysis, β-lg is less susceptible to pressure-induced changes at acidic pH, but pressure-induced changes in proteinases, thermolysin, and pepsin may confound this. However, NMR measurements of monomeric β-lg at pH 2 while under the pressure of up to 200 MPa have revealed that the two sheets unfold independently to produce two intermediate states of unfolded β-lg that are still characterized by significant secondary structure (Edwards and Jameson, 2020). At neutral pH and ambient temperature, a three-step mechanism has been proposed that during β-lg denaturation, the calyx collapses when the pressure is 50 MPa (resulting in a reduction of ligand-binding capacity) along with Cys121 exposure. At 200 MPa, further (partially reversible) disruption of the hydrophobic structure occurs, accompanied by a decrease in the molecular volume. When pressure is increased, disulfide interchange reactions take place irreversibly, causing aggregation reactions (Nagy, 2013).

1.16.8. Effect of co-solvents

A cosolvent immiscible with a mixture increases the solvent power of the primary substance in the mixture. Generally, Protein stability is enhanced by cosolvents such as glycerol, trehalose, sucrose, glucose, and stachyose. It is found that trehalose induces remarkable stability of β-lg against chemical denaturation by guanidinium chloride (Gdn.HCl) (D'alfonso et al., 2003).

According to Maity et al. (2016), β-lactoglobulin can fold and self-assemble from a reversible unfolded state at pH 10.5 when methanol, 2-propanol, t-butanol, and 2,2,2-trifluoroethanol (TFE) are present (Maity et al., 2016). The following order describes the degree of secondary and tertiary structure formation: methanol < 2-propanol < t-butanol < TFE. Because the hydrophobic core of the protein molecules is exposed in the apolar environment of TFE, a higher order intermolecular cluster is produced. While isopropanol and t-butanol favor the creation of the β-structure, which leads to aggregation at greater concentrations, methanol and TFE induce aggregation through the α-helical structure.

When cosolvents such as sorbitol, glycerol, and sucrose are added to β-lg, they include hydrogen bonds; this process causes preferential hydration of the protein, which is the exclusion of cosolvent molecules from the protein surface, and alters the thermodynamic properties of proteins with longer thermal stability.

1.16.9. Immobilization

Immobilization is a physical method that involves the attachment of β-lg to a support material, such as a matrix or nanoparticles. This attachment can be achieved through various techniques such as covalent bonding, electrostatic interactions, or encapsulation. Immobilization methods vary depending on the desired modification. Covalent attachment involves chemically modifying the protein's surface, while electrostatic interactions involve the use of charged matrices or nanoparticles. Encapsulation involves the entrapment of β-lg within a matrix or nanoparticles.

Zinc ion binding to β-lg is a heterogeneous process with three main stages, as revealed by the nature of the binding/immobilization process. The first stage was linked to the fast sorption of zinc ions on the micelle surface of β-lg, whereas stages two and three were the consequence of intramolecular diffusion of zinc ions. Furthermore, it was demonstrated through experimental and stability studies that aromatic (Tyr, Trp, Phe) and acidic (Glu, Asp) amino acid groups contribute to the production of Zn-β-lg complex, a metal complex with potential applications in nutraceuticals (Buszewsky et al., 2020).

1.16.10. The effect of chemical modification

A chemical modification is the process of chemically reacting a protein with chemical reagents. During this process, specific amino acid residue side chains are covalently grafted with modifying agents of interest. During chemical modification, the goal is to understand the "relative reactivity of side chain groups, to quantify amino acids individually, and to develop affinity reagents, mechanism-based reagents for pharmaceutical use, cross-linking reagents, bioprostheses techniques, blocking reagents for peptide synthesis, and cleavage reagents (Feeny et al., 1987). In addition to primary structural analysis, specific amino acid residues' contribution to the tertiary and secondary structural components has also been studied. Several chemical transformations available for selective modification of proteins include the studies of protein-protein interaction, protein-ligand interactions, processing of bio-conjugates, and protein micro-arrays (Baslé et al., 2010). Side chain residues of asparagine, cysteine, glutamine, histidine, lysine, tryptophan, and tyrosine have been modified chemically in different proteins for several purposes. Modifications of β-lg serve the purpose of “structural biology” as a model protein and have a direct significant approach in the “protein chemistry” field. Another point for the β-lg-derivatives is related to the developments in the design of

therapeutics and toward the selective manipulation of bio-materials of precise uses. The different modifying agents for β-lg's modification have been discussed below briefly.

1.16.11. Alkylation/Acylation

Recent progress in the structure-activity relationship (SAR) of small proteins interacting with ligands/small organic molecules has shed a new light on the molecules of β-lg. Modifying β-lg by chemical means or enzyme may induce conformational change and binding properties (Zheng et al., 2016).

The adsorption behavior of lysine-modified β-lg by acetylation and succinylation has been extensively studied in air-water and alumina-water interfaces. These results imply that the electrostatic forces manipulated after modification play a key role in the aggregation/dissociation properties of β-lg. The aggregation behavior was also studied in other protein systems, Concanavalin A, after succinylation, where the succinyl derivatives were reluctant to participate in aggregation and fibril formation (Vetri et al., 2005). Results from other groups of researchers showed that the succinylation of lysine residues exploited as an indirect proof of £-amino groups of some specific lysine residues are likely to be the binding sites of β-lg in the activation of β-galactosidase activity (Del Moral-ramirez et al., 2008). Modification of lysines and glutamines of β-lg with transglutaminase from Streptoverticillium mobaraense (MTgase) can be exploited for several physicochemical processes such as surface tension, viscosity, etc. Earlier, it was said that the importance of chemical modification is associated with improvements in the design of therapeutic agents (Boutureira and Bernard, 2015). Recent reports suggest that modified β-lg, acetylation, succinylation, and/or hydroxy pthalylation in the lysine residues shows a great extent of anti-viral activities. On the other hand, fine-stranded, transparent gels were formed at pH away from the isoelectric point and low ionic strength (Arnaudov et al., 2003).

1.16.12. Glycosylation

The glycosylation technique is a well-accepted phenomenon in the field of chemical modification of β-lg. In this process, carbohydrates, such as glucose, maltose, lactose, gluconic acid, etc., are covalently linked to β-lg and alter many physio-chemical properties of the protein. The effects of glycosylation/ maltosylation greatly affect the properties like hydrophobicity, viscosity, and fluorescence properties of modified protein (Waniska et al., 1984). The synthetic glycoproteins showed higher solubility and heat stability at isoelectric pH and lower ionic strength with increasing glycosylation (Zhang et al., 2019). Changes in β-lg

glycation with lactose in powdered form and aqueous solution affected the association behavior of the multi-step denaturation and aggregation process of β-lg. The dimer interface of β-lg (AB loop, GH loop, P-strand "I," and helix part) that was involved in non-covalent interaction was characterized by means of immunochemical method after glycosylation (Morgan et al., 1999). The properties like antigenicity and immunogenicity of β-lg were also reduced by glycosylation (Yuan et al., 2018). Besides all, recent work shows that the enzymatic activity of β-galactosidase was very likely to be affected when the lysine group of β-lg was modified by lactose and was concluded into the significance of lysine e-amino groups on its activating effect of the enzyme (Del Moral-Ramirez et al., 2008).

1.16.13. Free thiol modification

Cysteine is the most closely targeted residue for amino acid modification in the protein structure with chemical reagents. Free thiol of bovine β-lg at Cysl21 of β-H strand is completely buried under the C-terminal α-helix and has been targeted both in native and denaturing conditions with several cysteine specific reagents such as Dithioerythritol (DTT); 5,5‟-dithiobis (2-nitrobenzoic acid) (DTNB) or 4,4‟-dithiopyridine; 2-mercaptoethanol (MCE); mercapto-propanoic acid and other fluorophore tagged maleimide derivatives for different structural elucidation purposes (Le Maux et al., 2014). As the free thiol is very much susceptible to involve in disulfide-linked oligomerization/aggregation pathways of heat treated β-lg, different thiol modifying agents have been employed to trace its specific role in the aggregation process as well as to insight the conformation and stability of the pristine protein (Sakai et al., 2000).

1.16.14. Methionine modification

One of the most oxidation-prone amino acids is methionine (Met). It can be transformed into derivatives of methionine sulfoxide or sulfone through a variety of processes, including UV exposure, metal-catalyzed reactions, and hydrogen peroxide treatment. The impact of oxidation caused by t-butyl hydroperoxide (tBHP) on the structure, compactness, and fibrillation tendency of β-lg at physiological pH was examined by Sanhita et al. The structural orientation of β-lg is impacted by t-BHP-induced selective Met oxidation, which changes the protein's internal polarity and decreases its susceptibility to thermal instability. This causes the introduction of an internal strain (Maity et al., 2021).

1.16.15. Esterification

As the amount of ionizable carboxyl groups decreases, proteins that have undergone esterification acquire a greater positive charge. Moderate esterification of β-lg results in minor modifications to both its secondary and tertiary structures. As a result, the β-lg molecule opens, causing the peptide link to break. Because 22 more pepsin cleavage sites introduce esterification, esterified β-lg is more susceptible to hydrolysis by pepsin (Chobert, 2012). Changes in the imposed tertiary structure cause the exposing of 14 pepsin-specific cleavage sites. Pepsin recognizes eight of the novel cleavage sites as esterified carboxylates. According to M. I. Halpin, the methyl-, ethyl-, and butyl-esters of β-lg exhibited increased surface activity and hydrophobic probe binding activity, with the methyl esters showing the most effect (Halpin et al., 1985). because the protein molecules' positive charges allow them to interact with viral proteins or DNA, influencing the transcription, translation, and replication of viruses and, ultimately, their contagiousness. At pH 7, highly esterified β-lg demonstrated DNA-binding abilities similar to natural basic proteins like histones and lysozymes. β-lg's antiviral activity against the HSV-1 virus, the influenza virus A subtype H1N1, and the avian influenza A virus (H5N1) was boosted by esterification. Esterified β-lg peptic hydrolyzates also showed antiviral properties (Sitohy et al., 2007).

1.16.16. Modification by physical methods

The structure and stability of β-lg can also be altered by physical factors such as electrolysis, high hydrostatic pressure, UV, gamma, and ultrasound radiation. The β-lg forms that were subjected to the sonication method exhibited greater hydrophobic surfaces compared to their native form, which made them more amenable to phenol oxidase cross-linking. The ability of β-lg to bind to IgE in vitro and in vivo was hardly affected by sonication (Zhang et al., 2021). According to Stanic-Vucinic et al. (2013), ultrasound-mediated glycation in the Maillard reaction demonstrated superior reducing power, a higher ferrous ion-chelating activity, and the ability to scavenge radicals.

The ordered structure of β-lg is disrupted, and the molecule size distribution is altered by UV exposure. This resulted in modifications to the antigenicity of β-lg and changed the way that β-lg regulated the generation of immunoglobulins. After being exposed to UV light for 24 hours, it was discovered that 18.8% of the protein had become denatured and that some of it had begun to aggregate, which had changed the protein's secondary structure. Jia et al. (2019) have shown a drop in the overall number of sulfhydryl groups during the photo-oxidation process, accompanied by an increase in the number of exposed sulfhydryl groups.

The γ-irradiation-induced modifications to the secondary and tertiary structures of β-lg are comparable to those seen in mildly thermally treated β-lg. Both modifications lead to an increase in the agglomeration and a decrease in the protein's solubility. Although γ-radiation up to a dose level of 10 kGy decreased the solubility and enhanced the antigenicity of β-lg, it had no effect on its molecular-weight distribution (Kaddouri et al., 2008).

Only dimers and trimers developed as a result of the SH/S–S interaction in the β-lg aggregation generated by high hydrostatic pressure (HHP) (Reznikov et al., 2011). The thiol group buried inside the native globule became more reactive as a result of the high-pressure denaturation of β-lg. The thiol group's exposure to the protein surface was the cause of this. Various enzymes were able to hydrolyze β-lg more effectively due to the increased hydrostatic pressure (Bamdad et al., 2017).

When high-intensity PEF was applied to β-lg, the protein was partially denatured and aggregated, resulting in covalent cross-linking. The PEF treatment raised β-lg's gelation rate and thermal stability by 4 to 5 °C (Perez et al., 2004). Following electrolysis treatment, there was a noticeable reduction in the allergenic characteristics of β-lg on the cathode. This was explained by the allergenic peptides being dislocated from the protein surface (Matsumoto et al., 2011).

1.16.17. Enzymatic modifications

Enzymes provide numerous advantages, including the capacity to make alterations under physiological conditions with great specificity and without undesirable side effects. One such enzyme is transglutaminase (TG), which enables the cross-linking of proteins. TG triggers an acyl group transfer between the ε-amino group of lysine residues and the γ-carboxamide group of glutaminyl residues in proteins, creating an iso-peptide bond. When treated with excess TG, β-lg's thermostability improves, possibly due to the protein molecule's partial unfolding and subsequent conformational rearrangement (Tang et al., 2007).

The use of laccase in protein cross-linking relies on the availability of phenolic moieties in proteins, which are typically scarce. Laccase formed irreducible intermolecular cross-links in β-lg and caused oxidative modifications, including dityrosine formation, fluorescent tryptophan oxidation product formation, and the creation of carbonyl derivatives of histidine, tryptophan, and methionine, resulting in protein molecules with heightened surface tension (Steffensen et al., 2008).

Research by Thalmann et al. suggests that only Agaricus bisporus tyrosinase, when accompanied by a low molecular weight phenolic compound as a bridging agent between protein subunits, can cross-link β-lg (Thalmann et al., 2002). Enzymatic hydrolysis of β-lg under HHP yields more short bioactive peptides with potential antioxidant and anti-inflammatory effects (Bamdad et al., 2017).

1.17. Biological functions of β-lg

β-lg is the most abundant protein found in cow's milk. It is responsible for a significant portion of the total protein content of milk, accounting for approximately 25%. β-lg is known for its high nutritional value and is an excellent source of essential amino acids, making it an important component of infant formulas.

β-lg has also been investigated as a drug delivery carrier, particularly for oral administration. Its ability to bind and transport drugs within the digestive system makes it an attractive candidate for drug delivery applications. β-lg has been shown to enhance the stability of drugs and reduce their degradation, allowing for better absorption and improved therapeutic outcomes.

Vitamin A (retinol) is bound by it in a hydrophobic pocket, shielded from oxidation, and transported from the stomach to the small intestine, where it binds to a retinol-binding protein that resembles β-Lg. The mechanism of retinol's transfer from the milk's fat globule core to β-Lg and the reasons for certain species' absence of this protein are unknown. The fact that β-Lg can bind retinol may be coincidental because it may bind a variety of hydrophobic compounds. β-Lg belongs to the family of lipocalins, which are all capable of binding (Goulding et al., 2020).

It can bind with tri-glycerides and transport other small and long-chain hydrophobic molecules (Mansouri et al., 1998; Sawyer et al., 2000).

The hydrolyzed peptides are also believed to enhance passive immunity in infants. β-lg participates in the removal of harmful organisms from the neonatal after attaching to the gut wall. β-lg acts as a transporter of small, sparingly soluble molecules such as retinol or long-chain fatty acids and vitamin D (Kontopidis et al., 2004), but species distribution and variation in binding profile do not all fit with such a role. This has been supported by evidence that β-lg has been isolated with free fatty acids, mainly palmitic acid and oleic acids, from fresh milk (Le Maux et al., 2014). So, β-lg shows a wide variety of functions, most of which involve some ligand-binding function.

1.18. Aggregation of β-lactoglobulin

Thermal aggregation is a crucial phenomenon in protein science and engineering, yet the exact mechanisms by which protein aggregates form and their biological significance remain unclear. Unfolding and aggregation are two distinct processes, with unfolding involving successive unimolecular reactions, while aggregation is a bimolecular second-order reaction. Notably, temperature, pH, protein concentration, and ionic strength affect the two reactions differently (Mounsey et al., 2009). Of particular interest are proteins such as α-lactoglobulin and β-lactalbumin found in milk serum, which are sensitive to heating between 60-100 degrees Celsius. Heating leads to denaturation, aggregation, and intramolecular reactions. During dairy processing, heating results in a conformational change in β-lg. Additionally, partial unfolding of polypeptide chains also leads to aggregation. Despite extensive research on the subject, the lack of a clear physical picture and precise knowledge of the mechanisms involved have resulted in heuristic approaches being widely used. At room temperature and physiological pH, β-lg exists mainly as a dimer, with the monomers noncovalently linked. However, at elevated temperatures, β-lg dissociates into monomers, which is a necessary step in the heat-induced aggregation mechanism. Further heating (above 50°C) results in the protein undergoing a conformational change, exposing previously buried hydrophobic groups and thiol groups. This state is referred to as a "molten globule state" due to the retention of the nativelike backbone secondary structure. In the molten-globule state, hydrophobic interactions can cause protein molecules to aggregate. Roefs and de Kruif proposed an analogous polymerization mechanism via thiol catalysts for β-lg heated at 65°C with neutral pH and low ionic strength. A progressive loss of β-sheet structure was observed with increasing temperature, while an abrupt loss of the helical conformation was detected near 65ºC (Roefs and de Kruif et al., 1994).

According to Jung et al. (2008), β-lg partially denatures and aggregates when the temperature rises above 70ºC. If the protein concentration is below the critical gelation concentration, this results in the formation of soluble aggregates, and if it is above, it forms a continuous network known as gel (Jung et al., 2008). Noncovalent interactions become increasingly important at temperatures above 80ºC, and the aggregation process is dominated by both interchange of disulphide bonds and hydrophobic interactions. The kinetics of protein denaturation/aggregation are governed by various factors, including the heating conditions, temperature, time, chemical environment, protein concentration, pH, ionic strength, calcium, and lactose concentrations. Kinetic experiments using ^{1}H NMR at 70°C suggest that the folded form unfolds within several minutes, while subsequent aggregation and gel formation from the unfolded form is a slow process that takes several hours. The thermally induced aggregation

pathway of β-lg appears to proceed through a series of steps involving quaternary, tertiary, and secondary structural changes. Vetri et al. reported that conformational changes expose and/or cover specific residues and hydrophobic regions that play a critical role in the process, resulting in aggregates with different structures, even at the secondary and tertiary levels. At 70°C and 90°C, protein conformations form nuclei by adding partially and/or fully unfolded monomers, forming spherical aggregates (Vetri et al., 2005).

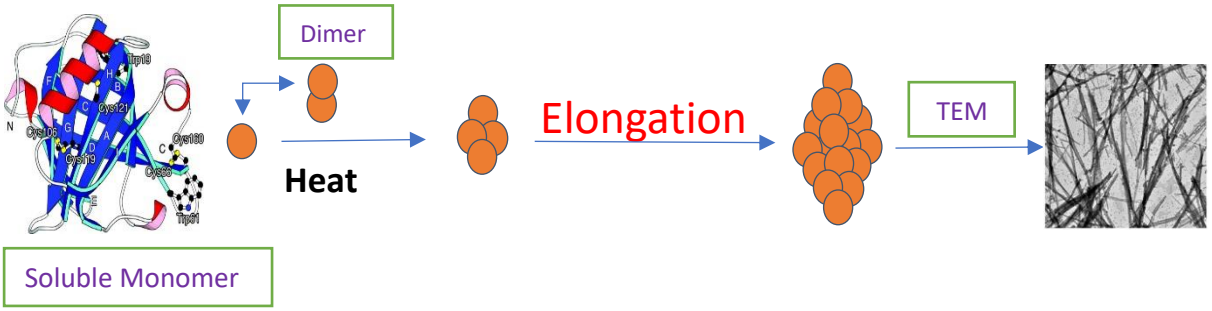

Figure 22: Schematic representation: Aggregation occurs when complementary hydrophobic surfaces interact again through intermolecular interaction. The common intermediate in folding and aggregation can be seen.

Protein aggregation is a complex phenomenon that is influenced by various factors, including protein concentration, temperature, and pH. At a pH close to the isoelectric pH (IEP), the frequency of disulfide bond interchange is reduced, and the aggregation process is dominated by electrostatic attractions and hydrophobic interactions (Krebs et al., 2009). In contrast, at a pH below the IEP, i.e., pH 2, the formation of covalent bonds is inhibited due to the low reactivity of the sulfhydric group, and noncovalent interactions, such as ionic, dipole, van der Waals, and hydrophobic interactions, result in the formation of aggregates.

The denaturation and aggregation of β-lg protein follow a radical-addition polymerization reaction at near-neutral pH, with the free thiol group of β-lg acting as the radical. The optimal pH range for maximum aggregation rates has been reported to be between 4.3 and 4.8. Additionally, the structural changes in the folding of alkaline β-lg are influenced by the presence of non-fluorinated alcohols MeOH, i-PrOH, t-BuOH, and a fluorinated alcohol, 2,2,2-trifluoroethanol (TFE). TFE favors intermolecular hydrogen bonding at lower concentrations, while t-BuOH induces secondary and tertiary structures. Both fluorinated and non-fluorinated alcohols accelerate the formation of non-native secondary structures, leading to protein self-assembly. Intriguingly, only α-helical structure formation induces β-lg aggregation when TFE is present (Maity et al., 2016).

Protein aggregates can have widely varying structures, ranging from densely branched clusters to rigid rods. Thermal incubation of β-lg aqueous dispersions at increasing pH from 2.0 to 5.8 to 7.0 results in rod-like aggregates, spherical aggregates, and worm-like primary aggregates, respectively (Jung et al., 2008). Protein aggregates categorized as amyloid-like are characterized by varying size and flexibility depending on the assembly process. Shorter and more flexible amyloid-like aggregates typically form when molecules are assembled quickly and less precisely due to low repulsion force, high concentration, or the presence of a solvent. Destabilizing factors, such as high temperatures, zinc, solvent, hydrolysis, interfaces, or oxidation, generally accelerate the aggregation process, while stabilizing factors, such as glycerol, or hindering factors, such as phenolic compounds or sugars, slow it down. Therefore, understanding the various factors that influence protein aggregation is crucial for developing effective strategies to prevent or control protein aggregation (Hoppenreijs et al., 2022).

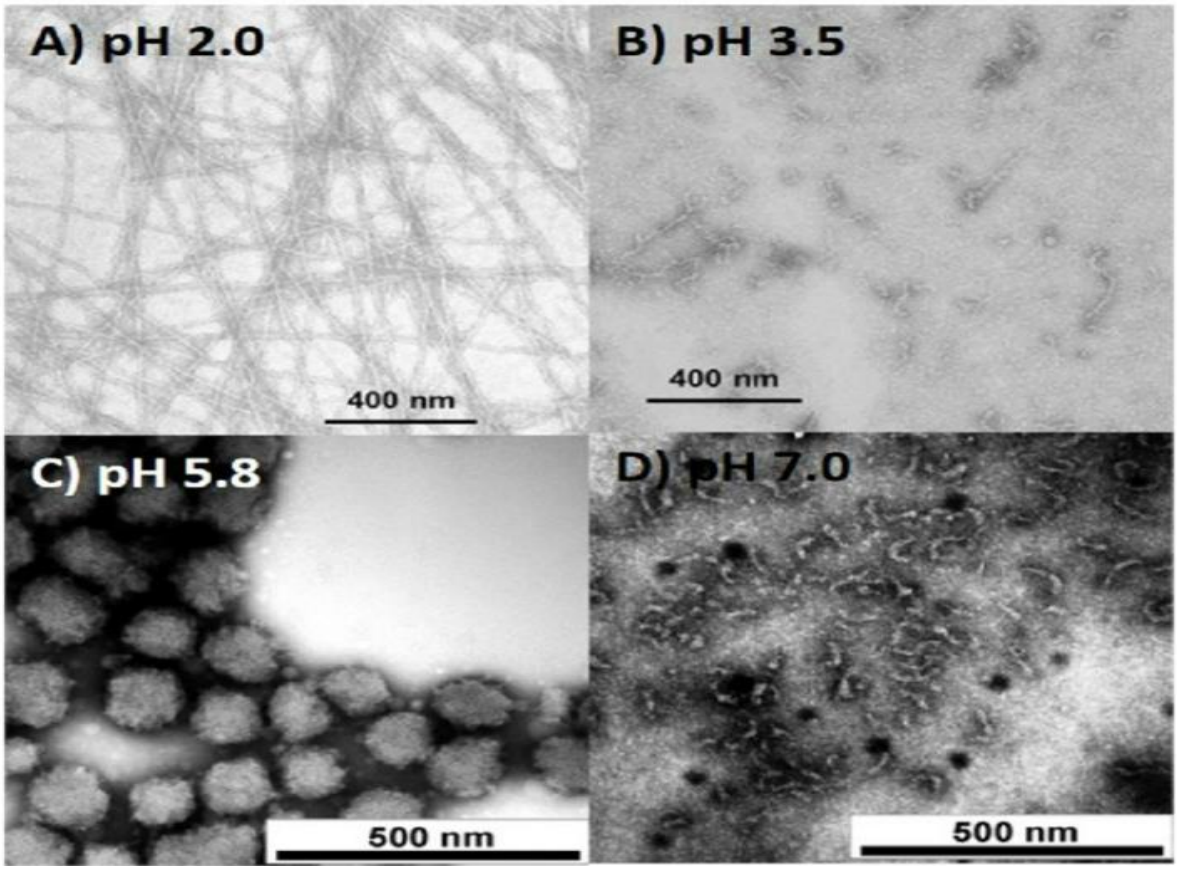

Figure 23: TEM images of BLG aggregates prepared at (A) pH 2.0 and (B) pH 3.5 (both 2.5% β-lg at 90ºC for 5 h, from Keppler et al. (2019), and (C) pH 5.8 and (D) pH 7.0 (both 1.0% β-lg at 85ºC for 15 min, from Jung et al. (2008).

1.19. Amyloid fibril formation by β-lactoglobulin

Certain aggregates, known as amyloid fibrils, are created when partially or fully unfolded proteins or peptides bind together. These fibrils have a cross-β structure, which is an organized and repeating molecular architecture. In this structure, a prolonged, intermolecular β-sheet with a parallel or antiparallel arrangement is formed by the association of β-strands from different protein or peptide chains (Baldassarre et al., 2016). According to Ma et al. (2013), there is a lag time for the nucleation (creation of stable nuclei) and an apparent rate constant for the elongation (growing of fibrils) phases of the fibrillation process at neutral pH (pH 7.0) (Ma et al., 2013). Heating at low pH does not promote disulfide bonding between β-lg molecules as cysteine residues become protonated. Prolonged heating (20 h) at 85ºC and pH 2 causes several chemical modifications to amino acid side chains, but no covalent crosslinking occurs. Hydrolysis of peptide bonds can occur at low pH and high temperature. Heat-denatured β-lg fibrils at pH 2 assume a multistranded helical shape with twisted ribbon-like structures. Amyloidal aggregation cannot be stopped by strong repulsive electrostatic forces or low ionic strength; rather, aggregation at pH 2 requires the presence of a strong, energetic driving force (Akkermans et al., 2013). One proposed explanation for the attractive forces that cause aggregation is the amphoteric nature of the protein fibrils. Periodically spaced neutral residues along the fibrils' contour length can encourage potent, alluring "hydrophobic" interactions. A considerable population of unfolded or partially unfolded molecules is necessary for the development of fibrils of β-lg, although circumstances that substantially disrupt intermolecular connections must also be avoided. At pH 1.6, β-lg amyloid fibrils have spherulite structures. At neutral pH, macromolecular crowding agents such as polyethylene glycols (PEG) and Dextran 70 can efficiently hasten the fibril production of β-lg (Ma et al., 2013). According to Navarra et al. (2014), β-lactoglobulin can be efficiently induced to aggregate when exposed to heat by use of metal ions like copper and zinc ions (Navarra et al., 2014).

1.20. References

Achari, A.E. and Jain, S.K., 2017. l-Cysteine supplementation increases insulin sensitivity mediated by upregulation of GSH and adiponectin in high glucose treated 3T3-L1 adipocytes. Archives of biochemistry and biophysics, 630, pp.54-65.

Ahern, T.J. and Manning, M.C., 1992. Stability of protein pharmaceuticals. Part A. Chemical and physical pathways of protein degradation. Pharmaceutical Biotechnology Series, 2.

Aich, R., Batabyal, S. and Joardar, S.N., 2014. Simple purification method for betalactoglobulin from buffalo milk. Adv. Anim. Vet. Sci, 2(2), pp.78-80.

Aich, R., Batabyal, S. and Joardar, S.N., 2015. Isolation and purification of beta-lactoglobulin from cow milk. Veterinary World, 8(5), p.621.

Akbay, E., Tıras, M.B., Yetkin, I., Törüner, F.Ü.S.U.N., Ersoy, R., Uysal, S. and Ayvaz, G., 2003. Insulin secretion and insulin sensitivity in normal pregnancy and gestational diabetes mellitus. Gynecological endocrinology, 17(2), pp.137-142.

Akkermans, C., Venema, P., van der Goot, A.J., Boom, R.M. and van der Linden, E., 2008. Enzyme-induced formation of β-lactoglobulin fibrils by AspN endoproteinase. Food Biophysics, 3, pp.390-394.

Alam, P., Beg, A.Z., Siddiqi, M.K., Chaturvedi, S.K., Rajpoot, R.K., Ajmal, M.R., Zaman, M., Abdelhameed, A.S. and Khan, R.H., 2017. Ascorbic acid inhibits human insulin aggregation and protects against amyloid induced cytotoxicity. Archives of biochemistry and biophysics, 621, pp.54-62.

Amaral, M.D. and Kunzelmann, K., 2007. Molecular targeting of CFTR as a therapeutic approach to cystic fibrosis. Trends in pharmacological sciences, 28(7), pp.334-341.

Ando, T., Uchihashi, T., Kodera, N., Yamamoto, D., Miyagi, A., Taniguchi, M. and Yamashita, H., 2008. High-speed AFM and nano-visualization of biomolecular processes. PflügersArchiv-European Journal of Physiology, 456, pp.211-225.

Andrews, J.M. and Roberts, C.J., 2007. A Lumry− Eyring nucleated polymerization model of protein aggregation kinetics: 1. Aggregation with pre-equilibrated unfolding. The Journal of Physical Chemistry B, 111(27), pp.7897-7913.

Andrews, J.M. and Roberts, C.J., 2007. Non-native aggregation of α-chymotrypsinogen occurs through nucleation and growth with competing nucleus sizes and negative activation energies. Biochemistry, 46(25), pp.7558-7571.

Araki, K., Yagi, N., Aoyama, K., Choong, C.J., Hayakawa, H., Fujimura, H., Nagai, Y., Goto, Y. and Mochizuki, H., 2019. Parkinson's disease is a type of amyloidosis featuring accumulation of amyloid fibrils of α-synuclein. Proceedings of the National Academy of Sciences, 116(36), pp.17963-17969.

Armstrong, J.M., McKenzie, H.A. and Sawyer, W.H., 1967. On the fractionation of β-lactoglobulin and α-lactalbumin. Biochimica et Biophysica Acta (BBA)-Protein Structure, 147(1), pp.60-72.

Arnaudov, L.N., de Vries, R., Ippel, H. and van Mierlo, C.P., 2003. Multiple steps during the formation of β-lactoglobulin fibrils. Biomacromolecules, 4(6), pp.1614-1622.

Arora, A., Ha, C. and Park, C.B., 2004. Inhibition of insulin amyloid formation by small stress molecules. FEBS letters, 564(1-2), pp.121-125.

Aschaffenburg, R. and Drewry, J., 1957. Improved method for the preparation of crystalline β-lactoglobulin and α-lactalbumin from cow's milk. Biochemical Journal, 65(2), p.273.

Aschaffenburg, R., Green, D.W. and Simmons, R.M., 1965. Crystal forms of β-lactoglobulin.

Astwood, J.D., Leach, J.N. and Fuchs, R.L., 1996. Stability of food allergens to digestion in vitro. Nature biotechnology, 14(10), pp.1269-1273.

Atkins, P. and De Paula, J., 2009. Elements of physical chemistry. Macmillan.

Azuaga, A.I., Dobson, C.M., Mateo, P.L. and Conejero-Lara, F., 2002. Unfolding and aggregation during the thermal denaturation of streptokinase. European journal of biochemistry, 269(16), pp.4121-4133.

Báez, G.D., Moro, A., Ballerini, G.A., Busti, P.A. and Delorenzi, N.J., 2011. Comparison between structural changes of heat-treated and transglutaminase cross-linked beta-lactoglobulin and their effects on foaming properties. Food Hydrocolloids, 25(7), pp.1758-1765.

Baldassarre, M., Bennett, M. and Barth, A., 2016. Simultaneous acquisition of infrared, fluorescence and light scattering spectra of proteins: direct evidence for pre-fibrillar species in amyloid fibril formation. Analyst, 141(3), pp.963-973.

Bamdad, F., Bark, S., Kwon, C.H., Suh, J.W. and Sunwoo, H., 2017. Anti-inflammatory and antioxidant properties of peptides released from β-lactoglobulin by high hydrostatic pressure-assisted enzymatic hydrolysis. Molecules, 22(6), p.949.

Baslé, E., Joubert, N. and Pucheault, M., 2010. Protein chemical modification on endogenous amino acids. Chemistry & biology, 17(3), pp.213-227.

Bély, M. and Makovitzky, J., 2006. Sensitivity and specificity of Congo red staining according to Romhanyi. Comparison with Puchtler's or Bennhold's methods. Actahistochemica, 108(3), pp.175-180.

Bhattacharjee, C., Saha, S., Biswas, A., Kundu, M., Ghosh, L. and Das, K.P., 2005. Structural changes of β-lactoglobulin during thermal unfolding and refolding–an FT-IR and circular dichroism study. The Protein Journal, 24(1), pp.27-35.

Biolo, G. and Wolfe, R.R., 1993. Insulin action on protein metabolism. Bailliere's clinical endocrinology and metabolism, 7(4), pp.989-1005.

Blázquez, E., Velázquez, E., Hurtado-Carneiro, V. and Ruiz-Albusac, J.M., 2014. Insulin in the brain: its pathophysiological implications for States related with central insulin resistance, type 2 diabetes and Alzheimer's disease. Frontiers in endocrinology, 5, p.161.

Boland, B.B., Rhodes, C.J. and Grimsby, J.S., 2017. The dynamic plasticity of insulin production in β-cells. Molecular metabolism, 6(9), pp.958-973.

Boutureira, O. and Bernardes, G.J., 2015. Advances in chemical protein modification. Chemical reviews, 115(5), pp.2174-2195.

Brange, J., Andersen, L., Laursen, E.D., Meyn, G. and Rasmussen, E., 1997. Toward understanding insulin fibrillation. Journal of pharmaceutical sciences, 86(5), pp.517-525.

Bridgman, P.W., 1964. The coagulation of albumen by pressure. In Papers 12-31 (pp. 735-736). Harvard University Press.

Broersen, K., 2020. Milk processing affects structure, bioavailability and immunogenicity of β-lactoglobulin. Foods, 9(7), p.874.

Brownlow, S., Cabral, J.H.M., Cooper, R., Flower, D.R., Yewdall, S.J., Polikarpov, I., North, A.C. and Sawyer, L., 1997. Bovine β-lactoglobulin at 1.8 Å resolution—still an enigmatic lipocalin. Structure, 5(4), pp.481-495.

Brylinski, M. and Skolnick, J., 2011. FINDSITE-metal: integrating evolutionary information and machine learning for structure-based metal-binding site prediction at the proteome level. Proteins: Structure, Function, and Bioinformatics, 79(3), pp.735-751.

Buszewski, B., Rodzik, A., Railean-Plugaru, V., Sprynskyy, M. and Pomastowski, P., 2020. A study of zinc ions immobilization by β-lactoglobulin. Colloids and Surfaces A: Physicochemical and Engineering Aspects, 591, p.124443.

Buyanbadrakh, B., 2014. Isolation of beta-lactoglobulin from cow milk. Research.

Caessens, P.W., Visser, S. and Gruppen, H., 1997. Method for the isolation of bovine β-lactoglobulin from a cheese whey protein fraction and physicochemical characterization of the purified product. International dairy journal, 7(4), pp.229-235.

Cao, A., Hu, D. and Lai, L., 2004. Formation of amyloid fibrils from fully reduced hen egg white lysozyme. Protein Science, 13(2), pp.319-324.

Cao, P., Marek, P., Noor, H., Patsalo, V., Tu, L.H., Wang, H., Abedini, A. and Raleigh, D.P., 2013. Islet amyloid: from fundamental biophysics to mechanisms of cytotoxicity. FEBS letters, 587(8), pp.1106-1118.

Carta, G. and Jungbauer, A., 2020. Protein chromatography: process development and scale-up. John Wiley & Sons.

Carullo, D., Donsì, F. and Ferrari, G., 2020. Influence of high-pressure homogenization on structural properties and enzymatic hydrolysis of milk proteins. Lwt, 130, p.109657.

Carvalho, P.M., Felício, M.R., Santos, N.C., Gonçalves, S. and Domingues, M.M., 2018. Application of light scattering techniques to nanoparticle characterization and development. Frontiers in chemistry, 6, p.237.

Cavanagh, J., 1996. Protein NMR spectroscopy: principles and practice. Academic press.

Chaturvedi, S.K., Ahmad, E., Khan, J.M., Alam, P., Ishtikhar, M. and Khan, R.H., 2015. Elucidating the interaction of limonene with bovine serum albumin: a multi-technique approach. Molecular BioSystems, 11(1), pp.307-316.

Chaturvedi, S.K., Khan, J.M., Siddiqi, M.K., Alam, P. and Khan, R.H., 2016. Comparative insight into surfactants mediated amyloidogenesis of lysozyme. International journal of biological macromolecules, 83, pp.315-325.

Chaturvedi, S.K., Siddiqi, M.K., Alam, P. and Khan, R.H., 2016. Protein misfolding and aggregation: Mechanism, factors and detection. Process Biochemistry, 51(9), pp.1183-1192.

Chen, B.L., Arakawa, T., Morris, C.F., Kenney, W.C., Wells, C.M. and Pitt, C.G., 1994. Aggregation pathway of recombinant human keratinocyte growth factor and its stabilization. Pharmaceutical research, 11, pp.1581-1587.

Chen, Y.Y., Xiao, L., Cui, J.H., Chen, G.F., Zhang, J. and Wang, P., 2013. Biological relevance of the interaction between resveratrol and insulin. Food Biophysics, 8, pp.282-289.

Chiti, F. and Dobson, C.M., 2009. Amyloid formation by globular proteins under native conditions. Nature chemical biology, 5(1), pp.15-22.

Chiti, F. and Dobson, C.M., 2017. Protein misfolding, amyloid formation, and human disease: a summary of progress over the last decade. Annual review of biochemistry, 86, pp.27-68.

Chobert, J.M., 2012. Milk protein tailoring to improve functional and biological properties. Journal of BioScience & Biotechnology, 1(3).

Cleland, J.L., Powell, M.F. and Shire, S.J., 1993. The development of stable protein formulations: a close look at protein aggregation, deamidation, and oxidation. Critical reviews in therapeutic drug carrier systems, 10(4), pp.307-377.

Coles, M., Diercks, T., Muehlenweg, B., Bartsch, S., Zölzer, V., Tschesche, H. and Kessler, H., 1999. The solution structure and dynamics of human neutrophil gelatinase-associated lipocalin. Journal of molecular biology, 289(1), pp.139-157.

Conti, A., Godovac-Zimmermann, J., Liberatori, J., Braunitzer, G., The primary structure of monomeric beta-lactoglobulin I from horse colostrum (Equus caballus, Perissodactyla). Hoppe Seylers Z Physiol Chem, 1984, 365, 1393-401.

Cowan, S.W., Newcomer, M.E. and Jones, T.A., 1990. Crystallographic refinement of human serum retinol binding protein at 2Å resolution. Proteins: Structure, Function, and Bioinformatics, 8(1), pp.44-61.

Crowfoot, D. and Riley, D., 1938. Crystal Structures of the Proteins An X-Ray Study of Palmar's Lactoglobulin. Nature, 141(3568), pp.521-522.

Crowther, J., 2017. Unravelling the mysteries of the milk protein β-lactoglobulin.

Crowther, J.M., Allison, J.R., Smolenski, G.A., Hodgkinson, A.J., Jameson, G.B. and Dobson, R.C., 2018. The self-association and thermal denaturation of caprine and bovine β-lactoglobulin. European Biophysics Journal, 47(7), pp.739-750.

Czech, M.P., Tencerova, M., Pedersen, D.J. and Aouadi, M., 2013. Insulin signalling mechanisms for triacylglycerol storage. Diabetologia, 56, pp.949-964.

Das, A., Shah, M. and Saraogi, I., 2022. Molecular aspects of insulin aggregation and various therapeutic interventions. ACS bio & med Chem Au, 2(3), pp.205-221.

Das, S. and Bhattacharyya, D., 2017. Destabilization of human insulin fibrils by peptides of fruit bromelain derived from Ananascomosus (pineapple). Journal of Cellular Biochemistry, 118(12), pp.4881-4896.

De Baets, G., Schymkowitz, J. and Rousseau, F., 2014. Predicting aggregation-prone sequences in proteins. Essays in Biochemistry, 56, pp.41-52.

De Jongh, H.H.J., Gröneveld, T. and De Groot, J., 2001. Mild isolation procedure discloses new protein structural properties of β-lactoglobulin. Journal of Dairy Science, 84(3), pp.562-571.

De Meyts, P., 2016. The insulin receptor and its signal transduction network. Endotext [Internet].

DeLano, W.L., 2002. Pymol: An open-source molecular graphics tool. CCP4 Newsl. Protein Crystallogr, 40(1), pp.82-92.

Dill, K.A., 1990. Dominant forces in protein folding. Biochemistry, 29(31), pp.7133-7155.

Dubey, K., Anand, B.G., Badhwar, R., Bagler, G., Navya, P.N., Daima, H.K. and Kar, K., 2015. Tyrosine-and tryptophan-coated gold nanoparticles inhibit amyloid aggregation of insulin. Amino acids, 47, pp.2551-2560.

Duerkop, M., Berger, E., Dürauer, A. and Jungbauer, A., 2018. Impact of cavitation, high shear stress and air/liquid interfaces on protein aggregation. Biotechnology journal, 13(7), p.1800062.

Dusa, A., Kaylor, J., Edridge, S., Bodner, N., Hong, D.P. and Fink, A.L., 2006. Characterization of oligomers during α-synuclein aggregation using intrinsic tryptophan fluorescence. Biochemistry, 45(8), pp.2752-2760.

Eaton, W.A. and Bunn, H.F., 2017. Treating sickle cell disease by targeting HbS polymerization. Blood, The Journal of the American Society of Hematology, 129(20), pp.2719-2726.

Edwards, P.J. and Jameson, G.B., 2020. Structure and stability of whey proteins. In Milk proteins (pp. 251-291). Academic Press.

Farrell Jr, H.M., Jimenez-Flores, R., Bleck, G.T., Brown, E.M., Butler, J.E., Creamer, L.K., Hicks, C.L., Hollar, C.M., Ng-Kwai-Hang, K.F. and Swaisgood, H.E., 2004. Nomenclature of the proteins of cows' milk—Sixth revision. Journal of dairy science, 87(6), pp.1641-1674.

Fekete, S., Beck, A., Veuthey, J.L. and Guillarme, D., 2014. Theory and practice of size exclusion chromatography for the analysis of protein aggregates. Journal of pharmaceutical and biomedical analysis, 101, pp.161-173.

FELIPE, X. and LAW, A.J., 1997. SHORT COMMUNICATIONS Preparative-scale fractionation of bovine, caprine and ovine whey proteins by gel permeation chromatography. Journal of Dairy Research, 64(3), pp.459-464.

Fernandez-Flores, A., 2011. A review of amyloid staining: methods and artifacts. Biotechnic&Histochemistry, 86(5), pp.293-301.

Findeis, M.A., Musso, G.M., Arico-Muendel, C.C., Benjamin, H.W., Hundal, A.M., Lee, J.J., Chin, J., Kelley, M., Wakefield, J., Hayward, N.J. and Molineaux, S.M., 1999. Modified-peptide inhibitors of amyloid β-peptide polymerization. Biochemistry, 38(21), pp.6791-6800.

Fink, A.L., 1999. Chaperone-mediated protein folding. Physiological reviews, 79(2), pp.425-449.

Fogolari, F., Ragona, L., Zetta, L., Romagnoli, S., De Kruif, K.G. and Molinari, H., 1998. Monomeric bovine β-lactoglobulin adopts a β-barrel fold at pH 2. FEBS letters, 436(2), pp.149-154.

Fox, K.K., Holsinger, V.H., Posati, L.P. and Pallansch, M.J., 1967. Separation of β-lactoglobulin from other milk serum proteins by trichloroacetic acid. Journal of Dairy Science, 50(9), pp.1363-1367.

Franks, F., Hatley, R.H.M. and Friedman, H.L., 1988. The thermodynamics of protein stability: cold destabilization as a general phenomenon. Biophysical chemistry, 31(3), pp.307-315.

Gancar, M., Kurin, E., Bednarikova, Z., Marek, J., Mucaji, P., Nagy, M. and Gazova, Z., 2020. Amyloid aggregation of insulin: an interaction study of green tea constituents. Scientific Reports, 10(1), p.9115.

Gluvic, Z., Zaric, B., Resanovic, I., Obradovic, M., Mitrovic, A., Radak, D. and R Isenovic, E., 2017. Link between metabolic syndrome and insulin resistance. Current vascular pharmacology, 15(1), pp.30-39.

Goedert, M. and Spillantini, M.G., 2006. A century of Alzheimer's disease. science, 314(5800), pp.777-781.

Goedert, M., 2001. Alpha-synuclein and neurodegenerative diseases. Nature reviews neuroscience, 2(7), pp.492-501.

Goldstein, B.J., 2002. Insulin resistance as the core defect in type 2 diabetes mellitus. The American journal of cardiology, 90(5), pp.3-10.

Gołębiowski, A., Pomastowski, P., Rodzik, A., Król-Górniak, A., Kowalkowski, T., Górecki, M. and Buszewski, B., 2020. Isolation and self-association studies of beta-lactoglobulin. International Journal of Molecular Sciences, 21(24), p.9711.

Gong, H., He, Z., Peng, A., Zhang, X., Cheng, B., Sun, Y., Zheng, L. and Huang, K., 2014. Effects of several quinones on insulin aggregation. Scientific reports, 4(1), p.5648.

Goulding, D.A., Fox, P.F. and O'Mahony, J.A., 2020. Milk proteins: An overview. Milk proteins, pp.21-98.

Grant, C.S., 2005. Insulinoma. Best practice & research Clinical gastroenterology, 19(5), pp.783-798.

Green, D.W. and Aschaffenburg, R.J., 1959. Twofold symmetry of the β-lacto-globulin molecule in crystals.

Guaiquil, V.H., Vera, J.C. and Golde, D.W., 2001. Mechanism of vitamin C inhibition of cell death induced by oxidative stress in glutathione-depleted HL-60 cells. Journal of Biological Chemistry, 276(44), pp.40955-40961.

Guliyeva, A.J. and Gasymov, O.K., 2020. ANS fluorescence: Potential to discriminate hydrophobic sites of proteins in solid states. Biochemistry and Biophysics Reports, 24, p.100843.

Haghighi-Poodeh, S., Kurganov, B., Navidpour, L., Yaghmaei, P. and Ebrahim-Habibi, A., 2020. Characterization of arginine preventive effect on heat-induced aggregation of insulin. International journal of biological macromolecules, 145, pp.1039-1048.

Hagihara, Y., Aimoto, S., Fink, A.L. and Goto, Y., 1993. Guanidine hydrochloride-induced folding of proteins. Journal of molecular biology, 231(2), pp.180-184.

Halliday, J.A., Bell, K. and Shaw, D.C., 1991. The complete amino acid sequence of feline β-lactoglobulin II and a partial revision of the equine β-lactoglobulin II sequence. Biochimica et Biophysica Acta (BBA)-Protein Structure and Molecular Enzymology, 1077(1), pp.25-30.

Halttunen, M., Kämäräinen, M. and Koistinen, H., 2000. Glycodelin: a reproduction-related lipocalin. Biochimica et Biophysica Acta (BBA)-Protein Structure and Molecular Enzymology, 1482(1-2), pp.149-156.

Hamada, D., Segawa, S.I. and Goto, Y., 1996. Non-native α-helical intermediate in the refolding of β-lactoglobulin, a predominantly β-sheet protein. Nature structural biology, 3(10), pp.868-873.

Hameed, I., Masoodi, S.R., Mir, S.A., Nabi, M., Ghazanfar, K. and Ganai, B.A., 2015. Type 2 diabetes mellitus: from a metabolic disorder to an inflammatory condition. World journal of diabetes, 6(4), p.598.

Han, Q., Brown, S.J., Drummond, C.J. and Greaves, T.L., 2022. Protein aggregation and crystallization with ionic liquids: Insights into the influence of solvent properties. Journal of Colloid and Interface Science, 608, pp.1173-1190.

Hardy, J. and Selkoe, D.J., 2002. The amyloid hypothesis of Alzheimer's disease: progress and problems on the road to therapeutics. science, 297(5580), pp.353-356.

Hawe, A., Wiggenhorn, M., van de Weert, M., Garbe, J.H., Mahler, H.C. and Jiskoot, W., 2012. Forced degradation of therapeutic proteins. Journal of pharmaceutical sciences, 101(3), pp.895-913.

Heddleson, R.A., Allen, J.C., Wang, Q. and Swaisgood, H.E., 1997. Purity and yield of β-lactoglobulin isolated by an N-Retinyl-Celite bioaffinity column. Journal of Agricultural and Food Chemistry, 45(7), pp.2369-2373.

Heremans, K., 2005. Protein dynamics: hydration and cavities. Brazilian journal of medical and biological research, 38, pp.1157-1165.

Hinnenkamp, C.L., 2020. Blending of Procream with Functionally Enhanced Whey Protein Concentrate: A Structure-Function Approach to Whey Coproduct Utilization (Doctoral dissertation, University of Minnesota).

Hoffmann, M.A. and van Mil, P.J., 1997. Heat-induced aggregation of β-lactoglobulin: role of the free thiol group and disulfide bonds. Journal of Agricultural and Food Chemistry, 45(8), pp.2942-2948.

Hong, Y., Meng, L., Chen, S., Leung, C.W.T., Da, L.T., Faisal, M., Silva, D.A., Liu, J., Lam, J.W.Y., Huang, X. and Tang, B.Z., 2012. Monitoring and inhibition of insulin fibrillation by a small organic fluorogen with aggregation-induced emission characteristics. Journal of the American Chemical Society, 134(3), pp.1680-1689.

Hoppenreijs, L.J.G., Fitzner, L., Ruhmlieb, T., Heyn, T.R., Schild, K., Van der Goot, A.J., Boom, R.M., Steffen-Heins, A., Schwarz, K. and Keppler, J.K., 2022. Engineering amyloid and amyloid-like morphologies of β-lactoglobulin. Food Hydrocolloids, 124, p.107301.

Housmans, J.A., Wu, G., Schymkowitz, J. and Rousseau, F., 2023. A guide to studying protein aggregation. The FEBS journal, 290(3), pp.554-583.

Hudson, S.A., Ecroyd, H., Kee, T.W. and Carver, J.A., 2009. The thioflavin T fluorescence assay for amyloid fibril detection can be biased by the presence of exogenous compounds. The FEBS journal, 276(20), pp.5960-5972.

Invernizzi, G., Papaleo, E., Sabate, R. and Ventura, S., 2012. Protein aggregation: mechanisms and functional consequences. The international journal of biochemistry & cell biology, 44(9), pp.1541-1554.

Ivanova, M.I., Sievers, S.A., Sawaya, M.R., Wall, J.S. and Eisenberg, D., 2009. Molecular basis for insulin fibril assembly. Proceedings of the National Academy of Sciences, 106(45), pp.18990-18995.

Jawasreh, K., Amareen, A.A. and Aad, P., 2019. Effect and interaction of β-lactoglobulin, kappa casein, and prolactin genes on milk production and composition of awassi sheep. Animals, 9(6), p.382.

Jayamani, J., Shanmugam, G. and Singam, E.R.A., 2014. Inhibition of insulin amyloid fibril formation by ferulic acid, a natural compound found in many vegetables and fruits. RSC advances, 4(107), pp.62326-62336.

Jha, N.K., Jha, S.K., Kumar, D., Kejriwal, N., Sharma, R., Ambasta, R.K. and Kumar, P., 2015. Impact of insulin degrading enzyme and neprilysin in Alzheimer's disease biology: characterization of putative cognates for therapeutic applications. Journal of Alzheimer's disease, 48(4), pp.891-917.

Jia, Y., Zhao, T., Zhao, N., Wei, H., Zhang, W. and Qiu, R., 2019. Effects of light irradiation on the complexes of cadmium and humic acids: The role of thiol groups. Chemosphere, 225, pp.174-181.

Jiménez, J.L., Nettleton, E.J., Bouchard, M., Robinson, C.V., Dobson, C.M. and Saibil, H.R., 2002. The protofilament structure of insulin amyloid fibrils. Proceedings of the National Academy of Sciences, 99(14), pp.9196-9201.

Johnson, I.S., 1983. Human insulin from recombinant DNA technology. Science, 219(4585), pp.632-637.

Judy, E. and Kishore, N., 2019. A look back at the molten globule state of proteins: Thermodynamic aspects. Biophysical Reviews, 11, pp.365-375.

Jung, J.M., Savin, G., Pouzot, M., Schmitt, C. and Mezzenga, R., 2008. Structure of heat-induced β-lactoglobulin aggregates and their complexes with sodium-dodecyl sulfate. Biomacromolecules, 9(9), pp.2477-2486.

Jung, J.M., Savin, G., Pouzot, M., Schmitt, C. and Mezzenga, R., 2008. Structure of heat-induced β-lactoglobulin aggregates and their complexes with sodium-dodecyl sulfate. Biomacromolecules, 9(9), pp.2477-2486.

Kaddouri, H., Mimoun, S., El-Mecherfi, K.E., Chekroun, A., Kheroua, O. and Saidi, D., 2008. Impact of γ-radiation on antigenic properties of cow's milk β-lactoglobulin. Journal of food protection, 71(6), pp.1270-1272.

Kaffe-Abramovich, T. and Unger, R., 1998. A simple model for evolution of proteins towards the global minimum of free energy. Folding and Design, 3(5), pp.389-399.

Katsarou, A., Gudbjörnsdottir, S., Rawshani, A., Dabelea, D., Bonifacio, E., Anderson, B.J., Jacobsen, L.M., Schatz, D.A. and Lernmark, Å., 2017. Type 1 diabetes mellitus. Nature reviews Disease primers, 3(1), pp.1-17.

Kaul, K., Apostolopoulou, M. and Roden, M., 2015. Insulin resistance in type 1 diabetes mellitus. Metabolism, 64(12), pp.1629-1639.

Keane, K. and Newsholme, P., 2014. Metabolic regulation of insulin secretion. Vitamins & Hormones, 95, pp.1-33.

Kella, N.K.D. and Kinsella, J.E., 1988. Structural stability of β-lactoglobulin in the presence of kosmotropic salts A kinetic and thermodynamic study. International Journal of Peptide and Protein Research, 32(5), pp.396-405.

Kerstens, S., Mugnier, C., Murray, B.S. and Dickinson, E., 2006. Influence of ionic surfactants on the microstructure of heat-set β-lactoglobulin-stabilized emulsion gels. Food Biophysics, 1, pp.133-143.

Khurana, R., Gillespie, J.R., Talapatra, A., Minert, L.J., Ionescu-Zanetti, C., Millett, I. and Fink, A.L., 2001. Partially folded intermediates as critical precursors of light chain amyloid fibrils and amorphous aggregates. Biochemistry, 40(12), pp.3525-3535.

Koistinen, H., Koistinen, R., Seppälä, M., Burova, T.V., Choiset, Y. and Haertlé, T., 1999. Glycodelin and β-lactoglobulin, lipocalins with a high structural similarity, differ in ligand binding properties. FEBS letters, 450(1-2), pp.158-162.

Komatsu, H., Kandeel, F. and Mullen, Y., 2018. Impact of oxygen on pancreatic islet survival. Pancreas, 47(5), p.533.

Kontopidis, G., Holt, C. and Sawyer, L., 2002. The ligand-binding site of bovine β-lactoglobulin: evidence for a function?. Journal of molecular biology, 318(4), pp.1043-1055.

Kontopidis, G., Holt, C. and Sawyer, L., 2004. Invited review: β-lactoglobulin: binding properties, structure, and function. Journal of dairy science, 87(4), pp.785-796.

Koradi, R., Billeter, M. and Wüthrich, K., 1996. MOLMOL: a program for display and analysis of macromolecular structures. Journal of molecular graphics, 14(1), pp.51-55.

Krebs, M.R., Devlin, G.L. and Donald, A.M., 2009. Amyloid fibril-like structure underlies the aggregate structure across the pH range for β-lactoglobulin. Biophysical journal, 96(12), pp.5013-5019.

Kulkarni, R.N., 2004. The islet β-cell. The international journal of biochemistry & cell biology, 36(3), pp.365-371.

Kuwata, K., Hoshino, M., Forge, V., Era, S., Batt, C.A. and Goto, Y., 1999. Solution structure and dynamics of bovine β-lactoglobulin A. Protein Science, 8(11), pp.2541-2545.

Langer, O., Berkus, M., Brustman, L., Anyaegbunam, A. and Mazze, R., 1991. Rationale for insulin management in gestational diabetes mellitus. Diabetes, 40(Supplement_2), pp.186-190.

Larson, B.L., 1972. Methionine stimulation of milk protein synthesis in bovine mammary cell cultures. Journal of dairy science, 55(5), pp.629-631.

Le Maux, S., Bouhallab, S., Giblin, L., Brodkorb, A. and Croguennec, T., 2014. Bovine β-lactoglobulin/fatty acid complexes: binding, structural, and biological properties. Dairy science & technology, 94, pp.409-426.

Leiske, D.L., Shieh, I.C. and Tse, M.L., 2016. A method to measure protein unfolding at an air–liquid interface. Langmuir, 32(39), pp.9930-9937.

Len, J.S., Koh, W.S.D. and Tan, S.X., 2019. The roles of reactive oxygen species and antioxidants in cryopreservation. Bioscience reports, 39(8), p.BSR20191601.

Lewis, G.F., Carpentier, A.C., Pereira, S., Hahn, M. and Giacca, A., 2021. Direct and indirect control of hepatic glucose production by insulin. Cell metabolism, 33(4), pp.709-720.

Li, Y.I., Weiss IV, W.F. and Roberts, C.J., 2009. Characterization of high-molecular-weight nonnative aggregates and aggregation kinetics by size exclusion chromatography with inline multi-angle laser light scattering. Journal of pharmaceutical sciences, 98(11), pp.3997-4016.

Liu, Q.R., Zhu, M., Zhang, P., Mazucanti, C.H., Huang, N.S., Lang, D.L., Chen, Q., Auluck, P., Marenco, S., O'Connell, J.F. and Ferrucci, L., 2021. Novel Human Insulin Isoforms and Ca-Peptide Product in Islets of Langerhans and Choroid Plexus. Diabetes, 70, p.1.

Lizcano, J.M. and Alessi, D.R., 2002. The insulin signalling pathway. Current biology, 12(7), pp.R236-R238.

Louros, N., Orlando, G., De Vleeschouwer, M., Rousseau, F. and Schymkowitz, J., 2020. Structure-based machine-guided mapping of amyloid sequence space reveals uncharted sequence clusters with higher solubilities. Nature communications, 11(1), p.3314.

Low, K.J.Y., Venkatraman, A., Mehta, J.S. and Pervushin, K., 2022. Molecular mechanisms of amyloid disaggregation. Journal of Advanced Research, 36, pp.113-132.

Lozano, J.M., Giraldo, G.I. and Romero, C.M., 2008. An improved method for isolation of β-lactoglobulin. International Dairy Journal, 18(1), pp.55-63.

M Ashraf, G., H Greig, N., A Khan, T., Hassan, I., Tabrez, S., Shakil, S., A Sheikh, I., K Zaidi, S., Akram, M., R Jabir, N. and K Firoz, C., 2014. Protein misfolding and aggregation in Alzheimer's disease and type 2 diabetes mellitus. CNS & Neurological Disorders-Drug Targets (Formerly Current Drug Targets-CNS & Neurological Disorders), 13(7), pp.1280-1293.

Ma, B., Xie, J., Wei, L. and Li, W., 2013. Macromolecular crowding modulates the kinetics and morphology of amyloid self-assembly by β-lactoglobulin. International journal of biological macromolecules, 53, pp.82-87.

MacFarlane, N.G., 2018. Digestion and absorption. Anaesthesia & Intensive Care Medicine, 19(3), pp.125-127.

Mahadevi, A.S. and Sastry, G.N., 2016. Cooperativity in noncovalent interactions. Chemical reviews, 116(5), pp.2775-2825.

Mahler, H.C., Friess, W., Grauschopf, U. and Kiese, S., 2009. Protein aggregation: pathways, induction factors and analysis. Journal of pharmaceutical sciences, 98(9), pp.2909-2934.

Maqbool, M., Dar, M.A., Gani, I. and Geer, M.I., 2019. Insulin resistance and polycystic ovary syndrome: a review. Journal of drug delivery and therapeutics, 9(1-s), pp.433-436.

Marek, P.J., Patsalo, V., Green, D.F. and Raleigh, D.P., 2012. Ionic strength effects on amyloid formation by amylin are a complicated interplay among Debye screening, ion selectivity, and Hofmeister effects. Biochemistry, 51(43), pp.8478-8490.

MATÉ, J.I. and KROCHTA, J.M., 1994. β-Lactoglobulin separation from whey protein isolate on a large scale. Journal of Food Science, 59(5), pp.1111-1114.

Matthews, C.R., 1993. Pathways of protein folding. Annual review of biochemistry, 62(1), pp.653-683.

McKenzie, H.A. and Sawyer, W.H., 1967. Effect of p H on β-Lactoglobulins. Nature, 214(5093), pp.1101-1104.

Mercadante, D., Melton, L.D., Norris, G.E., Loo, T.S., Williams, M.A., Dobson, R.C. and Jameson, G.B., 2012. Bovine β-lactoglobulin is dimeric under imitative physiological conditions: dissociation equilibrium and rate constants over the pH range of 2.5–7.5. Biophysical journal, 103(2), pp.303-312.

Mikhail, N., 2009. The metabolic syndrome: insulin resistance. Current hypertension reports, 11(2), pp.156-158.

Minj, S. and Anand, S., 2020. Whey proteins and its derivatives: Bioactivity, functionality, and current applications. Dairy, 1(3), pp.233-258.

Mlinar, B., Marc, J., Janež, A. and Pfeifer, M., 2007. Molecular mechanisms of insulin resistance and associated diseases. Clinicachimicaacta, 375(1-2), pp.20-35.

Monaco, H.L., Zanotti, G., Spadon, P., Bolognesi, M., Sawyer, L. and Eliopoulos, E.E., 1987. Crystal structure of the trigonal form of bovine beta-lactoglobulin and of its complex with retinol at 2.5 Å resolution. Journal of Molecular Biology, 197(4), pp.695-706.

Mounsey, J.S. and O'KENNEDY, B.T., 2009. Stability of β-lactoglobulin/micellar casein mixtures on heating in simulated milk ultrafiltrate at pH 6.0. International journal of dairy technology, 62(4), pp.493-499.

Nagy, P., 2013. Kinetics and mechanisms of thiol–disulfide exchange covering direct substitution and thiol oxidation-mediated pathways. Antioxidants & redox signaling, 18(13), pp.1623-1641.

Naiki, H., Higuchi, K., Hosokawa, M. and Takeda, T., 1989. Fluorometric determination of amyloid fibrils in vitro using the fluorescent dye, thioflavine T. Analytical biochemistry, 177(2), pp.244-249.

Naqvi, Z., Khan, R.H. and Saleemuddin, M., 2010. A procedure for the purification of beta-lactoglobulin from bovine milk using gel filtration chromatography at low pH. Preparative Biochemistry & Biotechnology, 40(4), pp.326-336.

Navarra, G., Tinti, A., Di Foggia, M., Leone, M., Militello, V. and Torreggiani, A., 2014. Metal ions modulate thermal aggregation of beta-lactoglobulin: A joint chemical and physical characterization. Journal of Inorganic Biochemistry, 137, pp.64-73.

Newcomer, M.E., Jones, T.A., Aqvist, J., Sundelin, J., Eriksson, U., Rask, L. and Peterson, P.A., 1984. The three-dimensional structure of retinol-binding protein. The EMBO journal, 3(7), pp.1451-1454.

Newsholme, P., Cruzat, V., Arfuso, F. and Keane, K., 2014. Nutrient regulation of insulin secretion and action. Journal of Endocrinology, 221(3), pp.R105-R120.

Nicoud, L., Sozo, M., Arosio, P., Yates, A., Norrant, E. and Morbidelli, M., 2014. Role of cosolutes in the aggregation kinetics of monoclonal antibodies. The Journal of Physical Chemistry B, 118(41), pp.11921-11930.

Norton, L., Shannon, C., Gastaldelli, A. and DeFronzo, R.A., 2022. Insulin: The master regulator of glucose metabolism. Metabolism, 129, p.155142.

Okamura, S., Hayashino, Y., Kore-Eda, S. and Tsujii, S., 2013. Localized amyloidosis at the site of repeated insulin injection in a patient with type 2 diabetes. Diabetes Care, 36(12), pp.e200-e200.

Oliva, A., Fariña, J.B. and Llabrés, M., 2016. Pre-study and in-study validation of a size-exclusion chromatography method with different detection modes for the analysis of monoclonal antibody aggregates. Journal of Chromatography B, 1022, pp.206-212.

Oliveira, K.M., Valente-Mesquita, V.L., Botelho, M.M., Sawyer, L., Ferreira, S.T. and Polikarpov, I., 2001. Crystal structures of bovine β-lactoglobulin in the orthorhombic space group C2221: Structural differences between genetic variants A and B and features of the Tanford transition. European Journal of Biochemistry, 268(2), pp.477-484.

Oren, Z. and Shai, Y., 1998. Mode of action of linear amphipathic α-helical antimicrobial peptides. Peptide Science, 47(6), pp.451-463.

Ornellas, F., Karise, I., Aguila, M.B. and Mandarim-de-Lacerda, C.A., 2020. Pancreatic islets of langerhans: adapting cell and molecular biology to changes of metabolism. Obesity and Diabetes: Scientific Advances and Best Practice, pp.175-190.

Ovalle, F. and Azziz, R., 2002. Insulin resistance, polycystic ovary syndrome, and type 2 diabetes mellitus. Fertility and sterility, 77(6), pp.1095-1105.

Palmer, A.H., 1933. The preparation of a crystalline globulin from the albumin fraction of cow's milk. Journal of biological chemistry, 100.

Papiz, M.Z., Sawyer, L., Eliopoulos, E.E., North, A.C.T., Findlay, J.B.C., Sivaprasadarao, R., Jones, T.A., Newcomer, M.E. and Kraulis, P.J., 1986. The structure of β-lactoglobulin and its similarity to plasma retinol-binding protein. Nature, 324(6095), pp.383-385.

Patel, P., Parmar, K. and Das, M., 2018. Inhibition of insulin amyloid fibrillation by Morin hydrate. International journal of biological macromolecules, 108, pp.225-239.

Pedersen, K.O., 1936. Ultracentrifugal and electrophoretic studies on the milk proteins: Introduction and preliminary results with fractions from skim milk. Biochemical Journal, 30(6), p.948.

Perez, M.D., Sanchez, L., Aranda, P., Ena, J., Oria, R. and Calvo, M., 1992. Effect of β-lactoglobulin on the activity of pregastric lipase. A possible role for this protein in ruminant milk. Biochimica et Biophysica Acta (BBA)-Lipids and Lipid Metabolism, 1123(2), pp.151-155.

Pervaiz, S. and Brew, K., 1986. Purification and characterization of the major whey proteins from the milks of the bottlenose dolphin (Tursiops truncatus), the Florida manatee (Trichechus manatus latirostris), and the beagle (Canis familiaris). Archives of biochemistry and biophysics, 246(2), pp.846-854.

Powers, E.T., Morimoto, R.I., Dillin, A., Kelly, J.W. and Balch, W.E., 2009. Biological and chemical approaches to diseases of proteostasis deficiency. Annual review of biochemistry, 78, pp.959-991.

Privalov, P.L. and Gill, S.J., 1988. Stability of protein structure and hydrophobic interaction. Advances in protein chemistry, 39, pp.191-234.

Prusiner, S.B., 1998. Prions. Proceedings of the National Academy of Sciences, 95(23), pp.13363-13383.

Qi, X.L., Holt, C., Mcnulty, D., Clarke, D.T., Brownlow, S. and Jones, G.R., 1997. Effect of temperature on the secondary structure of β-lactoglobulin at pH 6.7, as determined by CD and IR spectroscopy: a test of the molten globule hypothesis. Biochemical Journal, 324(1), pp.341-346.

Qin, B.Y., Bewley, M.C., Creamer, L.K., Baker, E.N. and Jameson, G.B., 1999. Functional implications of structural differences between variants A and B of bovine β-lactoglobulin. Protein Science, 8(1), pp.75-83.

Qin, B.Y., Bewley, M.C., Creamer, L.K., Baker, H.M., Baker, E.N. and Jameson, G.B., 1998. Structural basis of the Tanford transition of bovine β-lactoglobulin. Biochemistry, 37(40), pp.14014-14023.

Quevedo, M., Jandt, U., Kulozik, U., Karbstein, H.P. and Emin, M.A., 2019. Investigation on the influence of high protein concentrations on the thermal reaction behaviour of β-lactoglobulin by experimental and numerical analyses. International dairy journal, 97, pp.99-110.

Rabbani, G. and Choi, I., 2018. Roles of osmolytes in protein folding and aggregation in cells and their biotechnological applications. International journal of biological macromolecules, 109, pp.483-491.

Rahaman, T., Vasiljevic, T. and Ramchandran, L., 2017. Digestibility and antigenicity of β-lactoglobulin as affected by heat, pH and applied shear. Food chemistry, 217, pp.517-523.

Rahman, M.S., Hossain, K.S., Das, S., Kundu, S., Adegoke, E.O., Rahman, M.A., Hannan, M.A., Uddin, M.J. and Pang, M.G., 2021. Role of insulin in health and disease: an update. International journal of molecular sciences, 22(12), p.6403.

Rajan, R., Ahmed, S., Sharma, N., Kumar, N., Debas, A. and Matsumura, K., 2021. Review of the current state of protein aggregation inhibition from a materials chemistry perspective: Special focus on polymeric materials. Materials Advances, 2(4), pp.1139-1176.

Ramakrishna, D., Prasad, M.D. and Bhuyan, A.K., 2012. Hydrophobic collapse overrides Coulombic repulsion in ferricytochrome c fibrillation under extremely alkaline condition. Archives of biochemistry and biophysics, 528(1), pp.67-71.

Rambaran, R.N. and Serpell, L.C., 2008. Amyloid fibrils: abnormal protein assembly. Prion, 2(3), pp.112-117.

Recasens, A. and Dehay, B., 2014. Alpha-synuclein spreading in Parkinson's disease. Frontiers in neuroanatomy, 8, p.159.

Reddy, I.M., Kella, N.K. and Kinsella, J.E., 1988. Structural and conformational basis of the resistance of. beta.-lactoglobulin to peptic and chymotryptic digestion. Journal of agricultural and food chemistry, 36(4), pp.737-741.

Redl, B. and Habeler, M., 2022. The diversity of lipocalin receptors. Biochimie, 192, pp.22-29.

Remmele, R.L., Bhat, S.D., Phan, D.H. and Gombotz, W.R., 1999. Minimization of recombinant human Flt3 ligand aggregation at the T m plateau: a matter of thermal reversibility. Biochemistry, 38(16), pp.5241-5247.

Rocha, T.L., Brownlow, S., Saddler, K.N., Fothergill-Gilmore, L.A. and Sawyer, L., 1996. New crystal form of β-lactoglobulin. Journal of dairy research, 63(4), pp.575-584.

Roefs, S.P. and De Kruif, K.G., 1994. A model for the denaturation and aggregation of β-lactoglobulin. European journal of biochemistry, 226(3), pp.883-889.

Roefs, S.P. and De Kruif, K.G., 1994. A model for the denaturation and aggregation of β-lactoglobulin. European journal of biochemistry, 226(3), pp.883-889.

Rogol, A.D., Laffel, L.M., Bode, B. and Sperling, M.A., 2023. Celebration of a century of insulin therapy in children with type 1 diabetes. Archives of Disease in Childhood, 108(1), pp.3-10.

Rovnyagina, N.R., Sluchanko, N.N., Tikhonova, T.N., Fadeev, V.V., Litskevich, A.Y., Maskevich, A.A. and Shirshin, E.A., 2018. Binding of thioflavin T by albumins: An underestimated role of protein oligomeric heterogeneity. International journal of biological macromolecules, 108, pp.284-290.

Rovoli, M., Gortzi, O., Lalas, S. and Kontopidis, G., 2014. β-Lactoglobulin improves liposome's encapsulation properties for vitamin E delivery. Journal of liposome research, 24(1), pp.74-81.

Rutter, G.A., Pullen, T.J., Hodson, D.J. and Martinez-Sanchez, A., 2015. Pancreatic β-cell identity, glucose sensing and the control of insulin secretion. Biochemical Journal, 466(2), pp.203-218.

Rytkönen, J., 2006. Effect of heat denaturation of bovine milk beta-lactoglobulin on its epithelial transport and allergenicity.

Sacchettini, J.C. and Kelly, J.W., 2002. Therapeutic strategies for human amyloid diseases. Nature Reviews Drug Discovery, 1(4), pp.267-275.

Sadrjavadi, K., Barzegari, E., Khaledian, S., Derakhshankhah, H. and Fattahi, A., 2020. Interactions of insulin with tragacanthic acid biopolymer: Experimental and computational study. International journal of biological macromolecules, 164, pp.321-330.

Saha, S., Bhattacharjee, S. and Chowdhury, J., 2023. Interaction of plant alkaloid berberine with β-lactoglobulin: an account from spectroscopic, thermodynamic, and small-angle X-ray scattering studies aided by theoretical calculations. New Journal of Chemistry, 47(37), pp.17525-17539.

Sahin, E. and Roberts, C.J., 2012. Size-exclusion chromatography with multi-angle light scattering for elucidating protein aggregation mechanisms. Therapeutic proteins: methods and protocols, pp.403-423.

Sakai, K., Sakurai, K., Sakai, M., Hoshino, M. and Goto, Y., 2000. Conformation and stability of thiol-modified bovine β lactoglobulin. Protein Science, 9(9), pp.1719-1729.

Sakurai, K. and Goto, Y., 2002. Manipulating monomer-dimer equilibrium of bovine β-lactoglobulin by amino acid substitution. Journal of Biological Chemistry, 277(28), pp.25735-25740.

Sakurai, K., Oobatake, M. and Goto, Y., 2001. Salt-dependent monomer–dimer equilibrium of bovine β-lactoglobulin at pH 3. Protein Science, 10(11), pp.2325-2335.

Saltiel, A.R. and Kahn, C.R., 2001. Insulin signalling and the regulation of glucose and lipid metabolism. Nature, 414(6865), pp.799-806.

Samant, M., Banerjee, S.S., Taneja, N., Zope, K., Ghogale, P. and Khandare, J.J., 2014. Biophysical interactions of polyamidoamine dendrimer coordinated Fe3O4 nanoparticles with insulin. Journal of Biomedical Nanotechnology, 10(7), pp.1286-1293.

Sawyer, L. and Kontopidis, G., 2000. The core lipocalin, bovine β-lactoglobulin. Biochimica et Biophysica Acta (BBA)-Protein Structure and Molecular Enzymology, 1482(1-2), pp.136-148.

Sawyer, L., 2012. β-Lactoglobulin. In Advanced Dairy Chemistry: Volume 1A: Proteins: Basic Aspects, 4th Edition (pp. 211-259). Boston, MA: Springer US.

Sawyer, L., Brownlow, S., Polikarpov, I. and Wu, S.Y., 1998. β-Lactoglobulin: structural studies, biological clues. International Dairy Journal, 8(2), pp.65-72.

Sawyer, L., Kontopidis, G. and Wu, S.Y., 1999. β-Lactoglobulin–a three-dimensional perspective. International journal of food science & technology, 34(5-6), pp.409-418.

Seo, J.A., Hédoux, A., Guinet, Y., Paccou, L., Affouard, F., Lerbret, A. and Descamps, M., 2010. Thermal denaturation of beta-lactoglobulin and stabilization mechanism by trehalose analyzed from Raman spectroscopy investigations. The Journal of Physical Chemistry B, 114(19), pp.6675-6684.

Serno, T., Carpenter, J.F., Randolph, T.W. and Winter, G., 2010. Inhibition of agitation-induced aggregation of an IgG-antibody by hydroxypropyl-β-cyclodextrin. Journal of pharmaceutical sciences, 99(3), pp.1193-1206.

Sharma, G.S., Krishna, S., Khan, S., Dar, T.A., Khan, K.A. and Singh, L.R., 2021. Protecting thermodynamic stability of protein: The basic paradigm against stress and unfolded protein response by osmolytes. International journal of biological macromolecules, 177, pp.229-240.

Shin, J.J., Gorden, P. and Libutti, S.K., 2010. Insulinoma: pathophysiology, localization and management. Future oncology, 6(2), pp.229-237.

Sitohy, M., Billaudel, S., Haertlé, T. and Chobert, J.M., 2007. Antiviral activity of esterified α-lactalbumin and β-lactoglobulin against herpes simplex virus type 1. Comparison with the effect of acyclovir and L-polylysines. Journal of agricultural and food chemistry, 55(25), pp.10214-10220.

Sluzky, V., Klibanov, A.M. and Langer, R., 1992. Mechanism of insulin aggregation and stabilization in agitated aqueous solutions. Biotechnology and bioengineering, 40(8), pp.895-903.

Srivastava, A.K. and Pandey, S.K., 1998. Potential mechanism (s) involved in the regulation of glycogen synthesis by insulin. Molecular and cellular biochemistry, 182, pp.135-141.

Steffensen, C.L., Andersen, M.L., Degn, P.E. and Nielsen, J.H., 2008. Cross-linking proteins by laccase-catalyzed oxidation: importance relative to other modifications. Journal of agricultural and food chemistry, 56(24), pp.12002-12010.

Steiner, D.F., Park, S.Y., Støy, J., Philipson, L.H. and Bell, G.I., 2009. A brief perspective on insulin production. Diabetes, Obesity and Metabolism, 11, pp.189-196.

Stetefeld, J., McKenna, S.A. and Patel, T.R., 2016. Dynamic light scattering: a practical guide and applications in biomedical sciences. Biophysical reviews, 8, pp.409-427.

Stojadinovic, M., Burazer, L., Ercili-Cura, D., Sancho, A., Buchert, J., Velickovic, T.C. and Stanic-Vucinic, D., 2012. One-step method for isolation and purification of native β-lactoglobulin from bovine whey. Journal of the Science of Food and Agriculture, 92(7), pp.1432-1440.

Straub, S.G. and Sharp, G.W., 2002. Glucose-stimulated signaling pathways in biphasic insulin secretion. Diabetes/metabolism research and reviews, 18(6), pp.451-463.

Su, Z. and Dias, C.L., 2017. Molecular interactions accounting for protein denaturation by urea. Journal of Molecular Liquids, 228, pp.168-175.

Sulatskaya, A.I., Volova, E.A., Komissarchik, Y.Y., Snigirevskaya, E.S., Maskevich, A.A., Drobchenko, E.A., Kuznetsova, I.M. and Turoverov, K.K., 2014. Investigation of the kinetics of insulin amyloid fibrils formation. Cell and Tissue Biology, 8, pp.186-191.

Sumi, T. and Koga, K., 2019. Theoretical analysis on thermodynamic stability of chignolin. Scientific reports, 9(1), p.5186.

Surin, A.K., Grishin, S.Y. and Galzitskaya, O.V., 2019. Identification of amyloidogenic regions in the spine of insulin fibrils. Biochemistry (Moscow), 84, pp.47-55.

Surin, A.K., Grishin, S.Y. and Galzitskaya, O.V., 2020. Determination of amyloid core regions of insulin analogues fibrils. Prion, 14(1), pp.149-162.

Svedberg, T., 1939. A discussion on: The protein molecule. Proceedings of the Royal Society of London. Series A. Mathematical and Physical Sciences, 170(940), pp.40-79.

Sweeney, P., Park, H., Baumann, M., Dunlop, J., Frydman, J., Kopito, R., McCampbell, A., Leblanc, G., Venkateswaran, A., Nurmi, A. and Hodgson, R., 2017. Protein misfolding in neurodegenerative diseases: implications and strategies. Translational neurodegeneration, 6, pp.1-13.

Takagi, K., Teshima, R., Okunuki, H. and Sawada, J.I., 2003. Comparative study of in vitro digestibility of food proteins and effect of preheating on the digestion. Biological and Pharmaceutical Bulletin, 26(7), pp.969-973.

Tanford, C. and Nozaki, Y., 1959. Physico-chemical comparison of β-lactoglobulins A and B.

Tang, C.H. and Ma, C.Y., 2007. Modulation of the thermal stability of β-lactoglobulin by transglutaminase treatment. European Food Research and Technology, 225, pp.649-652.

Taulier, N. and Chalikian, T.V., 2001. Characterization of pH-induced transitions of β-lactoglobulin: ultrasonic, densimetric, and spectroscopic studies. Journal of molecular biology, 314(4), pp.873-889.

Taylor, A.I. and Staniforth, R.A., 2022. General principles underpinning amyloid structure. Frontiers in Neuroscience, 16, p.878869.

Taylor, J.P., Brown Jr, R.H. and Cleveland, D.W., 2016. Decoding ALS: from genes to mechanism. Nature, 539(7628), pp.197-206.

Thalmann, C. and Lötzbeyer, T., 2002. Enzymatic cross-linking of proteins with tyrosinase. European Food Research and Technology, 214, pp.276-281.

Torisu, T., Maruno, T., Hamaji, Y., Ohkubo, T. and Uchiyama, S., 2017. Synergistic effect of cavitation and agitation on protein aggregation. Journal of pharmaceutical sciences, 106(2), pp.521-529.

Torres, N., Noriega, L. and Tovar, A.R., 2009. Nutrient modulation of insulin secretion. Vitamins & Hormones, 80, pp.217-244.

Tranter, G.E., 2017. Protein structure analysis by CD, FTIR, and Raman spectroscopies.

Trivedi, M.V., Laurence, J.S. and Siahaan, T.J., 2009. The role of thiols and disulfides on protein stability. Current Protein and Peptide Science, 10(6), pp.614-625.

Tsai, A.M., van Zanten, J.H. and Betenbaugh, M.J., 1998. I. Study of protein aggregation due to heat denaturation: a structural approach using circular dichroism spectroscopy, nuclear magnetic resonance, and static light scattering. Biotechnology and bioengineering, 59(3), pp.273-280.

Uhrínová, S., Smith, M.H., Jameson, G.B., Uhrín, D., Sawyer, L. and Barlow, P.N., 2000. Structural changes accompanying pH-induced dissociation of the β-lactoglobulin dimer. Biochemistry, 39(13), pp.3565-3574.

van den Berg, B., Ellis, R.J. and Dobson, C.M., 1999. Effects of macromolecular crowding on protein folding and aggregation. The EMBO journal.

Verdian-Doghaei, A. and Housaindokht, M.R., 2015. Spectroscopic study of the interaction of insulin and its aptamer–sensitive optical detection of insulin. Journal of Luminescence, 159, pp.1-8.

Vestergaard, B., Groenning, M., Roessle, M., Kastrup, J.S., de Weert, M.V., Flink, J.M., Frokjaer, S., Gajhede, M. and Svergun, D.I., 2007. A helical structural nucleus is the primary elongating unit of insulin amyloid fibrils. PLoS biology, 5(5), p.e134.

Vetri, V. and Militello, V., 2005. Thermal induced conformational changes involved in the aggregation pathways of beta-lactoglobulin. Biophysical chemistry, 113(1), pp.83-91.

Vincenzi, M., Mercurio, F.A. and Leone, M., 2019. About TFE: Old and new findings. Current Protein and Peptide Science, 20(5), pp.425-451.

Virtanen, T., 2001. Lipocalin allergens. Allergy, 56, pp.48-51.

Viseu, M.I., Melo, E.P., Carvalho, T.I., Correia, R.F. and Costa, S.M., 2007. Unfolding kinetics of β-lactoglobulin induced by surfactant and denaturant: A stopped-flow/fluorescence study. Biophysical journal, 93(10), pp.3601-3612.

Walker, F.O., 2007. Huntington's disease. The Lancet, 369(9557), pp.218-228.

Wang, Q., Pan, M.H., Chiou, Y.S., Li, Z., Wei, S., Yin, X. and Ding, B., 2022. Insights from alpha-Lactoalbumin and beta-Lactoglobulin into mechanisms of nanoliposome-whey protein interactions. Food Hydrocolloids, 125, p.107436.

Wang, W., Nema, S. and Teagarden, D., 2010. Protein aggregation—Pathways and influencing factors. International journal of pharmaceutics, 390(2), pp.89-99.

Wankhede, N.L., Kale, M.B., Upaganlawar, A.B., Taksande, B.G., Umekar, M.J., Behl, T., Abdellatif, A.A., Bhaskaran, P.M., Dachani, S.R., Sehgal, A. and Singh, S., 2022. Involvement of molecular chaperone in protein-misfolding brain diseases. Biomedicine & Pharmacotherapy, 147, p.112647.

Watson, R.T. and Pessin, J.E., 2001. Subcellular compartmentalization and trafficking of the insulin-responsive glucose transporter, GLUT4. Experimental cell research, 271(1), pp.75-83.

Waudby, C.A., Dobson, C.M. and Christodoulou, J., 2019. Nature and regulation of protein folding on the ribosome. Trends in biochemical sciences, 44(11), pp.914-926.

Wilcox, G., 2005. Insulin and insulin resistance. Clinical biochemist reviews, 26(2), p.19.

Wu, C., Scott, J. and Shea, J.E., 2012. Binding of Congo red to amyloid protofibrils of the Alzheimer Aβ9–40 peptide probed by molecular dynamics simulations. Biophysical journal, 103(3), pp.550-557.

Wu, H., 1995. Studies on denaturation of proteins XIII. A theory of denaturation. In Advances in protein chemistry (Vol. 46, pp. 6-26). Academic Press.

Xu, J., Hao, M., Sun, Q. and Tang, L., 2019. Comparative studies of interaction of β-lactoglobulin with three polyphenols. International journal of biological macromolecules, 136, pp.804-812.

Xu, R., 2001. Particle characterization: light scattering methods (Vol. 13). Springer Science & Business Media.

Yakupova, E.I., Bobyleva, L.G., Vikhlyantsev, I.M. and Bobylev, A.G., 2019. Congo Red and amyloids: history and relationship. Bioscience reports, 39(1), p.BSR20181415.

Yanti, S., Wu, Z.W., Agrawal, D.C. and Chien, W.J., 2021. Interaction between phloretin and insulin: a spectroscopic study. Journal of Analytical Science and Technology, 12, pp.1-16.

Yoshikawa, M., Mizukami, T., Sasaki, R. and Chiba, H., 1978. Pre-β-lactoglobulin synthesis by mRNA from bovine mammary gland. Agricultural and Biological Chemistry, 42(11), pp.2185-2186.

Yuan, F., Ahmed, I., Lv, L., Li, Z., Li, Z., Lin, H., Lin, H., Zhao, J., Tian, S. and Ma, J., 2018. Impacts of glycation and transglutaminase-catalyzed glycosylation with glucosamine on the conformational structure and allergenicity of bovine β-lactoglobulin. Food & function, 9(7), pp.3944-3955.

Zapadka, K.L., Becher, F.J., Gomes dos Santos, A.L. and Jackson, S.E., 2017. Factors affecting the physical stability (aggregation) of peptide therapeutics. Interface focus, 7(6), p.20170030.

Zhang, Q., Cheng, Z., Chen, R., Wang, Y., Miao, S., Li, Z., Wang, S. and Fu, L., 2021. Covalent and non-covalent interactions of cyanidin-3-O-glucoside with milk proteins revealed modifications in protein conformational structures, digestibility, and allergenic characteristics. Food & Function, 12(20), pp.10107-10120.

Zhang, Q., Li, L., Lan, Q., Li, M., Wu, D., Chen, H., Liu, Y., Lin, D., Qin, W., Zhang, Z. and Liu, J., 2019. Protein glycosylation: A promising way to modify the functional properties and extend the application in food system. Critical reviews in food science and nutrition, 59(15), pp.2506-2533.

Zheng, G., Liu, H., Zhu, Z., Zheng, J. and Liu, A., 2016. Selenium modification of β-lactoglobulin (β-Lg) and its biological activity. Food chemistry, 204, pp.246-251

Zhou, H.X. and Pang, X., 2018. Electrostatic interactions in protein structure, folding, binding, and condensation. Chemical reviews, 118(4), pp.1691-1741.

CHAPTER 2

STRUCTURAL MODULATION OF INSULIN BY HYDROPHOBIC AND HYDROPHILIC MOLECULES

Structural modulation of insulin by hydrophobic and hydrophilic molecules

2.1. Introduction and literature review

2.1.1. General overview of insulin and its structure

Insulin, a pivotal hormone in mammalian physiology, plays a critical role in regulating glucose metabolism and energy balance within the body (Marshall 2006). Comprised of 51 amino acid residues, insulin is a remarkable example of molecular elegance, its structure finely tuned for its biological function. Its compact, globular form is organized into two polypeptide chains linked by disulfide bonds, with the A-chain and B-chain collaborating synergistically to form a tertiary structure vital for insulin's activity. Despite its relatively short length, the A-chain plays a significant role in the hormone's stability, harboring a critical disulfide bond between cysteine residues at positions 7 and 11. Meanwhile, the B-chain boasts two disulfide bridges, linking cysteine residues at positions 6 to 11 and 7 to 19, further bolstering insulin's structural integrity (Figure 1). Within the tertiary structure, hydrophobic interactions, hydrogen bonds, and van der Waals forces delicately sculpt the spatial arrangement of amino acid residues, fostering a conformation conducive to insulin's binding to its receptor.

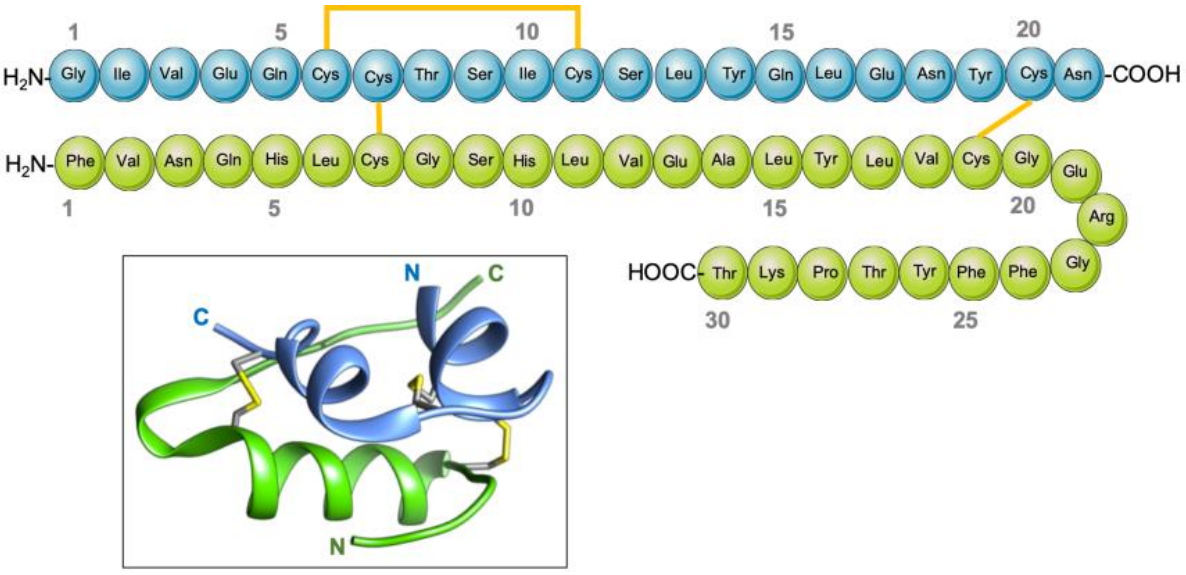

Figure 1: Diagrammatic depiction of the three-dimensional structure of human insulin (inset). Green represents the B-chain and blue the A-chain. Yellow indicates the intra- and inter-chain disulfide bridges connecting cysteine residues. (Adapted from https://pdb101.rcsb.org/global-health/diabetes-mellitus/drugs/insulin/insulin)

Functionally, insulin is a master regulator of glucose homeostasis, exerting its effects through binding to insulin receptors located on the surface of target cells, notably hepatocytes, adipocytes, and myocytes (Norton et al., 2022; Saltiel, 2016). Upon ligand binding, the insulin receptor undergoes conformational changes, initiating a cascade of intracellular events culminating in the translocation of glucose transporter proteins, particularly GLUT4, to the cell membrane, facilitating glucose uptake into cells. Additionally, insulin orchestrates anabolic processes, promoting glycogen synthesis in the liver and skeletal muscles while inhibiting gluconeogenesis and glycogenolysis (Kruszynska et al., 1986; Bouskila et al., 2008). Furthermore, insulin stimulates lipogenesis in adipose tissue, fostering the storage of excess glucose as triglycerides, thereby averting hyperglycemia and maintaining energy balance. Beyond its metabolic roles, insulin exerts profound effects on cellular growth, differentiation, and gene expression, underscoring its multifaceted significance in physiological regulation.

The synthesis and secretion of insulin are intricately regulated processes orchestrated by pancreatic β-cells nestled within the islets of Langerhans. Proinsulin, the precursor of insulin, emerges from ribosomal translation as a single polypeptide chain, subsequently undergoing post-translational modification within the endoplasmic reticulum and Golgi apparatus. Proteolytic cleavage mediated by prohormone convertases liberates the C-peptide segment from proinsulin, yielding mature insulin ready for secretion. Notably, the concomitant release of C-peptide alongside insulin serves as a valuable biomarker in clinical settings, reflecting endogenous insulin production and aiding in the assessment of pancreatic function. Under physiological conditions, insulin secretion is tightly regulated by myriad signals, including glucose, amino acids, incretin hormones, neural inputs, and metabolic substrates. Glucose, the primary stimulus for insulin release, triggers a cascade of events culminating in the depolarization of β-cell membranes and the influx of calcium ions, facilitating the exocytosis of insulin-containing vesicles into the bloodstream (Bisht et al., 2024).

Dysregulation of insulin signaling underlies the pathogenesis of various metabolic disorders, prominently type 1 and type 2 diabetes mellitus (Eizirik et al., 2020). Type 1 diabetes, characterized by autoimmune destruction of pancreatic β-cells, precipitates an absolute deficiency of insulin secretion, necessitating exogenous insulin administration for glycemic control. Conversely, type 2 diabetes ensues from a multifaceted interplay of genetic predisposition, environmental factors, and lifestyle choices, culminating in insulin resistance and impaired pancreatic β-cell function. In the early stages of type 2 diabetes, compensatory hyperinsulinemia strives to overcome peripheral insulin resistance, yet progressive β-cell

dysfunction ultimately leads to declining insulin secretion and overt hyperglycemia. Pharmacological interventions targeting insulin signaling pathways, including insulin analogs, insulin sensitizers, and incretin-based therapies, stand as cornerstones in the management of diabetes, aiming to restore euglycemia and mitigate the risk of long-term complications.

2.1.2. Introduction to Schiff's base compounds

Schiff's base compounds were first synthesized by the renowned German chemist Hugo Schiff in the late 19th century and have since been widely employed in various fields of chemistry and beyond (Subasi et al., 2022). These compounds are characterized by the presence of an imine or azomethine group (-C=N-) resulting from the condensation reaction between a primary amine and a carbonyl compound, usually an aldehyde or a ketone. The carbon-nitrogen double bond in the imine group imparts unique properties and reactivity to Schiff base compounds, making them highly versatile in structural design and molecular engineering.

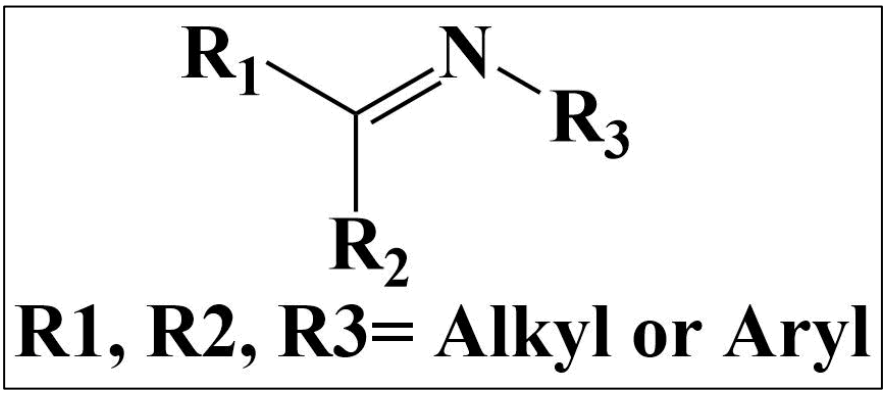

Schiff base compounds can be tailored to meet specific requirements for a wide range of applications by carefully selecting different amine and carbonyl components, allowing for the development of Schiff base compounds with diverse functionalities, including fluorescent probes, catalysts, ligands for metal complexes, and molecular switches. Additionally, Schiff bases have garnered significant attention due to their biological activities, with many naturally occurring compounds featuring Schiff base functionalities. Synthetic Schiff bases have also been explored for their pharmacological properties, including antimicrobial, antiviral, anticancer, and antioxidant activities.

The unique electronic structure of Schiff base compounds contributes to their diverse reactivity. The carbon-nitrogen double bond in the imine group can undergo various chemical transformations, including hydrolysis, reduction, and addition reactions. These reactions enable the functionalization of Schiff bases to introduce different substituents or modify their

chemical properties. Moreover, the imine bond can serve as a site for coordination with metal ions, leading to the formation of metal complexes with intriguing properties and catalytic activities.

Schiff base compounds have found applications in many areas of chemistry, including organic synthesis, coordination chemistry, materials science, and catalysis. In organic synthesis, they are employed as versatile intermediates for constructing complex molecules, allowing for forming of carbon-carbon and carbon-heteroatom bonds through efficient and selective reactions. In coordination chemistry, Schiff base ligands are widely used for the preparation of metal complexes with diverse structures and functionalities, which find applications in catalysis, sensing, and materials synthesis.

The development of new methodologies for synthesizing and functionalizing Schiff base compounds continues to be an active area of research in contemporary organic chemistry. Advances in catalysis, green chemistry, and computational methods have enabled the discovery of novel reactions and applications of Schiff bases, expanding their utility and relevance in modern chemical research. The interdisciplinary nature of Schiff base chemistry, bridging organic, inorganic, and biological chemistry, offers exciting opportunities for collaboration and innovation in addressing complex scientific challenges.

2.1.3. Chemical properties of Schiff bases

The characteristics of Schiff bases vary depending on the substituents attached to the azomethine group. An electronegative group bound to the nitrogen atom improves the stability of the azomethine molecule. Schiff bases with alkyl or aryl substituents on the nitrogen atom are considerably less stable against hydrolysis than oximes with hydroxyl groups on the nitrogen atom, phenylhydrazone, and semicarbazones with -NH groups. Schiff bases are resistant to alkalies, but in an acidic environment, they can hydrolyze to form amine and carbonyl compounds.

One mole of water is produced by the reversible reaction that forms Schiff bases, and the reaction is pushed to the left by the presence of water in the surrounding environment. Consequently, the reaction is typically conducted in solvents that generate an azeotrope by distilling water out of the surrounding environment. When amines with an electronegative atom and unpaired electrons in the nitrogen atom are used in the reaction, the reaction completes, and high-efficiency Schiff bases can be produced without hydrolysis.

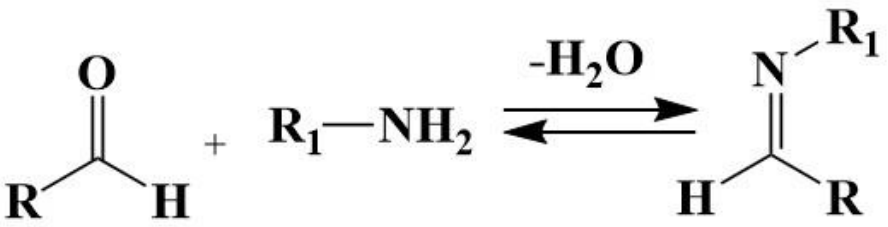

Scheme 1: Schiff base formation reaction.

2.1.4. Interactions of various Schiff bases with human insulin

Schiff bases are versatile organic compounds that feature a unique functional group formed by substituting a carbon atom for a nitrogen atom in a primary amine. These compounds are widely used in organic synthesis and coordination chemistry, and ongoing research has shown that they interact with human insulin in a variety of ways. Given their potential implications for diabetes treatment, scientists continue to explore the many applications of Schiff bases.

In a recent study by Chigurupati and colleagues (2021), 4-Hydroxy-3-methoxybenzaldehyde Schiff bases were successfully prepared using an environmentally friendly, time-saving green synthesis process. These compounds have demonstrated potential for stabilizing insulin levels and could serve as a therapeutic option for type 2 diabetes mellitus (T2DM) due to their insulin-degrading function. S2 has shown the most promising potential among all the compounds analyzed. While S1 and S3 also show potential as drug candidates, they are slightly inferior to S2 in all analytical data. Further in-depth investigations on S1 and S3 are therefore advisable. With its convincing prospects in the synthesis of insulin-degrading enzyme (IDE), S2 could emerge as a promising lead compound in reversing the negative impact of T2DM on quality of life (Chigurupati et al., 2021).

A study by Halevas et al. (2015) showed that Schiff base ligands were synthesized with varying numbers of alcoholic moieties attached to a vanillin core and used to synthesize binary V(V)-Schiff compounds. The resulting materials had distinct structural properties and were assessed for toxicity. Those with the lowest toxicity were selected for further cell-differentiation studies, which showed that V(V) has insulin-like behavior and can promote pre-adipocyte differentiation into mature adipocytes. The number of alcoholic moieties tethered to the vanillin core bound to V(V) likely contributes to that metal ion's insulin-like bioactivity. These findings could lead to the development of efficient anti-diabetic vanadodrugs in the future (Halevas et al., 2015).

2.1.5. Interaction of human insulin with various hydrophilic and hydrophobic molecules

Two magnetic imprinted polymers, MMIP2 and MMIP3, were created in a recent study by Gheybalizadeh et al. (2022) with the goal of enhancing insulin bioseparation. The results of the study showed that during the pre-polymerization phase, complex formation was improved by the imprinted polymer based on insulin structure. The imprinting effect, adsorption capacity, and imprinted site configuration were all improved by MMIP3, which has hydrophilic and hydrophobic functional groups that closely resemble those of natural antibodies. Conversely, the hydrophobic effect of MMIP2 demonstrated a higher imprinting factor and selectivity coefficient towards insulin despite forming a weaker hydrophobic association in an aqueous environment. The investigation also demonstrated that the effectiveness of MMIPs in each scenario is highly dependent on the proper kind and molar ratio of functional monomers toward the target insulin structure and surface charge (Gheybalizadeh et al., 2022).

The phenomenon of insulin amyloidal aggregates forming on material surfaces is well-known and has significant implications for pharmaceutical and medical applications. In a study by Nault et al. (2013), surface plasmon resonance imaging was used to monitor real-time insulin adsorption on hydrophobic surfaces. Insulin adsorbs in two stages: a quick phase that lasts less than a minute and creates a protein monolayer and a longer phase that can last up to an hour and involves the formation of multilayered protein aggregates. The kinetics of dissociation identifies two insulin populations: a pool of tightly bound insulin aggregates and a quickly dissociating pool. These populations interconvert slowly. The adsorbed insulin has essentially stopped dissociating from the surface after an hour of contact between the protein solution and the surface. Attenuated total reflection–Fourier transform infrared spectroscopy is used to investigate the structure of adsorbed insulin (Figure 2). Insulin adsorption is linked to distinct shifts in the amide A and amide II′ bands. Unlike soluble or aggregated insulin, the amide I band changes gradually over time. A peak of 1708 cm−1 is detected, representing insulin adsorbed for durations over half an hour. Ultimately, after 30 to 40 minutes, thioflavin T, a hallmark of elongated β-sheet structures found in amyloid fibers, binds to adsorbed insulin. These results imply that more insulin binding from the solution is made possible by the conformational change in insulin that is brought about by binding to hydrophobic surfaces. According to Nault et al. (2013), adsorbed insulin functions as a mediator in the α-to-β structural transition that generates amyloidal fibers on these material surfaces. (Nault et al., 2013).

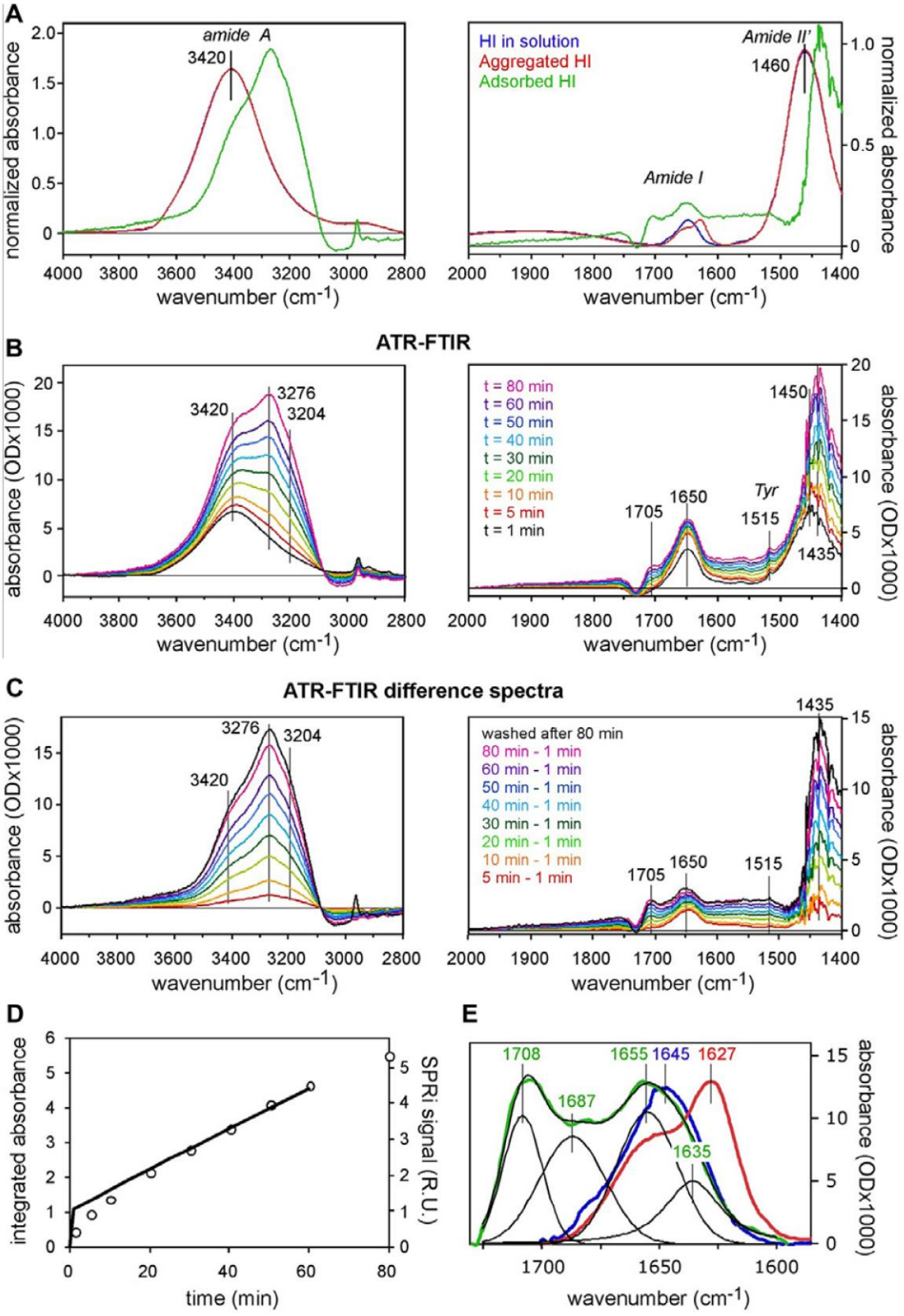

Figure 2: ATR-FTIR spectra of HI adsorbed on hydrophobic surfaces. The left and right panels in (A), (B), and (C) show the spectra in the 4000–2800 cm^{-1} and 2000–1400 cm^{-1} ranges, respectively. The baseline was zeroed at 4000 or 2000 cm^{-1} in the left and right panels,

respectively, with the exception of the right panel of (A), where the zero was set at the minimum. Three experiments' worth of data are represented. (A) Transmission FTIR spectra of aggregated (red) and soluble (blue) HI. ATR-FTIR spectra of hydrogen adsorbed on a hydrophobic surface for 80 minutes and then cleaned (green). The same total area has been used to standardize the spectra. (B) Using the same hydrophobic surface, successive ATR-FTIR spectra were obtained for 80 minutes while an 86 μM HI solution was passed over it. The right panel shows the current time. (C) The identical data as in (B). To display the increase in adsorbed HI, the ATR-FTIR spectra recorded after one minute has been subtracted from those recorded later. Furthermore, the spectrum acquired following an 80-minute interaction with the HI solution and a 1-minute washing is also presented. (D) Total absorbance of adsorbed HI computed as a function of time using Eq. (3) integrated over the ranges of 2000–1400 cm^{-1} and 4000–2800 cm^{-1}. The association SPRi differential signal is shown as a thick line for comparison. (E) HI adsorbed for 80 minutes on hydrophobic surfaces (green), aggregated HI (red), and the amide I band of soluble HI (blue). Information comes from (A). For soluble HI and aggregated HI spectra, the baseline is linearly adjusted between 1700 and 1570 cm^{-1}, and for the adsorbed HI spectrum, it is modified between 1730 and 1570 cm^{-1}. The breakup of the band into four peaks in the instance of the adsorbed HI spectra is shown as thin lines that indicate the individual peaks and their sum (Adapted from Nault et al., 2013)

Insulin has become a popular choice for biomedical research due to its small size and simple tertiary structure. Researchers have recently focused on studying how insulin adsorbs to various surfaces, as it can provide insight into how surface/protein hydrophilic/hydrophobic interactions affect protein refolding and aggregation (Figure 3). However, the model surfaces used in these studies are vastly different from physiological surfaces. In 2015, Mauri et al. conducted a study to better understand how insulin interacts with biological surfaces by investigating its adsorption at lipid monolayers and studying the effects of minor mutations in its primary amino acid sequence on its interaction with 1,2-Dipalmitoyl-sn-glycero-3-phosphoglycerol (DPPG) model lipid layers. The team used sum frequency generation spectroscopy (SFG) to examine the structure of bovine and human insulin at the lipid/water interface and complemented their findings with XPS analysis of Langmuir-Schaefer deposited lipid/insulin films. Interestingly, the group discovered that bovine and human insulin, despite their sequence similarities, behave differently when interacting with lipid films (Mauri et al., 2015).

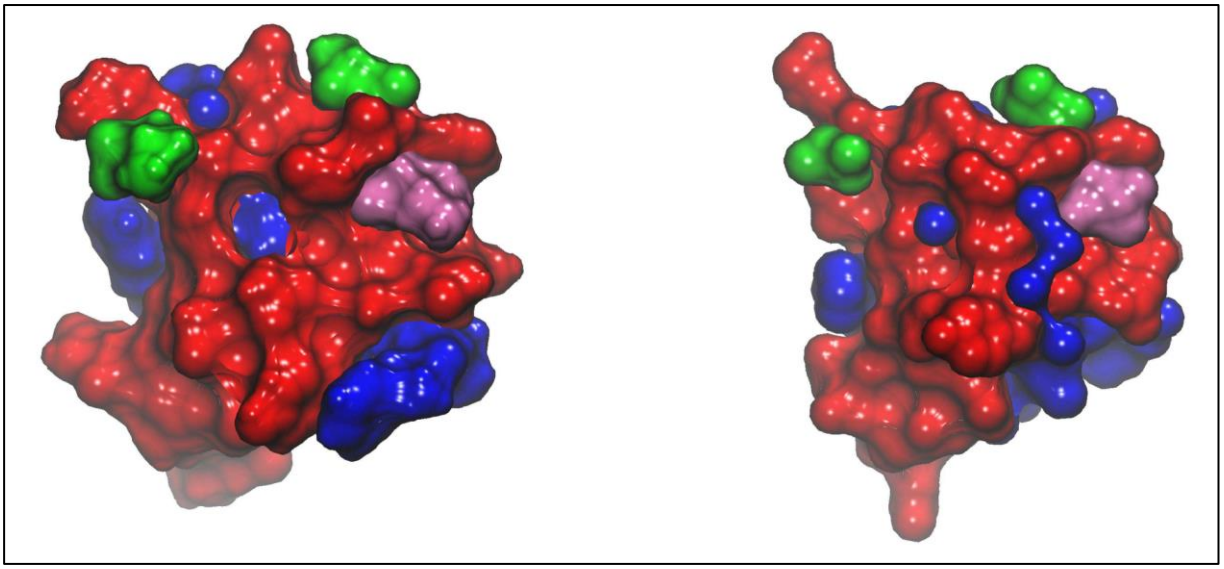

Figure 3: Right: human insulin. Left: bovine insulin. Hydrophilic residues are shown in red. Hydrophobic residues are shown in blue. Residue A8 (top right) and B30 (top left) are shown in green. Residue A10 is shown in pink. (Adapted from Mauri et al., 2015)

In 2019, Salar et al. conducted a study to examine how chitosan and cholesterol-grafted chitosan polymers impact the structure and dynamics of human insulin. The goal was to evaluate the important interactions involved in the peptide hormone's encapsulation process by carbohydrate polymers. The study found that the presence of chitosan and cholesterol-modified chitosan polymers did not significantly alter the native conformation of insulin (Figure 4). However, increasing the cholesterol content of the chitosan derivatives decreased the interactions between the carbohydrate polymer and the peptide hormone. The research also revealed that aromatic residues, such as phenylalanine and tyrosine, as well as negatively charged residues, played a critical role in forming insulin-polymer complexes. The MD simulation results also suggested that van der Waals, electrostatic, and CH-π interactions were the primary factors controlling insulin encapsulation. Overall, the study concluded that chitosan polymers were a more suitable carrier for human insulin than cholesterol-modified chitosan polymers (Salar et al., 2019).

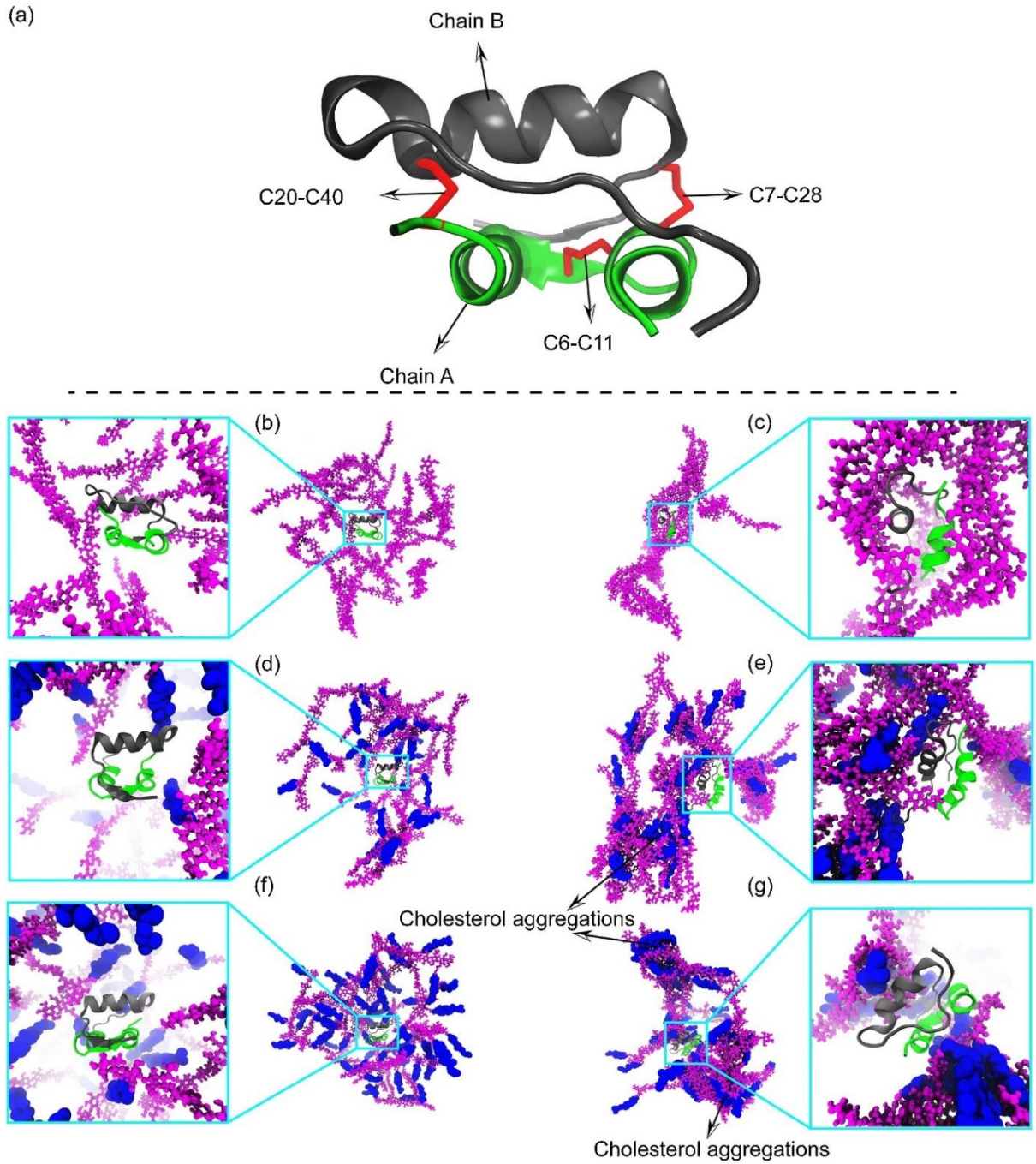

Figure 4: (a) Human insulin's native conformation is depicted as a new cartoon model. Chain A and chain B are colored in green and gray, respectively. C6-C11, C7- C28, and C20-C40 represent disulfide bonds between Cys6-Cys11, Cys7-Cys28, and Cys20-Cys40, respectively. The first frame of the trajectory of the chitosan (b), chit_1chl (d), and chit_2chl (f) systems. (c), (e) and (g) show the last frame of the trajectory of the chitosan, chit_1chl, and chit_2chl systems, respectively. The chitosan polymers and the cholesterol moieties are colored magenta and blue, respectively. (Adapted from Salar et al., 2019)

Human insulin exhibits a significant attraction for hydrophobic Teflon particles, even in the presence of electrostatic repulsion, as reported by Mollmann et al. in 2006. The hydrophobic amino acids on the outside of insulin and the Teflon surface's dryness are to blame for this. Insulin adsorption modifies its secondary structure by enhancing the unordered structure and lowering the α-helix. Fluorescence investigations in TrpB30 insulin also reveal alterations in the surrounding environment of tryptophan. Furthermore, adsorbed insulin's thermal stability differs from that of insulin in solution. The immediate environment of the tryptophan in TrpB30 insulin appears to be impacted, although TIRF experiments show that the N-terminal end of the B-chain is not implicated in adsorption. Interestingly, the desorption mechanism changes when washing with human insulin, and adsorbed insulin molecules cannot be removed from the surface by dilution (Mollmann et al., 2006).

In 1991, Nilsson et al. conducted a study using in situ ellipsometry to investigate the adsorption of insulin on different silica surfaces. The study explored three surfaces: clean hydrophilic silica, methylated hydrophobic silica, and silica with a wettability gradient. The researchers utilized both human insulin and modified monomeric insulin in their investigation. The study concluded that insulin adsorption depended on the surface properties of the different oligomeric forms of insulin. Regarding the hydrophilic negatively charged silica surface, the adsorption of insulin, which carries a negative net charge, was found to rely on the concentration, ionic strength, and type of ions present. However, the study did not observe any adsorption of monomeric insulin on the hydrophilic surface. The hexameric form of insulin is believed to be responsible for adsorbing to the hydrophilic surface, with electrostatic forces governing the adsorption process. In contrast, the adsorption of insulin on the hydrophobic surface was discovered to be independent of the concentration and largely independent of the ionic strength and type of ions added. The study found that the amounts of human insulin and monomeric insulin adsorbed on the hydrophobic surface were identical. There is substantial evidence to support the idea that the monomeric form of insulin adsorbs to the hydrophobic surface, with hydrophobic interaction driving the adsorption process (Nilsson et al., 1991).

Developing alternative methods for diabetes therapy is a significant challenge due to the unwanted aggregation of aqueous insulin solutions. In 1992, Sluzky and colleagues conducted research on the aggregation mechanism and proposed stabilization strategies based on a mathematical model. They employed UV spectroscopy and quasielastic light scattering (QELS) to monitor insulin aggregation kinetics in the presence of solid-liquid and air-liquid interfaces. The observations confirmed the model of monomer denaturation at hydrophobic

surfaces, leading to the formation of stable intermediate species that facilitated subsequent macroaggregation. The model was then utilized to predict insulin aggregation behavior, propose stabilization strategies, and elucidate stabilization mechanisms. Insulin solutions without additives aggregated entirely within 24 hours, resulting in the loss of over 95% of the soluble protein. However, no significant loss was detected with sugar-based nonionic detergents for more than six weeks (Sluzky et al., 1992).

In 2009, Rekha et al. conducted a research study that resulted in the development of a new form of chitosan known as lauryl succinyl chitosan (LSC). The primary objective of this development was to assess its potential as a drug delivery system for oral peptides. Sodium tripolyphosphate (TPP) cross-linking was used to create nano/microparticles from this derivative. Human insulin was utilized as the model protein drug to examine the release kinetics at gastrointestinal pH. The presence of succinyl carboxyl groups inhibited the release kinetics of insulin at pH 1.2, reducing it by approximately 8.5 ± 0.45% in two hours. The results demonstrated that hydrophobic moieties controlled the release of insulin from the particles at intestinal pH. The particles ranged in size from 315 nm to 1.090 μm and had a negative charge. Rat intestinal jejunum was used to assess the mucoadhesive capability ex vivo. The tight junction permeability in Caco 2 cells and the rat intestinal epithelium's in vivo uptake of the FITC-insulin from loaded nanoparticles were both validated by confocal microscopy investigations. In comparison to native chitosan particles, the results demonstrated that the modified chitosan containing both hydrophilic (succinyl) and hydrophobic (lauryl) moieties enhanced the release properties, mucoadhesivity, and permeability of insulin. According to Rekha et al. (2009), the LSC2 particles were observed to lower blood glucose levels in diabetic rats for roughly six hours, suggesting that this novel derivative is a viable option for oral peptide delivery. (Rekha et al., 2009).

The structure of proteins is highly sensitive to their microenvironments, which can be altered by various factors such as pH, temperature, salt concentration, and different types of small molecules. These changes may significantly affect the function of proteins, making the study of modulator-protein interactions an important area of research within the scientific community.

Human insulin is a protein hormone that plays a crucial role in regulating blood sugar levels. Its exposure and availability in the body have been linked to several widespread medical conditions, such as hypertension, coronary heart disease, stroke, cancer, and type II diabetes.

Insulin is a small monomeric protein consisting of fifty-one amino acids and two α-helical structures held together by three disulfide bonds (intra-chain and inter-chain). Due to its small size, insulin is highly unstable, and various factors can influence its structure. Insulin frequently interacts with glucose, a polar poly-hydroxyl group-containing molecule in the serum. However, the presence of hydrophobic molecules in the serum can significantly affect insulin's structure and function, leading to insulin-related diseases. Thus, investigating the effect of hydroxyl and hydrophobic molecules on insulin's structure is crucial.

Protein-small molecule interaction studies play a significant role in examining the structural effects of proteins under diverse microenvironments. The microenvironment can be tuned through the proper selection of small molecules. Schiff's base is a widely used class of compounds that can be synthesized through simple organic reactions, such as the reaction between an aldehyde and a primary amine. The products of this reaction are known as Schiff's bases, which can be used to generate hydrophilic and hydrophobic molecules by selecting the appropriate substituents attached to the amine and aldehyde parts. Schiff's bases are used extensively in various fields of science, such as coordination chemistry, hydrogels, sensing, analytical chemistry, electronics, optics, etc.

To investigate the interaction of insulin with different microenvironments, we synthesized two Schiff's bases, one hydrophobic, (E)-2-((tert-butylimino) methyl)-6-methoxyphenol (**3a**), and one hydrophilic, (E)-2-((2-hydroxy-3-methoxybenzylidene)amino)-2-(hydroxymethyl)propane-1,3-diol (**3b**), and studied their interactions with insulin. Thus, this study provides an opportunity to monitor insulin's structure in two opposite microenvironments.

2.2. Aims and objectives of the study

- To synthesize two novel Schiff base compounds having extremely hydrophilic and hydrophobic side chains.
- To investigate the effect of molecules with hydroxyl groups and hydrophobic groups on the insulin's structure.
- The effects of hydrophilic and hydrophobic molecules on the insulin binding process have been investigated through a multi-spectroscopic approach.
- Investigation of insulin stability in the presence of the developed compounds.

2.3. Materials

Table 1. List of materials/chemicals used in the study

Serial No	Name	Source
1.	Human insulin (Huminsulin)	Eli Lilly, USA
2.	*o*-vanillin	Sigma-Aldrich, USA
3.	Tris(hydroxymethyl)aminomethane	Sigma-Aldrich, USA
4.	Tert-butyl amine	Sigma-Aldrich, USA
5.	Acetic acid	Merck, Germany
6.	Hydrochloric acid (HCl)	Merck, Germany
7.	8-anilinonaphthalene-1-sulfonic acid ammonium salts (ANS)	Sigma Chemical (St. Louis, USA)
8.	Thioflavin T (ThT)	Sigma Chemical (St. Louis, USA)

2.4. Methodology

2.4.1. Preparation and purification of monomeric state of insulin

The hexameric state of insulin, which is marketed at a concentration of 100 IU/mL (equivalent to 2 mg/mL), typically contains *m*-cresol as a preservative, glycerin as a tonicity modifier, and HCl/NaOH to adjust the pH. However, these substances were removed via extensive dialysis with water. To convert the hexameric insulin to a monomeric state, 80% acetic acid was added, resulting in a final concentration of 20%. To ensure the formation of amyloid-like fibrils, the solution was subsequently filtered through a 0.22 μm (Millipore) filter membrane to eliminate any traces of hexameric molecules. The filtrate was then allowed to incubate at 37°C overnight, resulting in a homogeneous solution of monomeric insulin with a concentration of 1.5 mg/mL. During this process, an optical value of ε (276 nm) = 10.0 was measured (Paul et al., 2024).

2.4.2. Synthesis of Schiff base compounds

In a round-bottomed flask of 10 mL volume, which is equipped with a condenser and a stirring bar, a mixture consisting of ethanol (3 mL), ortho-vanillin (1.0 mmol), amine (1.2 mmol), and a single drop of acetic acid was added. After the addition of the aforementioned components,

the solution turned yellow in color. The mixture was then subjected to reflux for three hours with continuous stirring and subsequently allowed to cool down to room temperature. Following cooling, 10 mL of water was added to the mixture, and the resulting mixture was extracted with CH_2Cl_2 (3 × 5 mL). The combined organic layer was then dried over anhydrous Na_2SO_4 and evaporated in a vacuum. Finally, the compounds obtained (**3a**, **3b**) were purified either by crystallization or column chromatography, followed by crystallization.

2.4.3. UV-visible spectroscopy

The present study employed a JASCO Spectrophotometer model number V700 (Serial Number B184461798) to precisely measure the absorbance at room temperature (25°C) for determining the binding affinity and binding constants (Yanti et al., 2021). The UV titration technique was implemented by gradually increasing the concentration of insulin (1-20 μM) for **3a** and **3b**, which were kept at a constant concentration of 20 μM in Milli-Q water in a 1 cm quartz cuvette. The UV-visible spectra were recorded between 200-600 nm. Additionally, the stability of the compounds was evaluated through UV-vis spectroscopy in water at a concentration of 20 μM over time. These experimental procedures were carried out to ascertain the physicochemical properties of the compounds under investigation.

2.4.4. Intrinsic fluorescence study of insulin in the presence of Schiff base compounds

At room temperature, a fluorescence quenching study was carried out utilizing a HORIBA machine (Model: FLUOROMAX-4C, serial no. 1734D-4018-FM). The solutions were excited at 276 nm, and the emission was monitored in the range of 290-400 nm, with the excitation and emission slits set at 5 nm. The concentration of insulin was kept constant at 25 μM while **3a** and **3b** were sequentially added in concentrations ranging from 2 to 24 μM. The excitation wavelength for **3a** and **3b** derivatives was 335 nm and 325 nm, respectively, and the emission was recorded between 350-550 nm. In order to gain a better understanding of the spectroscopic behavior of both compounds, concentration-dependent fluorescence spectroscopy was recorded in water at the given excitation wavelength (Chauhan et al., 2017).

2.4.5. ANS assay for monitoring the hydrophobicity changes

The hydrophobicity of protein molecules was evaluated using a fluorescent probe, 1-anilinonapthalene-8-sulfonate (ANS), which selectively binds to the hydrophobic pockets of the protein molecules (Alavi et al., 2013). This assay is a commonly employed tool in the domains of biochemistry and molecular biology to investigate the intricate aspects of protein

folding, stability, and interactions. ANS, a hydrophobic dye, is known for its relatively weak fluorescence in aqueous environments. However, when ANS binds to the hydrophobic regions of proteins, it exhibits a remarkable increase in fluorescence intensity. Our study determined the hydrophobicity by preparing a stock solution of ANS and adding it to 2 mL of monomeric insulin samples. The final concentration of ANS in each sample was maintained at a constant value of 30 μM. The protein samples were subsequently treated with **3a** and **3b** chemicals at doses ranging from 2 to 60 μM and 2 to 60 μM, respectively. The emission spectra were measured from 390 to 600 nm, with excitation at 350 nm, using a Shimadzu Spectrofluorometer (Shimadzu 5301 PC). The path length was set to 1 cm, and both the excitation and emission slits were set at 5 nm. The results obtained from this study can provide significant insights into the hydrophobicity of protein molecules, which is a critical factor in various biological processes such as protein-protein interactions and protein folding.

2.4.6. Circular dichroism (CD) spectroscopy

Circular dichroism (CD) spectroscopy is an analytical technique that has significantly contributed to the fields of chemistry, biochemistry, and structural biology. This technique is widely used to investigate molecules' secondary structure, conformational changes, and interactions, particularly proteins, nucleic acids, and chiral small molecules (Falconi et al., 2001). By measuring the differential absorption of left-handed circularly polarized light (L-CPL) and right-handed circularly polarized light (R-CPL) by optically active molecules, CD spectroscopy provides valuable information that can be used to unravel the complex structures and functions of biomolecules. We conducted a study to investigate the impact of Schiff bases **3a** and **3b** on insulin employing a Jasco spectropolarimeter (Model: J-815). The experiments were performed under a nitrogen atmosphere with a quartz cell of path length 0.2 cm in the far-UV region (200–260 nm). The insulin concentration remained constant at 6 μM, while the concentrations of **3a** and **3b** were varied between 1-6 μM. We acquired spectral data ranging from 260 to 200 nm at a scan speed of 50 nm per minute. The sample temperature was maintained at 25 °C using a Neslab circulating water bath connected to water-jacketed quartz cuvettes. We employed CDNN 2.1 software to compute the secondary structures of insulin.

2.4.7. Molecular docking

Molecular docking represents a fundamental computational technique employed extensively within the field of structural biology (Muhammad et al., 2016). Its primary purpose is to predict the optimal binding mode and affinity of a small molecule (ligand) to a protein target. The

crystal structure of human insulin was obtained from the RCSB Protein Data Bank website (PDB ID: 3I40), which was then analyzed and prepared for a docking experiment. The **3a** and **3b** structures were optimized using the Density Functional Theory (DFT) B3LYP/6-31G level of theory to minimize energy. MEP was carried out using the same functional and basis sets. These optimized structures were docked with insulin protein to determine the most probable site and mode of binding, utilizing the grid-based docking program Auto Dock 4.2. To ensure accuracy, the protein and water molecules' ligands were removed from the protein, Atom Kollman charges were assigned, and polar hydrogen was added to the protein. The default parameters of Auto Dock and the generic algorithm were utilized for the calculation. The visualization effects were expertly generated using Discovery Studio 4.1 Client. The accuracy and validity of our findings are confidently asserted. SwissADMET was employed to predict the polar surface area, lipophilicity, and water solubility.

2.5. Results and discussion

2.5.1. Synthesis of Schiff's base and choice of compounds

Insulin, a hormone that regulates glucose metabolism, binds with glucose, a polar polyhydroxy compound. We have designed a polyhydroxy compound to investigate the effect of attaching a hydrophobic molecule to insulin. To achieve this, we have designed a similar molecule without the hydroxyl group. Our study has revealed that electron-rich aromatic molecules possess a unique protein binding ability. Therefore, we plan to separately attach a polyhydroxyl group containing a hydrophobic moiety and an aromatic moiety with a hydroxyl group. For this purpose, we will use Schiff bases formation reaction, which is a convenient choice for joining these two moieties. To do this, we have selected two amine compounds: 2-amino-2-(hydroxymethyl) propane-1,3-diol for the polyhydroxyl moiety and 2-methylpropan-2-amine for the hydrophobic moiety. We require an electron-rich aldehyde for Schiff base formation, and ortho-vanillin is the optimal choice due to its ortho-hydroxy and meta-methoxy groups along with aldehyde at the benzene ring.

Under refluxing conditions in dry ethanol, the reaction between ortho-vanillin (1) and aliphatic amine (2) yielded corresponding Schiff bases. With the addition of one drop of glacial acetic acid, this reaction proceeded for three hours. When tert-butyl amine (2a) and 2-amino-2-(hydroxymethyl)propane-1,3-diol (2b) were employed in the reaction, high-yield production of compound **3a** and **3b** were achieved respectively (Scheme 2). The compounds were characterized through the use of ^{1}H NMR.

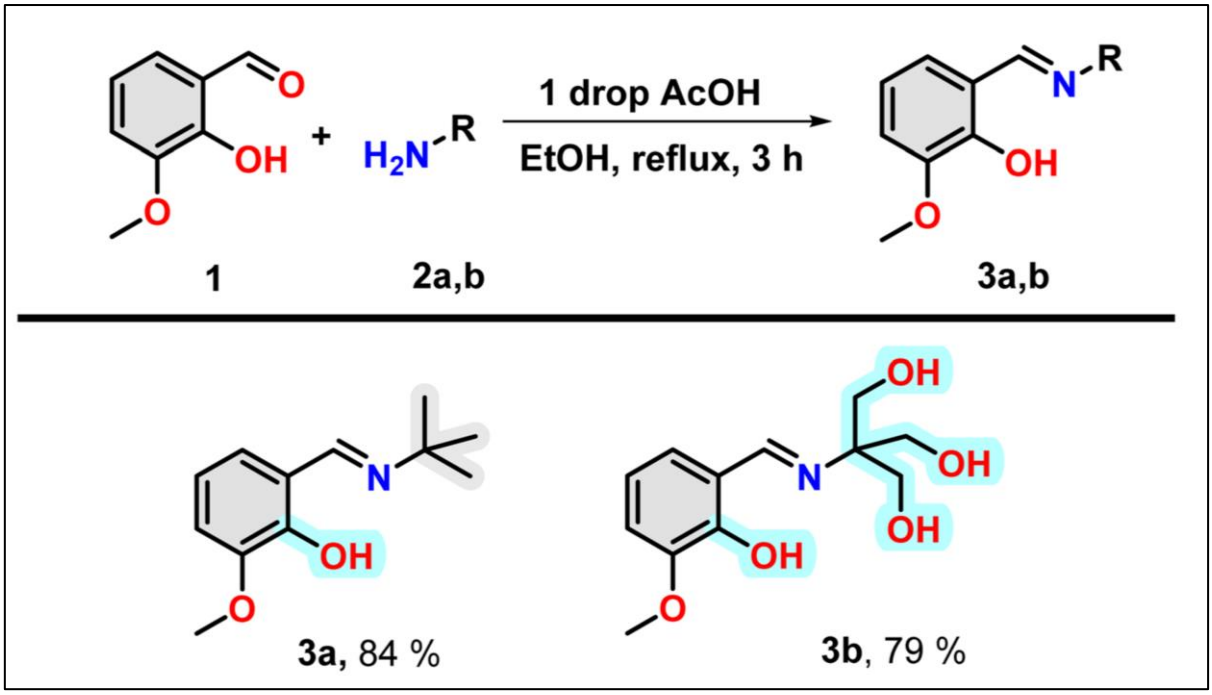

Scheme 2: Synthetic schemes of Schiff base compounds **3a** and **3b**.

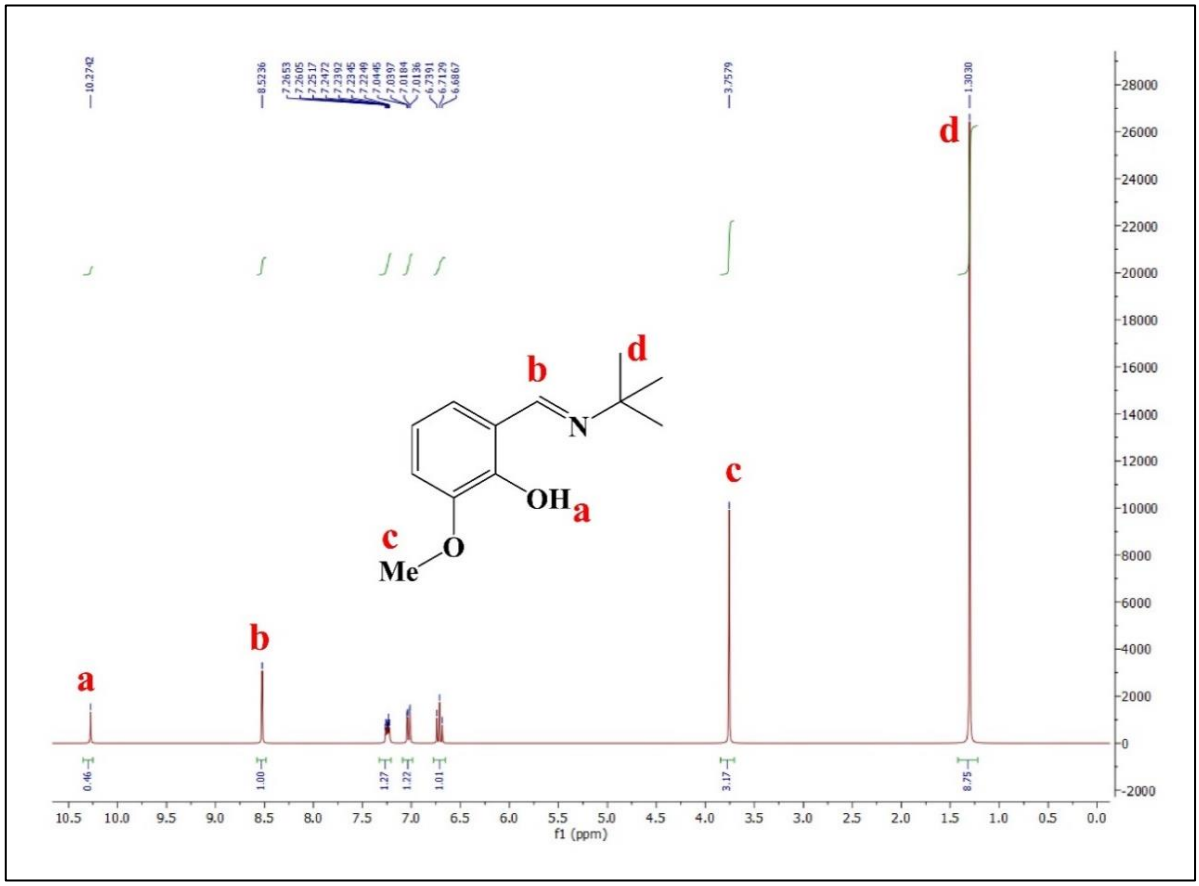

Figure 5: The ^{1}H NMR spectra of **3a**.

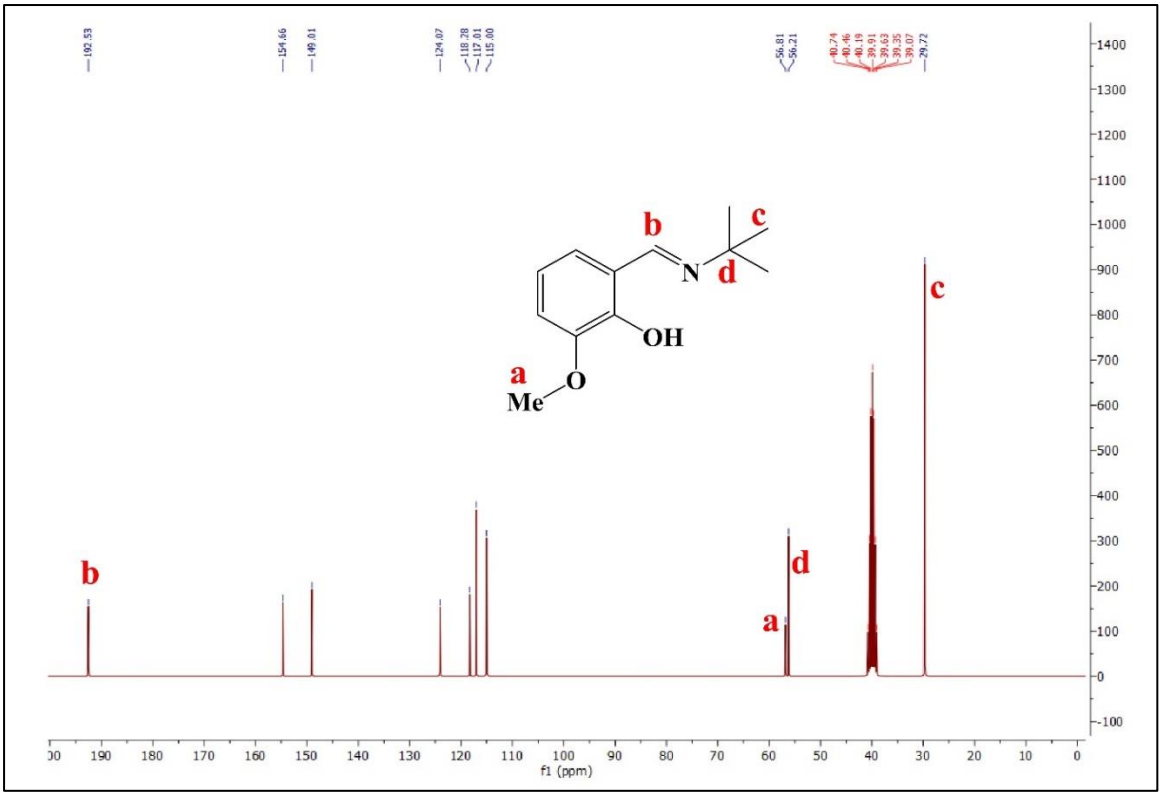

Figure 6: The ^{13}C NMR spectra of **3a**.

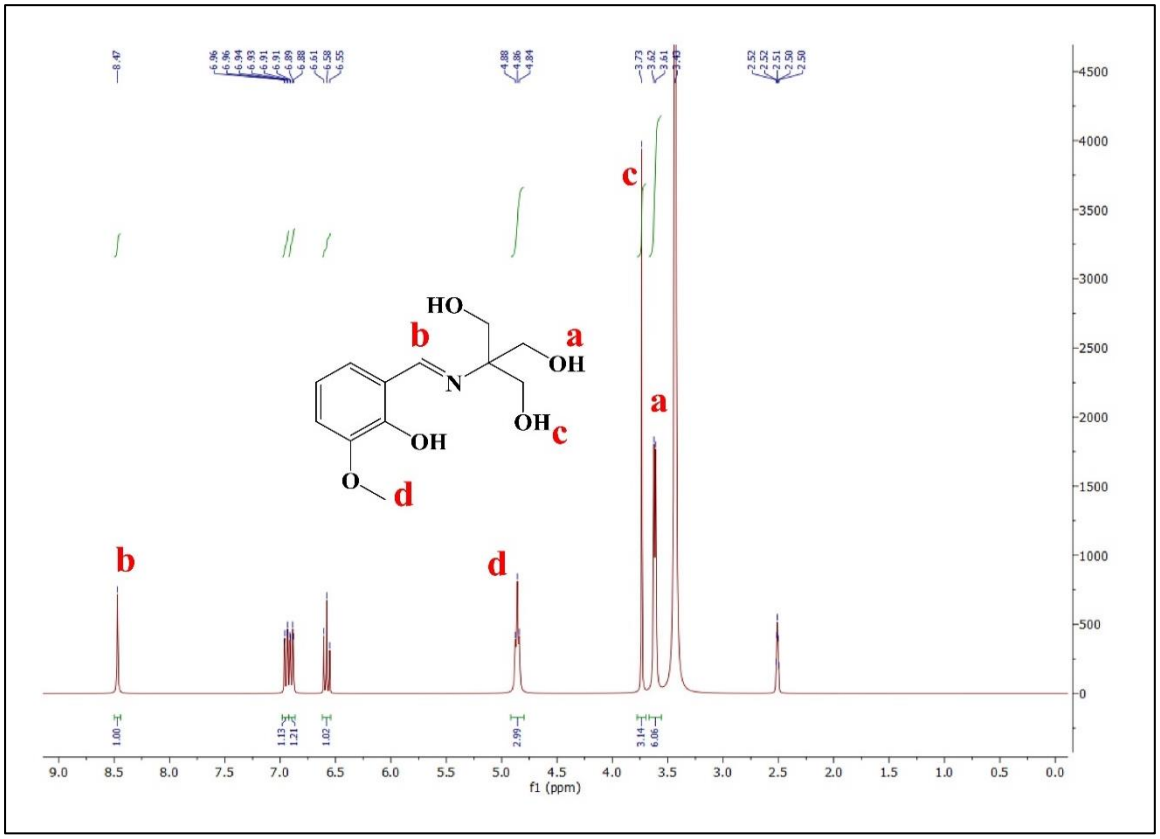

Figure 7: The ^{1}H NMR spectra of **3b**.

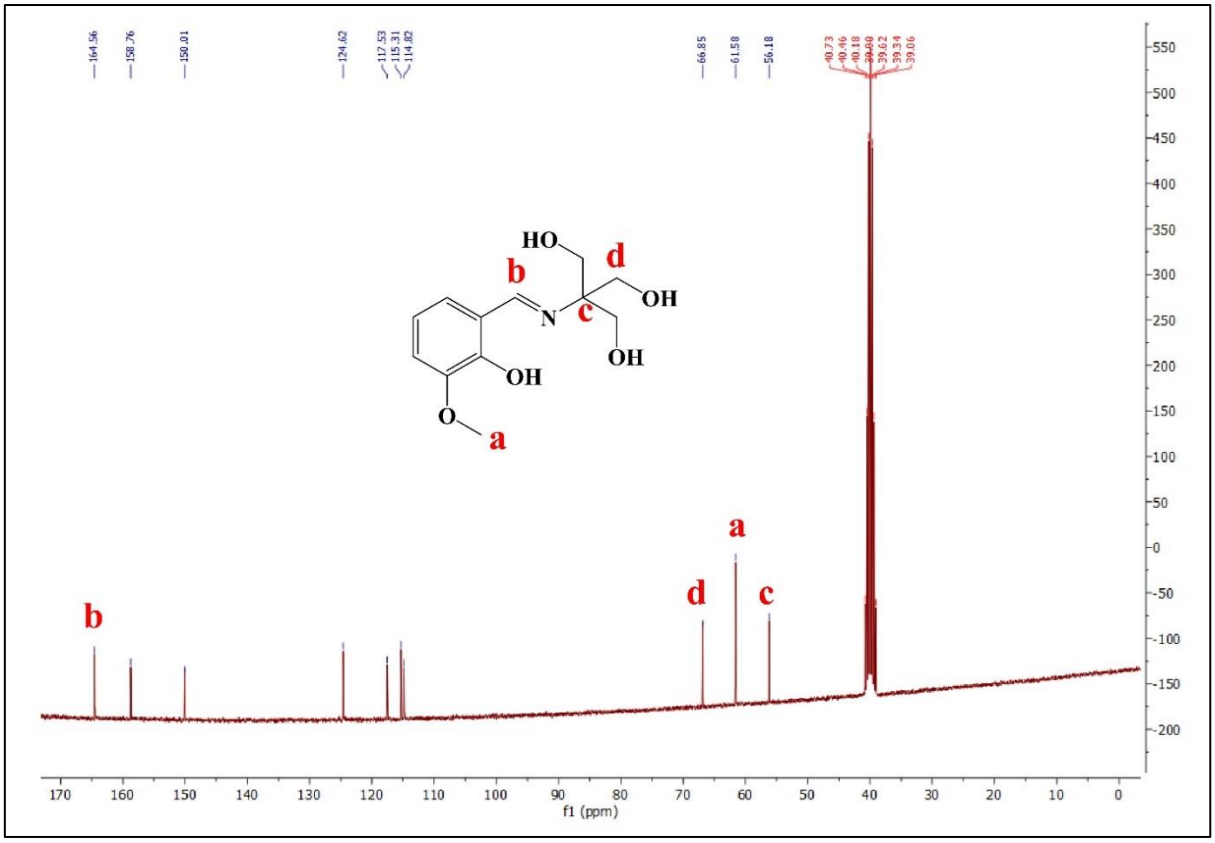

Figure 8: The ^{13}C NMR spectra of **3b**.

It is imperative to note that compound **3a** features one hydrogen bond forming group, i.e., a hydroxyl group, a hydrophobic t-Bu group, and an aromatic ring (grey highlighted). Therefore, it is hydrophobic in nature. However, in the case of **3b**, the presence of three OH groups in the nitrogen-containing part instead of a t-Bu group renders this region hydrophilic (cyan highlighted). Therefore, compounds **3a** and **3b** will offer a purely hydrophobic and largely hydrophilic environment in the vicinity of insulin.

2.5.2. Spectroscopic study of the Schiff base compounds

2.5.2.1. UV-vis spectroscopy study

The present study investigates the small molecules **3a** and **3b** and their response in UV-vis spectroscopy, which were found to exhibit peaks at 402, 285, and 232 nm for **3a** and 412, 292, and 237 nm for **3b** (Figure 9).

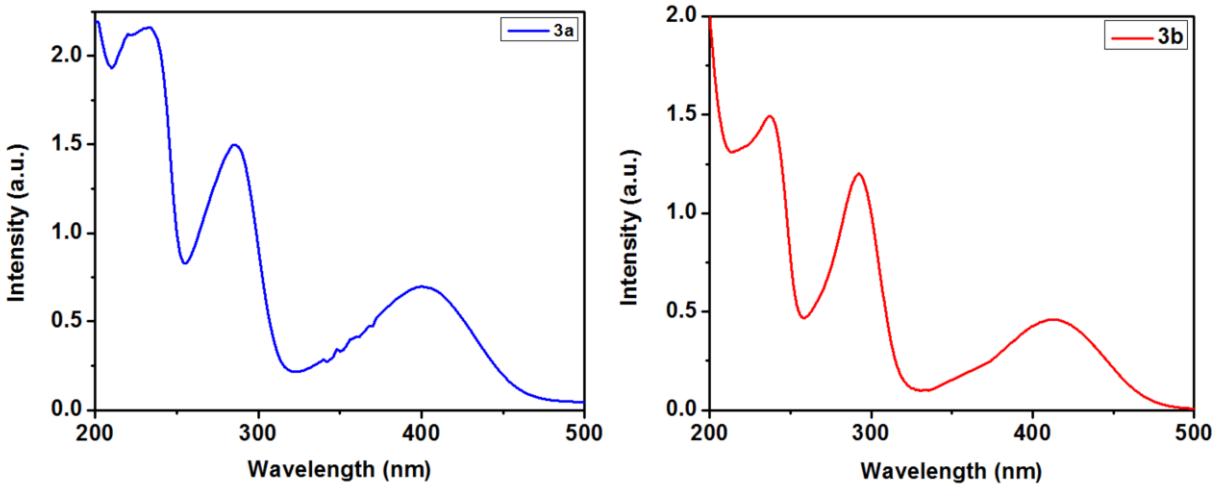

Figure 9: UV-vis spectroscopy of **3a** and **3b**

To assess the stability of these compounds in the solvent system, each compound was individually mixed into the solvent system, and their resulting UV-vis spectra were recorded over time. The results of this investigation suggest that both compounds remain stable in these conditions, with only slight changes observed over the course of 3.5 hours (Figure 10).

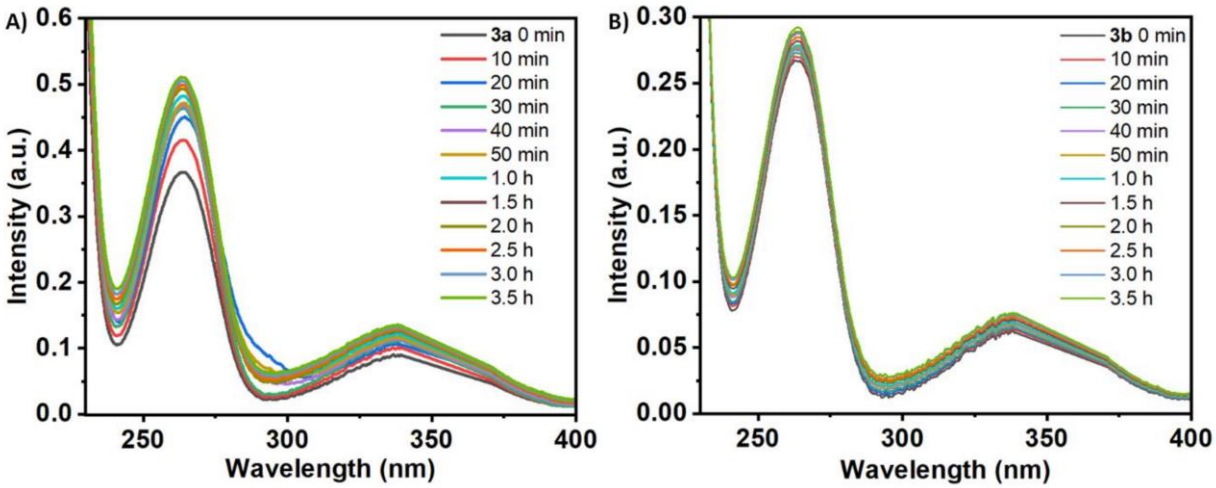

Figure 10: UV-vis spectroscopy of (A) **3a** and (B) **3b** with time.

2.5.2.2. Fluorescence study

The current investigation involves the analysis of two compounds, **3a** and **3b**, with fluorescence properties. These compounds exhibit three hump emission spectra, with peaks at 322, 333, and 347 nm upon excitation at 276 nm (Figure 11).

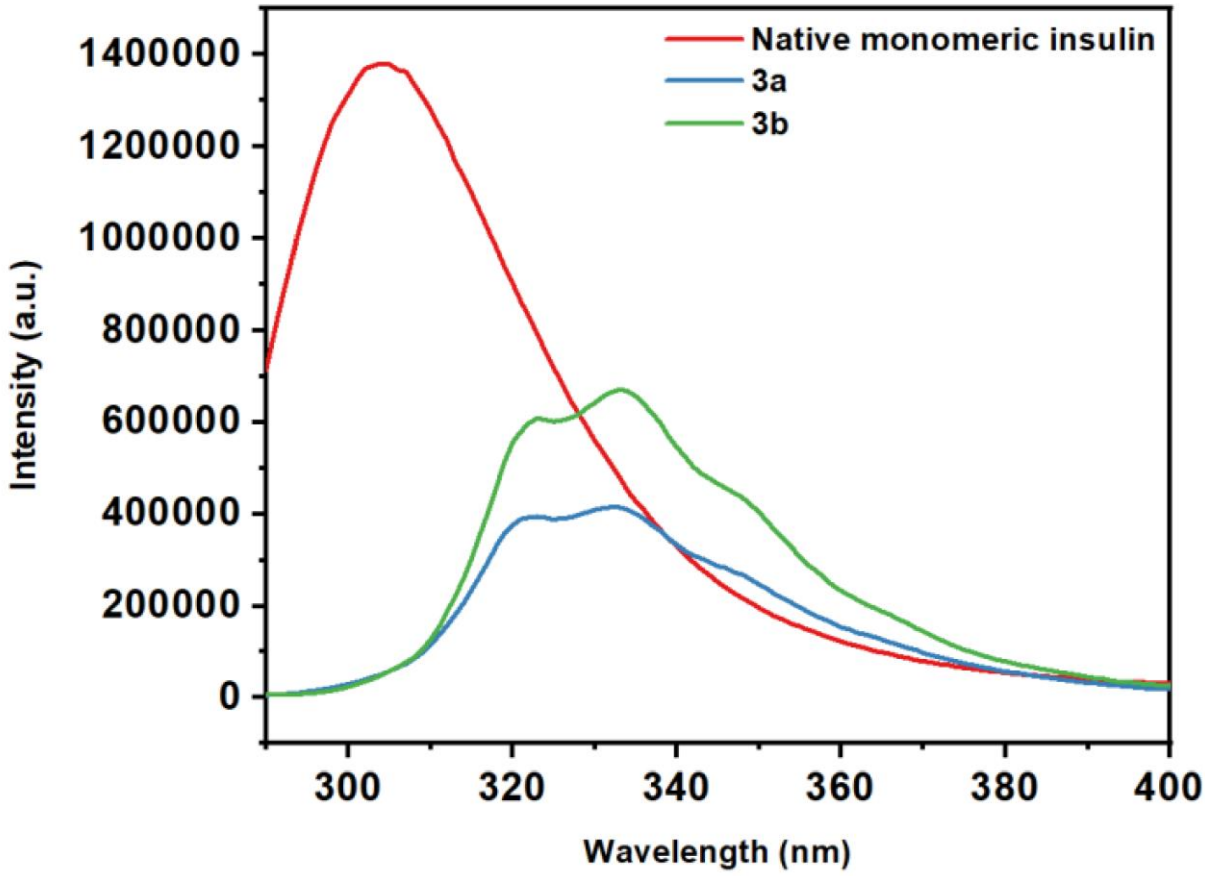

Figure 11: Fluorescence spectra of insulin and synthesized compounds **3a** and **3b** on excitation 276 nm.

Compound **3a** is hydrophobic in nature, and its aggregation-caused quenching (ACQ) or aggregation-induced emission (AIE) in water can be influenced by its hydrophobicity. To investigate this effect, an experiment was conducted where the compound was gradually added to the experimental conditions without insulin. The results indicated that **3a** experiences ACQ at high concentrations (Figure 12A). However, a linear relationship between concentration and fluorescence intensity is observed at lower concentrations, and self-aggregation of the compound is absent. This linear behavior breaks down after 25 μM and follows a polynomial curve, indicating self-aggregation in the experimental solvent system (Figure 12B).

Compound **3b** is a hydrophilic molecule and self-aggregates at high concentrations in the experimental conditions (Figure 12C). The compound shows aggregation-induced emission as the fluorescence intensity slowly increases with the concentration of **3b**. However, at low concentrations (2-25 μM), a linear relationship between concentration and **3b** fluorescence intensity is observed, implying that self-aggregation cannot proceed rapidly at lower concentrations of both compounds (Figure 12D).

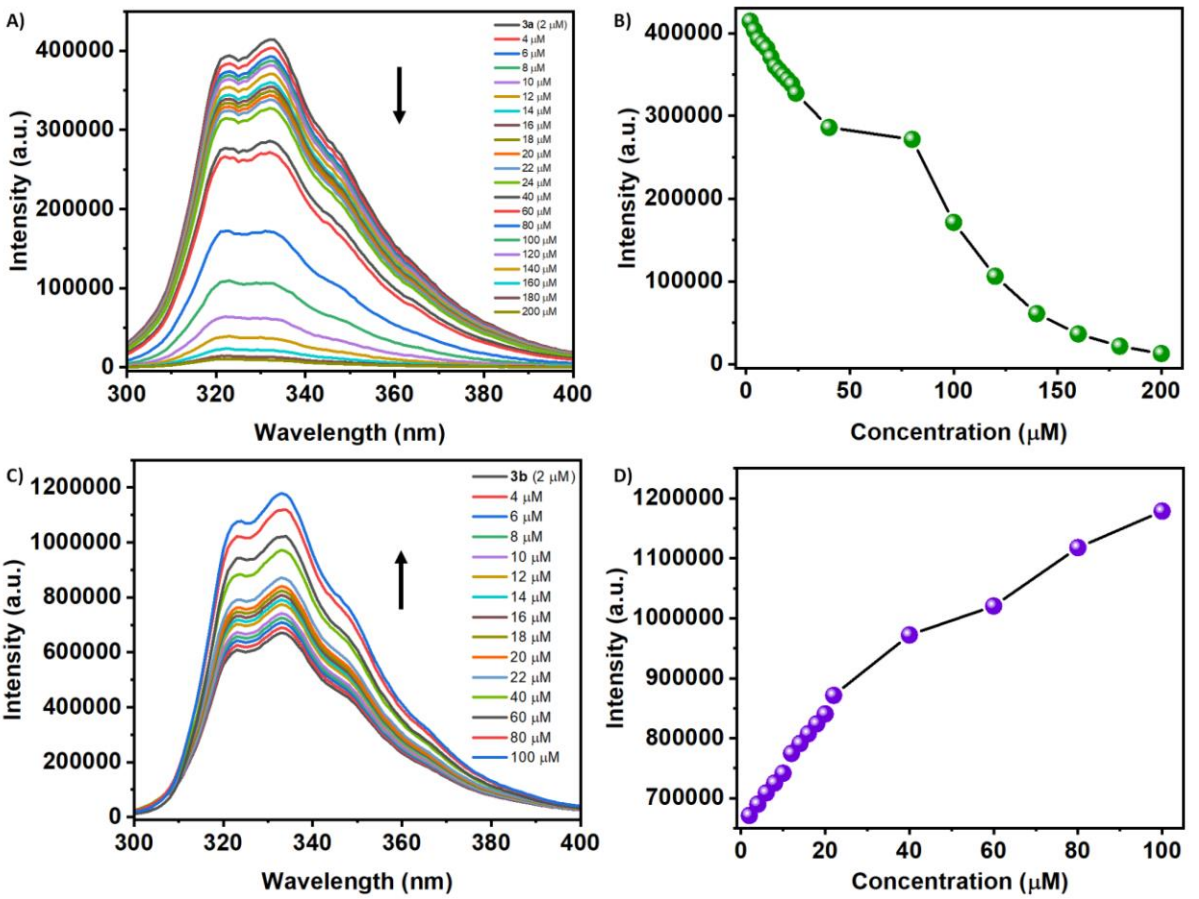

Figure 12: (A) Change of fluorescence of **3a** with increasing concentration, (B) Fluorescence intensity vs concentration plot of **3a**, (C) Change of fluorescence of **3b** with increasing concentration, (D) Fluorescence intensity vs concentration plot of **3b**.

2.5.3. Study of interactions of the Schiff bases with human insulin

2.5.3.1. UV-vis spectroscopy study of insulin in the presence of hydrophobic and hydrophilic compounds

Ultraviolet-visible spectroscopy is a valuable tool for examining the environment surrounding the chromophore of proteins or small molecules during interactions. For this particular study, insulin was selected as the model protein, with the p-hydroxyphenyl group in the Tyr residue serving as the chromophore. Monomeric insulin contains four Tyr residues and exhibits a peak at λmax = 276 nm. If the environment of the Tyr residues changes during interactions with small molecules, the nature of this peak may also change.

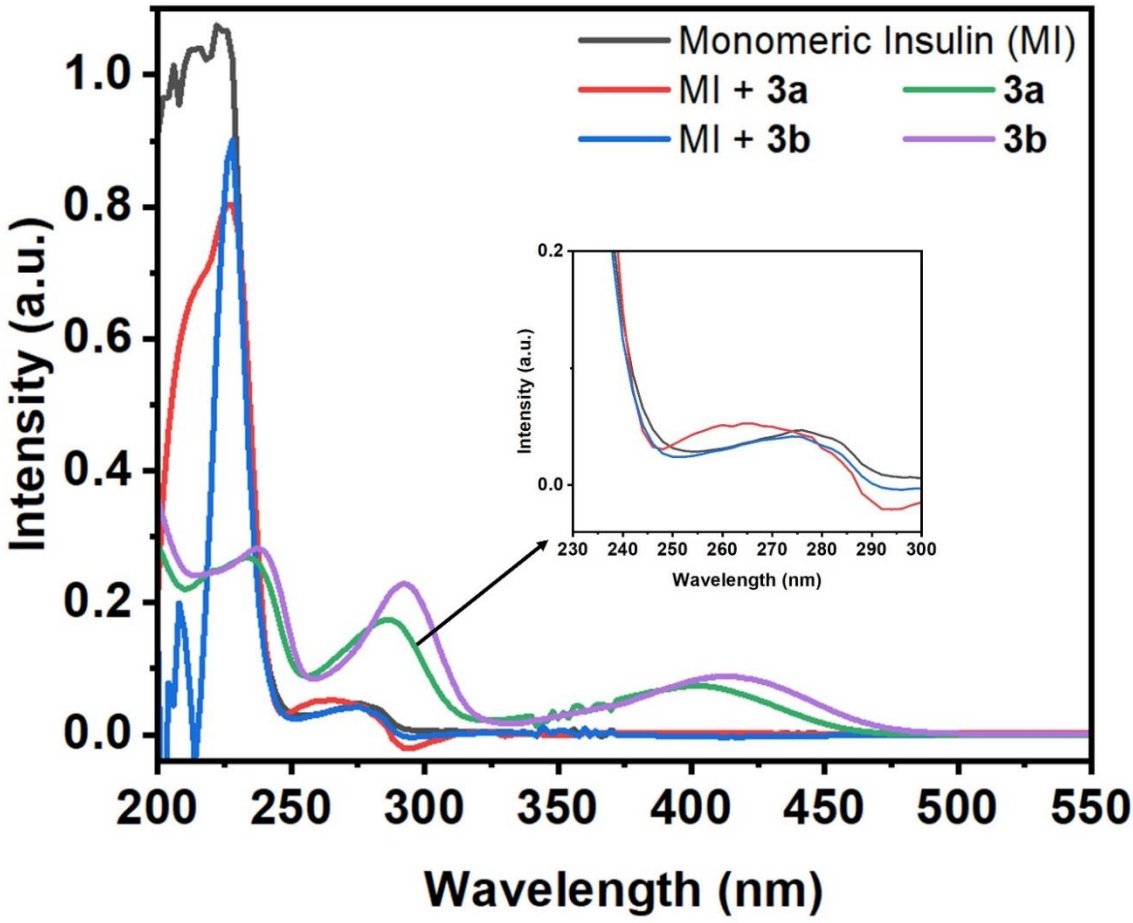

Figure 13: Absorption spectra of monomeric insulin (10 μM in pH 2.0) in the absence and presence of Schiff base compounds **3a** and **3b**. Absorption spectra of **3a** and **3b** (50 μM in pH 2.0).

When the protein was exposed to compound **3a**, the peak at 276 nm shifted to a blue wavelength of 11 nm while also increasing in intensity. In contrast, when exposed to compound **3b**, the protein peak shifted slightly to a blue wavelength of 2 nm (Figure 13). Despite the fact that the compounds themselves have peaks at 286 and 289 nm for **3a** and **3b**, respectively, the protein peak (276 nm) shifted towards the blue end of the spectrum when these compounds were added. Based on these initial findings, it is reasonable to assume that these compounds can interact with the protein.

2.5.3.2. Intrinsic fluorescence study of insulin in the presence of synthesized hydrophobic and hydrophilic compounds

Insulin's monomeric form features Tyr residues that emit light at 304 nm when excited at 276 nm. Upon the addition of **3a** or **3b** to a 25 μM insulin solution at 283 K, the intensity of the

protein's emission peak at 304 nm decreases rapidly with a 7 nm red shift. The appearance of a peak at 312 nm is also characteristic of **3a**. As more **3b** is added, the protein's intensity gradually decreases (Figure 14).

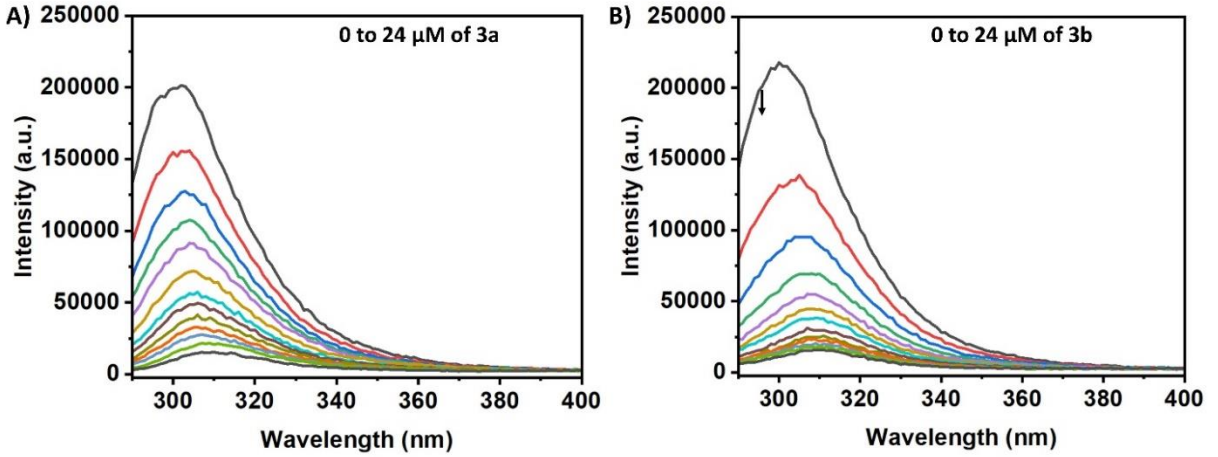

Figure 14: Fluorescence spectral change of insulin on gradual addition of (A) **3a** and (B) **3b**.

The Stern-Volmer equation (Equation-1) is a useful tool for evaluating the affinity of compounds to bind to proteins. This formula gauges the strength of the interaction between a compound and a protein.

The equation is- $I_0/I = 1 + K_{sv}[C]$…….(1)

Where I_0 is the initial protein fluorescence intensity, I is the intensity after adding **3a** or **3b**, and [C] is the compound concentration. The quenching constant (K_{sv}) relates to the slope of the plot of I_0/I vs. C and can help with its calculation.

The Stern-Volmer equation was used to assess fluorescence quenching, with Table 1 presenting quenching constants for different temperatures. Results indicate that the Ksv for **3a** is inversely proportional, while for **3b**, it has a direct correlation with temperature. These findings suggest that the protein-binding mechanisms of these compounds differ (Figure 15).

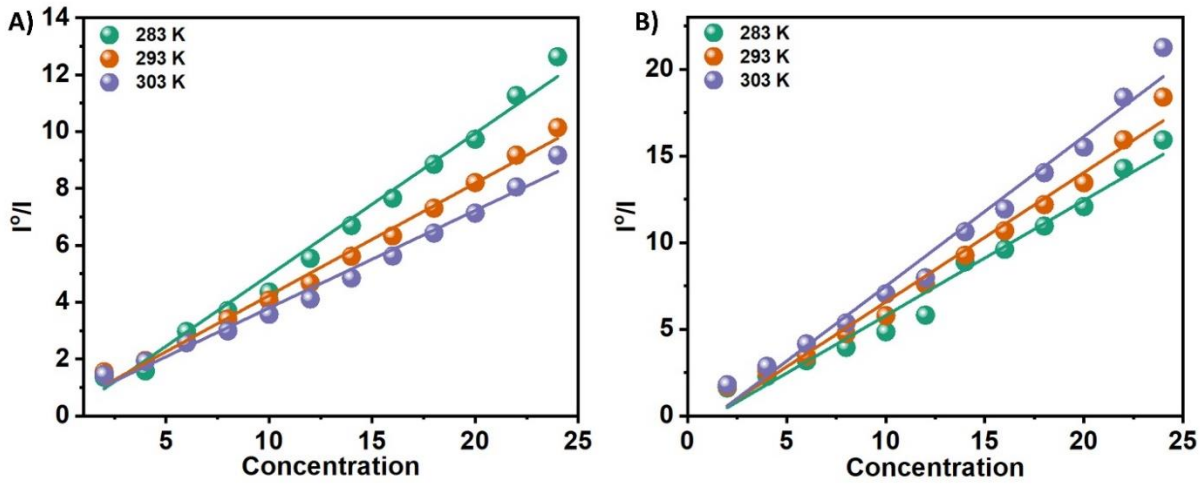

Figure 15: Stern–Volmer plots for the quenching of Tyr-fluorescence of insulin at 283, 293, and 303 K in the presence of two Schiff base **3a** (Panel A) and **3b** (Panel B) in solution.

2.5.3.3. Binding parameters

The interaction between small molecules **3a** and **3b** and protein can be measured by assessing the binding constant (K) and free energy change (ΔG) of the synthesized compounds' interaction with insulin. The effectiveness of these small molecules relies on their ability to bind to the target protein and impact its stability, which significantly influences their binding potential. To quantify K and ΔG, we apply the following equation (Equation-2) to examine fluorescence quenching data:

$$\ln((I_0 - I)/I) = \ln K_b + n \ln[C] \text{.....(2)}$$

In this equation, n represents the number of binding sites, and K_b is the binding constant. The equation describes the balance between free and bound species when complementary species bind autonomously to equal sites in a macromolecule. This equation has been widely utilized to determine binding parameters from fluorescence quenching data, serving as a technique for predicting binding parameters. Table 2 summarizes the outcomes of this study, which was conducted at various temperatures. Figure 16 shows cases representative plots of $\ln((I_0 - I)/I)$ versus ln[C], which gauges how protein-compound interactions were influenced by temperature.

The results of the study indicate that **3a**'s binding is weaker than **3b**'s. Thus, insulin has a greater affinity to bind with polar molecules rather than hydrophobic molecules. The binding of **3a** to insulin decreases with increasing temperature, while the opposite was observed in **3b**'s case.

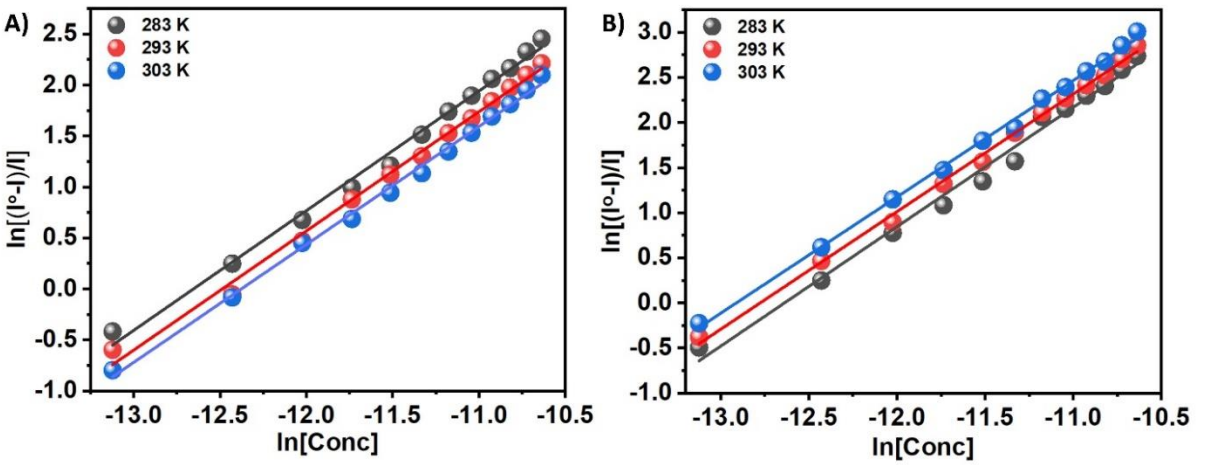

Figure 16: ln((I^0 − I)/I) versus ln[C] plots for the quenching of Tyr-fluorescence of insulin at 283, 293, and 303 K in the presence of two Schiff base **3a** (Panel A) and **3b** (Panel B) in solution.

Table 2 The Stern–Volmer (K_{sv}) and binding (K_b) constant of **3a** and **3b** at different temperature

	K_{sv}, 10^4 (M^{-1})			**K_b, 10^4 (M^{-1})**		
Compound	**283 K**	**293 K**	**303 K**	**283 K**	**293 K**	**303 K**
3a	4.99	3.94	3.65	2.83	2.18	1.65
3b	6.64	7.47	8.64	16.08	17.09	18.57

2.5.3.4. Binding forces and thermodynamic parameters

In a broader sense, the interactions between small molecules and biomolecules can be categorized into various types of forces. These include electrostatic forces, hydrogen bonds, van der Waals interactions, and hydrophobic and steric contact. The principal forces of binding between small molecules and proteins are traditionally accounted for by the signs and magnitudes of thermodynamic parameters. By considering the assumption that there is no significant alteration in the enthalpy change (H) over a particular temperature range, the enthalpy change (H) and the entropy change (S) can both be calculated using the Van't Hoff equation.

$$\ln K = \Delta H/RT + \Delta S/R$$

R represents the universal gas constant, and T represents the Kelvin temperature. Change in the free energy (ΔG) resulting from the process in this study was estimated by using the relationship given below:

$$\Delta G = \Delta H - T\Delta S$$

Table 2 presents a comprehensive list of various thermodynamic parameters, whereas Figure 17 illustrates the Van't Hoff plot (ln K vs. 1/T) in a graphical format.

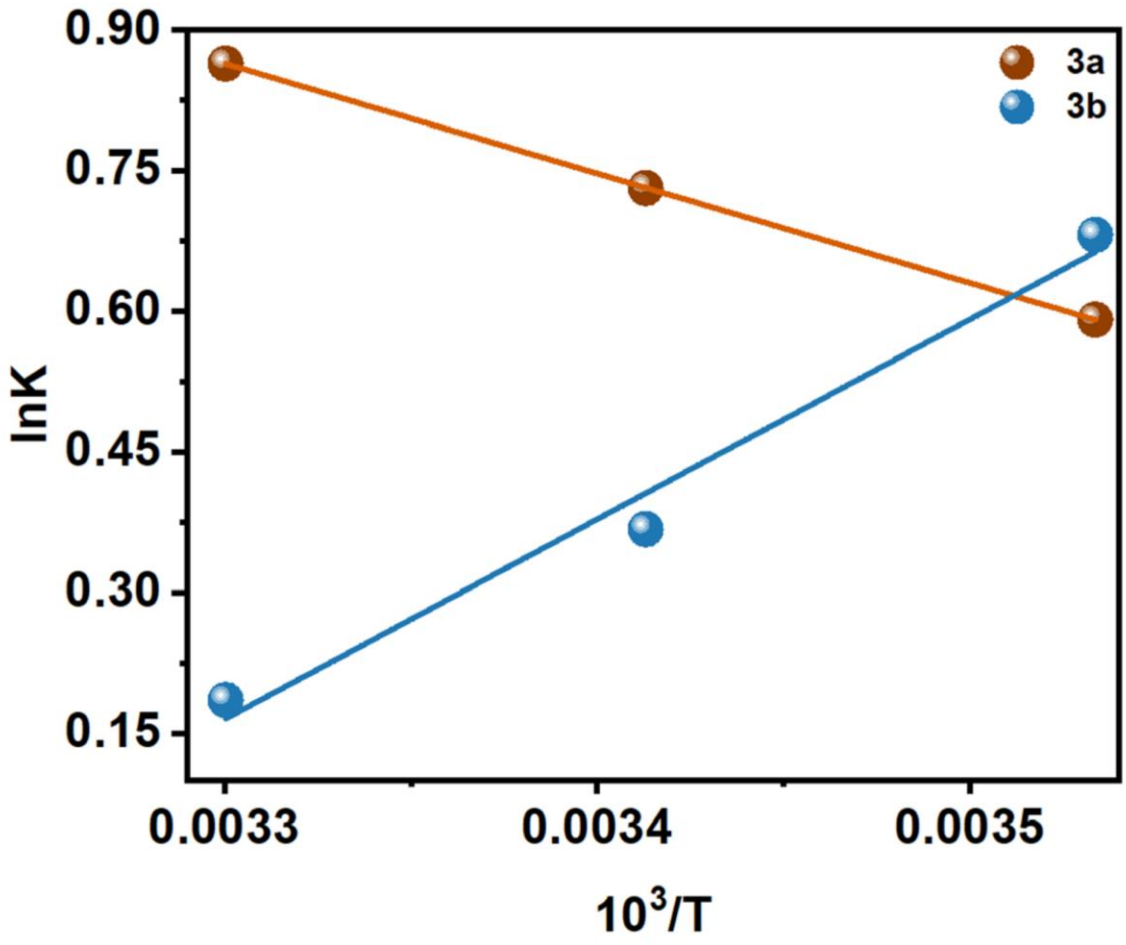

Figure 17: ln K vs. 1/T plot at 283, 293, and 303 K of two Schiff bases **3a** and **3b**.

Table 3 Thermodynamic parameters involved in the insulin–**3a**/**3b** interactions

Compounds	**Temperature (K)**	**ΔG° kJ mol^{-1}**	**ΔH° kJ mol^{-1}**	**ΔS° kJ mol^{-1}**
3a	283	−5.41	+10.72	+0.057
	293	−5.98		
	303	−6.55		
3b	283	−12.16	−35.65	−0.083
	293	−11.33		
	303	−10.50		

During protein-small molecule interactions, various types of interactions occur. Ross and Subramanian have documented thermodynamic parameters that are associated with these interactions. These parameters provide essential insights into the mechanisms by which each interaction occurs. Based on the thermodynamic data, the following models of interaction can be summarized:

(i) $\Delta H > 0$, $\Delta S > 0$ correspond to hydrophobic forces.

(ii) $\Delta H < 0$, $\Delta S < 0$ correspond to hydrogen bond formation and van der Waals interaction.

(iii) $\Delta H < 0$, $\Delta S > 0$ correspond to electrostatic/ionic interactions.

Table 3 indicates that the thermodynamic parameters for the interaction between **3a** and insulin are enthalpically unfavorable and entropically favorable, with a negative Gibbs free energy change suggesting that the interaction may occur spontaneously. However, the **3b**-insulin interaction is enthalpically favorable and entropically unfavorable, with a negative Gibbs free energy change. Notably, the positive enthalpy and entropy change demonstrate that hydrophobic forces dominate the interaction process between **3a** and insulin. Conversely, **3b** and insulin interact through hydrogen bond formation and van der Waals interaction, as demonstrated by negative enthalpy and entropy changes.

2.5.3.5. Monitoring the hydrophobicity changes in the microenvironment of insulin: ANS assay

8-Anilinonaphthalene-1-sulfonic acid (ANS) is a highly useful fluorescent probe that exhibits increased fluorescence intensity upon binding to the hydrophobic pocket of a protein surface,

including insulin. If a compound has the ability to displace ANS from the protein binding site, the intensity of ANS bound to insulin will decrease, which evidences that the compound can also bind to the hydrophobic site of the protein surface. In this regard, compound **3a** has been observed to gradually decrease the intensity of the ANS-insulin system upon its addition due to its sufficient hydrophobicity. This is attributed to the presence of only one OH group and a hydrophobic tert-butyl group in its molecular structure, which enables it to bind to the hydrophobic protein surface. Conversely, compound **3b** has four hydroxyl groups, rendering it polar and incapable of binding to the hydrophobic protein surface. This causes the decrease in fluorescence intensity to be less pronounced upon its addition, as seen in Panel B of Figure 18.

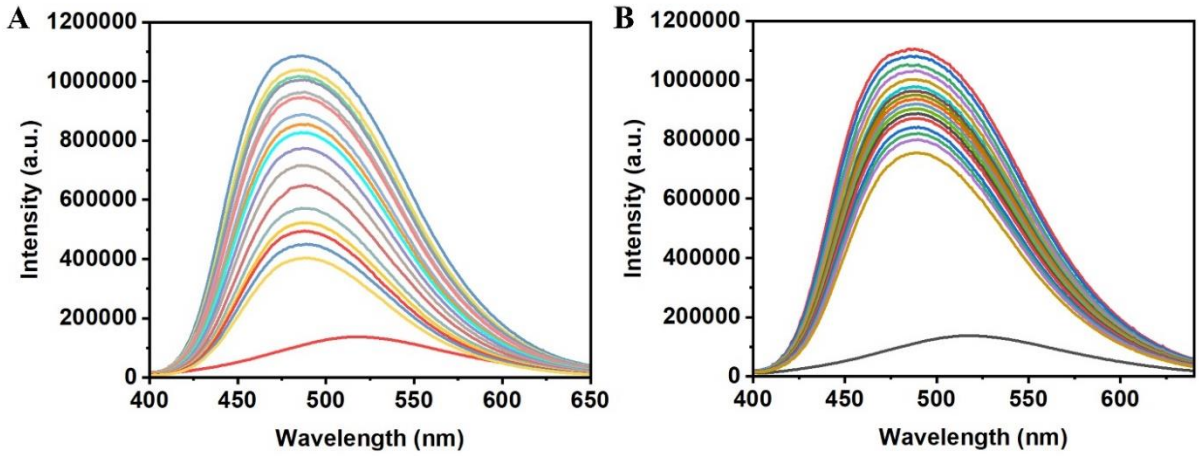

Figure 18: ANS-fluorescence emission spectra of monomeric insulin incubated separately at 25°C and at pH 2.0 in the absence and presence of Schiff base **3a** (Panel A) and in the absence and presence of Schiff base **3b** (Panel B). Insulin concentrations throughout all the experiments were kept at 25 μM. The results were the average of three different experiments.

In the presence of insulin, which has a limited number of hydrophobic pockets on its protein surface, both ANS and **3a** have been observed to bind to it. Due to its lower solubility and higher binding ability, **3a** moves from the polar aqueous medium to the hydrophobic protein sites to replace ANS in their binding site on insulin. This is evidenced by the observed decrease in ANS intensity. In contrast, **3b**, which is hydrophilic and has four hydroxyl groups, has a binding site different from **3a**. The observed slight decrease in ANS fluorescence intensity upon the addition of **3b** may be attributed to the displacement of ANS from their binding sites due to the conformational change of the protein during **3b** binding. To further confirm these results, circular dichroism (CD) spectroscopy was employed to monitor the secondary

structural changes. This technique has been demonstrated to be highly effective in providing evidence of secondary structural changes in proteins.

2.5.3.6. Application of circular dichroism (CD) spectroscopy to monitor the secondary structural changes of insulin in the hydrophobic and hydrophilic compounds

Circular dichroism (CD) is a powerful technique utilized to elucidate the secondary and tertiary structural changes in proteins. Insulin, a protein enriched in alpha-helices, exhibits a characteristic peak at 208 nm in the far-UV CD spectral region, corresponding to its alpha-helical structure. The interaction of small molecules, such as Schiff bases, with insulin can perturb its secondary structure, causing a shift or change in the aforementioned peaks.

In this study, purified monomeric insulin (6 μM) was analyzed through CD, which revealed peak values at 208 nm and 221 nm, indicative of the presence of alpha-helix and beta-sheet structures, respectively. The interaction of insulin with the hydrophobic compound **3a** resulted in a significant change in the far-UV CD spectrum, indicating a perturbation of its secondary structure. A greater shift in the CD spectrum was observed at higher concentrations of **3a** (2 and 6 μM), suggesting a higher percentage of random structure. This indicates that the hydrophobic compound **3a** interacts strongly with insulin, disrupting its secondary structure. Conversely, the hydrophilic compound **3b** interacted differently with insulin. At lower concentrations (1 and 2 μM), **3b** caused a red-shift of the peaks with a greater negative ellipticity value compared to monomeric insulin, indicating a slightly higher beta-structure content formation. At higher concentrations, **3b** caused a transition in the structure of insulin, with a lesser MRE value at 215 nm and an increased MRE at 207 nm compared to insulin alone (Figure 19). This indicates that the hydrophilic compound **3b** has an influence on both the secondary and tertiary structure of insulin. The stability of insulin is highly dependent on the hydrophilic and hydrophobic environment. The results of this study suggest that the hydrophobic molecule **3a** has a high potential for disrupting the secondary structure of insulin, while the hydrophilic molecule **3b** has an influence on both the secondary and tertiary structure of insulin. These findings provide valuable insights into the structural changes induced by small molecules and their impact on protein function, thereby highlighting the importance of identifying and characterizing such interactions. Secondary structural contents of different insulin samples with or without **3a** and **3b** were calculated using CDNN 2.1 software, and the results are shown in Table 4.

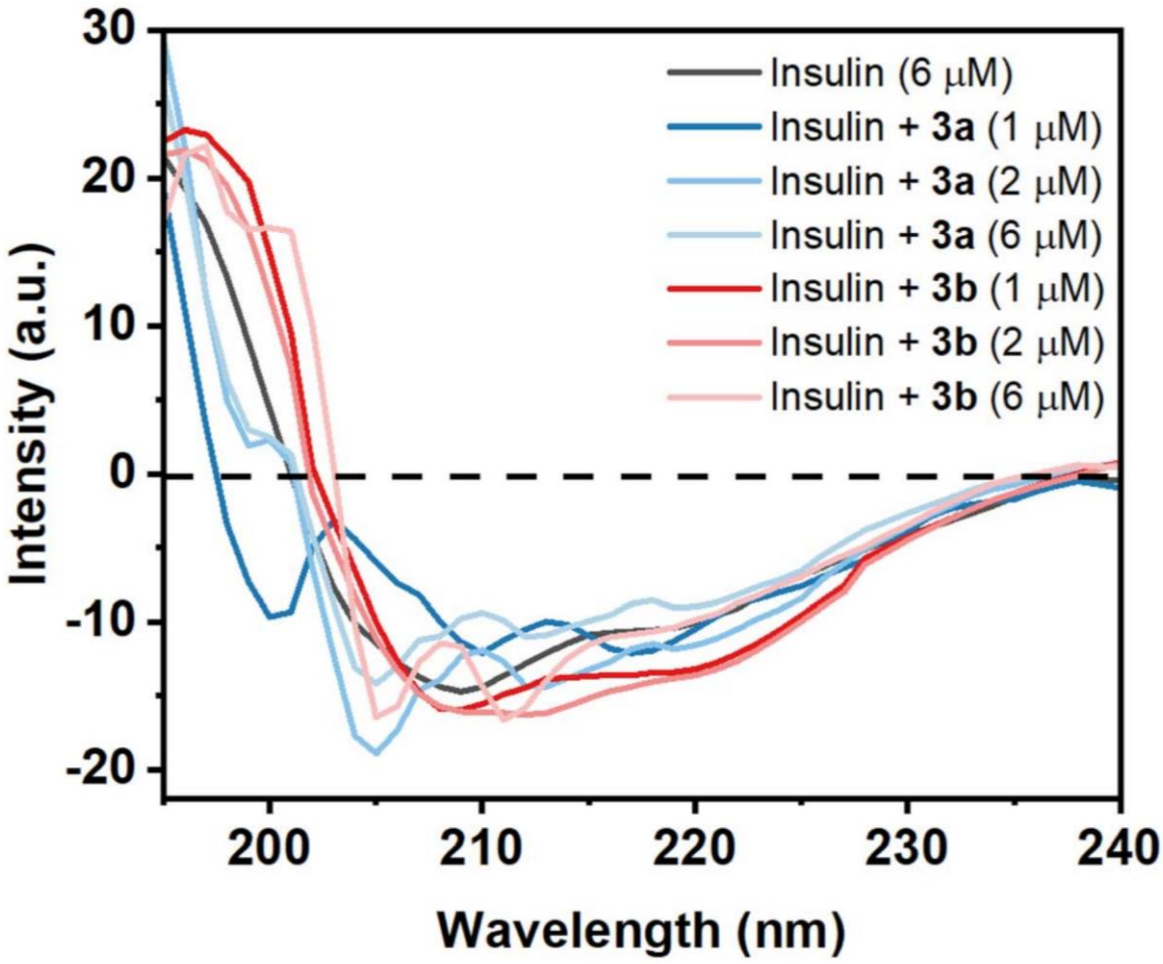

Figure 19: Far-UV CD spectra (190–250 nm) of monomeric insulin in the absence and presence of two small molecules (Schiff bases) **3a** and **3b** at 25 °C and at pH 2.0, showing the secondary structural changes of insulin.

Table 4: Structural integrity of monomeric insulin in the absence and presence of the Schiff bases **3a** and **3b** determined by CD calculations

Samples	% of α-helix	% of β-sheet	% of Random coil
Insulin (6 μM)	89.93	0.68	1.45
Insulin + 3a **(1 μM)**	87.18	1.20	2.50
Insulin + 3a **(2 μM)**	83.19	0.38	2.671
Insulin + 3a **(6 μM)**	79.34	0.97	3.934
Insulin + 3b **(1 μM)**	93.28	0.29	1.25
Insulin + 3b **(2 μM)**	92.67	0.28	1.96
Insulin + 3b **(6 μM)**	81.93	2.07	5.23

2.5.3.7. Theoretical studies

The structural investigation of Schiff bases is a crucial aspect that provides valuable insights into the nature of the molecule and the functional groups' contribution to the molecule's properties. The molecular electrostatic potential map (MEP) of the energy-minimized structure of Schiff bases, using density functional theory (DFT), is a significant tool that provides insight into the electronic distribution around the molecular backbone. The MEP map is color-coded to indicate electron-rich (red), neutral (green), and electron-poor (blue) regions (Figure 20). The **3a** molecule comprises polar atoms such as methoxy, phenolic oxygen, and imine nitrogen, while **3b** has three additional hydroxyl groups. Depending upon the group, these groups can form an H-bond with protein through either H-bond donation or acceptance. The MEP of both compounds depicts a red color on oxygen atoms, while nitrogen atoms are buried in the neutral region, indicating that imine nitrogen is less capable of H-bond formation.

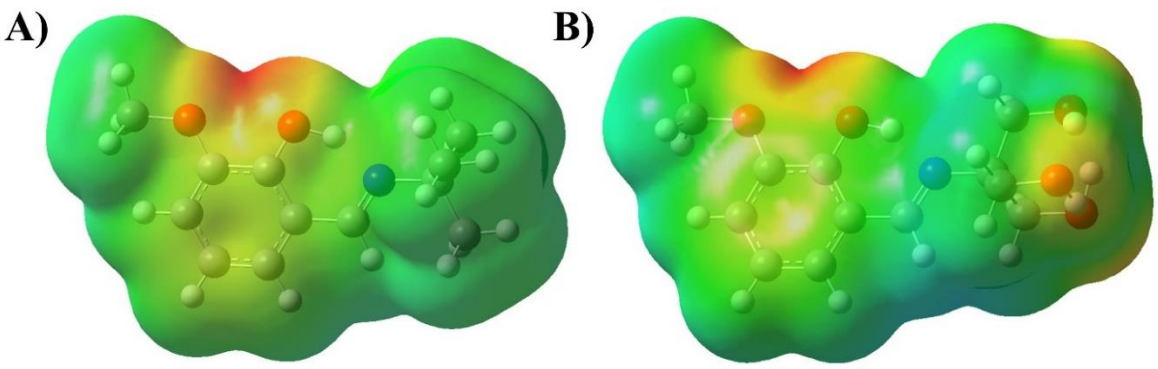

Figure 20: Molecular electrostatic map of the synthesized compounds. (A) **3a** and (B) **3b**

The polar surface area of **3a** and **3b** was calculated to be 41.82 Å2 and 102.51 Å2, respectively. Thus, **3b** has more than double the polar surface area than **3a**. As a result, the lipophilicity of **3a** (log Po/w = 2.83) is higher than that of **3b** (log Po/w = 1.73). However, despite being small molecules, both compounds are somewhat water-soluble, and the log S of **3a** and **3b** were calculated to be −2.41 and −0.48, respectively. These parameters suggest that both molecules have the potential to form H-bonds with molecules and enough polarity.

Molecular docking is a fascinating computational technique used to predict the binding site of a small molecule to a protein, the mechanism of protein binding, and the weak forces involved in the binding process. This study used the method to predict the binding mode of **3a** and **3b** in human insulin. The structure of the molecules was energy-minimized using density functional

theory (DFT). The molecular docking of these compounds to human insulin showed that compound **3b** has a higher binding affinity than **3a**. The change of free energy for this binding process was observed to be −6.83 and −5.74 kcal mol^{-1} for **3b** and **3a**, respectively, which was also observed experimentally.

The molecular docking results revealed that compound **3a** is bound at the hydrophobic cavity on the protein surface, while **3b** is attached to the protein's surface. In the binding process of **3a**, amino acid residues Q4, L6, H10, and A14 were involved. In the case of **3b**, the binder amino acids are Q21, F24, F25, and Y26. In the binding sites, the N–H of the amide group formed hydrogen bonds with the imine and hydroxyl group of **3a**, while the imidazole ring of H10 showed C–H···π interactions with the tert-butyl group of **3a**. The methyl group of A14 interacted with C–H···π to the benzene ring of **3a**, and L6 interacted through hydrophobic interaction with the tert-butyl group of **3a**. However, hydrogen bonding was the primary driving force for the binding of **3b** to insulin. The amide CO of F25 was involved in hydrogen bonding with two hydroxyl groups at the side-chain of **3b**. Another hydrogen bonding was found between amide N–H of N21 and the side-chain OH. The aliphatic C–H of F25 was involved in non-conventional H-bonding interactions with the OH group. Amide N–H of Y26 showed N–H···π interactions with the benzene ring of **3b** (Figure 21).

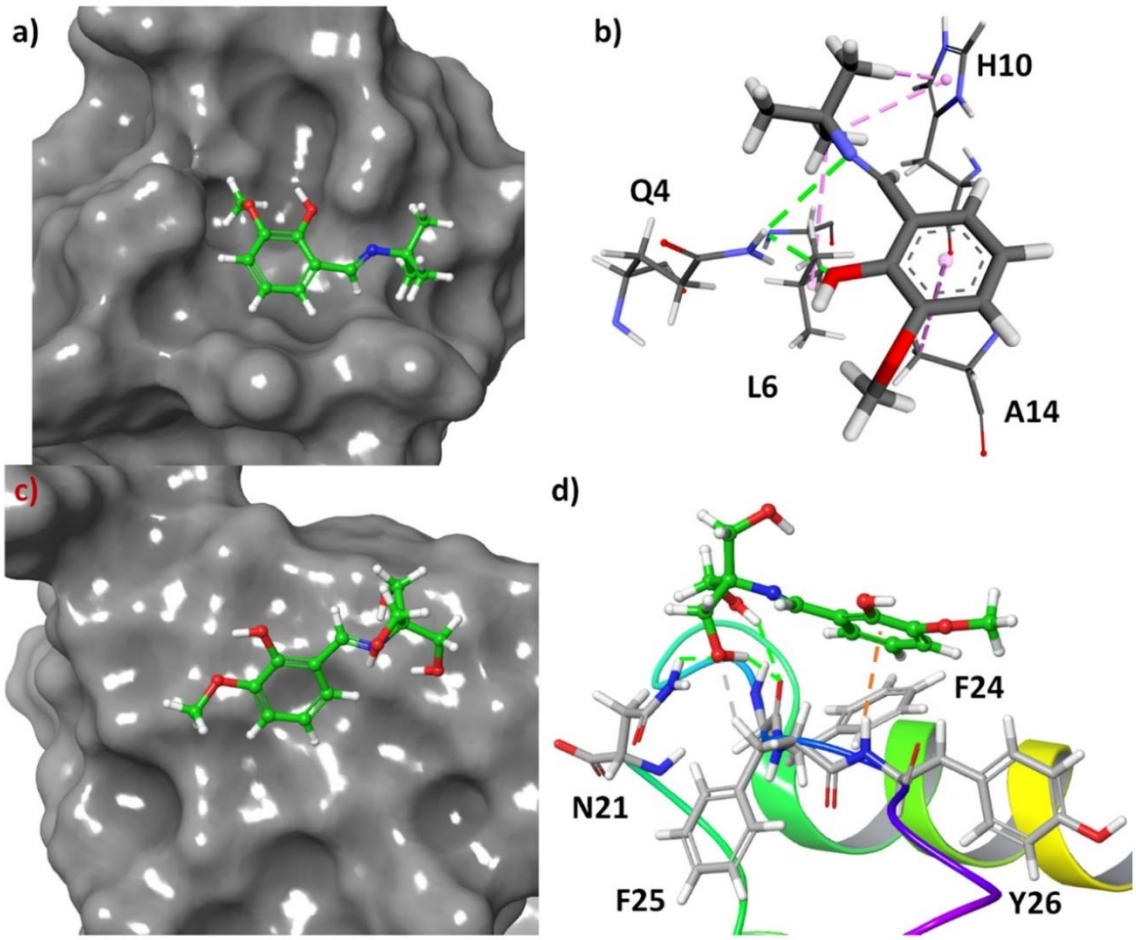

Figure 21: (a) Docking pose of **3a** in the hydrophobic pocket of the insulin, (b) different non-covalent interactions between **3a** and active site amino acids, (c) docking pose of **3b** on the surface of insulin, (d) different non-covalent interactions in the binding site of the protein with **3b**.

2.6. Summary of the work

Insulin is a key hormone that regulates glucose metabolism in our body. Its functionality is dependent on its ability to interact with various molecules, which may alter its structure and modulate its activity. It is noteworthy that insulin can bind with the hydrophilic molecule in a manner analogous to glucose binding. To understand how different molecules can affect insulin's activity, we studied the effects of two synthetic molecules with different hydrophilic and hydrophobic properties on insulin binding and stability.

Our investigation of the effects of hydrophilic and hydrophobic molecules on the insulin binding process was conducted through a multi-spectroscopic approach. To synthesize the

molecules, we created two Schiff base compounds, one with a hydrophilic side chain and the other with a hydrophobic side chain. Our research discovered that insulin, a hydrophilic binding protein, has a remarkably strong affinity for hydrophilic and hydrophobic molecules. At a temperature of 283 K, the binding constant was found to be 6.64×10^4 M^{-1} for hydrophilic molecules and 4.99×10^4 M^{-1} for hydrophobic molecules. On binding with hydrophobic molecules, insulin's secondary structure is greatly perturbed, mainly in the hydrophobic pocket. On the other hand, when insulin binds with hydrophilic molecules, it only causes slight alterations in the secondary structural contents. Consequently, the presence of hydrophobic molecules diminishes the stability of insulin.

2.7. References

Alavi, P., Yousefi, R., Amirghofran, S., Karbalaei-Heidari, H.R. and Moosavi-Movahedi, A.A., 2013. Structural analysis and aggregation propensity of reduced and nonreduced glycated insulin adducts. Applied biochemistry and biotechnology, 170, pp.623-638.

Bisht, S. and Singh, M.F., 2024. The triggering pathway, the metabolic amplifying pathway, and cellular transduction in regulation of glucose-dependent biphasic insulin secretion. Archives of Physiology and Biochemistry, pp.1-12.

Bouskila, M., Hirshman, M.F., Jensen, J., Goodyear, L.J. and Sakamoto, K., 2008. Insulin promotes glycogen synthesis in the absence of GSK3 phosphorylation in skeletal muscle. American journal of physiology-endocrinology and metabolism, 294(1), pp.E28-E35.

Chauhan, P., Velappan, A.B., Sahoo, B.K., Debnath, J. and Ghosh, K.S., 2017. Studies on molecular interactions between Schiff bases and eye lens chaperone human αA-crystallin. Journal of Luminescence, 192, pp.148-155.

Chigurupati, S., Palanimuthu, V.R., Kanagaraj, S., Sundaravadivelu, S. and Varadharajula, V.R., 2021. Green synthesis and in silico characterization of 4-Hydroxy-3-methoxybenzaldehyde Schiff bases for insulysin inhibition–a potential lead for type 2 diabetes mellitus. Journal of Applied Pharmaceutical Science, 11(7), pp.063-071.

Eizirik, D.L., Pasquali, L. and Cnop, M., 2020. Pancreatic β-cells in type 1 and type 2 diabetes mellitus: different pathways to failure. Nature Reviews Endocrinology, 16(7), pp.349-362.

Falconi, M., Bozzi, M., Paci, M., Raudino, A., Purrello, R., Cambria, A., Sette, M. and Cambria, M.T., 2001. Spectroscopic and molecular dynamics simulation studies of the interaction of insulin with glucose. International journal of biological macromolecules, 29(3), pp.161-168.

Gheybalizadeh, H. and Hejazi, P., 2022. Influence of hydrophilic and hydrophobic functional monomers on the performance of magnetic molecularly imprinted polymers for selective recognition of human insulin. Reactive and Functional Polymers, 171, p.105152.

Halevas, E., Tsave, O., Yavropoulou, M.P., Hatzidimitriou, A., Yovos, J.G., Psycharis, V., Gabriel, C. and Salifoglou, A., 2015. Design, synthesis and characterization of novel binary V (V)-Schiff base materials linked with insulin-mimetic vanadium-induced differentiation of 3T3-L1 fibroblasts to adipocytes. Structure–function correlations at the molecular level. Journal of Inorganic Biochemistry, 147, pp.99-115.

Kruszynska, Y.T., Home, P.D. and Alberti, K.G.M.M., 1986. In vivo regulation of liver and skeletal muscle glycogen synthase activity by glucose and insulin. Diabetes, 35(6), pp.662-667.

Marshall, S., 2006. Role of insulin, adipocyte hormones, and nutrient-sensing pathways in regulating fuel metabolism and energy homeostasis: a nutritional perspective of diabetes, obesity, and cancer. Science's STKE, 2006(346), pp.re7-re7.

Mauri, S., Pandey, R., Rzeźnicka, I., Lu, H., Bonn, M. and Weidner, T., 2015. Bovine and human insulin adsorption at lipid monolayers: a comparison. Frontiers in Physics, 3, p.51.

Mollmann, S.H., Jorgensen, L., Bukrinsky, J.T., Elofsson, U., Norde, W. and Frokjaer, S., 2006. Interfacial adsorption of insulin: Conformational changes and reversibility of adsorption. European journal of pharmaceutical sciences, 27(2-3), pp.194-204.

Muhammad, E.F., Adnan, R., Latif, M.A.M. and Abdul Rahman, M.B., 2016. Theoretical investigation on insulin dimer-β-cyclodextrin interactions using docking and molecular dynamics simulation. Journal of Inclusion Phenomena and Macrocyclic Chemistry, 84, pp.1-10.

Nault, L., Guo, P., Jain, B., Bréchet, Y., Bruckert, F. and Weidenhaupt, M., 2013. Human insulin adsorption kinetics, conformational changes and amyloidal aggregate formation on hydrophobic surfaces. Acta biomaterialia, 9(2), pp.5070-5079.

Nilsson, P., Nylander, T. and Havelund, S., 1991. Adsorption of insulin on solid surfaces in relation to the surface properties of the monomeric and oligomeric forms. Journal of colloid and interface science, 144(1), pp.145-152.

Norton, L., Shannon, C., Gastaldelli, A. and DeFronzo, R.A., 2022. Insulin: The master regulator of glucose metabolism. Metabolism, 129, p.155142.

Paul, S., Begum, S., Parvej, H., Dalui, R., Sardar, S., Mondal, F., Sepay, N. and Halder, U.C., 2024. In vitro retardation and modulation of human insulin amyloid fibrillation by Fe 3+ and Cu 2+ ions. New Journal of Chemistry, 48(7), pp.3120-3135.

Rekha, M.R. and Sharma, C.P., 2009. Synthesis and evaluation of lauryl succinyl chitosan particles towards oral insulin delivery and absorption. Journal of Controlled Release, 135(2), pp.144-151.

Salar, S., Jafari, M., Kaboli, S.F. and Mehrnejad, F., 2019. The role of intermolecular interactions on the encapsulation of human insulin into the chitosan and cholesterol-grafted chitosan polymers. Carbohydrate polymers, 208, pp.345-355.

Saltiel, A.R., 2016. Insulin signaling in the control of glucose and lipid homeostasis. Metabolic control, pp.51-71.

Sluzky, V., Klibanov, A.M. and Langer, R., 1992. Mechanism of insulin aggregation and stabilization in agitated aqueous solutions. Biotechnology and bioengineering, 40(8), pp.895-903.

Subasi, N.T., 2022. Overview of Schiff Bases. In Schiff Base in Organic, Inorganic and Physical Chemistry. IntechOpen.

Yanti, S., Wu, Z.W., Agrawal, D.C. and Chien, W.J., 2021. Interaction between phloretin and insulin: a spectroscopic study. Journal of Analytical Science and Technology, 12, pp.1-16.

CHAPTER 3

ANION–INDUCED AMYLOID FIBRILLATION OF HUMAN INSULIN IN VITRO

Anion–Induced Amyloid Fibrillation of Human Insulin In vitro

3.1. Biological importance of ions

Ions are an essential component of biological systems. These charged particles have a wide range of functions, from conducting nerve impulses and muscle contractions to regulating cellular signaling and enzymatic reactions (Funk et al.,2009). Ions play a crucial role in regulating physiological processes at both the cellular and systemic levels. They profoundly impact the human body and are necessary for maintaining proper physiological functioning and overall health. Maintaining the balanced presence and regulation of ions is essential for achieving optimal health and well-being.

The presence of metal ions is crucial for the growth and maintenance of life in plants, animals, and humans. These essential elements have long been recognized for their fundamental role in biological systems. Without them, growth disorders, severe malfunction, carcinogenesis, and even death can occur. Metal ions serve as macro or microelements in various functional and structural roles (Nieder et al.,2018). They participate in a multitude of biochemical reactions and can exist in diverse forms. Furthermore, they are key players in intra and intercellular communications, regulating electrical charges and osmotic pressure, photosynthesis, and electron transfer processes. They also help maintain nucleotide bases pairing, stacking, and stability and regulate DNA transcription. Metal ions are crucial for the proper functioning of nerve cells, muscle cells, the brain, and the heart, aiding in the transport of oxygen and many other biological processes. In short, metals are essential for life as we know it (Moustakas, 2021).

Some key points highlighting the importance of ions in biological systems are given below.

3.1.1. Electrolyte balance

The proper balance of electrolytes in bodily fluids, which is imperative for hydration, nerve function, muscle contraction, and cellular homeostasis, is maintained by essential ions such as sodium (Na^+), potassium (K^+), chloride (Cl^-), calcium (Ca^{2+}), and magnesium (Mg^{2+}) (Blaine et al.,2015).

3.1.2. Nerve signal transmission

Ion channels play a crucial role in the transmission of nerve signals as they facilitate the selective movement of ions across cell membranes. The flow of ions, such as sodium (Na^+),

potassium (K^+), and calcium (Ca^{2+}), generates electrical impulses that travel along nerve cells (Pessia, 2004). This intricate process is vital for sensory perception, motor coordination, and cognitive function.

3.1.3. Muscle contraction

Calcium ions (Ca^{2+}) play a pivotal role in the process of muscle contraction. Upon release from intracellular stores, calcium ions bind to regulatory proteins, namely troponin and tropomyosin, which in turn initiate the contraction process by enabling actin-myosin interactions (Rüegg, 2012). Similarly, Chloride ions (Cl^-) play an integral role in muscle function, including muscle contraction and relaxation. Chloride ions assist in maintaining the electrical neutrality of muscle cells and contribute to the generation of action potentials, which are fundamental for muscle contraction (Goto and Kitazono, 2022).

3.1.4. Cellular signaling

Ions are essential in intracellular signaling pathways that impact various processes, such as cell growth, differentiation, metabolism, and gene expression. For instance, calcium ions (Ca^{2+}) act as second messengers by binding to specific proteins and enzymes, triggering diverse cellular responses (McAinsh et al.,1997). Additionally, phosphate ions play a crucial role in cell signaling pathways. Phosphorylation, which involves the addition of phosphate groups to proteins, is a key mechanism that regulates protein function and cellular processes such as cell growth, differentiation, and apoptosis (Ardito et al., 2017).

3.1.5. pH regulation

Ions play a crucial role in regulating the pH levels in bodily fluids and tissues. Buffers containing ions, particularly bicarbonate (HCO_3^-), are essential for maintaining the body's acid-base balance, which is paramount for optimal enzyme activity, protein function, and overall physiological well-being (Muir, 2015)

3.1.6. Nutrient transport

Ions play a crucial role in facilitating the transportation of nutrients across cellular membranes. Specifically, the sodium ion (Na^+) is fundamental to the process of nutrient absorption, including glucose, amino acids, and other essential nutrients in the intestines, through sodium-dependent transporters (Hediger and Rhoads, 1994).

3.1.7. Cellular metabolism

Anions such as phosphate ($HPO_4^{2-}/H_2PO_4^-$) play a critical role in energy metabolism and cellular signaling. Phosphate ions are essential components of molecules such as ATP (adenosine triphosphate), which serves as the primary energy currency in cells, and cAMP (cyclic adenosine monophosphate), a crucial signaling molecule (Peacock, 2021).

3.1.8. Water balance

The presence of ion gradients across the membranes of cells is critical in controlling osmotic pressure, which in turn governs the movement of water into and out of cells (Schwab et al.,2007). Adequate water balance is necessary for the hydration of cells, regulation of blood pressure, and overall fluid homeostasis.

3.1.9. Enzyme activation

Some ions serve as cofactors for enzymes, modulating their activity and specificity. Examples include magnesium (Mg^{2+}), which is required for ATP-dependent reactions, and zinc (Zn^{2+}), which is involved in various enzymatic processes.

3.1.10. Cell adhesion and communication

The presence of Calcium ions (Ca^{2+}) is essential for cell adhesion as they enable cells to attach to each other and to the extracellular matrix (Nayab et al.,2005). Moreover, cell-cell interactions and communication within tissues are facilitated by Calcium-dependent cell adhesion molecules.

3.2. Effect of various ions on protein misfolding

Protein aggregation is a complex process whereby proteins misfold and assemble into insoluble structures. This phenomenon assumes critical significance in both physiological and pathological contexts. The interaction between ions and proteins is a fundamental issue in a range of fields, including life sciences and industrial processes (Niemeyer, 2001). Ions play a pivotal role in controlling cell physiological processes and are known to influence the oligomerization of charged rod-like biopolymers, such as DNA, microtubules, and actin (Wong and Pollack, 2010). Moreover, they also affect the aggregation of disease-associated amyloidogenic proteins. During the 19th century, Hofmeister's pioneering work brought to light the effect of various ions on protein solubility (Nostro and Ninham, 2012). His findings showed that certain ions are capable of inducing protein precipitation (salt-out), while others

promote protein solubilization (salting-in). Subsequent research has revealed the existence of ion-selective effects that can influence ion channel permeability and enzyme activity, which parallel the observations made by Hofmeister. These observations suggest a common molecular basis underlying the intricate interplay between ions and proteins in biological systems.

The relationship between ions and protein aggregation is complex and multi-faceted. Ions can have a variety of effects on protein stability, conformation, and intermolecular interactions (Zhou and Pang, 2018). It is important to understand these effects in order to better understand protein aggregation-related diseases and to develop effective therapeutic strategies. In this context, we explore the different ways in which ions can influence protein aggregation, providing relevant examples and references to support our discussion.

3.2.1. Ionic strength and protein aggregation

The concentration of ions in solution, known as ionic strength, is a key factor in regulating protein aggregation kinetics. By adding salts to increase the ionic strength, the electrostatic repulsion between protein molecules can be shielded, thereby promoting protein aggregation. Isaacs et al. (2006) demonstrated this phenomenon in a study on the aggregation of amyloid beta (Aβ) peptides associated with Alzheimer's disease (Isaacs et al., 2006). As the NaCl concentration increased, the aggregation of Aβ peptides accelerated. When the ionic strength is higher, the electrostatic repulsion between Aβ peptides is reduced, enabling them to come closer, which facilitates the nucleation and growth of aggregates. This example highlights the profound influence of ionic strength on protein aggregation and underscores its importance in understanding the mechanisms of protein misfolding diseases and developing therapeutic interventions.

3.2.2. Specific ion effects

Specific ion effects refer to the impact that different ions have on protein behavior due to their distinct properties. These effects greatly influence the dynamics of protein aggregation. For example, Nostro and Ninham's research in 2012 showed how magnesium ions, known as kosmotropes, and guanidinium ions, known as chaotropes, had contrasting effects on the aggregation of the prion protein PrP (Nostro and Ninham, 2012). Magnesium ions, classified as kosmotropes, typically stabilize protein structures and inhibit aggregation by enhancing hydration and shielding protein-protein interactions. Conversely, guanidinium ions, categorized as chaotropes, disrupt hydrogen bonding networks and promote non-native

interactions, leading to protein destabilization and an acceleration of the aggregation process. These findings underscore the importance of considering specific ion effects when investigating protein aggregation and provide insights into potential therapeutic strategies for protein misfolding diseases.

3.2.3. pH dependence and ion effects

Changes in pH can affect the way proteins aggregate, as pH can alter the protonation state of amino acid residues, leading to changes in protein charge distribution and electrostatic interactions. One example of this is the aggregation behavior of insulin, which has been demonstrated by Ahmad et al. in 2011. Depending on the pH of the solution, insulin can exhibit different patterns of aggregation (Ahmad et al.,2011). Zinc ions have been found to play a crucial role in regulating insulin solubility and preventing aggregation when present at a neutral pH. However, in acidic conditions, zinc ions trigger conformational changes in insulin that result in the formation of aggregates. This pH-dependent effect highlights the intricate interplay between ion effects and pH in modulating protein aggregation dynamics. It is crucial to comprehend these complexities to unravel the mechanisms underlying protein misfolding diseases and to develop targeted therapeutic strategies to mitigate protein aggregation.

3.2.4. Metal ions and oxidative stress

Metal ions are known to play a crucial role in regulating protein aggregation via oxidative stress mechanisms. Among various transition metal ions, copper and iron have been found to be particularly involved in promoting protein aggregation by facilitating the generation of reactive oxygen species (ROS). For instance, copper ions have been shown to catalyze the aggregation of alpha-synuclein, a protein that is strongly associated with Parkinson's disease, through ROS-mediated pathways (Rasia et al., 2005). The combination of copper ions and alpha-synuclein results in the production of hydrogen peroxide and hydroxyl radicals. These radicals cause oxidative damage to proteins, DNA, and lipids, which eventually leads to protein aggregation. This example highlights the crucial part metal ions play in worsening protein misfolding diseases through oxidative stress mechanisms. It highlights the intricate interplay between metal ions and protein aggregation.

3.2.5. Hydration and solvation effects

Hydration and solvation effects significantly influence protein aggregation behavior (Thirumalai et al.,2012). These effects impact the solubility and interactions of proteins in

solution. The introduction of ions can modify the hydration shell surrounding proteins, which can affect their propensity for aggregation. A classic example of this was demonstrated by Collins and Washabaugh (1985), who showcased the hydration effects of ions on protein behavior at interfaces (Collins and Washabaugh, 1985). The presence of kosmotropic ions, including sulfate ions, can effectively stabilize the hydration shells of proteins. These ions enhance the structure of water and decrease protein-protein interactions, ultimately inhibiting the process of aggregation. In contrast, chaotropic ions, such as thiocyanate ions, have the opposite effect. They destabilize protein structures and promote aggregation by disrupting hydration and encouraging protein-protein interactions. This example clearly demonstrates the significant role that hydration and solvation effects play in determining the kinetics of protein aggregation. It underscores the importance of comprehending the changes induced by ions in the structure of water in order to gain a better understanding of the mechanisms underlying protein misfolding diseases.

3.2.6. Salt bridges and electrostatic interactions

Salt bridges and electrostatic interactions between charged residues on protein surfaces are fundamental aspects that play a pivotal role in determining the stability and aggregation propensity of proteins. These interactions can either stabilize protein structures or promote aggregation, depending on the balance between attractive and repulsive forces. For instance, Hung et al. (2010) conducted a study to investigate the role of electrostatic interactions in lysozyme aggregation induced by sodium dodecyl sulfate (SDS) (Hung et al.,2010). The researchers observed that the electrostatic interactions between positively charged lysine residues on lysozyme and negatively charged sulfate groups on SDS played a significant role in protein aggregation. The stability of protein structures under physiological conditions can be attributed to the formation of salt bridges and electrostatic interactions between oppositely charged residues (Panja et al.,2020). However, excessive ionic interactions may promote protein aggregation, as they facilitate the assembly of misfolded protein aggregates. This example underscores the significance of comprehending salt bridges and electrostatic interactions in elucidating the mechanisms of protein aggregation and highlights the need for further research in this area.

3.3. Interaction of insulin with metal ions

The efficacy of insulin is known to be influenced by its interaction with various components of the cellular milieu. Specifically, insulin coordinated with Zn^{2+} ions at the site of production,

i.e., in the pancreas. In vitro studies have revealed that metal ions, such as Co^{2+} and Cd^{2+}, in conjunction with Zn^{2+}, facilitate the formation of insulin crystals. Moreover, Hudecek et al. have demonstrated that Zn^{2+}, Co^{2+}, and Cd^{2+} induce a red shift in the tyrosyl bands present in insulin's absorbance spectra. Interestingly, Ca^{2+} and Mg^{2+} were found to have no such effect (Hudeček et al.,1979). This spectral shift was attributed to conformational changes in insulin hexamers, which arise due to the presence of the aforementioned interacting metal ions in the proximity of tyrosine residues.

In a study conducted by Coffman and Dunn, two insulin hexamers were synthesized, each with or without Co^{3+} ions bound to HisB10 (Coffman and Dunn, 1988). Their results indicated that the hexameric form of insulin could be stabilized by only one Co^{3+} ion at the HisB10 site. In addition to HisB10, GluB13, another amino acid residue, also binds to other metal ions such as Zn^{2+}, Cd^{2+}, and Pb^{2+} (Coffman and Dunn, 1988). Although Zn^{2+} can bind to both B10 and B13 residues, coordinating with HisB10 provides additional thermodynamic stabilization to insulin. Xu et al. discovered that an excess of zinc encourages insulin to form the hexameric structure, whereas, under zinc-free conditions at low ionic strength and a pH close to its pI, insulin remains in the dimeric state (Xu et al.,2012). Conversely, Co^{2+} binds to HisB10, while Ca^{2+} has a higher affinity for GluB13. Like Zn^{2+}, Ca^{2+} also stabilizes the insulin hexamer. This knowledge is critical because metal ion contamination during insulin purification and packaging could negatively affect insulin aggregation (Lougheed et al.,1980).

3.4. Effect of various ions on insulin aggregation

Insulin is a peptide hormone consisting of 51 amino acids. It has been observed to readily form amyloid fibrils in vitro. In the pancreatic secretory granules, insulin is stored in a dense packing with Zn(II) to form crystals of $Zn_2Insulin_6$ hexamer. This helps to maintain the stability of the vesicles and prevent the formation of fibrils. However, once insulin is released from the pancreatic β-cells, it dissociates into active monomers, which tend to fibrillate at acidic pH values and physiological levels.

Noormagi et al. (2010) conducted a study that examined the impact of co-secreted Zn(II) ions on the fibrillation of monomeric insulin. The findings revealed that Zn(II) forms a soluble complex with insulin, which inhibits the fibrillation of monomeric insulin at physiological pH values. At pH 7.3, the inhibitory effect of Zn(II) ions was particularly strong (IC_{50} = 3.5 μM), while it gradually weakened at pH 5.5, suggesting the involvement of histidine residue(s) in complex formation. Overall, these results suggest that Zn(II) ions may suppress insulin

fibrillation at release sites and in circulation. It was also proposed that misfolded oligomeric intermediates, which may occur in zinc-deficient conditions, could trigger autoantibodies against insulin, leading to β-cell damage and autoimmune Type 1 diabetes (Noormägi et al.,2010).

In a study on insulin aggregation in artificial delivery systems, Lougheed et al. found that Zn^{2+}, Cu^{2+}, and Fe^{2+} induce large insulin aggregates with molecular weights ranging from 10^5 to 2×10^5 Da at neutral pH (Lougheed et al.,1980). They also observed visible precipitation in vials containing Cu^{2+} within 4 hours when insulin was slowly rocked at physiological pH, whereas visible aggregation appeared only after 3-4 days in copper-free controls. Because zinc plays a physiological role in stimulating the development of insulin hexamers, its effect on insulin aggregation is complex. The insulin dimer is thought to be the initiating species for aggregation because of its predominance or quicker aggregation rate in the absence of zinc. A nucleation-dependent process is shown by insulin's greater inclination to assemble at increasing monomer concentrations (Dunn, 2005). Because the coordination of Zn^{2+} with HisB10 promotes the production of insulin hexamers at concentrations above 0.01 mM Zn-insulin, insulin fibrillation rises with a reduction in insulin concentration in solutions of Zn-insulin at physiological pH (Yip et al., 1998). Hexameric Zn-insulin must dissociate into its dimeric form in order for insulin to aggregate (Dathe et al., 1990). Because HisB10 is protonated at low pH, insulin is in its monomeric state and has a higher aggregation tendency because zinc coordination is prevented. Less fibrillation results from insulin's greater propensity to form hexamers at doses over 0.01 mM in a neutral environment when zinc is present.

Researchers have discovered that amyloid fibrils, which can be used to create advanced biomaterials, are heavily influenced by the properties of the solvent used to create them. A study by Vanik et al. in 2023 examined the effect of ionic liquids on insulin fibrillation (Figure 1). These alternative solvents have adjustable properties and have been proven to help regulate the formation of amyloid fibrils. The scientists analyzed the effect of five different ionic liquids, all containing the 1-ethyl-3-methylimidazolium cation [$EMIM^+$] and anions of Hofmeister series hydrogen sulfate [HSO_4^-], acetate [AC^-], chloride [Cl^-], nitrate [NO_3^-], and tetrafluoroborate [BF_4^-], on insulin fibrillization. They used fluorescence spectroscopy, AFM, and ATR-FTIR spectroscopy to examine the kinetics, morphology, and structure of insulin fibrils. Their findings indicated that the ionic liquids studied could speed up the fibrillization process in a concentration-dependent manner that varied with the type of anion used. The results of the study indicate that anions can successfully enhance insulin amyloid fibrillization

at concentrations of IL up to 100 mM in the reverse Hofmeister series. This suggests that ions interact directly with the surface of proteins. Amyloid fibrils with varying forms were generated at a concentration of 25 mM, although they shared a comparable secondary structure composition. No correlation was found between the kinetics parameters and the Hofmeister ranking. To be more precise, in the IL-free solvent, fibrils with needle-like morphologies formed when IL was combined with the kosmotropic strongly hydrated [HSO_4^-] anion. In contrast, other kosmotropic anions, such as [AC^-] and [Cl^-], produced large amyloid fibril clusters. Conversely, ILs containing chaotropic anions [BF_4^-] and [NO_3^-] produced longer fibrils that were laterally linked. A careful balance and interaction between particular protein-ion and ion-water interactions and non-specific long-range electrostatic shielding controlled the impact of particular ILs (Vanik et al., 2023).

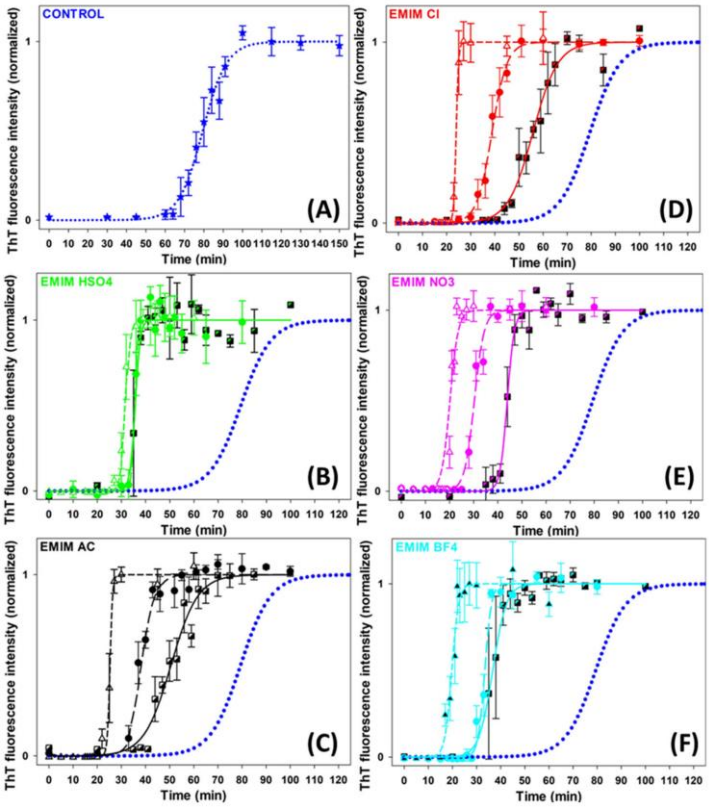

Figure 1: Graphic representation of insulin fibrillization in the absence (blue dotted line in (A–F)) and presence of (B) [$EMIM^+$] [HSO_4^-], (C) [$EMIM^+$] [AC^-], (D) [$EMIM^+$] [Cl^-], (E) [$EMIM^+$] [NO_3^-], (F) [$EMIM^+$] [BF_4^-]. IL-concentrations: CIL = 10 mM (semi-filled square, solid line); CIL = 25 mM (circle, long-dash line); CIL = 100 mM (open triangle, short-dash line). (Adapted from Vanik et al., 2023)

The research conducted by Paul et al. (2024) elucidated the inhibition of amyloid fibrillation of human insulin by two transition metal ions, Fe^{3+} and $Cu^{2+,}$ at acidic pH and elevated temperature. The researcher conducted a study to investigate the inhibitory effects of two biologically relevant transition metal chloride salts - iron and copper, in very low concentrations on the in vitro fibrillation of insulin. The results of their research work indicated that Fe^{3+} exhibited greater inhibitory potential than Cu^{2+} in suppressing the formation of β-sheet-rich fibrillar structures (Figure 2). Dynamic light scattering and circular dichroism techniques were employed to demonstrate that Cu^{2+} was effective in reducing the interaction ratios with insulin, while Fe^{3+} was effective in maintaining the size and alpha-helical conformation of monomeric insulin. The metal complexes of insulin-Fe^{3+} or insulin-Cu^{2+} were found to delay the nucleation step of aggregation, with Fe^{3+} emerging as the more potent inhibitor. Both metal ions demonstrated their efficacy in preventing amyloid fibrillation in vitro and were able to modulate the morphology of the aggregates, as revealed by TEM studies (Paul et al.,2024).

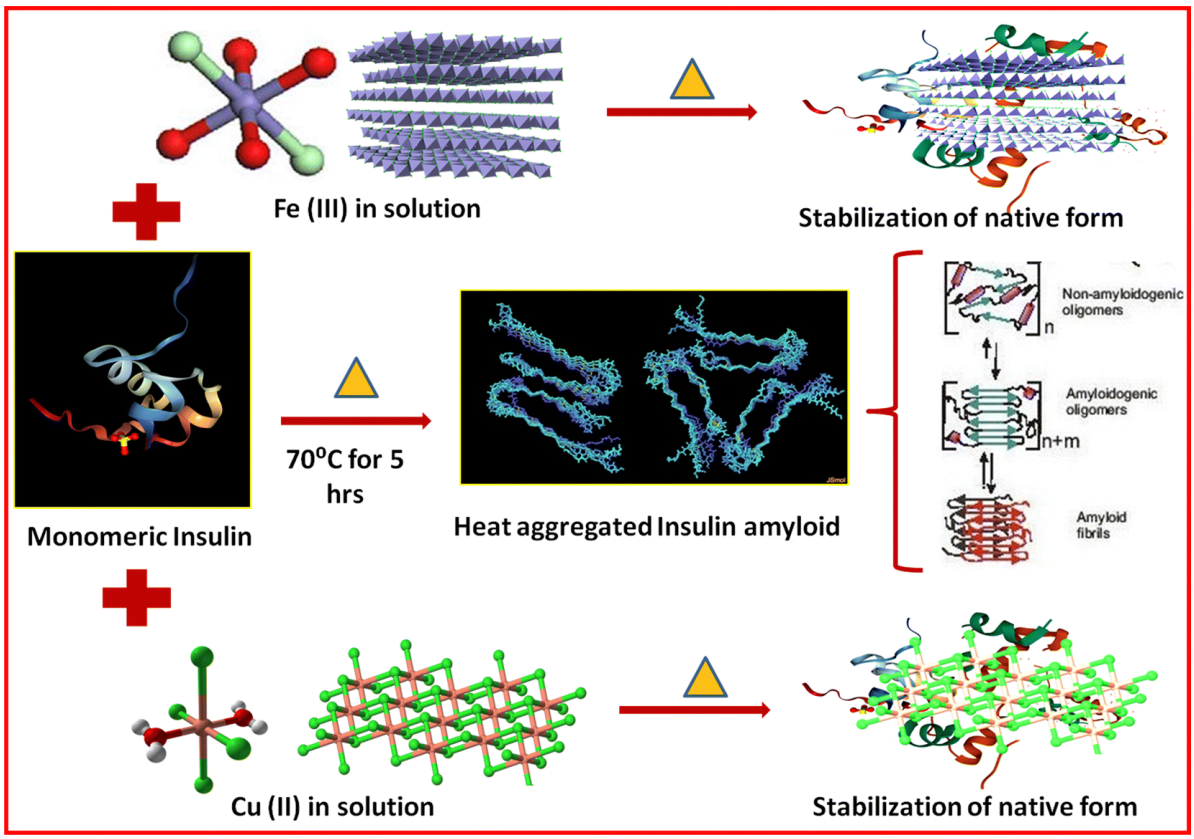

Figure 2: Schematic depiction of partial unfolding and self-assembly formation of human insulin in the absence and presence of Fe^{3+} and Cu^{2+} metal ions when co-incubated separately with insulin. (Adapted from Paul et al., 2024).

The impact of anions on insulin aggregation has been studied and documented. A report by Owczarz and Arosio discovered that sulfate anions can hinder the conversion of insulin monomers to aggregates by altering the insulin aggregation path (Owczarz and Arosio, 2014). Insulin followed a nucleation-dependent polymerization route at low sulfate concentrations (0–5 mM) and an acidic pH, which is commonly reported to produce thin fibrils. But beyond 5 mM, sulfate ions led to a delayed fibrillation process by salting out about 18–20% of insulin monomers into reversible amorphous aggregates with a high alpha-helix structure. These amorphous aggregates underwent structural rearrangement over time, evolving into beta-sheet-rich fibrils that recruited monomer molecules to elongate into mature fibrils. By sheltering the charge on the insulin surface, chloride ions, on the other hand, increased the aggregation rate rather than having an inhibitory effect on insulin aggregation at any concentration. On the other hand, the amount of sulfate ions present determined whether or not insulin accumulated. Aggregation was characterized by a larger activation energy in the presence of a substantial excess of sulfate ions than chloride ions (Figure 3). The elongation interaction between monomeric proteins and seed-component aggregates or structural rearrangements of insulin caused by sulfate ions may be responsible for this phenomena.

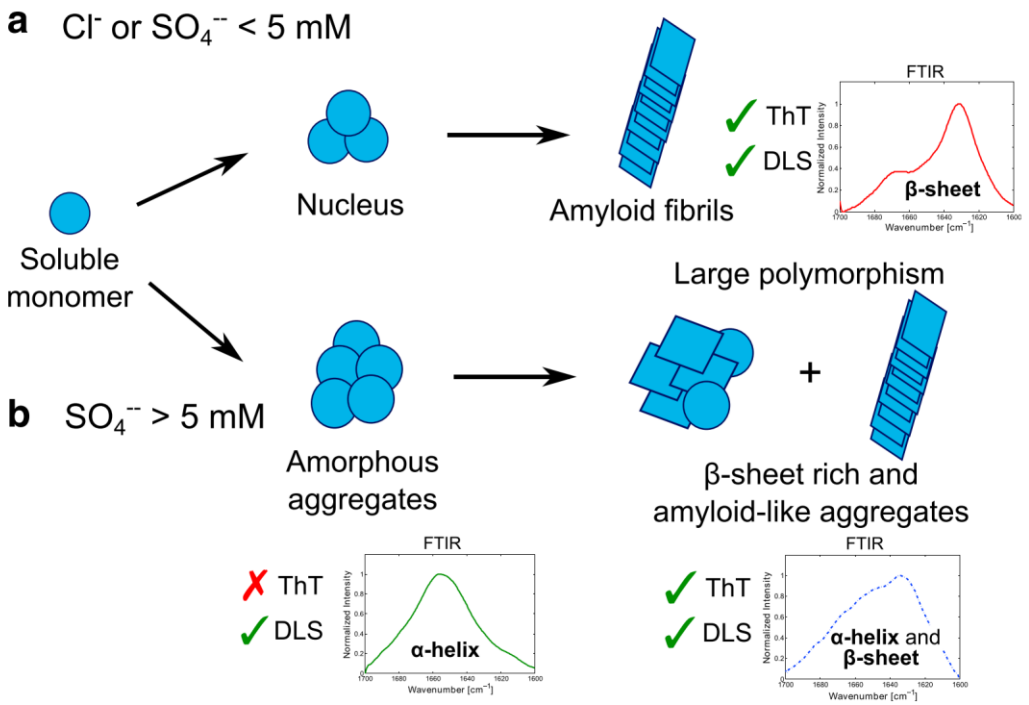

Figure 3: Schematic diagram showing the several ways that insulin aggregates when sulfate is present. (a) Insulin forms amyloid fibrils at low sulfate concentrations (0–5 mM) by the nucleated polymerization mechanism, which is frequently observed in acidic conditions in the

presence of monovalent anions; (b) As the sulfate concentration rises above 5 mM, the sulfate anion causes ~18–20% of insulin molecules to salt out into reversible amorphous aggregates that retain a significant amount of a-helix structures. These aggregates change structurally throughout time to become polymorphic species with b-sheet architectures. (Adapted from Owczarz and Arosio,2014).

Previous studies have demonstrated that NaCl can cause a specific type of amyloid superstructure with strong chiroptical properties to form from agitated, acidified insulin solutions (Dzwolak et al., 2007; Loksztejn and Dzwolak, 2008; Babenko et al., 2011). A 2015 study by Babenko et al. discovered that adding NaCl at the beginning of insulin aggregation leads to structural variations in amyloid that exhibit unique fingerprint infrared features (Figure 4). However, when salt is added later to previously formed fibrils under calm conditions, a "condensation effect" occurs, forming amyloid superstructures with strong chiroptical properties. These superstructures are stabilized by chloride ions, much like how polyvalent cations stabilize DNA condensates. When bovine insulin fibrils grown in 0.1 M NaCl at pD 1.9 were thoroughly washed with water afterward, ion chromatography revealed that the concentration of residual chloride ions trapped within the fibrils was less than one anion per 16 insulin monomers. This suggests that there are no clearly defined solvent-sequestered nesting sites for chloride counterions. Their findings have implications for understanding the mechanisms of insulin aggregation (Babenko et al., 2015).

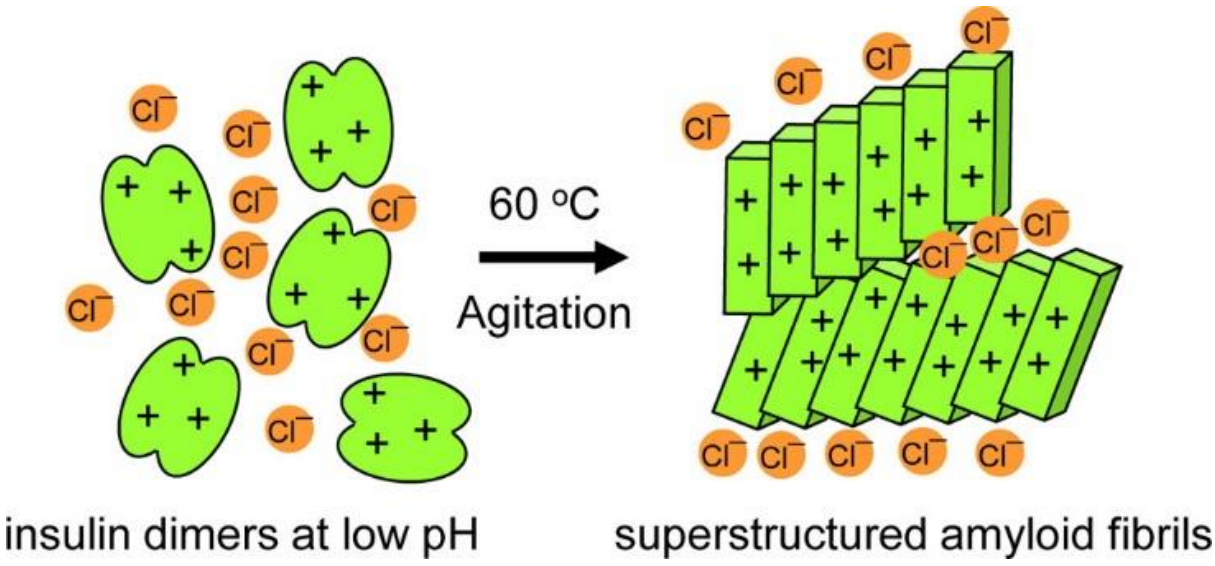

Figure 4: Influence of Cl^- ions on insulin aggregation. (Adapted from Babenko et al., 2015).

A study conducted by Muzaffar and Ahmad in 2011 demonstrated that NaCl enhances insulin fibrillation due to subtle structural changes rather than just a salt effect. The study was

conducted in the presence and absence of urea and Gdn.HCl, and aimed to compare the relationship between the conformation of insulin induced by urea and Gdn.HCl and its relation to NaCl at both pH 7.4 (hexamer) and pH 2 (monomer). Fibril formation was evaluated using a Thioflavin T assay, while circular dichroism and size-exclusion chromatography were used to keep track of structural changes. The results indicated that salt-insulin interactions cannot be classified as commonly accepted Debye-Hückel or Hofmeister series interactions. Instead, a strong correlation was observed between the association states and conformational states of insulin and their propensity to fibrillate (Muzaffar and Ahmad, 2011).

3.5. Effect of selected anions on the amyloid fibrillation of insulin

Protein function is closely related to its structure, which can be classified into four levels: primary, secondary, tertiary, and quaternary (Yu et al.,2006). Primary structure refers to the arrangement of amino acids in a polypeptide chain. Secondary structure encompasses alpha-helices and beta-sheets, which are formed locally within the polypeptide chain due to interactions between atoms in the protein backbone. These structures are also known as motifs.

The tertiary structure of a polypeptide encompasses its complete three-dimensional configuration. While some proteins consist of a single polypeptide chain and exhibit only primary, secondary, and tertiary structures, others, such as hemoglobin, possess a quaternary structure comprising multiple polypeptide chains arranged in coordination (Khan et al.,2017). Molecular machine proteins play a crucial role in biological functions. The unique sequence of amino acids in their three-dimensional structure determines their ability to bind to specific molecules, catalyze reactions, and interact with other proteins (Dorn et al.,2014). The impact of protein structure on function is multi-faceted, influencing everything from enzyme-substrate binding to catalytic efficiency. Additionally, protein structure affects how these molecules interact with other proteins and small molecules, which is essential for critical cell signaling processes.

Protein structure plays a significant role in determining the stability and folding of a protein. As a result, any changes in protein structure due to mutations, post-translational modifications, or environmental factors can affect the functional properties of a protein (Ramazi and Zahiri, 2021). These changes can lead to altered or impaired function and lead to the development of diseases.

Under stress due to misfolding, many proteins and peptides can form stable self-assemblies called amyloid fibrils (Selkoe, 2003; Chiti and Dobson, 2006). These fibrils have a common cross-β sheet structure, regardless of the nature of the proteins (Eisenberg and Sawaya, 2017). Researchers have tried to understand the formation of oligomeric intermediates of amyloid fibrils, which play a key role in the pathology of amyloid diseases (Eisenberg and Jucker, 2012). There are over twenty diseases in humans associated with "amyloidosis," including Alzheimer's disease, Parkinson's disease, cataracts, systemic amyloidosis, type 2 diabetes mellitus, and cardiovascular diseases (Khan and Khan, 2022). To trigger the protein oligomerization process, researchers have studied the fibril-forming events and the structural intermediates. The formation of worm-like protofibrillar assemblies with less organized structures than the resulting fibrillar aggregates is induced by the nucleation and subsequent growth of these oligomers (Lambrecht et al.,2019).

The rate and morphology of aggregates resulting from unfolded peptides and proteins are often governed by two key factors: the intrinsic parameter of the amino acid sequence and the surrounding physicochemical or environmental conditions. The intrinsic parameter is closely associated with the primary structure, types, and distribution of the amino acid residues that constitute the peptides or proteins, as well as their charge and beta-sheet propensity for adopting the crossed β-structure. On the other hand, physicochemical or environmental factors are influenced by a range of variables such as pH, temperature, salt ions, small additives, cosolvents, or solutes (Munishkina et al.,2004; Madeira et al.,2022; Banerjee and Das, 2012). Our bodies contain salts at lower concentrations, ranging from nanomolar to micromolar levels, which act as micronutrients (Morris and Mohiuddin, 2020). These salts' ions can play a crucial role in the amyloid formation, particularly in the aggregation of proteins such as α-synuclein (Munishkina et al.,2004), Aβ peptide (Klement et al.,2007), prion protein (Yeh et al.,2010), HypF (Campioni et al.,2012) and bovine serum albumin (Madeira et al.,2022). The protein aggregation ability of different ions is typically related to the electroselectivity principle or the Hofmeister series, which ranks ions commonly used to explain various chemical and biological phenomena (Vanik et al.,2023). The Hofmeister effect typically comes into play at moderate to high (>0.3 M) salt concentrations, with 'kosmotropic' ions enhancing protein stability by structuring water and decreasing protein solubility. Conversely, 'chaotropic' ions are believed to disrupt water structure, increasing protein solubility by reducing conformational stability (Ball and Hallsworth, 2015). Nonetheless, these effects are generally considered insignificant at lower and physiological salt concentrations. At salt concentrations below 0.1 M, protein-ion

interactions are mainly controlled by nonspecific electrostatic interactions, which screen the charges on protein surfaces (Kunz, 2010). However, there are instances where ion-specific effects play a significant role in protein solubility (Zhang and Cremer, 2009), stability (Yao et al.,2021), and amyloid fibrillation (Munishkina et al.,2004) in this concentration range. While some anions, such as sulfates, can cause the native protein solution to precipitate, their impact on non-native protein solutions is complex, and only a few have been reported. On the other hand, some anions can stabilize the protein structure under non-native conditions, reducing the likelihood of forming aggregation-prone structures (Rajan et al.,2021). The presence of ions with different charges can significantly alter the electrostatic fields and ionic environment surrounding proteins. The aggregation of protein can either be inhibited or promoted by the differential electrostatic effects imposed by anions that have varying charges (Wang, 2005). When anions bind to the positively charged residues of protein at low pH, not only does it affect the rate of oligomerization, but it also impacts the morphology of the aggregates. The effectiveness of different ions in controlling the protein fibrillation phenomenon is highly dependent on the anion type, its concentration, pH, and temperature of the medium, as well as the particular protein being studied (Nielsen et al., 2001). For our current research, we have chosen some biologically important monovalent salt anions and focused on their influence at physiologically relevant concentrations on the fibrillation mechanism and fibril morphology of human insulin under an acidic environment.

Insulin is a hormone made up of 51 amino acids that regulate blood glucose levels. It has two peptide chains, known as chain A and chain B, and a mostly α-helical structure when in its natural state (Rahman et al.,2021). In the body, insulin is found primarily in a hexameric form that is stabilized by Zn^{2+} (Arya et al.,2021). However, at low pH, it exists as a monomer. When the environment changes, the hexameric form dissociates into its monomeric state. This process exposes hydrophobic residues that are normally buried in the hexamer (Ivanova et al.,2009). The insulin B chain residues B11-B18 and B24-B26 play a significant role in this fibrillation pathway (Nielsen et al.,2001). Under stress-induced conditions, insulin undergoes structural changes that lead to different oligomeric forms, including amyloid structures. It has been studied as a model system for amyloid fibril formation. However, this raises concerns regarding the efficacy of insulin in treating type II diabetes (Ahmad et al.,2005).

Insulin amyloid deposition is observed in patients with type II diabetes and after repeated injection and subcutaneous insulin infusion. Under high temperatures and low pH, insulin forms a fibrillar network with greater β-structure (Whittingham et al., 2002). Existing reports

indicate that strong acids can trigger the formation of insulin's molten globule. It is believed that the molten globule state plays a role in both protein folding and amyloid formation (GoTo et al.,1990). For our study, we focused on three crucial salt anions: acetate, iodide, and nitrate. These anions occur in our cellular components in very small concentrations (in the micromolar range) and hold different positions in the Hofmeister and electroselectivity series.

The study focused on the effect of selected salt anions at very low concentrations of 1 μM and 50 μM. This allowed for an examination of specific ion binding with charged side chains and Debye-Huckel charge screening. The Hofmeister effect, on the other hand, was not significant at these low concentrations. The experiment utilized sodium acetate (NaOAc), sodium iodide (NaI), and sodium nitrate (NaNO3) to analyze the aggregation kinetics and morphology changes of insulin at pH 1.6 and 60°C. With protein surfaces being primarily dominated by positive charges at low pH, the impact of cations was minimal compared to that of the anions.

Previous studies on the anion-induced fibrillation of insulin have shown the involvement of higher salt concentrations in the millimolar (mM) range. However, in our present study, we have maintained the anion concentrations at levels relevant to our physiological conditions in the micromolar (μM) range. Through a variety of multi-spectroscopic techniques, including ANS fluorescence, Thioflavin T (ThT) assay, dynamic light scattering (DLS), circular dichroism (CD) spectroscopy, and transmission electron microscopy (TEM), we explored the mechanism and morphology of insulin amyloid aggregates and their fibrillation process.

3.6. Materials and methods

3.6.1. Materials

Human insulin, sold under the trade name 'Huminsulin,' was acquired from Eli Lilly in India through a local medicine shop. Other chemicals, such as sodium acetate, sodium iodide, sodium nitrate, acetic acid, and hydrochloric acid, were obtained from Merck in India. Various fluorescent probes, including Thioflavin T (Th T) and 8-anilinonaphthalene-1-sulfonic acid ammonium salt (ANS), were purchased from Sigma Chemical Co. in the USA. All chemicals used were of the highest available purity. Furthermore, we filtered all buffer solutions through a 0.22 μM Micro Syringe filter made by Millipore in the USA.

3.6.2. Monomeric insulin preparation

The current study involves the preparation of an insulin solution with a concentration of 100 IU/mL of Insulin Human I.P. (rDNA origin) that predominantly exists in a hexameric state

(Bakaysa et al.,1996). An extensive dialysis process was carried out to eliminate glycerine, the tonicity modifier, and m-cresol, the preservative. The pH of the solution was then adjusted using HCl/NaOH. The solution was then converted to the monomeric state by adding 80% acetic acid to a final concentration of 20% (Whittingham et al.,2002). To prevent the formation of amyloid-like fibrils, the solution was filtered through a Millex-G 0.22 mm (Millipore) membrane filter to exclude any residual hexameric insulin. The filtrate was then incubated at 37°C overnight in a temperature-controlled oven to achieve a homogeneous solution containing monomeric insulin with a concentration of 1.5 mg/mL (Whittingham et al.,2002) (Ahmad et al., 2003). The extinction coefficient of insulin was calculated as $\varepsilon_{1\%}$ 276 nm= 10.0 (Nielsen et al.,2001).

3.6.3. Preparation of insulin oligomers

A 20% monomeric insulin (MI) solution in acetic acid was prepared and then diluted to 1.0 g/L with 1(N) HCl. The solution was then subjected to thermal treatment at 65°C and pH 1.6 for 4 hours to initiate the amyloid fibrillation of insulin (Nilsson, 2004). To investigate the influence of salt anions, monomeric insulin at pH 1.6 was incubated with separate solutions of 1μM and 50 μM NaOAc, NaI, and $NaNO_3$ at 65°C for 4 hours. The aggregation process was monitored using ThT and ANS fluorescence, dynamic light scattering (DLS), and transmission electron microscopy (TEM).

3.6.4. Intrinsic fluorescence measurements

The intrinsic fluorescence of tyrosine was investigated in monomeric insulin (20μM) and heat-treated insulin (65^0C for 4 hours). The measurements were carried out under controlled conditions of temperature (200 C) and pH (1.6) in the presence and absence of 1 μM and 50 μM NaOAc, NaI, and NaNO3 salt solutions. The excitation wavelength was set at 276 nm, and spectra were recorded within the 280−400 nm wavelength range. The slit width was maintained at 5 nm for both excitation and emission. The findings of this study could potentially provide insights into the effects of salt solutions on the intrinsic fluorescence of tyrosine in insulin.

3.6.5. ANS fluorescence measurements

During the aggregation process of insulin, its hydrophobic patches were opened up. This process was monitored with the help of a polarity-sensitive fluorescent probe called ANS. In this regard, a stock solution of ANS was added to each insulin sample at 20μM concentration. Two different strengths of NaOAc, NaI, and $NaNO_3$ solutions were added to the samples at a pH of 1.6. The concentration of ANS in each aliquot was kept at 30 mM, using a 50-fold molar

excess of insulin. Following a 15-minute incubation in the dark, the ANS fluorescence intensities were measured upon excitation at 380 nm. Subsequently, the emission spectra were recorded between 400 and 600 nm using a fluorescence spectrophotometer (Horiba, Fluoro Max FM-4). Blank corrections were performed with ANS as a control for all sets. The excitation and emission slit widths were maintained at 3 and 5 nm, respectively. The presented data points represent the mean of three consecutive measurements.

3.6.6. Th T fluorescence measurements

Th T is a commonly used dye that helps to identify amyloid fibrils by binding with the crossed beta-sheet structure of amyloid fibrils (Biancalana and Koide, 2010). The Th T fluorescence assay was conducted utilizing a Horiba fluorescence spectrophotometer (FluoroMax FM-4). The stock solution of ThT was prepared with miliQ water, and its concentration was calculated by using the molar extinction coefficient of 36,000 M^{-1} cm^{-1} and the absorbance value at 412 nm (Freire et al.,2014). Insulin samples were thermally incubated separately with or without 1μM and 50μM OAc^-, I^- and NO_3^- solutions having pH 1.6. From each sample set, insulin samples were withdrawn and added to Th T to detect the amyloid fibrils, keeping the final protein and dye concentrations at 20 μM. The fluorescence spectra of Th T were recorded from 450 to 600 nm while exciting at 440 nm. The excitation and emission slit widths were maintained at 3 and 5 nm, respectively. The sample spectrum was corrected using the respective blank. The data points reported are the mean of three consecutive measurements.

3.6.7. Measurement of hydrodynamic radius (RH) of insulin oligomers by DLS

Dynamic light scattering (DLS) is a commonly utilized technique in the field of biophysics and biomolecular sciences to determine the size of macromolecules, such as proteins and aggregates present in a solution. It is known that the diffusion of small nano-sized particles can alter the intensity of scattered light, and DLS is capable of monitoring these fluctuations based on autocorrelation (Rupert et al.,2017). This analysis allows for the distribution of particles and fibrillar aggregates to be evaluated due to the technique's sensitivity to particle size.

This study conducted DLS measurements using heat-incubated insulin (65°C for 4h) in the presence and absence of ^-OAc, I^-, and NO_3^- anions. The measurements were performed using a Zetasizer Nanos (Malvern Instrument, U.K.) equipped with a 633 nm laser. A rectangular cuvette with a path length of 10 mm and a volume of 2 mL was employed for this purpose. Prior to measurements, the solutions were filtered through a syringe filter with a pore size of

0.22 μM. All measurements were conducted at a temperature of 20°C. Twelve acquisitions were made for each run to achieve the time-dependent autocorrelation function.

3.6.8. Monitoring the secondary structural changes of insulin by circular dichroism (CD) Spectroscopy

The present study aimed to assess the impact of anions OAc^-, I^-, and NO_3^- of varying concentrations on the conformational changes of insulin. To this end, far-UV CD spectra were recorded in the 195-255 nm wavelength range at 20°C using a JASCO-815 Spectropolarimeter equipped with a 1mm rectangular cuvette. Insulin solutions (pH 1.6) were subjected to incubation at 75°C for 4 hours in a temperature-controlled water bath, both in the presence and absence of the aforementioned anions. Aliquots of different insulin solutions were then diluted to a concentration of 0.2mg/mL to monitor the secondary structural changes of insulin, utilizing the CD spectropolarimeter. The final spectra of the protein samples were recorded by subtracting the corresponding buffer spectrum and averaging three consecutive scans. Finally, the secondary structural contents of different insulin samples were calculated using the CDNN 2.1 curve-fitting program.

3.6.9. High-resolution transmission electron microscopy (HR-TEM)

In order to characterize and differentiate the fibrils of insulin samples in different anionic environments, a series of TEM images were acquired using a high-resolution transmission electron microscopy (JEOL-HRTEM-2011, Japan), which operated with an accelerating voltage of 80-85 kV, and captured images at different magnifications. Each insulin sample (15 μL), in the absence and presence of OAc^-, I^-, and NO_3^- ions, was carefully placed on a carbon-coated copper grid of mesh size 300C (ProSci Tech) and allowed to rest for 20 seconds before the excess liquid was removed from the grid. Following this, two drops of 2% uranyl acetate (Sigma, Steinheim, Germany) were added for staining and removed after 15 seconds. The specimens were then left to dry in the air before imaging. All specimens were left for 6 hours before imaging to ensure optimal imaging conditions.

3.7. Results and discussion

3.7.1. Effect of salt anions on the intrinsic fluorescence of insulin

This study aimed to measure the intrinsic fluorescence of tyrosine (Tyr) residues in insulin by analyzing the monomeric insulin (MI), which contains only tyrosine residues (at the position

of 14, 19 of chain A and 16, 26 of chain B) as a fluorophore, and is devoid of any tryptophan residue. The results of this analysis indicated that the microenvironment around the excited fluorophore of insulin does not alter its normal fluorescence characteristics.

The study observed a decrease in fluorescence intensity in heat-incubated insulin in the absence of any salt anions, as it led to a change in the conformation and microenvironment around the excited fluorophore. The fluorescence intensity decreased upon incubation with anions OAc^-, I^-, and NO_3^- separately at 65^0 C for 4 hours (Figure 5). The decrease in emission intensity observed in the presence of salt anions indicates that the anions interact with insulin molecules, and the Tyr residues of the protein are exposed in an anionic environment. This decrease suggests that the anions interact with insulin molecules, exposing the Tyr residues of the protein in an anionic environment. Interestingly, the decrease in emission intensity is smaller in the presence of salt anions than in heat-treated (HT) insulin alone, indicating a lesser change in the insulin structure in an anionic environment. The positively charged residues on the insulin backbone in the acidic medium are stabilized by the anions, leading to this difference.

Furthermore, the study found that iodide ions had a greater effect on intrinsic fluorescence intensity than acetate and nitrate ions when salt concentrations were at a physiological level of 50 μM. This is due to the greater negative charge density and quenching ability of iodide ions compared to acetate and nitrate ions.

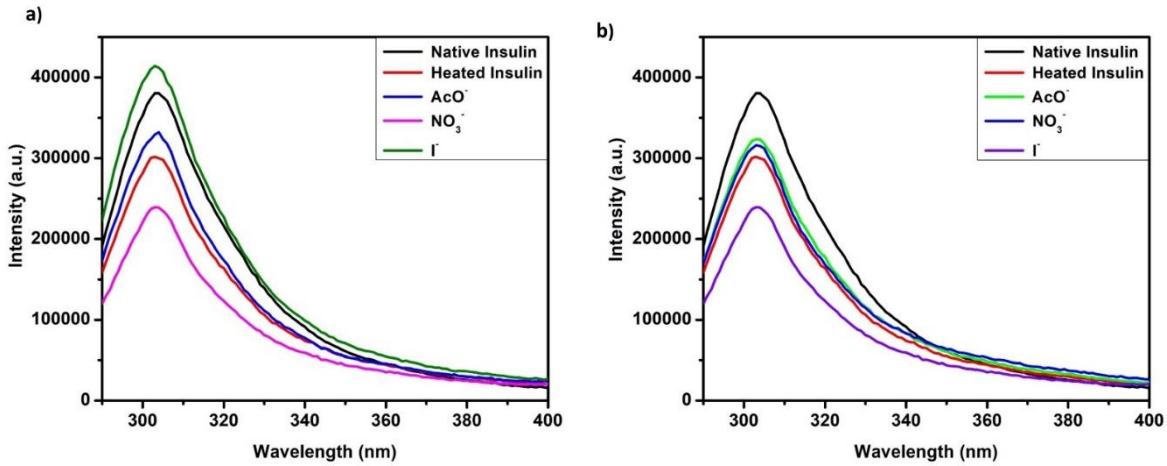

Figure 5: Intrinsic fluorescence emission spectra of monomeric insulin and thermally incubated insulin (65°C for 4 h) in the absence and presence of salt anions OAc^-, I^-, and NO_3^-.

3.7.2. Monitoring the change of the microenvironment of insulin in the presence of salt anions

The process of hydrophobic collapse leads to the formation of protein aggregates in the nucleation state. Upon thermal incubation of insulin (65^0 C for 4h, pH 1.6) in an acidic medium, patches of hydrophobic residues are exposed. In this study, we aimed to investigate the influence of selected salt anions $^-$OAc, I^- and NO_3^- of two different concentrations (1μM and 50 μM) on the exposure of hydrophobic clusters in insulin. We monitored the interactions between the protein samples and 8-anilinonaphthalene-1-sulfonate (ANS), a hydrophobic fluorescent probe, to determine the effect of salt anions. Our results indicate that the interactions between ANS and the exposed hydrophobic clusters of heat-treated insulin led to an increased fluorescence emission of ANS, accompanied by a blue shift of its emission maxima. Notably, ANS binding to native insulin was observed to be low, owing to the limited exposure of hydrophobic residues. On the other hand, ANS bound strongly to the newly exposed hydrophobic sites in the insulin samples incubated under acidic conditions, which resulted in a blue shift of the emission maxima to 490 nm. Moreover, ANS binding to insulin was significantly increased in the presence of anions, which resulted in a similar blue shift of the emission maxima from 515 nm to 490 nm (Figure 6). At a lower salt concentration of 10 μM, all the selected anions demonstrated a similar ANS fluorescence intensity to that of heat-treated insulin alone. This suggests that there was little interaction with the heat-induced insulin at low salt anion concentration. However, when 50 μM salt solutions were added to the thermally incubated insulin, the ANS-fluorescence emission increased in each case with blue shifts. This modulation of electrostatic forces was due to interactions of the anions with positively charged residues of insulin. Iodide ions (I^-) showed stronger interaction with positively charged residues in acidic pH compared to acetate (CH_3COO^-) and nitrate (NO_3^-) ions of the same strength. This led to the modification of electrostatic forces, exposing hydrophobic clusters in acid and heat-induced insulin molecules. The greater interaction of I- compared to CH_3COO^- and NO_3^- ions with the positively charged residues of insulin at acidic pH was due to the greater charge density on I^- ions. At this low salt concentration (physiological concentration range), the anions' efficacy in modulating the electrostatic forces in the acid-induced insulin follows the order I- > CH_3COO^- > NO_3^-.

These findings support the observations made in previous studies of aggregation kinetics, secondary structural changes, and electron microscopic studies (Morris et al.,2009). It is

important to note that ANS can also affect the partially unfolded structure's form in an acidic medium. Therefore, spectral data was acquired at a lower protein concentration than necessary during the aggregation kinetics study to avoid the formation of oligomers.

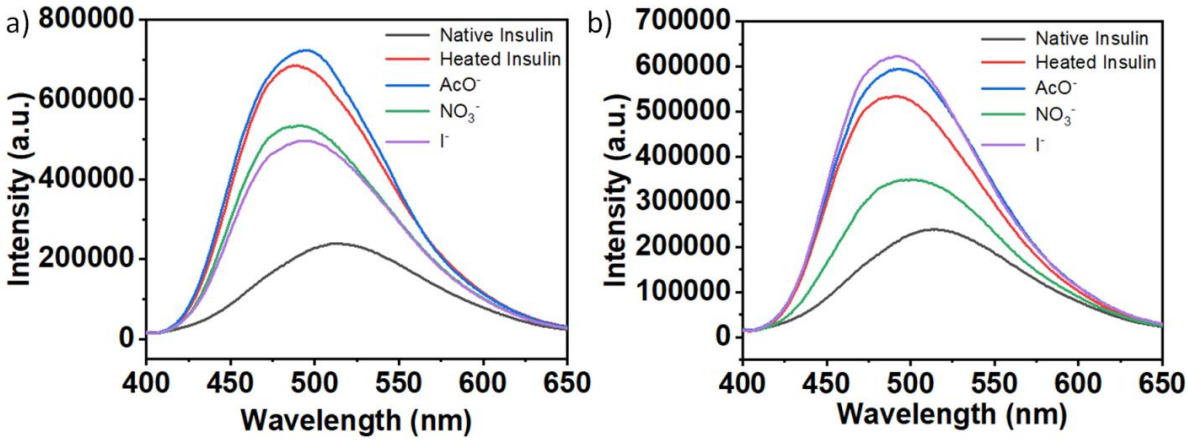

Figure 6: ANS-fluorescence of monomeric insulin and thermally incubated insulin (65°C for 4 h) without or with the salt anions OAc^-, I^-, and NO_3^-.

3.7.3. Effect of salt anions on the propensity of fibrillation of insulin

ThT-fluorescence measurements were carried out to explore the impact of distinct salt anions on insulin's amyloid fibril formation rate and likelihood. ThT, a benzothiazole dye, was utilized to specifically bind with amyloid aggregates and cause an enhancement of ThT fluorescence intensity. This method is a commonly used technique to identify the cross beta-structure of protein aggregates and measure the extent of amyloid formation. The ThT emission spectra of insulin were monitored in the absence and presence of OAc^-, I^-, and NO_3^- ions under low physiological salt concentrations, stressed conditions at pH 1.6, and a temperature of 65°C is represented in Figure 7a. The results obtained indicated that the monomeric insulin exhibited weak interaction with the ThT probe, resulting in the lowest ThT intensity. However, upon thermal incubation at 65°C, the monomeric insulin without any salt anion showed an enhanced ThT fluorescence intensity, thus indicating the formation of cross β-sheet structures during amyloid fibrillation of the protein. All other insulin samples were incubated with OAc^-, I^-, and NO_3^- ions at two different concentrations for four hours at pH 1.6. The ThT emission intensities produced by these samples were proportional to the amount of fibrillar aggregates in the solution. From the comparative analysis of the ThT-fluorescence emission spectra, it is apparent that the selected salt anions of biological significance promote the aggregation propensity of insulin at acidic pH differently depending on the concentrations used. At the lowest concentration range of approximately 1 μM, the anions OAc^-, I^-, and NO_3^- showed ThT-

fluorescence intensity similar to that of heat-incubated monomeric insulin alone. This indicates that the anions are unable to interact effectively with the positively charged residues of insulin at this very low salt concentration and have little influence on the thermal aggregation of insulin.

The present study investigated the interaction of three anions, $NaNO_3$, NaOAc, and NaI, with acid-denatured insulin at their higher salt concentrations (50 μM) to evaluate their effect on the fibrillation of insulin. The findings revealed that all three anions had a strong effect on the insulin fibrillation process and led to increased ThT emission intensities compared to heat-treated insulin. This indicates that the cross β-sheet structure formation increased when insulin was incubated with the three anions separately, which implies that they promote insulin fibrillation more efficiently.

Moreover, the ThT fluorescence emission intensity was highest when NaI was used at a 50 μM concentration level, while the other two anions, NO_3^- and OAc^-, also increased the fluorescence signals compared to heat-treated insulin. This suggests that the anionic environments created by these anions have a significant impact on the ThT emission intensities of insulin.

The study also suggests that anions with higher ionic strength have a greater ability to interact with positively charged side chain residues in acid-denatured insulin, which modulates the electrostatic forces and brings the aromatic and other hydrophobic amino acid residues closer to each other during beta-amyloid formation. The study found that the efficiency of beta-amyloidogenesis of the anions increases in the order $I^- > CH_3COO^- > NO_3^-$.

Overall, the present study provides valuable insights into the role of salt anions in insulin fibrillation and highlights the potential of these anions in modulating amyloid formation. This could have implications for the development of amyloid-based biosensors and therapeutics.

The current research focuses on the Th T-fluorescence curve of insulin with incubation time in the presence of selected anions, which is illustrated in Figure 7c. The results reveal a two-phase sigmoidal growth curve, characterized by an initial lag phase, followed by a sharp increase in intensity value, and ultimately reaching a constant curve. The ThT kinetic assay was monitored for up to 4 hours, and the final reading was taken after 24 hours, indicating that the ThT intensity did not change any further after reaching the plateau.

The middle phase of the ThT kinetic curve reflects the growth of amyloid fibrils, where ThT-fluorescence increases rapidly. The plateau, or the last phase, signifies the completion of the

nucleation, leading to the maturation of the fibrils. Such ThT kinetic curves are commonly observed in the protein aggregation phenomenon and have been reported by many researchers.

The impact of selected anions on insulin fibrillation was also investigated in this study. Insulin exhibited a shorter lag time in the presence of I^- and CH_3COO^- ions, while a longer lag phase was observed with nitrate anions (Figure 7d). Thus, NO_3^- ions delayed the aggregation of insulin, while I^- and CH_3COO^- ions accelerated the fibrillation process. An earlier report on anion-induced oligomerization of insulin revealed that at low (< 5mM) and high chloride salt concentrations, the nucleation-polymerization mechanism operates, leading to the generation of the amyloid fibrillar state of insulin.

In the context of insulin fibrillation, it has been observed that low sulfate concentrations (< 5mM) result in the formation of fibrillar aggregates that bear resemblance to their monovalent chloride ion counterparts. However, when sulfate salt concentration is higher than 5mM, it initially leads to the formation of amorphous aggregates. These aggregates subsequently change to both amorphous and fibrillar types of aggregates, ultimately causing a slowdown in insulin fibrillation.

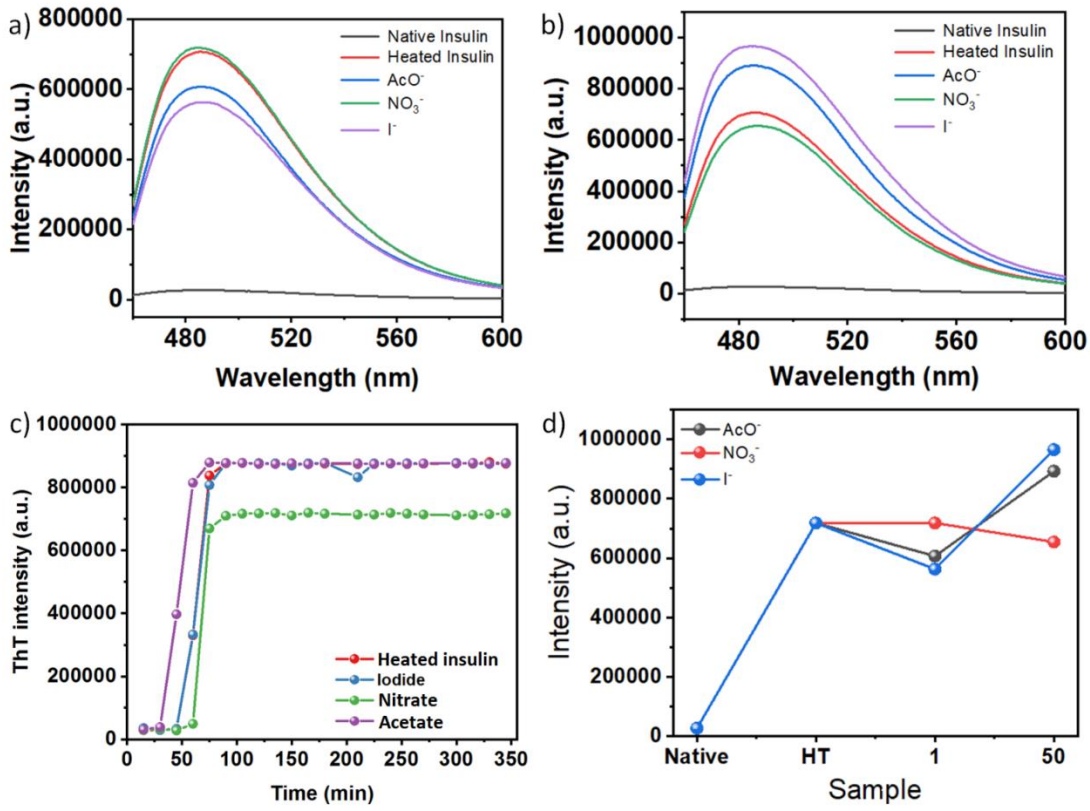

Figure 7: ThT-fluorescence profile of monomeric insulin and thermally incubated insulin (65°C for 4 h) with or without different salt anions at pH 1.6: (a) 1 μM and (b) 50 μM

concentration. The excitation wavelength was set at 440 nm, and fluorescence emissions were monitored from 450 to 600 nm. Slit widths were set at 3 nm (excitation) and 5 nm (emission). Each spectrum was the average of three scans within a 5% error limit. (c) The ThT fluorescence kinetics have been shown with the salt anions (50 μM) at pH 1.6; (d) Relative ThT fluorescence intensity curves (at 485 nm) of insulin in the presence of different salts anions at two different concentrations (1 and 50 μM).

3.7.4. Dynamic light scattering (DLS) study to measure Rh of the insulin oligomers in the presence of salt anions

Dynamic light scattering, or DLS, was carried out to determine the hydrodynamic radii (R_h) of insulin oligomers in the presence of salt anions. The size distribution of insulin aggregates and the size of the protein and its aggregates were estimated using DLS profiles represented in Figure 8. The hydrodynamic radii (R_h) of monomeric insulin (MI) were found to be between 32-60 nm, while the hydrodynamic radius of insulin aggregate (IA) was ~200 nm after incubation of insulin solution at 65°C for 4 hours. When insulin was co-incubated with salt anions, the R_h values of the insulin aggregates increased significantly. Iodide ions induced the formation of the largest aggregates with a R_h value of around 750 nm. In contrast, the formation of relatively smaller aggregates with R_h values of around 450 nm and 225 nm was observed with monovalent acetate and nitrate ions, respectively. During the experiment, sample solutions (0.1 mg/mL) were prepared with a total volume of 1 mL. The binding of anions with insulin reduced the protein's net positive charge, which enhanced hydrophobic interactions. Due to preferential exclusion, insulin molecules' net attractive forces promoted protein-protein interactions, leading to the nucleation of aggregates into fibrillar morphology, as revealed later by TEM. The charge density and shape of the anions employed explained the increasing trend in the size of insulin aggregates (IA).

In conclusion, the aggregation efficiency of the selected anions followed the order of Iodide > Acetate > Nitrate based on the fibrils' size and morphology.

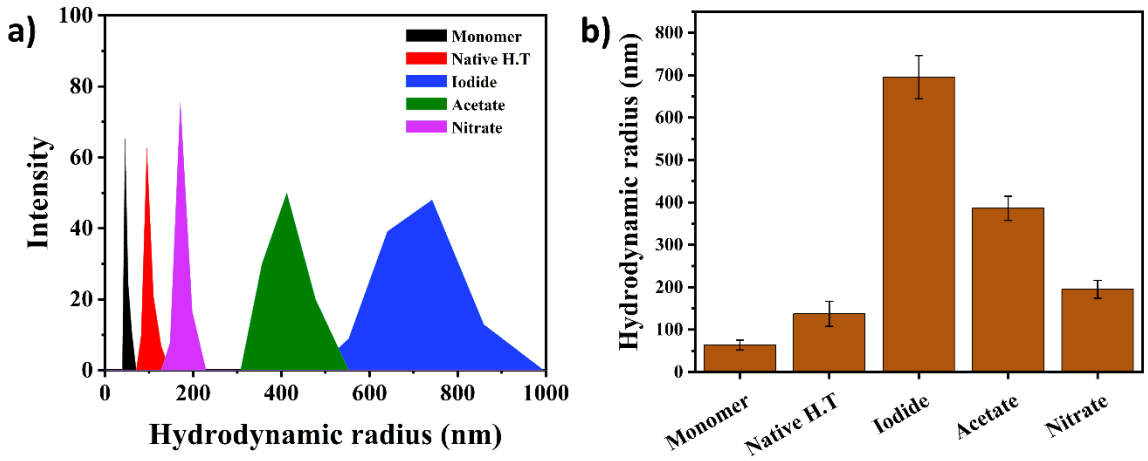

Figure 8: Intensity vs. particle size distribution in DLS studies of monomeric insulin and different insulin aggregates obtained after incubation at 65 °C for 4 h with or without the salt anions OAc^-, I^-, and NO_3^-.

3.7.5. Zeta potential measurement

The zeta-potential values of insulin and its aggregates were investigated in the presence of various anions, including nitrate, acetate, and iodide ions (Figure 9). The zeta-potential values of insulin were found to be 22.86 mV and 27.87 mV for native and heat-incubated insulin, respectively. The higher zeta-potential value of heat-incubated insulin suggests the formation of fibrillar aggregates. When incubated with insulin, acetate ions exhibited higher zeta-potential values of 29.4 mV and 35.36 mV at ion concentrations of 1 μM and 50 μM, respectively. The zeta-potential value of heat-incubated insulin with iodide ions was found to be the highest, while nitrate ions had the lowest zeta-potential value among other anions under the same experimental conditions. In all cases, positive zeta-potential values were observed. The zeta potential of the ions followed the order of nitrate > acetate > iodide, which was consistent with the trends observed in the aforementioned experiments. These findings shed light on the role of anions in modulating the zeta-potential values of insulin and its aggregates, which has implications for protein aggregation and stability.

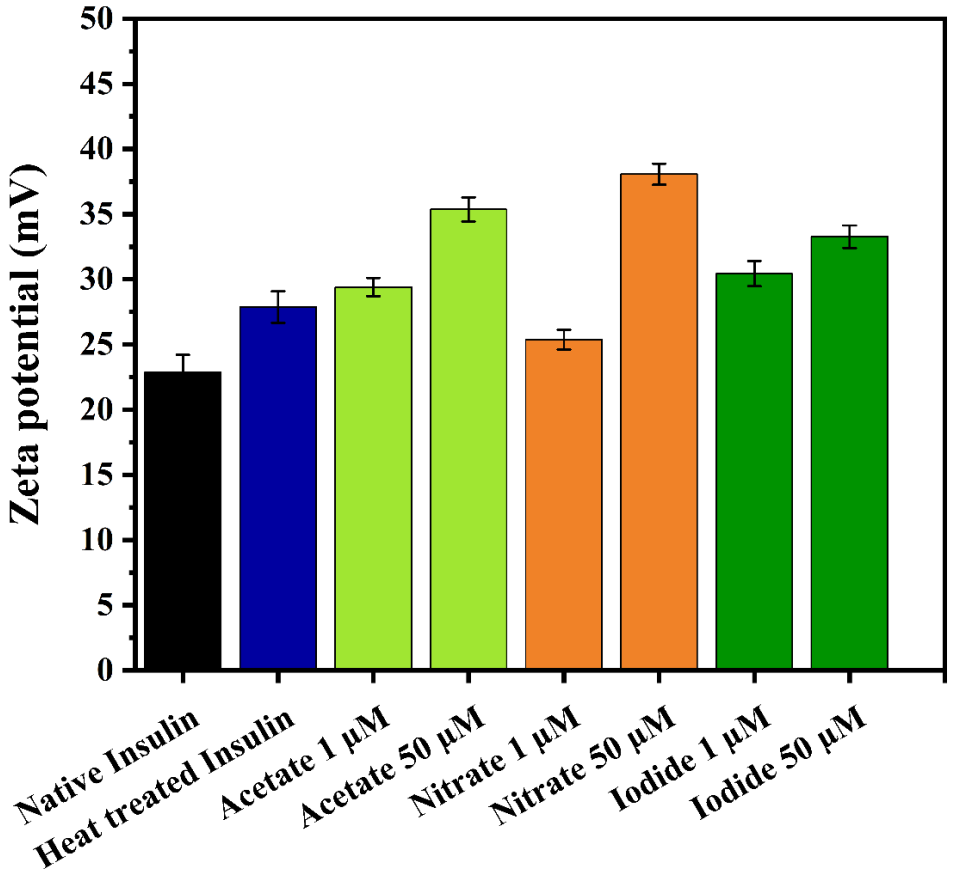

Figure 9: Zeta potential of insulin and different insulin aggregates obtained after incubation at 65°C for 4 h with or without the salt anions OAc^-, I^-, and NO_3^-.

3.7.6. The secondary structural changes in insulin during fibril formation are monitored by circular dichroism (CD) spectroscopy

Circular Dichroism (CD) is a well-established and widely used spectroscopic technique for investigating the secondary structures of peptides and proteins in solution. Far-UV CD (190-260 nm) spectroscopy is particularly useful for studying the interconversion of various secondary structures, such as alpha-helices, beta-sheets, and random coils, during insulin amyloid fibril formation. In this context, the appearance of a characteristic negative CD signal at 218 nm is indicative of a crossed β-sheet structure formation during aggregation.

The present study sought to explore the influence of different salt anions (I^-, CH_3COO^-, and NO_3^-) on the conformation of insulin after thermal incubation at 65°C for 4 hours. This analysis aimed to determine whether these anions could perturb the secondary structures of the protein in the non-native condition. To this end, we analyzed the corresponding far-UV CD spectra of insulin with or without 50 µM NaNO3, NaOAc, and NaI, respectively (Figure 10).

Our findings indicate that in the absence of any salt anion, the CD spectrum of native insulin exhibits two negative ellipticities around 207 nm and 222-224 nm, respectively, along with a positive maximum at 196 nm, which are consistent with the existence of a predominantly α-helical structure-rich protein. Conversely, the far-UV CD spectrum of insulin after incubation at 65°C for 4 hours in the absence of any anion shows significant structural transitions, characterized by the appearance of a single minima at 217 nm and the disappearance of the two negative ellipticities for α-helices. These observations confirm the formation of a β-sheet rich structure during amyloid fibrillation. Insulin solutions were subjected to coincubation with I-, CH_3COO^-, and NO_3^- ions, and the resulting secondary structural transitions were analyzed. The observed negative toughness at 217 nm, along with the increased negative ellipticity values compared to heat-treated insulin alone, indicate significant structural changes. Moreover, the thermal exposure of insulin in the presence of iodide, acetate, and nitrate ions displayed significant changes in intensity and band position, similar to heat-treated insulin. The presence of a single negative minima around 217-218 nm with all three anions indicates the presence of crossed β-structure, supporting the formation of insulin amyloid fibrils under the chosen conditions. Notably, the selected anions induced perturbations in the secondary structure of insulin even at their low physiological concentrations. Iodide, in particular, exhibited stronger interactions with the positively charged residues of the insulin backbone compared to acetate and nitrate ions. Consequently, maximum negative ellipticity was observed for iodide anions, while nitrate showed minimum negative ellipticity at 217 nm.

Our findings confirm that all three selected anions, I^-, CH_3COO^-, and NO_3^-, that have a common cationic counterpart, Na^+, accelerate insulin amyloid fibril formation even at their low physiological salt concentrations. The order of their effectiveness follows the series I- > CH_3COO^- > NO_3^-. Secondary structural contents of different insulin samples with or without the salt anions were calculated using CDNN 2.1 software, and the results clearly demonstrate the formation of increased β-structure (β sheet + β-turn) of insulin in the presence of the selected anions compared to native or heat-treated insulin in the absence of salt anions (Table 1). These findings represent a significant contribution to the understanding of insulin amyloid fibril formation and the role of salt anions in this process.

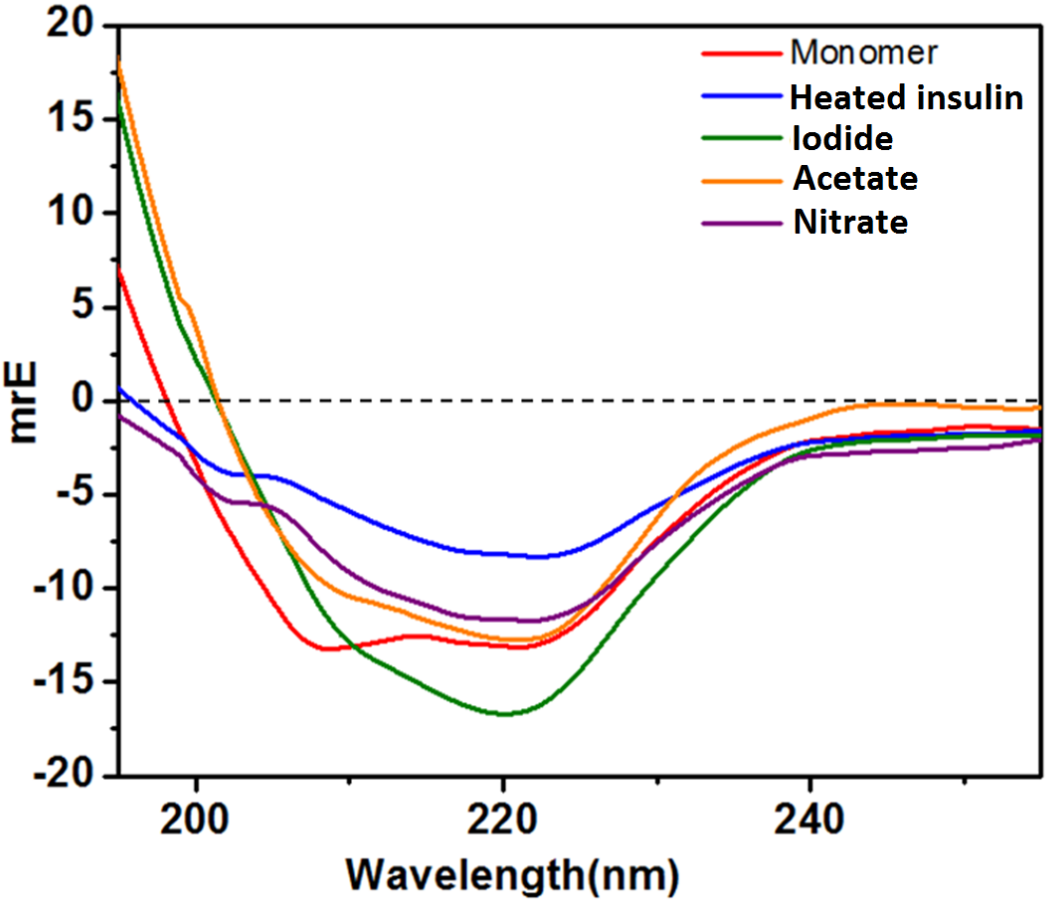

Figure 10: Far-UV CD curves of monomeric insulin (20 μM) and insulin incubated at 65 °C for 4 h in the presence and absence of I^-, CH_3COO^-, and NO_3^- anions (50 μM) at 25°C.

Table 1: Structural integrity of monomeric insulin and heat-stressed insulin (65 °C for 4h, pH 1.6) in the absence and presence of various salt anions as determined by calculations. (calculated by CDNN 2.1 Software)

Insulin Samples	% of α-Helix	% of β-Sheet	% of β-Turn	% of Random coil
Monomer	60.30	8.45	4.24	27.01
Heat-stressed insulin in the absence of salt anions	24.80	30.24	11.30	33.66
Heat-stressed insulin in the presence of iodide ion	15.40	40.85	12.90	30.85
Heat-stressed insulin in the presence of acetate ion	19.84	36.10	12.65	31.41
Heat-stressed insulin in the presence of nitrate ion	22.05	34.15	11.78	32.02

3.7.7. Morphological study of the aggregates with transmission electron microscopy (TEM)

In order to validate the results obtained from previous experiments, the morphology of insulin aggregates formed under various experimental conditions was examined with greater accuracy using Transmission Electron Microscopy (TEM). The TEM images of insulin fibrils were captured after thermal incubation at 65°C for 4 hours with and without certain salt anions (I^-, CH_3COO^-, and NO_3^-), as depicted in Figure 11. At a pH of 1.6 and room temperature, no fibrillar aggregate was observed with the insulin monomer (Figure 11a). The TEM image of insulin samples incubated at 65°C for 4 hours without any salt anion demonstrated the formation of matured, straight, long, and branched fibrils characteristic of amyloids (Figure 11b).

Upon incubation of insulin solutions with 50 µM iodide, 50 µM acetate, and 50 µM nitrate salts, the final aggregated forms are illustrated in the TEM images (Figure 11c-e). In acidic conditions, when insulin was coincubated with I- ions at 65°C for 4 hours, a larger number of mature, straight, long, and branched fibrils (Figure 11c) were formed by the nucleated polymerization mechanism in the presence of monovalent I^- anion. This suggests that the iodide ion plays a role in accelerating and modulating the amyloid fibrillation of insulin.

Insulin forms a reduced number of fibrils at a concentration of 50 µM NaOAc. However, the fibrils formed have a thinner, shorter, and more branched morphology compared to those formed with I^- ions (Figure 11d). On the other hand, 50 µM $NaNO_3$ induces the formation of shorter and fewer fibrillar aggregates than NaI and NaOAc of the same strength. The reduced efficiency of NO_3^- ions in inducing amyloid fibrillation of insulin is due to their lesser charge density and greater size compared to other monovalent ions ($^-$OAc). Despite the changes in insulin aggregate morphology in the presence of I^-, $^-$OAc, and NO_3^- ions, their kinetics for amyloid fibrillation are similar, as revealed by ThT kinetics and CD studies. These studies suggest that the selected anions accelerate amyloid fibril formation of insulin under stress-inducing conditions at their very low physiological salt concentrations.

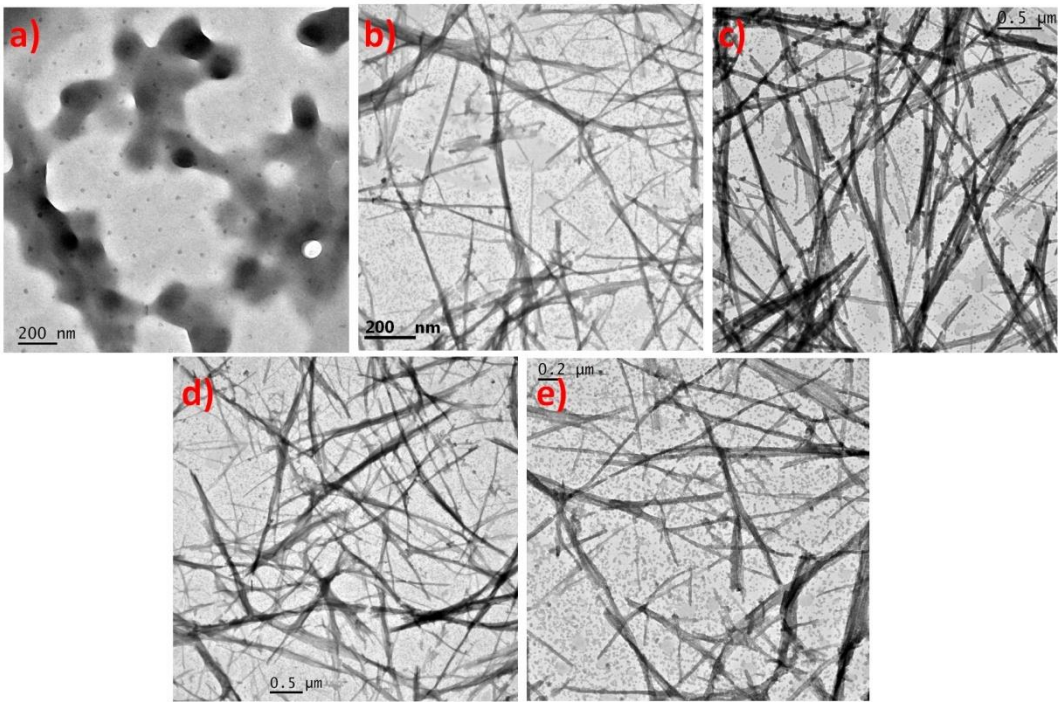

Figure 11: Selected images in transmission electron microscopy of monomeric insulin (a), insulin incubated at 65°C for 4 h (b), insulin incubated at 65°C for 4 h in the presence of iodide (c), acetate (d), and nitrate (e) anions.

3.8. Discussion

3.8.1. Mechanism of anion-induced amyloid fibrillation of insulin

According to our experimental results, insulin aggregation in an acidic environment is speeded up by the presence of salt anions with Na^+ as countercations. This acceleration effect varies among different types of anions at their low physiological concentrations. Therefore, it can be concluded that salt promotes insulin aggregation by its anions in acidic pH rather than the cationic counterpart. It should be noted that insulin carries a net positive charge of six units in this pH range. On the other hand, cations may play a crucial role in the process of oligomerization at basic pH in various experimental setups. For instance, the aggregation of lysozyme is mainly influenced by cations, while the role of anions is negligible. The findings of this study can help researchers understand the correct mechanism of interaction between anions and heat-incubated insulin in acidic pH.

Salts can influence the interaction between protein and anion in various ways by modulating electrostatic and hydrophobic forces. It was previously thought that insulin fibrillation in acidic environments was solely determined by the Debye-Hückel electrostatic effect, which screens the positive charges of insulin and reduces the repulsive electrostatic forces between insulin

chains. However, our observations show that the same concentrations of monovalent anions (I^-, AcO^-, and NO_3-) induce oligomerization at a faster rate than incubated insulin alone, which contradicts this theory. Both I^- and AcO^- induce nucleation and growth of the fibril at a faster rate than the nitrate ion of the same concentration. However, our ThT kinetics study demonstrates that nitrate ion delays the aggregation pathway and leads to the formation of smaller and fewer aggregates than I^- and AcO^- ions. Therefore, the aggregation mechanism of heat-induced insulin is not directly related to the solution's ionic strength, which can significantly impact insulin fibril formation. The anions in a solution not only help the nucleation mechanism but also stabilize intermediates. This effect was observed through the intrinsic fluorescence of insulin when anions were present (as shown in Figure 5). If the hydration shell of insulin is disrupted by salt anions, then the efficiency order of the selected anions should be equal, as all three ions carry a single negative charge. According to the Hofmeister series, the order should be $CH_3COO^->NO_3^->I^-$ since iodide and nitrate are chaotropic ions, while acetate ions are kosmotropic ions (Collins and Washabaugh, 1985). However, this order does not align with our experimental observations. Our findings suggest that the actual order is $I^- > CH_3COO^- > NO_3^-$. Therefore, the anion-induced aggregation of insulin does not follow either the Hofmeister series or electrosensitivity series at very low salt concentrations. It is worth noting that the electrostatic effect and electrosensitivity series are considered important factors only in dilute salt concentrations. The Hofmeister effect, on the other hand, plays a crucial role at higher salt concentrations (>100 mM). Our investigation procedure focused on exploring the ion-protein interactions even at very low salt concentrations in the micromolar range, similar to those present in the biological system.

According to the experimental results, iodide and acetate ions are more effective than nitrate ions in accelerating the fibrillation of insulin. This leads to the production of a larger number of fibrillar structures of insulin. Interestingly, the two anions (iodide and acetate) not only formed the final aggregate with different morphology but also showed different ThT signal intensities compared to nitrate ions. Long and greater numbers of fibrils are formed in the case of iodide ions, while shorter, lesser, and branched fibrils are observed in nitrate ions (see Figure 11c and e).

Previous studies have reported that salt anions are capable of promoting the formation of amyloid fibrils in numerous peptides and proteins, such as insulin (Babenko et al.,2015), β2-microglobulin (β2-m) (Raman et al., 2005), α-synuclein (Munishkina et al., 2004), glucagon (Pedersen et al.,2006), an immunoglobulin light chain (Sikkink and Ramirez-Alvarado, 2008),

the amyloid-β peptide (Aβ1–40) (Klement et al.,2007), HypF-N (Campioni et al.,2012), the mouse prion protein (Jain and Udgaonkar, 2010), and bovine serum albumin (Madeira et al.,2022). It is noteworthy that HypF-N and the aforementioned proteins exhibit an excess of positive charges at this pH. In contrast, the net charge on α-synuclein is nearly neutral at acidic pH due to the presence of a significant number of acidic residues in this protein. Furthermore, it has been observed that prion fibril growth is favored by 10 mM Na_2SO_4 (Jain and Udgaonkar, 2010), whereas insulin fibrillation is accelerated only in 5 mM NaCl (Owczarz and Arosio, 2014). These three anions, I^-, CH_3COO^-, and NO_3^-, differ markedly in their charge density, size, and shape. Among the three, the iodide ion is the smallest, spherical in shape, and carries the largest negative charge density. Consequently, it moves more quickly towards the positively charged side chain of insulin. Nitrate anion, on the other hand, has the lowest charge density, a larger size, and planar geometry compared to iodide. Due to its slow approach towards insulin's positively charged residues, it takes a longer time for insulin fibril formation than iodide and acetate ions.

Hydrophobic interactions and electrostatic interactions both play an important role in self-association and amyloid fibrillation. It's crucial to balance the two forces to achieve the desired outcome. Hydrophobic interactions are not significantly affected by low salt concentrations (Bonomo et al.,2006). However, adding chloride, sulfate, and iodide anions screens the positive charges on insulin, leading to enhanced hydrophobic interactions, which favor self-association and nucleation. Thus, both electrostatic and hydrophobic interactions control the nucleation of insulin. In the initial aggregation step, electrostatic forces between calcitonin monomers play a crucial role. Similarly, in amyloid-β peptide, both electrostatic and hydrophobic interactions are involved in fibril formation. The study provides evidence for the involvement of hydrophobic interactions in forming a partially folded insulin intermediate in the fibrillation pathway. This evidence comes from the ANS binding study (Figure 6a) and far UV-CD experiment (Figure 10). The ANS binding study observed that populated states/intermediates exhibit a greater affinity for the hydrophobic probe ANS. Additionally, it was observed that during thermal incubation at low pH in the presence of salt anions, insulin's tertiary and secondary structures were impacted, resulting in the formation of partially unfolded intermediates that trigger insulin fibrillation. The low pH and higher temperature promote the shift of the equilibrium between the native form of insulin and an increased population of the partially unfolded intermediate.

Upon formation, insulin's partially unfolded intermediate state exhibits a strong propensity to oligomerize into amyloid fibrils. However, our observations indicate that the nucleation of the monomer and the elongation of the fibril may not necessarily proceed in the same direction. Electrostatic and hydrophobic interactions govern both nucleation and fibril elongation, and the latter step is further influenced by the electronic structure of the anionic species involved. Despite deviating from the Hofmeister series, our findings demonstrate that the propensity for the formation of fibrillar aggregates of insulin at low pH is promoted by selected salt anions in the order of $I^- > CH_3COO^- > NO_3^-$. Remarkably, this order holds true even at very low salt concentration ranges (micromolar range) that are physiologically relevant. These results offer important insights into the mechanisms underlying insulin fibrillation and have implications for the development of strategies to prevent or treat amyloid-related disorders.

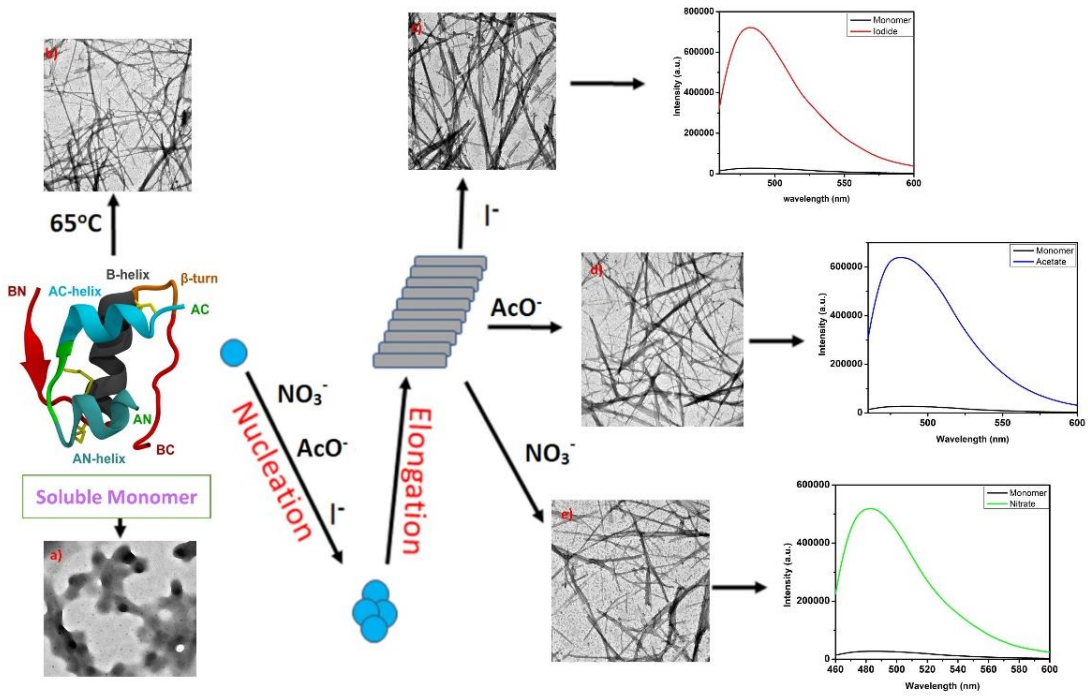

Scheme 1: Scheme for insulin fibrillation.

3.9. Summary of the work

The misfolding of proteins can lead to the formation of irreversible protein aggregates, which is the root cause of several human diseases. At the molecular level, it is difficult to determine the forces between different cellular components and protein molecules, which makes it a challenging task. When protein aggregation occurs in the presence of salt solutions, it can lead to serious problems during its separation, storage, and therapeutic applications. In this study, we focused on investigating the mechanism of fibrillation of human insulin, a peptide hormone

that plays a crucial role in glucose metabolism. We conducted our experiments in an acidic environment (in the presence of selected salt anions I^-, NO_3^-, and OAc^-) at very low salt concentrations, which fall within the physiological range. We used various spectroscopic and microscopic approaches, such as ANS and ThioflavinT (ThT) fluorescence, circular dichroism (CD), dynamic light scattering (DLS), and transmission electron microscopy (TEM) to elucidate the fibrillation mechanism and the fibril morphology.

After conducting investigations, it was found that in an acidic environment, anions preferentially bind to the positively charged residues on insulin. This perturbs the structure of insulin and causes salt-induced aggregation and amyloid-like oligomeric product formation. Nitrate anion, which has the smallest charge density and is larger and flatter than iodide (which has a spherical shape), slowly approaches insulin's positively charged residues. Therefore, it takes a longer lag time for insulin fibril formation than iodide and acetate ions. The findings of our study suggest that the nucleation kinetics of insulin following heat incubation and its subsequent fibril elongation in an acidic milieu are predominantly governed by hydrophobic and electrostatic interactions.

3.10. References

Ahmad, A., Millett, I.S., Doniach, S., Uversky, V.N. and Fink, A.L., 2003. Partially folded intermediates in insulin fibrillation. Biochemistry, 42(39), pp.11404-11416.

Ahmad, A., Uversky, V.N., Hong, D. and Fink, A.L., 2005. Early events in the fibrillation of monomeric insulin. Journal of Biological Chemistry, 280(52), pp.42669-42675.

Ahmad, E., Ahmad, A., Singh, S., Arshad, M., Khan, A.H. and Khan, R.H., 2011. A mechanistic approach for islet amyloid polypeptide aggregation to develop anti-amyloidogenic agents for type-2 diabetes. Biochimie, 93(5), pp.793-805.

Ardito, F., Giuliani, M., Perrone, D., Troiano, G. and Lo Muzio, L., 2017. The crucial role of protein phosphorylation in cell signaling and its use as targeted therapy. International journal of molecular medicine, 40(2), pp.271-280.

Arya, S., Gourley, A.J., Penedo, J.C., Blindauer, C.A. and Stewart, A.J., 2021. Fatty acids may influence insulin dynamics through modulation of albumin-Zn2+ interactions. BioEssays, 43(12), p.2100172.

Babenko, V., Harada, T., Yagi, H., Goto, Y., Kuroda, R. and Dzwolak, W., 2011. Chiral superstructures of insulin amyloid fibrils. Chirality, 23(8), pp.638-646.

Babenko, V., Surmacz-Chwedoruk, W. and Dzwolak, W., 2015. On the function and fate of chloride ions in amyloidogenic self-assembly of insulin in an acidic environment: salt-induced condensation of fibrils. Langmuir, 31(7), pp.2180-2186.

Bakaysa, D.L., Radziuk, J., Havel, H.A., Brader, M.L., Li, S., Dodd, S.W., Beals, J.M., Pekar, A.H. and Brems, D.N., 1996. Physicochemical basis for the rapid time-action of LysB28ProB29-insulin: Dissociation of a protein-ligand complex. Protein science, 5(12), pp.2521-2531.

Ball, P. and Hallsworth, J.E., 2015. Water structure and chaotropicity: their uses, abuses and biological implications. Physical Chemistry Chemical Physics, 17(13), pp.8297-8305.

Banerjee, V. and Das, K.P., 2012. Modulation of pathway of insulin fibrillation by a small molecule helix inducer 2, 2, 2-trifluoroethanol. Colloids and Surfaces B: Biointerfaces, 92, pp.142-150.

Biancalana, M. and Koide, S., 2010. Molecular mechanism of Thioflavin-T binding to amyloid fibrils. Biochimica et Biophysica Acta (BBA)-Proteins and Proteomics, 1804(7), pp.1405-1412.

Blaine, J., Chonchol, M. and Levi, M., 2015. Renal control of calcium, phosphate, and magnesium homeostasis. Clinical Journal of the American Society of Nephrology, 10(7), pp.1257-1272.

Bonomo, R.C., Minim, L.A., Coimbra, J.S., Fontan, R.C., da Silva, L.H.M. and Minim, V.P., 2006. Hydrophobic interaction adsorption of whey proteins: effect of temperature and salt concentration and thermodynamic analysis. Journal of Chromatography B, 844(1), pp.6-14.

Campioni, S., Mannini, B., López-Alonso, J.P., Shalova, I.N., Penco, A., Mulvihill, E., Laurents, D.V., Relini, A. and Chiti, F., 2012. Salt anions promote the conversion of HypF-N into amyloid-like oligomers and modulate the structure of the oligomers and the monomeric precursor state. Journal of molecular biology, 424(3-4), pp.132-149.

Chiti, F. and Dobson, C.M., 2006. Protein misfolding, functional amyloid, and human disease. Annu. Rev. Biochem., 75, pp.333-366.

Coffman, F.D. and Dunn, M.F., 1988. Insulin-metal ion interactions: the binding of divalent cations to insulin hexamers and tetramers and the assembly of insulin hexamers. Biochemistry, 27(16), pp.6179-6187.

Collins, K.D. and Washabaugh, M.W., 1985. The Hofmeister effect and the behaviour of water at interfaces. Quarterly reviews of biophysics, 18(4), pp.323-422.

Dathe, M., Gast, K., Zirwer, D., Welfle, H. and Mehlis, B., 1990. Insulin aggregation in solution. International journal of peptide and protein research, 36(4), pp.344-349.

Dorn, M., e Silva, M.B., Buriol, L.S. and Lamb, L.C., 2014. Three-dimensional protein structure prediction: Methods and computational strategies. Computational biology and chemistry, 53, pp.251-276.

Dunn, M.F., 2005. Zinc–ligand interactions modulate assembly and stability of the insulin hexamer–a review. Biometals, 18, pp.295-303.

Dzwolak, W., Loksztejn, A., Galinska-Rakoczy, A., Adachi, R., Goto, Y. and Rupnicki, L., 2007. Conformational indeterminism in protein misfolding: chiral amplification on amyloidogenic pathway of insulin. Journal of the American Chemical Society, 129(24), pp.7517-7522.

Eisenberg, D. and Jucker, M., 2012. The amyloid state of proteins in human diseases. Cell, 148(6), pp.1188-1203.

Eisenberg, D.S. and Sawaya, M.R., 2017. Structural studies of amyloid proteins at the molecular level. Annual review of biochemistry, 86, pp.69-95.

Freire, S., de Araujo, M.H., Al-Soufi, W. and Novo, M., 2014. Photophysical study of Thioflavin T as fluorescence marker of amyloid fibrils. Dyes and Pigments, 110, pp.97-105.

Funk, R.H., Monsees, T. and Özkucur, N., 2009. Electromagnetic effects–From cell biology to medicine. Progress in histochemistry and cytochemistry, 43(4), pp.177-264.

Goto, K. and Kitazono, T., 2022. Chloride ions, vascular function and hypertension. Biomedicines, 10(9), p.2316.

GoTo, Y., Calciano, L.J. and Fink, A.L., 1990. Acid-induced folding of proteins. Proceedings of the National Academy of Sciences, 87(2), pp.573-577.

Hediger, M.A. and Rhoads, D.B., 1994. Molecular physiology of sodium-glucose cotransporters. Physiological Reviews, 74(4), pp.993-1026.

Hudeček, J., Anzenbacher, P. and Kalous, V., 1979. Interaction of insulin with metal (II) ions. FEBS letters, 100(2), pp.374-376.

Hung, Y.T., Lin, M.S., Chen, W.Y. and Wang, S.S.S., 2010. Investigating the effects of sodium dodecyl sulfate on the aggregative behavior of hen egg-white lysozyme at acidic pH. Colloids and Surfaces B: Biointerfaces, 81(1), pp.141-151.

Isaacs, A.M., Senn, D.B., Yuan, M., Shine, J.P. and Yankner, B.A., 2006. Acceleration of amyloid β-peptide aggregation by physiological concentrations of calcium. Journal of biological chemistry, 281(38), pp.27916-27923.

Ivanova, M.I., Sievers, S.A., Sawaya, M.R., Wall, J.S. and Eisenberg, D., 2009. Molecular basis for insulin fibril assembly. Proceedings of the National Academy of Sciences, 106(45), pp.18990-18995.

Jain, S. and Udgaonkar, J.B., 2010. Salt-induced modulation of the pathway of amyloid fibril formation by the mouse prion protein. Biochemistry, 49(35), pp.7615-7624.

Khan, A.N. and Khan, R.H., 2022. Protein misfolding and related human diseases: A comprehensive review of toxicity, proteins involved, and current therapeutic strategies. International Journal of Biological Macromolecules, 223, pp.143-160.

Khan, R.H., Siddiqi, M.K. and Salahuddin, P., 2017. Protein structure and function. Basic biochemistry, 5, pp.1-39.

Klement, K., Wieligmann, K., Meinhardt, J., Hortschansky, P., Richter, W. and Fändrich, M., 2007. Effect of different salt ions on the propensity of aggregation and on the structure of Alzheimer's Aβ (1-40) amyloid fibrils. Journal of molecular biology, 373(5), pp.1321-1333.

Kunz, W., 2010. Specific ion effects in colloidal and biological systems. Current Opinion in Colloid & Interface Science, 15(1-2), pp.34-39.

Lambrecht, M.A., Jansens, K.J., Rombouts, I., Brijs, K., Rousseau, F., Schymkowitz, J. and Delcour, J.A., 2019. Conditions governing food protein amyloid fibril formation. Part II: Milk and legume proteins. Comprehensive reviews in food science and food safety, 18(4), pp.1277-1291.

Lo Nostro, P. and Ninham, B.W., 2012. Hofmeister phenomena: an update on ion specificity in biology. Chemical reviews, 112(4), pp.2286-2322.

Loksztejn, A. and Dzwolak, W., 2008. Chiral bifurcation in aggregating insulin: an induced circular dichroism study. Journal of molecular biology, 379(1), pp.9-16.

Lougheed, W.D., Woulfe-Flanagan, H., Clement, J.R. and Albisser, A.M., 1980. Insulin aggregation in artificial delivery systems. Diabetologia, 19, pp.1-9.

Madeira, P.P., Rocha, I.L., Rosa, M.E., Freire, M.G. and Coutinho, J.A., 2022. On the aggregation of bovine serum albumin. Journal of Molecular Liquids, 349, p.118183.

McAinsh, M.R., Brownlee, C. and Hetherington, A.M., 1997. Calcium ions as second messengers in guard cell signal transduction. Physiologia Plantarum, 100(1), pp.16-29.

Morris, A.L. and Mohiuddin, S.S., 2020. Biochemistry, nutrients.

Morris, A.M., Watzky, M.A. and Finke, R.G., 2009. Protein aggregation kinetics, mechanism, and curve-fitting: a review of the literature. Biochimica et Biophysica Acta (BBA)-Proteins and Proteomics, 1794(3), pp.375-397.

Moustakas, M., 2021. The role of metal ions in biology, biochemistry and medicine. Materials, 14(3), p.549.

Muir, W.W., 2015. Acid–base physiology. Veterinary Anesthesia and Analgesia: The Fifth Edition of Lumb and Jones, pp.355-371.

Munishkina, L.A., Henriques, J., Uversky, V.N. and Fink, A.L., 2004. Role of protein− water interactions and electrostatics in α-synuclein fibril formation. Biochemistry, 43(11), pp.3289-3300.

Muzaffar, M. and Ahmad, A., 2011. The mechanism of enhanced insulin amyloid fibril formation by NaCl is better explained by a conformational change model. PloS one, 6(11), p.e27906.

Nayab, S.N., Jones, F.H. and Olsen, I., 2005. Effects of calcium ion implantation on human bone cell interaction with titanium. Biomaterials, 26(23), pp.4717-4727.

Nieder, R., Benbi, D.K., Reichl, F.X., Nieder, R., Benbi, D.K. and Reichl, F.X., 2018. Microelements and their role in human health. Soil components and human health, pp.317-374.

Nielsen, L., Frokjaer, S., Brange, J., Uversky, V.N. and Fink, A.L., 2001. Probing the mechanism of insulin fibril formation with insulin mutants. Biochemistry, 40(28), pp.8397-8409.

Nielsen, L., Khurana, R., Coats, A., Frokjaer, S., Brange, J., Vyas, S., Uversky, V.N. and Fink, A.L., 2001. Effect of environmental factors on the kinetics of insulin fibril formation: elucidation of the molecular mechanism. Biochemistry, 40(20), pp.6036-6046.

Niemeyer, C.M., 2001. Nanoparticles, proteins, and nucleic acids: biotechnology meets materials science. Angewandte Chemie International Edition, 40(22), pp.4128-4158.

Nilsson, M.R., 2004. Techniques to study amyloid fibril formation in vitro. Methods, 34(1), pp.151-160.

Noormägi, A., Gavrilova, J., Smirnova, J., Tõugu, V. and Palumaa, P., 2010. Zn (II) ions co-secreted with insulin suppress inherent amyloidogenic properties of monomeric insulin. Biochemical Journal, 430(3), pp.511-518.

Owczarz, M. and Arosio, P., 2014. Sulfate anion delays the self-assembly of human insulin by modifying the aggregation pathway. Biophysical journal, 107(1), pp.197-207.

Panja, A.S., Maiti, S. and Bandyopadhyay, B., 2020. Protein stability governed by its structural plasticity is inferred by physicochemical factors and salt bridges. Scientific reports, 10(1), p.1822.

Paul, S., Begum, S., Parvej, H., Dalui, R., Sardar, S., Mondal, F., Sepay, N. and Halder, U.C., 2024. In vitro retardation and modulation of human insulin amyloid fibrillation by Fe 3+ and Cu 2+ ions. New Journal of Chemistry, 48(7), pp.3120-3135.

Peacock, M., 2021. Phosphate metabolism in health and disease. Calcified tissue international, 108, pp.3-15.

Pedersen, J.S., Flink, J.M., Dikov, D. and Otzen, D.E., 2006. Sulfates dramatically stabilize a salt-dependent type of glucagon fibrils. Biophysical journal, 90(11), pp.4181-4194.

Pessia, M., 2004. Ion channels and electrical activity. Molecular Biology of the Neuron, pp.103-137.

Rahman, M.S., Hossain, K.S., Das, S., Kundu, S., Adegoke, E.O., Rahman, M.A., Hannan, M.A., Uddin, M.J. and Pang, M.G., 2021. Role of insulin in health and disease: an update. International journal of molecular sciences, 22(12), p.6403.

Rajan, R., Ahmed, S., Sharma, N., Kumar, N., Debas, A. and Matsumura, K., 2021. Review of the current state of protein aggregation inhibition from a materials chemistry perspective: Special focus on polymeric materials. Materials Advances, 2(4), pp.1139-1176.

Raman, B., Chatani, E., Kihara, M., Ban, T., Sakai, M., Hasegawa, K., Naiki, H., Rao, C.M. and Goto, Y., 2005. Critical balance of electrostatic and hydrophobic interactions is required for β2-microglobulin amyloid fibril growth and stability. Biochemistry, 44(4), pp.1288-1299.

Ramazi, S. and Zahiri, J., 2021. Post-translational modifications in proteins: resources, tools and prediction methods. Database, 2021, p.baab012.

Rasia, R.M., Bertoncini, C.W., Marsh, D., Hoyer, W., Cherny, D., Zweckstetter, M., Griesinger, C., Jovin, T.M. and Fernández, C.O., 2005. Structural characterization of copper (II) binding to α-synuclein: insights into the bioinorganic chemistry of Parkinson's disease. Proceedings of the National Academy of Sciences, 102(12), pp.4294-4299.

Rüegg, J.C., 2012. Calcium in muscle contraction: cellular and molecular physiology. Springer Science & Business Media.

Rupert, D.L., Claudio, V., Lässer, C. and Bally, M., 2017. Methods for the physical characterization and quantification of extracellular vesicles in biological samples. Biochimica et Biophysica Acta (BBA)-General Subjects, 1861(1), pp.3164-3179.

Schwab, A., Nechyporuk-Zloy, V., Fabian, A. and Stock, C., 2007. Cells move when ions and water flow. Pflügers Archiv-European Journal of Physiology, 453, pp.421-432.

Selkoe, D.J., 2003. Folding proteins in fatal ways. nature, 426(6968), pp.900-904.

Sikkink, L.A. and Ramirez-Alvarado, M., 2008. Salts enhance both protein stability and amyloid formation of an immunoglobulin light chain. Biophysical chemistry, 135(1-3), pp.25-31.

Thirumalai, D., Reddy, G. and Straub, J.E., 2012. Role of water in protein aggregation and amyloid polymorphism. Accounts of chemical research, 45(1), pp.83-92.

Vanik, V., Bednarikova, Z., Fabriciova, G., Wang, S.S.S., Gazova, Z. and Fedunova, D., 2023. Modulation of Insulin Amyloid Fibrillization in Imidazolium-Based Ionic Liquids with Hofmeister Series Anions. International Journal of Molecular Sciences, 24(11), p.9699.

Wang, W., 2005. Protein aggregation and its inhibition in biopharmaceutics. International journal of pharmaceutics, 289(1-2), pp.1-30.

Whittingham, J.L., Scott, D.J., Chance, K., Wilson, A., Finch, J., Brange, J. and Dodson, G.G., 2002. Insulin at pH 2: structural analysis of the conditions promoting insulin fibre formation. Journal of molecular biology, 318(2), pp.479-490.

Wong, G.C. and Pollack, L., 2010. Electrostatics of strongly charged biological polymers: ion-mediated interactions and self-organization in nucleic acids and proteins. Annual review of physical chemistry, 61, pp.171-189.

Xu, Y., Yan, Y., Seeman, D., Sun, L. and Dubin, P.L., 2012. Multimerization and aggregation of native-state insulin: effect of zinc. Langmuir, 28(1), pp.579-586.

Yeh, V., Broering, J.M., Romanyuk, A., Chen, B., Chernoff, Y.O. and Bommarius, A.S., 2010. The Hofmeister effect on amyloid formation using yeast prion protein. Protein Science, 19(1), pp.47-56.

Yip, C.M., Brader, M.L., DeFelippis, M.R. and Ward, M.D., 1998. Atomic force microscopy of crystalline insulins: the influence of sequence variation on crystallization and interfacial structure. Biophysical journal, 74(5), pp.2199-2209.

Yu, X., Wang, C. and Li, Y., 2006. Classification of protein quaternary structure by functional domain composition. BMC bioinformatics, 7, pp.1-6.

Zhang, Y. and Cremer, P.S., 2009. The inverse and direct Hofmeister series for lysozyme. Proceedings of the National Academy of Sciences, 106(36), pp.15249-15253.

Zhou, H.X. and Pang, X., 2018. Electrostatic interactions in protein structure, folding, binding, and condensation. Chemical reviews, 118(4), pp.1691-1741.

CHAPTER 4

EFFECT OF ULTRAVIOLET LIGHT EXPOSURE ON MONOMERIC INSULIN

Effect of Ultraviolet Light Exposure on Monomeric Insulin

4.1. Introduction

In the electromagnetic spectrum, ultraviolet radiation lies between visible light and X-rays. The wavelengths of UV light range from 10 nanometers to 400 nanometers. A violet light's wavelength is approximately 400 nanometers (or 4,000 Å). The frequency of ultraviolet radiation ranges from 800 terahertz to 30,000 terahertz. The ultraviolet spectrum can be divided into three regions: near UV, far UV, and extreme UV. Wavelengths between 200 and 400 nm are included in the near UV region, which is closest to visible light (Levin, 2013). There is no doubt that ultraviolet radiation (UV) damages biological structures. The main target of UV radiation in humans is the lens of the eye, along with its protein constituents. This radiation is one of the leading causes of blindness worldwide due to cataract formation.

The stable native state and unfolded state of protein exist in a dynamic equilibrium. The minimum energy state of a stable protein is reached when the protein is stable. The protein reaches an unstable higher energy state when the external perturbation disturbs its internal energy milieu. As a result, if the external disturbance persists, the proteins undergo structural rearrangement, which results in protein aggregation.

UV light interacts with protein molecules to cause molecular alteration, leading to structural rearrangement in the molecule through photoionization. There has been evidence that UV-C radiation alters the conformation of albumin, thereby promoting aggregation (Das and Purkayastha, 2017). Espinoza et al. measured enthalpy, particle size, and fluorometry of the ovalbumin and crystallin proteins after exposure to UV-C radiation. Researchers also explored the possibility of mitigating UV-C radiation using red and green lights. In fact, the photoionization of ovalbumin produces free radicals, not thermal-induced unfolding, that have a deleterious impact on the protein (Espinoza and Mercado-Uribe, 2017). Molecular proteins are vulnerable to UV photons, which generate reactive oxygen species, leading to the unfolding and aggregation of proteins.

Near-UV light is known to induce disulfide bond splitting in proteins, resulting in thiyl radicals (CysS) (Prajapati et al., 2022). Cysteine residues or disulfide bonds can be oxidized by one electron or reduced by one electron to form thiyl radicals (Trujillo et al., 2016). The alteration of protein structures by UV irradiation has been extensively studied over the last few decades. Several aromatic amino acids, including tryptophan, Trp, tyrosine, Tyr, phenylalanine, Phe,

and histidine (His), were proposed to participate in the degradation process through the absorption of photons. Proteins' indole rings are among the strongest UV absorbers; thus, Trp residues are the primary components of photodegradation (Lundeen et al., 2014; Bastos et al., 2023; Prompers et al., 1999). Several proteins, including cutinase, bovine growth hormone, α-lactalbumin, and lysozyme, have been investigated in detail for their light-induced, Trp-mediated disulfide bridge breakdown. Numerous studies have attempted to determine the distance required between aromatic amino acid side chains and disulfide bridges, including studies involving major histocompatibility complexes (MHCs) class I and II, mannose-binding lectins (MBL) subunit A, immunoglobulins, triosephosphate isomerase (TIM) barrel glycosidases, alkaline phosphatases, and lysozymes. A study of goat-lactalbumin mutants containing substituted Trp residues revealed that their contribution to disulfide bond breaking is strongly influenced by the microenvironment of their side chains as well as their disulfide bonds (Espinoza and Mercado-Uribe, 2017; Vanhooren et al., 2006). In addition, thiyl radicals have been demonstrated to be involved in a variety of other chemical reactions, such as recombination with other radical intermediates (Trp-, Tyr-, and Phe radicals) (Wu et al., 2008; McLean et al., 2021), sulfenylation of Trp (or Tyr/Phe), or dimerization through interprotein cross-links (Mozziconacci et al., 2008; Nauser et al., 2005). In addition, antibodies are susceptible to photodegradation by near-UV light (Kaiser et al., 2021). As a result of the formation of thiyl radicals, the proteins might fragment and/or aggregate.

According to a number of studies, proteins' main responses to UV-C radiation (which ranges from 100 to 280 nm) include unfolding, aggregation, dimerization, secondary structure modification, and exposure of hydrophobic regions. Furthermore, several incidental consequences, such as ionization and radical production, have been noted (Nagy et al., 2018).

Protein stability may be significantly impacted by cation-π interactions, which involve positively charged amino acid side chains (Lys, Arg) and an aromatic ring of Trp, Tyr, or Phe (Dougherty, 1996).

It has been found that even visible light with lower energies can have adverse effects on some organisms. As an example, red light exposure stimulates plant development, affects DNA synthesis in HeLa cells, and increases the level of oxidative stress enzymes in E. coli in seawater as well as the growth of other types of bacteria (Espinoza et al., 2015; Espinoza and Mercado-Uribe, 2017; Gourmelon et al., 1994). As a result of green light, fungi's radial expansion decreases, HeLa cells grow slower, and rats' retinal DNA breaks are reduced (Lin

and Xu, 2020). Furthermore, collagenase enzyme activities are modulated by green light (Liu et al., 2018; Vincenti et al., 1996; Muneer et al., 2014).

According to reports, β-crystallins exposed to UV light change in charge, lose their natural three-dimensional structure, create cross-linked proteins, and have their methionine and tryptophan residues oxidized (Andley and Clark, 1989; Sergeev et al., 2005; Hott and Borkman, 1993). One-hit mechanism of protein denaturation under UV irradiation is demonstrated by Muranov et al. (Muranov et al., 2011).

Tyrosine (Tyr, Y), tryptophan, phenylalanine, cysteine, and the peptide backbone are the primary targets of UV-light-induced photodegradation in proteins. Two polypeptide chains, an A chain, and a B chain, each with 21 and 30 amino acid residues, make up the human insulin molecule (Weiss et al., 2015). Two inter-chain SS (CysA7-CysB7 and CysA20-CysA19) connect the two chains, and another SS (CysA6-CysA11) joins the two chains within the A chain. Numerous non-covalent interactions also involve the amino acids of the two chains. Here, we observed the effect on the structure of insulin during UV exposure. With huge biological importance, we chose insulin to measure its effect upon long exposure under UV irradiation.

4.2. Graphical abstract of the work

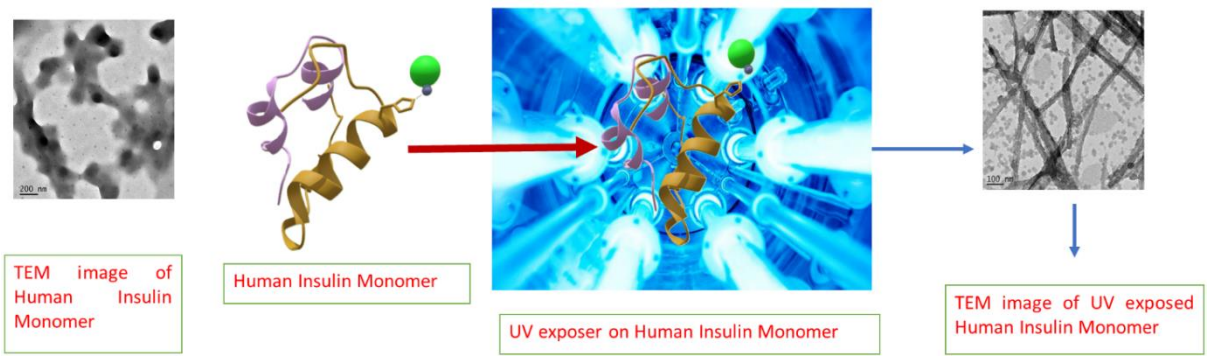

Figure 1: Graphical representation of the work.

4.3. Methods and materials

4.3.1. Protein and buffer solutions

Human insulin, marketed by Eli Lilly, India, under the trade name 'Huminsulin,' was purchased from a medicine shop. A few chemicals, such as acetic acid and HCl, were purchased from Merck, Germany. Different fluorescent probes, namely 8- anilinonaphthalene-1-sulfonic

acid ammonium salts (ANS) and thioflavin T (ThT), were purchased from Sigma Chemical (St. Louis, USA). All the other reagents used in our experiments were of analytical grade or of high purity reagents available.

4.3.2. Preparation and purification of monomeric state of insulin

The marketed hexameric insulin contains the preservative m-cresol, tonicity modifier glycerine, and pH-adjusting substances HCl/ NaOH. The concentration of this hexameric insulin is 100 IU $mL^{-1,}$ equivalent to 2 mg mL^{-1}. To remove the other particles, extensive dialysis with water is performed. Next, the hexameric to monomeric form is achieved by controlling the pH of the medium. In this step, 80% acetic acid was added to convert it to a monomer state with a final concentration of 20%. Next, the solution was filtered through a 0.22 mm (Millipore) filter membrane to remove traces of hexameric molecules. The filtrate was then kept at 37°C overnight, resulting in a homogeneous solution serving as the monomeric state of insulin (1.5 mg mL^{-1}). Insulin concentrations were determined by Abs 276 nm using a molar extinction coefficient of 1.0675 $cm^{-1}(mg/ml)^{-1}$ (Kamelnia et al., 2023). Milli-Q water with conductivity below 0.2 µS cm^{-1} was used. After that, the concentrated insulin monomer is diluted with HPLC water to prepare the stock 20 µM solution.

4.3.3. UV-excitation of insulin samples

For long exposure of Insulin monomer under UV irradiation, 2 mL of 20 µM insulin stock solution was placed in a four-side cleaned Perkin Elmer quartz cuvette (10mm path length) and continuously excited with UV-light over selected time periods using ISS P110 illuminator (Model no-81033) (DQS Inc., ISS Inc., using a 75-W Xenon arc lamp coupled to a monochromator (Wavelength range 230 nm to 850 nm). For each experiment, A fresh sample was used for each excitation session. Slits were set to 5 nm in every excitation. Lamp power at 276 nm was 142 mW, and the same lamp was used throughout the experiments. Different solutions of Native Human Insulin under UV light Exposure for 1 min, 3 mins, 7 mins, and 15 mins were prepared.

4.3.4. UV-visible spectroscopy

To understand the structural alteration, microenvironmental changes around the chromophore absorption spectra of native Insulin monomer and UV irradiated insulin of different time-lapses were recorded using a JASCO Spectrophotometer model no. V700 (Serial No. B184461798) and JASCO spectra manager software at room temperature (25°C). During this experiment,

two PerkinElmer Quartz cells of path length 10mm were used for both the reference cell and the sample cell. In the reference cell, 2 ml HPLC water was taken as a reference. The spectra were recorded between 200–600 nm. The concentration of Insulin monomer in each solution was kept at 20 µM.

4.3.5. ANS fluorescence study

Exposure of hydrophobic patches in the protein during structural alteration or the aggregation process was monitored using the polarity-sensitive fluorescent probe 1-anilinonapthalene-8-sulfonate (ANS) that shows specific binding with the hydrophobic pockets (Parvej et al., 2022).

A stock solution of ANS was added to each aliquot of different Insulin solutions (including monomer as well as UV irradiated samples) so that the final ANS concentration in each aliquot was 30 mM. The ANS fluorescence intensities were measured using a Horiba spectrofluorometer (Model: FLUOROMAX-4C, serial no. 1734D-4018- FM) instrument with excitation at 350 nm and by scanning the emission wavelength from 370 nm to 600 nm. Both the emission Slit and excitation slits were kept 5 nm. Data points were the average of triplicate measurements.

4.3.6. Thioflavin T (Th T) fluorescence assay

Thioflavin T is a cationic dye with a benzothiazole nucleus that binds with the beta-sheet structure of the amyloid fibrils and shows enhanced fluorescence emission intensity at around 460 nm for insulin. To explore and quantify the aggregates formed by protein sample (Human Insulin Monomer) after UV irradiation exposure of different time lapses, the following assay was employed using Th T as a probe. Th T stock solution of 3.136 mM (1 mg mL^{-1}) was prepared by dissolving Th T in HPLC water. To compare the fibril formation under different conditions, native Human Insulin and UV exposed Human Insulin monomer were mixed with 30 µM Th T solution. 30 µl of this stock solution was added to each sample solution, mixed thoroughly, and incubated for 30 minutes at room temperature 25°C. Using a Horiba spectrofluorometer (Model: FLUOROMAX-4C, serial no. 1734D-4018- FM), Th T fluorescence assay was performed by exciting each sample at λ_{max} 440 nm. Slit widths were maintained at 5 nm for both excitation and emission. Emission spectra were recorded in the wavelength range of 460 – 600 nm. The data are reported were means of three replicates.

The percent change in fluorescence intensity (Fp) was calculated using equation (1):

$$F_P = \{(F_t - F_0)/ F_0\} \times 100 \qquad (1)$$

where F_t is the fluorescence at a specific time point, and F_0 is the fluorescence at the starting time of incubation.

Percent inhibition was also calculated using equation (2):

$$F_X = 100 - (100F_S/F_C) \qquad (2)$$

Where F_X is the percent inhibition, F_S is the percent increase in fluorescence intensity in the presence of the metal ions, and F_C is the percent increase in the fluorescence intensity of the insulin monomer alone (Strasser et al., 2000).

4.3.7. Dynamic light scattering (DLS) measurement

There is a fluctuation in the intensity of scattered light due to the diffusion of particulates in solution. As DLS is sensitive to particle size, it detects these fluctuations using an autocorrelation on a microsecond time scale and is used to analyze the distribution of molecules and supramolecular aggregates. Generally, it measures the hydrodynamic radius of a particle diffused in a solution; thus, different sizes of molecules in the solution can be observed in different peaks, provided their sizes vary sufficiently. In this study, DLS measurements were performed with the samples containing 20 µM Insulin monomer. Insulin monomer and monomeric insulin under 1min, 3 mins, 7 mins, and 15 mins UV irradiation were sonicated and then filtered off using a Millipore filter paper for the DLS Measurements. The sample solutions were taken in a 2 ml rectangular Helma cuvette of 10 mm path length for DLS measurements using Zeta-sizer Nanos (Malvern Instrument, U.K.) equipped with a 633 nm laser at 25°C. The time-dependent autocorrelation function was acquired with twelve acquisitions for each run. Each data is an average of five such acquisitions.

4.3.8. Circular dichroism measurements

After sustained 276 nm excitation of insulin, the relative changes in ellipticity were observed using Circular Dichroism (CD) spectroscopy. Following each excitation session of one minute, three minutes, seven minutes, and fifteen minutes of UV light exposure at 276 nm excitation, the near- and far-UV CD spectra were collected right away. One milliliter of lighted insulin was put into a quartz microcuvette with a one-millimeter route length. 190–260 nm far-UV CD spectra were obtained with the following settings: 1.0 nm resolution, 3 accumulations, 100 nm/min scan speed, and 1.0 nm band width. The following settings were used to record near-UV CD spectra (250–310 nm): 10 nm band width, resolution 1.0 nm, 32 accumulations, scan speed 100 nm/min, 1 mdeg sensitivity, and 4 s response time. For the HPLC water and a fresh

insulin sample, far-UV and near-UV CDs were also obtained. Every spectrum had the buffer signal subtracted from it. A Peltier unit with a Multi Tech water circulator and a thermostatically controlled cell holder attached to the JASCO Spectropolarimeter (J-815, Jasco, Tokyo, Japan) was used to control each measurement. A Peltier element was used to maintain a consistent temperature of 22°C for all of the measurements.

MRE values were plotted against the wavelength to compare the CD spectra. Using the equation, the mean residual ellipticity (MRE) value having a unit in deg cm2 dmol-1 was obtained (Corrêa and Ramos, 2009).

$$MRE = \theta_{obs}\ (mdeg)/10 \times n \times Cp \times l$$

Here, θ_{obs} is the observed ellipticity (CD) in millidegree, n is the number of amino acid residues in the protein monomer (for insulin, n is 51), l is the path length of the cell in centimetres, and Cp is the molar fraction of proteins in solution.

4.3.9. Transmission electron microscopy

Imaging of the protein samples, before and after the UV exposure of different time-lapse, was captured using High-resolution Transmission Electron Microscopy (HR TEM) (JEOL – HRTEM- 2011, TOYKO, JAPAN) under an accelerating voltage of 80-85 kV in different magnifications. For this study, all the sample solutions were centrifuged and diluted. These diluted solutions were drop casted on a carbon-coated copper grid of mesh size 300C (Pro Sci Tech). After 20s the droplet was removed from the mesh grid by shocking it on a filter paper by the side of the grid, followed by a droplet of 2% uranyl acetate (Sigma) added to the stain. Next, the grids were air-dried in a desicator overnight. After incubation for a few hours, the grids were used for TEM imaging at a magnification of 12 - 30000.

4.4. Results and discussion

4.4.1. UV- Visible spectroscopy study

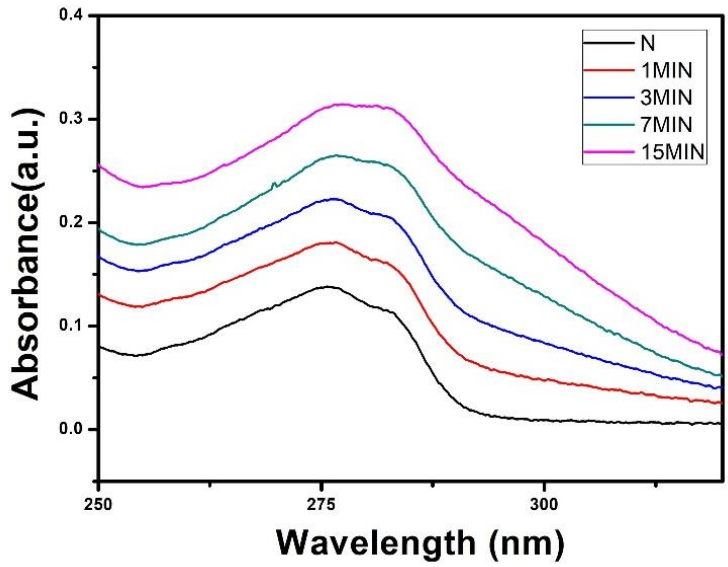

Figure 2: Absorbance Spectra of Human Insulin and Human Insulin under UV irradiation for 1 min, 3 mins, 7 mins, and 15 mins. In all samples, the insulin concentration is kept 20 µM.

The UV-vis spectroscopic study gives a preliminary understanding of the change of the microenvironment of chromophores in the protein during structural change. After incubation of native Human Insulin under UV irradiation for 1 min, 3 mins, 7 mins, and 15 mins the systems were investigated with UV-vis spectroscopy (Figure 2). Native Human Insulin showed λmax at 276 nm, a characteristic absorption band of a protein. Table 1 below shows the absorbance value at λmax for different samples.

Table 1: Absorbance value at λmax = 276 nm.

Samples	Absorbance value
Native Human Insulin	0.12
Native Human Insulin under UV light Exposure for 1min	0.16
Native Human Insulin under UV light Exposure for 3mins	0.20
Native Human Insulin under UV light Exposure for 7mins	0.24
Native Human Insulin under UV light Exposure for 15mins	0.30

The position of **λmax** peaks of the Native proteins and UV irradiated proteins remains unalter; however, a slight change is observed in the absorbance intensity of the different samples. The results thus indicate that the UV exposure on Insulin molecules can potentially change the positions of the chromophores.

4.4.2. ANS –Fluorescence to monitor the hydrophobicity changes

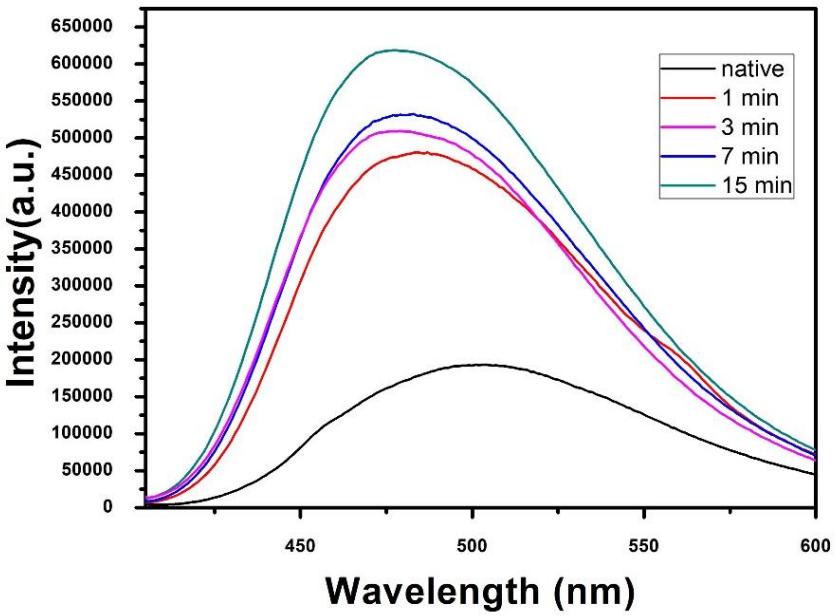

Figure 3: ANS fluorescence Spectra of Human Insulin and Human Insulin under UV irradiation for 1 min, 3 mins, 7 mins, and 15 mins. In all samples, the insulin concentration is kept 20 µM. The excitation wavelength is 350 nm, and emission spectra are 370 – 600 nm.

A fluorescence probe that detects the non-polarity of proteins, 1-anilino-8-naphthalene sulfonate (ANS), is mostly used to detect the contiguous hydrophobic surfaces of folding intermediates (Hofmann et al., 2014). As there are no exposed hydrophobic pockets, the ANS showed little affinity for native insulin. According to a publication, ANS exhibits nearly no fluorescence in water, but when it binds to hydrophobic protein patches, it creates a bright fluorescence with an emission maximum ranging from 510 to 480 nm. In the presence of ANS, the natural insulin spectrum displayed very little fluorescence (Figure 3).

After UV light irradiation for different time-lapses, Insulin showed enhanced ANS fluorescence intensity at 480 nm with a blue shift of the emission. During UV exposure of Human insulin monomer molecules with increased time, a significant increase in the ANS fluorescence intensity was observed, indicating the opening of more ANS binding sites.

Insulin exhibited maximum ANS fluorescence intensity at 480 nm with a blue shift of the emission after 15 minutes of UV light exposure. The greater access of ANS to the hydrophobic regions found in proteins following a 15-minute UV irradiation of native insulin is responsible for this rise in fluorescence intensity. β-lg aggregates thermally as a result of increased protein-protein interactions caused by these hydrophobic regions.

4.4.3. Th-T binding study to measure the aggregation propensity

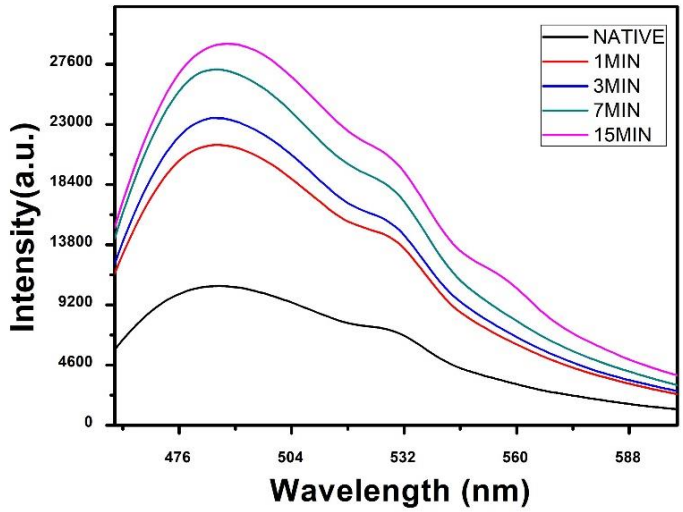

Figure 4: Fluorescence Spectra of Human Insulin and Human Insulin under UV irradiation for 1 min, 3 mins, 7 mins, and 15 mins. In all samples, the insulin concentration is kept 20 µM. The excitation wavelength is 440 nm, and emission spectra are 460 – 600 nm.

Since the thioflavin T (ThT) assay is thought to be a trustworthy method for measuring amyloid fibrils, we looked at the effects of UV light irradiation on monomer insulin in vitro by tracking changes in dye fluorescence over time. A dye called thioflavin T (ThT) attaches to amyloid fibrils and exhibits increased fluorescence intensity. The rotation of ThT's benzothiozole and benzaminic rings is controlled while binding to amyloid fibrils (if present in the reaction media). This reduces self-quenching and increases the quantum yield of fluorescence.

The external fluorescent probe ThT was used to monitor the change of monomer to insulin fibril formation. After UV light irradiation for different time-lapses, Insulin showed enhanced ThT fluorescence intensity at 482 nm. During UV exposure of Human insulin monomer molecules with increased time, a significant increase of the ThT fluorescence intensity was observed, indicating the formation of the amyloid fibrillar structure of insulin. The order of the ThT fluorescence intensity is native human insulin under UV light exposure for 15 mins > native human insulin under UV light exposure for 7 mins > native human insulin under UV

light exposure for 3 mins> native human insulin under UV light exposure for 1 mins > human insulin monomer (Figure 4).

4.4.4. Dynamic light scattering study

As a light-scattering technique, dynamic light scattering (DLS), or photon correlation spectroscopy (PCS), has become an increasingly powerful method for studying the properties of colloids, biomolecules, macromolecules, and polymers. In a solution with Brownian particles, flashing a monochromatic light beam causes a Doppler shift when it hits the moving particle, which changes the wavelength of the incoming light (typically red light at 633 nm or near infrared light at 830 nm for bimolecular applications). This change is related to the size of the particles (Nielsen et al., 2001).

Particle size distribution of human insulin monomer and UV light exposed human insulin monomer were monitored with DLS. Compared to native monomeric insulin, the UV light exposed insulin solutions showed a significant increase in particle size (Figure 5). The hydrodynamic radii of monomeric insulin ranged from 10 to 20 nm, but after irradiation with UV light, the human insulin monomer solution showed an increased hydrodynamic radius of particles present in the solution, which indicates the generation of insulin aggregates having greater light scattering properties. When we consider the time-lapse, it is observed that with more time of incubation with UV light, more scattering intensity by the particle of the solution, which in correspondence indicates the higher hydro dynamic radius formation of insulin monomer with long UV irradiation. The findings of the DLS studies are also consistent with the results of other experiments.

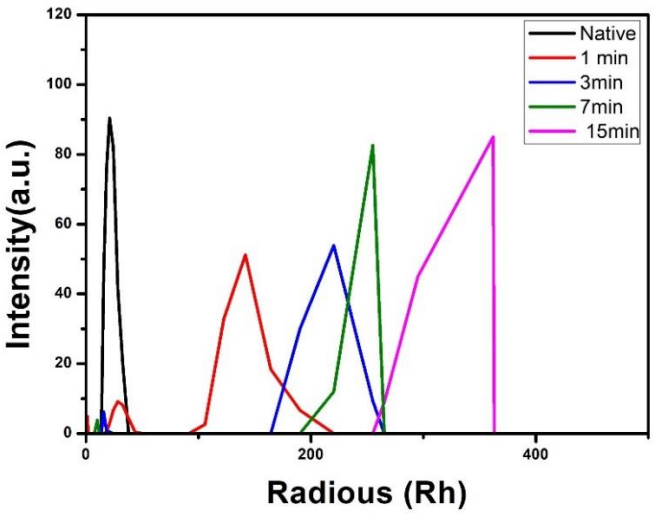

Figure 5: DLS Spectra of Human Insulin and Human Insulin under UV irradiation for 1 min, 3 mins, 7 mins, and 15 mins. In all samples, the insulin concentration is kept 20 µM.

4.4.5. Circular dichroism (CD) spectroscopy to monitor the secondary structural changes

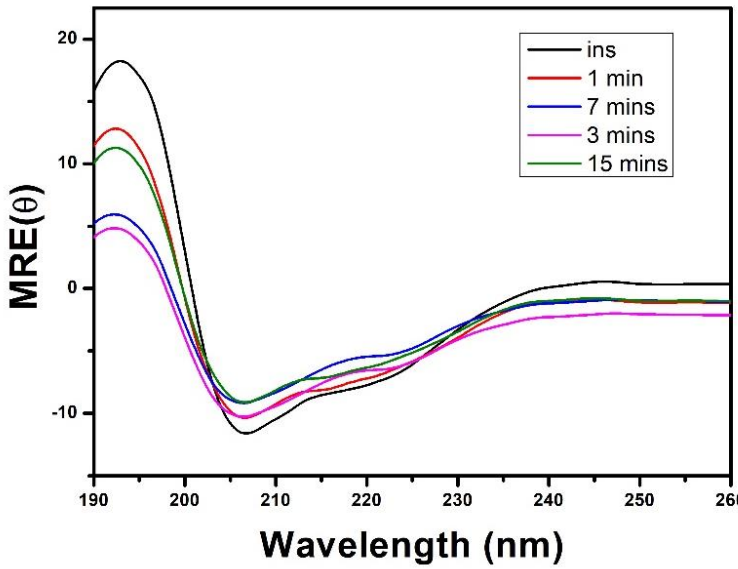

Figure 6: CD Spectra of Human Insulin and Human Insulin under UV irradiation for 1 min, 3 mins, 7 mins, and 15 mins. In all samples, the insulin concentration is kept 20 µM.

Circular dichroism (CD) spectroscopy is used to detect the secondary and tertiary structural change of the investigating protein. Insulin is an a-helix enriched protein that shows a peak at 208 nm in far-UV CD spectral regions for its a-helical structure. If any external force alters the secondary structure of the insulin, then there will be a change or shift of these Characteristic peaks. In this study, the monomeric insulin (20 µM) showed peaks at 208 nm and 221 nm, which are the characteristic peaks of an alpha helix-containing protein like insulin, along with the presence of beta-sheet structure. However, after irradiation with UV light, a significant change in the far- UV region was observed in the above-mentioned peak, indicating structural alteration and modification of the native protein's secondary structure. In Figure 6, it is observed that with an increasing time period of UV exposure of the native human insulin monomer, the negative ellipticity of the Charactertics peak at 208 nm and at 221 nm decreases rapidly. These results indicate the formation of a slightly higher content of b sheeted structure.

4.4.6. Transmission electron microscopy

For morphological changes of the Human insulin monomer after exposure to the UV light, the native insulin monomer solution and UV-exposed insulin monomer solutions were analyzed by high-resolution transmission electron microscopy (HRTEM). The structural effects imparted by UV light on the insulin monomer can be visualized by examining the TEM images

(Figure 7). The electron microscopic images also supported the results of ANS and ThT fluorescence measurements.

Under the TEM study, native human insulin shows very tiny irregular structures (Figure 7A), which are commonly observed for native human insulin reported in the literature. After UV irradiation for 15 mins, native insulin monomer formed fibrils through its self-assembly, which was subsequently converted to higher order aggregates that showed small spherical morphology (Figure 7B). Therefore, the UV light exposure of insulin promotes the structural modulation and formation of fibrillar aggregates.

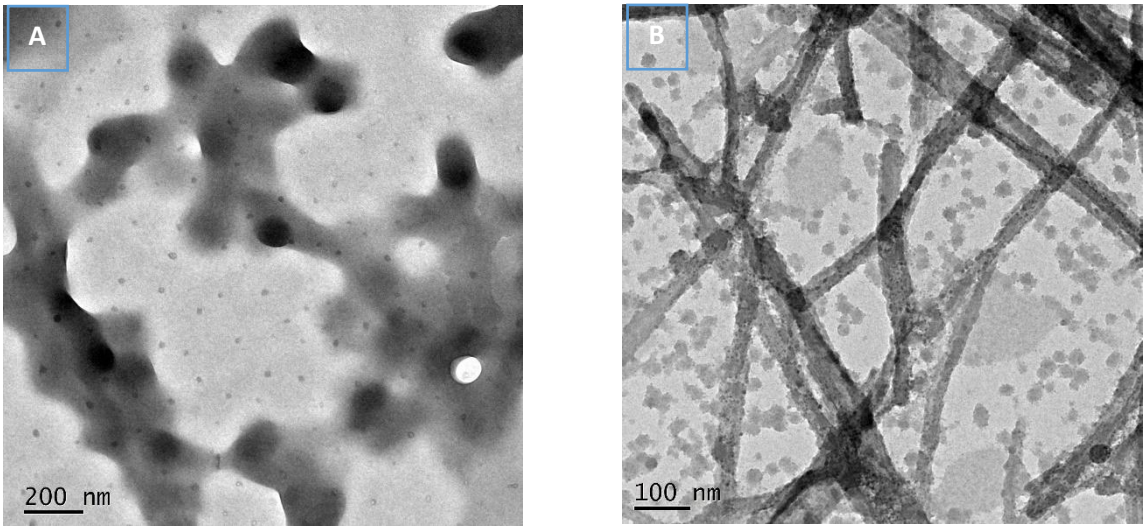

Figure 7: TEM images of Human Insulin and Human Insulin under UV irradiation for 1 min, 3 mins, 7 mins, and 15 mins. In all samples, the insulin concentration is kept 20 µM. 7A. TEM image of Native Human Insulin. 7B. TEM image of Native Human Insulin under UV light Exposure for 15mins.

4.5. Summary of the work

After correlating the results observed in different experiments of the present study, it can be concluded that upon UV exposure, human insulin aggregates. This effect is time-dependent, as higher structural modifications occur with long UV exposure. Upon UV exposure, the structure of Human Insulin gets altered as the secondary structure is altered and hydrophobic sites are exposed around the surface of the protein; thus, protein gets aggregates, and higher aggregates are formed under UV exposure for a long time.

Most proteins, including the pharmaceutically significant proteins insulin, insulin growth factors, nerve growth factors, and tumor necrosis factors, have several tyrosine residues.

Dityrosine cross-linking has the potential to cause long-term intermolecular aggregation in pharmaceutical preparations when they are subjected to both artificial and ambient UV radiation. Insulin structure can be altered at a wavelength of 254 nm, which is covered by UV sterilization lamps (Hg), which have irradiance values ranging from 10 to 2400 W. m22.

It is important to look into the light sources used when making drugs. It's crucial to stay away from UV light sources throughout production, including sunshine. UV-blocking materials should be incorporated into the pharmacological compositions.

4.6. References

Andley, U.P. and Clark, B.A., 1989. The effects of near-UV radiation on human lens β-crystallins: protein structural changes and the production of O2_ and H2O2. Photochemistry and photobiology, 50(1), pp.97-105.

Bastos, E.L., Quina, F.H. and Baptista, M.S., 2023. Endogenous photosensitizers in human skin. Chemical Reviews, 123(16), pp.9720-9785.

Corrêa, D.H. and Ramos, C.H., 2009. The use of circular dichroism spectroscopy to study protein folding, form and function. African Journal of Biochemistry Research, 3(5), pp.164-173.

Das, S. and Purkayastha, P., 2017. Gold nanocluster protection of protein from UVC radiation: a model study on bovine serum albumin. ACS omega, 2(6), pp.2451-2458.

Dougherty, D.A., 1996. Cation-π interactions in chemistry and biology: a new view of benzene, Phe, Tyr, and Trp. Science, 271(5246), pp.163-168.

Espinoza, J.H. and Mercado-Uribe, H., 2017. Visible light neutralizes the effect produced by ultraviolet radiation in proteins. Journal of Photochemistry and Photobiology B: Biology, 167, pp.15-19.

Espinoza, J.H., Reynaga-Hernández, E., Ruiz-García, J., Montero-Morán, G., Sanchez-Dominguez, M. and Mercado-Uribe, H., 2015. Effects of green and red light in βL-crystallin and ovalbumin. Scientific reports, 5(1), p.18120.

Gourmelon, M., Cillard, J. and Pommepuy, M., 1994. Visible light damage to Escherichia coli in seawater: oxidative stress hypothesis. Journal of Applied Bacteriology, 77(1), pp.105-112.

Hofmann, A., Simon, A., Grkovic, T. and Jones, M., 2014. Methods of molecular analysis in the life sciences. Cambridge University Press.

Hott, J.L. and Borkman, R.F., 1993. Concentration dependence of transmission losses in UV-laser irradiated bovine alpha-, beta H-, beta L-and gamma-crystallin solutions. Photochemistry and photobiology, 57(2), pp.312-317.

Kaiser, W., Schultz-Fademrecht, T., Blech, M., Buske, J. and Garidel, P., 2021. Investigating photodegradation of antibodies governed by the light dosage. International Journal of Pharmaceutics, 604, p.120723.

Kamelnia, R., Goliaei, B., Peyman Shariatpanahi, S., Mehrnejad, F., Ghasemi, A., Zare Karizak, A. and Ebrahim-Habibi, A., 2023. Chemical Modification of the Amino Groups of Human Insulin: Investigating Structural Properties and Amorphous Aggregation of Acetylated Species. The Protein Journal, 42(4), pp.383-398.

Levin, S.A., 2013. Encyclopedia of biodiversity. Academic Press.

Lin, L. and Xu, J., 2020. Fungal pigments and their roles associated with human health. Journal of Fungi, 6(4), p.280.

Liu, J., Tian, L., Zhang, R., Dong, Z., Wang, H. and Liu, Z., 2018. Collagenase-encapsulated pH-responsive nanoscale coordination polymers for tumor microenvironment modulation and enhanced photodynamic nanomedicine. ACS applied materials & interfaces, 10(50), pp.43493-43502.

Lundeen, R.A., Janssen, E.M.L., Chu, C. and McNeill, K., 2014. Environmental photochemistry of amino acids, peptides and proteins. Chimia, 68(11), pp.812-812.

McLean, J.T., Benny, A., Nolan, M.D., Swinand, G. and Scanlan, E.M., 2021. Cysteinyl radicals in chemical synthesis and in nature. Chemical Society Reviews, 50(19), pp.10857-10894.

Mozziconacci, O., Williams, T.D., Kerwin, B.A. and Schöneich, C., 2008. Reversible intramolecular hydrogen transfer between protein cysteine thiyl radicals and αC− H bonds in insulin: control of selectivity by secondary structure. The Journal of Physical Chemistry B, 112(49), pp.15921-15932.

Muneer, S., Kim, E.J., Park, J.S. and Lee, J.H., 2014. Influence of green, red and blue light emitting diodes on multiprotein complex proteins and photosynthetic activity under different light intensities in lettuce leaves (Lactuca sativa L.). International journal of molecular sciences, 15(3), pp.4657-4670.

Muranov, K.O., Maloletkina, O.I., Poliansky, N.B., Markossian, K.A., Kleymenov, S.Y., Rozhkov, S.P., Goryunov, A.S., Ostrovsky, M.A. and Kurganov, B.I., 2011. Mechanism of aggregation of UV-irradiated βL-crystallin. Experimental Eye Research, 92(1), pp.76-86.

Nagy, T.M., Knapp, K., Illyés, E., Timári, I., Schlosser, G., Csík, G., Borics, A., Majer, Z. and Kövér, K.E., 2018. Photochemical and Structural Studies on Cyclic Peptide Models. Molecules, 23(9), p.2196.

Nauser, T., Casi, G., Koppenol, W.H. and Schöneich, C., 2005. Intramolecular addition of cysteine thiyl radicals to phenylalanine in peptides: formation of cyclohexadienyl type radicals. Chemical communications, (27), pp.3400-3402.

Nielsen, L., Frokjaer, S., Brange, J., Uversky, V.N. and Fink, A.L., 2001. Probing the mechanism of insulin fibril formation with insulin mutants. Biochemistry, 40(28), pp.8397-8409.

Parvej, H., Begum, S., Dalui, R., Paul, S., Mondal, B., Sardar, S., Sepay, N., Maiti, G. and Halder, U.C., 2022. Coumarin derivatives inhibit the aggregation of β-lactoglobulin. RSC advances, 12(27), pp.17020-17028.

Prajapati, I., Subelzu, N., Zhang, Y., Wu, Y. and Schöneich, C., 2022. Near UV and visible light photo-degradation mechanisms in citrate buffer: one-electron reduction of peptide and protein disulfides promotes oxidation and cis/trans isomerization of unsaturated fatty acids of polysorbate 80. Journal of Pharmaceutical Sciences, 111(4), pp.991-1003.

Prompers, J.J., Hilbers, C.W. and Pepermans, H.A., 1999. Tryptophan mediated photoreduction of disulfide bond causes unusual fluorescence behaviour of Fusarium solani pisi cutinase. FEBS letters, 456(3), pp.409-416.

Sergeev, Y.V., Soustov, L.V., Chelnokov, E.V., Bityurin, N.M., Backlund, P.S., Wingfield, P.T., Ostrovsky, M.A. and Hejtmancik, J.F., 2005. Increased Sensitivity of Amino-Arm Truncated βA3-Crystallin to UV-Light–Induced Photoaggregation. Investigative ophthalmology & visual science, 46(9), pp.3263-3273.

Strasser, R.J., Srivastava, A. and Tsimilli-Michael, M., 2000. The fluorescence transient as a tool to characterize and screen photosynthetic samples. Probing photosynthesis: mechanisms, regulation and adaptation, 25, pp.445-483.

Trujillo, M., Alvarez, B. and Radi, R., 2016. One-and two-electron oxidation of thiols: mechanisms, kinetics and biological fates. Free radical research, 50(2), pp.150-171.

Vanhooren, A., Illyes, E., Majer, Z. and Hanssens, I., 2006. Fluorescence contributions of the individual Trp residues in goat α-lactalbumin. Biochimica et Biophysica Acta (BBA)-Proteins and Proteomics, 1764(10), pp.1586-1591.

Vincenti, M.P., White, L.A., Schroen, D.J., Benbow, U. and Brinckerhoff, C.E., 1996. Regulating expression of the gene for matrix metalloproteinase-1 (collagenase): mechanisms that control enzyme activity, transcription, and mRNA stability. Critical Reviews™ in Eukaryotic Gene Expression, 6(4).

Weiss, M., Steiner, D.F. and Philipson, L.H., 2015. Insulin biosynthesis, secretion, structure, and structure-activity relationships.

Wu, L.Z., Sheng, Y.B., Xie, J.B. and Wang, W., 2008. Photoexcitation of tryptophan groups induced reduction of disulfide bonds in hen egg white lysozyme. Journal of Molecular Structure, 882(1-3), pp.101-106.

CHAPTER 5

EFFECT OF POLARITY OF COUMARIN MOLECULES ON THE BINDING WITH BETA-LACTOGLOBULIN

Effect of polarity of coumarin molecules on the binding with beta-lactoglobulin

5.1. Literature review on recent developments in synthesis and applications of coumarin-3-carbamide derivative

Oxygen heterocycles are a highly significant group of building blocks in organic synthesis. Over time, synthetic organic chemists have taken great interest in numerous derivatives of these compounds. The key aim of synthesizing oxygen heterocycles and related compounds extends beyond creating a broader range of intricate and diverse compounds with various biological activities and exploring their structure-activity relationship (SAR) studies. Additionally, these compounds have other applications in medicinal chemistry and material science, including the development of diverse fluorescence probes due to their fascinating photophysical and photochemical properties.

Oxygen-containing heterocyclic compounds have been widely used in the construction of bicyclic ring systems (**1-6**). Benzene rings fused with the 5,6-positions of a 2H-pyran ring system give rise to 2H-1-benzopyran (commonly referred to as 2H-chromene) (**1**) and isochromene (**2**). Similarly, when a benzene ring is fused with the 5,6-positions of a 4H-pyran ring system, it gives rise to 4H-1-benzopyran (commonly referred to as 4H-chromene) (**3**) and 1-benzopyrylium ion (**4**). The partially reduced form of 2H-1-benzopyran is referred to as 3,4-dihydro-2H-1-benzopyran (chroman) (**5**), and its 2-phenyl derivative is known as flavan (**6**). Detailed information regarding the structural features of these compounds is provided in **Figure 1.**

Figure 1

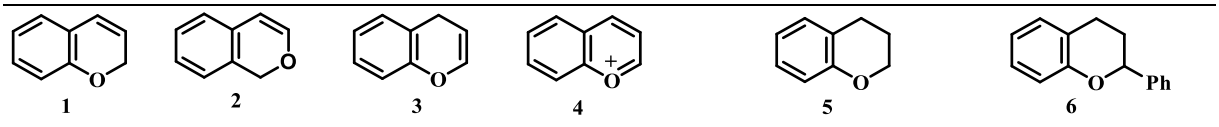

1 2*H*-chromene | **2** isochromene | **3** 4*H*-chromene | **4** 1-benzopyrylium | **5** 3,4-Dihydro-2*H*-1-benzo-pyran (Chroman) | **6** Flavan 2-Phenyl-3,4-dihydro-2*H*-1-benzo-pyran

There are ring systems **1-3** that have nine carbons, with eight of them being sp^2 hybridized and one being sp^3 hybridized. Depending on the position of the sp^3 carbon in relation to the ring oxygen, they can be either 2H- or 4H-chromenes. When the sp^3 carbon of the chroman ring system is replaced by a carbonyl functionality, the resulting compound is called a pyranone (commonly known as pyrones) (**Figure 2**). The compounds coumarin (**7**), isocoumarin (**8**),

dihydrocoumarin (**9**), chromone (**10**), xanthone (**11**), and chromanone (**12**) are named using this same nomenclature system. The 2-phenyl derivative of chromone is known as flavone (**13**), while the 2-phenyl derivative of chromanone is called flavanone (**14**).

Figure 2

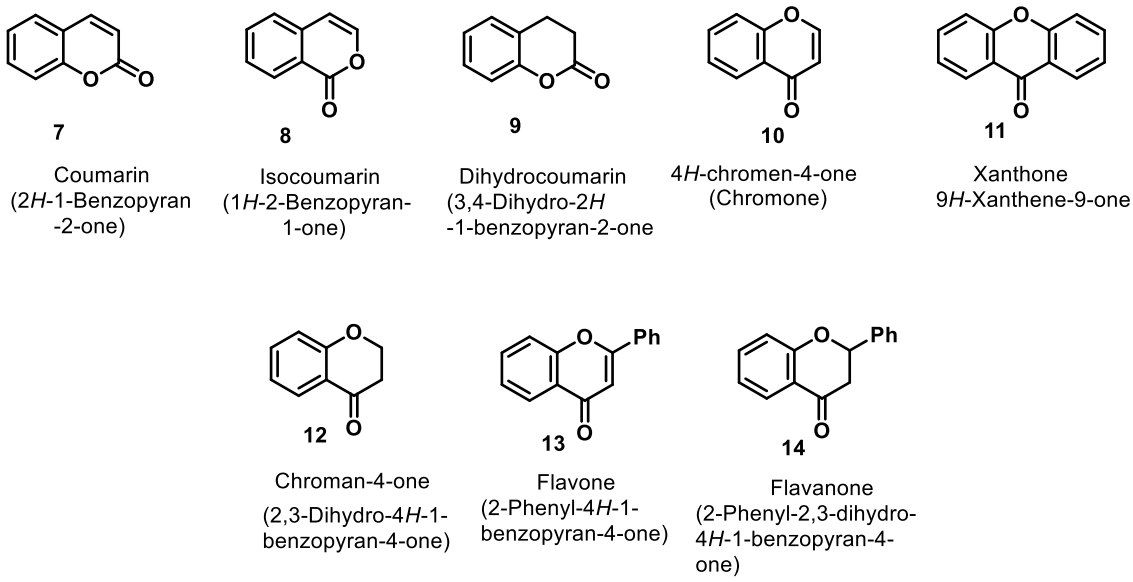

Coumarin (**7**) is a naturally occurring compound that belongs to the 2H-benzopyrone (2H-Chromene-2-one) family. Its first isolation from the tonka bean (Dipteryx odorata Wild) dates back to 1820, and it has since been found in various other plants (Bruneton, J., 1999; Tandon and Rastogi, 1979). Coumarins and their derivatives are widely distributed in the three kingdoms of life: plant, animal, and microbial (Annunziata et al., 2020). Essential oils, lavender, cinnamon bark, and cassia leaf are the primary plant sources of numerous coumarins (Lončar et al.,2020). Green tea, bilberry, and cloudberry fruits are also noteworthy sources of these compounds (Andrés-Lacueva et al., 2009; Pratap and Ram, 2014). Coumarins are also prevalent in the Rutaceae and Umbelliferae families. The fruits and stem bark of *Calophyllum dispar* are a minor source of new coumarins, which are utilized in traditional medicine and found in tropical rainforests (Pratap and Ram, 2014).

There are numerous coumarin derivatives found in nature that have been extensively documented in the literature. However, this review will only consider coumarin derivatives that have amide functionality at the 3-position. These compounds are divided into two categories based on whether the amide nitrogen or amide carbonyl is attached to the 3-position of the pyran moiety. The first category of coumarin amides was obtained from microbial sources, such as Novobiocin **15** and Coumermycin **16**, which are coumarin antibiotics and potent

inhibitors of DNA gyrase. They are found in streptomyces and aflotoxins from *Aspergillus* species, respectively. Chlorobiocin **17** also has similar source and activity (**Figure 3**) (Lacy and O'kennedy, 2004; Chen and Walsh, 2001).

Figure 3

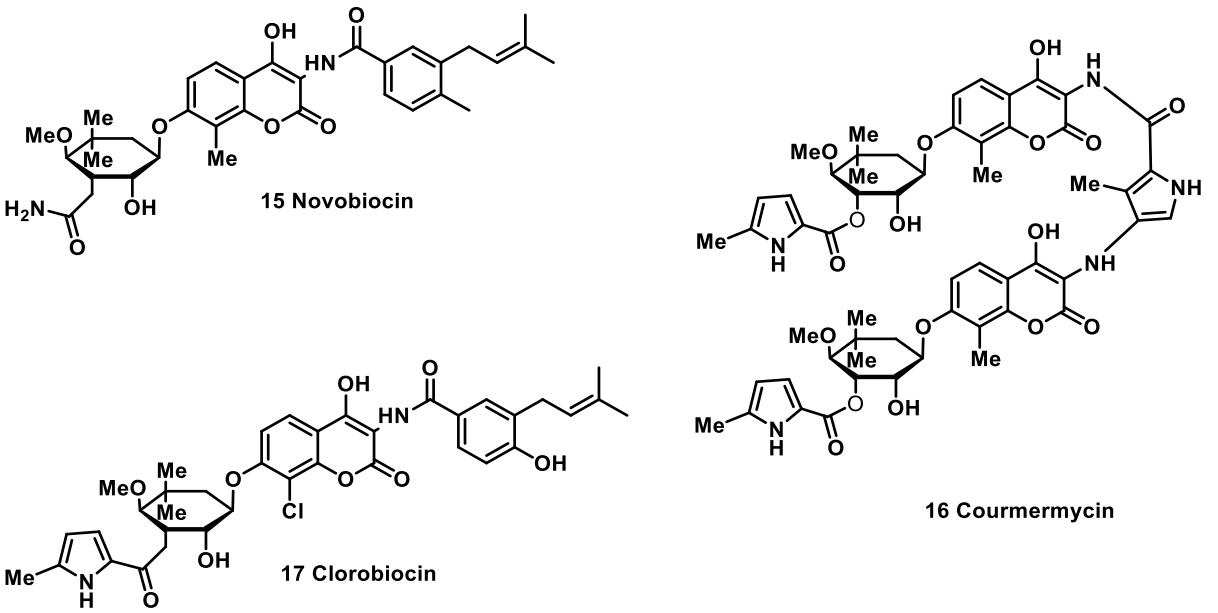

The second type of amides, namely coumarin-3-carbamide, are not found in natural sources, yet their synthetic production remains extensive due to their versatile application in different branches of science, including medicinal chemistry, material science, and nano science. The present review has been structured based on the significance and synthesis of specific coumarin-3-carbamide compounds.

5.1.1. Recently developed synthesis and biological activities of coumarin-3-carbamides

Coumarin-3-carbamides have garnered significant attention among organic chemists owing to their noteworthy biological activities, including antimicrobial, antithrombotic, anticholinesterase, and acetylcholinesterase. The classical route towards coumarin-3-carbamide synthesis entails four steps, including the Knoevenagel reaction between salicylaldehyde and suitable active methylene compounds (e.g., diethyl malonate) to obtain ethyl coumarin-3-carboxylate (**18**). Subsequently, the ester undergoes hydrolysis to yield the corresponding acid (**19**), which is then subjected to activation, followed by amide formation in the consecutive steps of the route (**Scheme 1**). Notably, the methodology for the synthesis of coumarin-3-carbamides involves primarily the modification of the Knoevenagel condensation and activation of acid steps (Sashidhara et al., 2011; Asadipour et al.,2013; Ghanei-Nasab et al., 2016; He et al., 2014)

Scheme 1

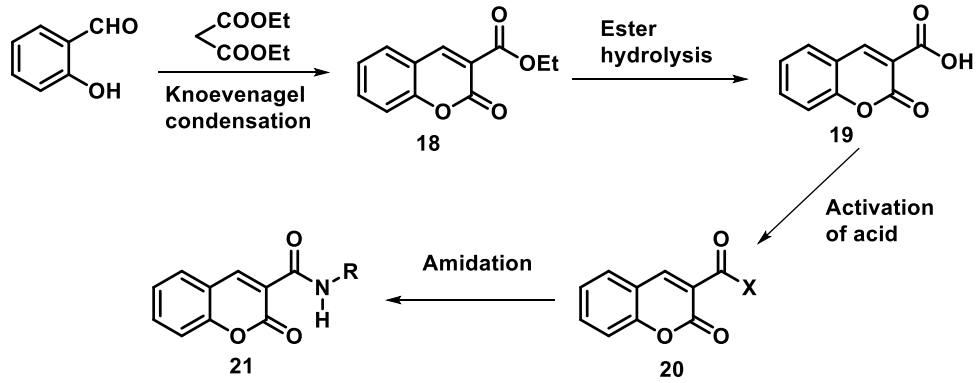

The synthesis of numerous biologically active coumarin-3-carbamide and their analogues remains a popular practice, with many compounds produced through this route. Sashidhara et al. utilized this method, activating the acid with $SOCl_2$ to obtain benzocoumarin-3-carbamide (**22**) derivatives as the final product (**Scheme 1**). These products have demonstrated orally active antithrombotic activity (Sashidhara et al., 2011), similar to the biologically active coumarin-3-carbamide **23**, **24**, and **25** (**Figure 4**), which showed anticholinesterase activity (Ghanei-Nasab et al., 2016), acetylcholinesterase (Asadipour et al.,2013), and hMAO inhibitory activity (He et al., 2014), respectively, through the same synthetic methodology.

Figure 4

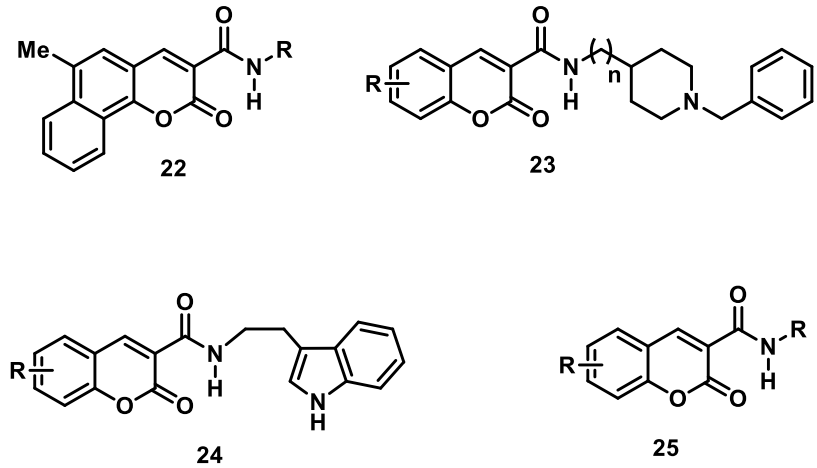

Danko and colleagues synthesized a novel derivative of coumarin-3-carbamide (27) by activating the acid group of coumarin-3-carboxylic acids using 4-(4,6-dimethoxy-1,3,5-triazin-2-yl)-4-methylmorpholin-4-ium chloride (**26**) as an activating agent at room temperature in a THF solution, as illustrated in **Scheme 2** (Danko et al., 2011).

Scheme 2

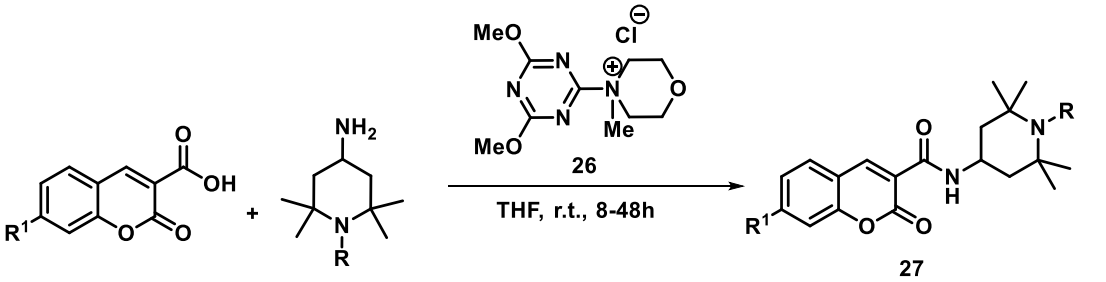

Tiwari et al. utilized coumarin-3-carbamide-amino acid conjugates as fluorescent-labels for quinolone antibiotics (ciprofloxacin, pipemidic acid, and norfloxacin) in **Scheme 3**. These conjugates are connected through amino acids by two peptide bonds (Tiwari et al., 2014).

Scheme 3

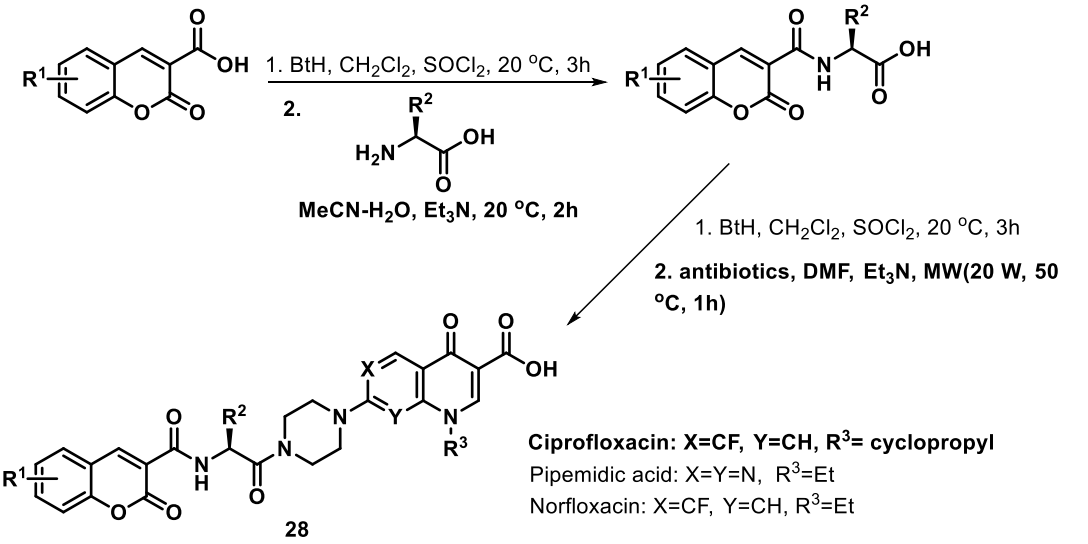

Liu and their team have developed a method to synthesize coumarin-3-carboxylic acids **29** using Meldrum's acid as a substitute for DEM, along with salicylaldehyde, in an aqueous medium. The acid was then converted into the corresponding amide with phenylethylamine through DCC-DMAP (**Scheme 4**). The final compounds, **30**, exhibit an excellent ability to protect DNA by acting as a radical scavenger (Yang et al., 2014).

Scheme 4

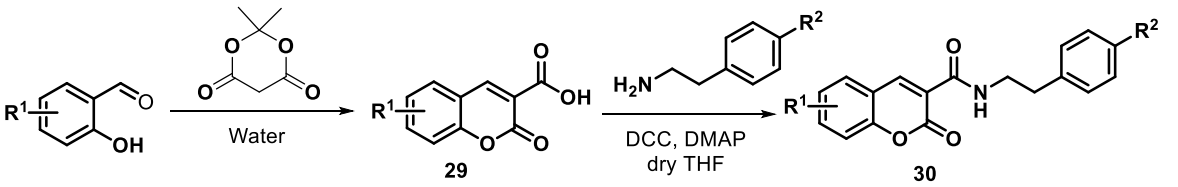

The work conducted by Fu et al. involved the utilization of Meldrum's acid as an active methylene compound in the Knoevenagel reaction, ultimately leading to the formation of coumarin-3-carboxylic acids. The acid was then employed to transform a selection of antiproliferative coumarin-3-carbamide **31** through a conventional route (**Scheme 1**), as demonstrated in **Scheme 5** (Fu et al., 2015).

Scheme 5

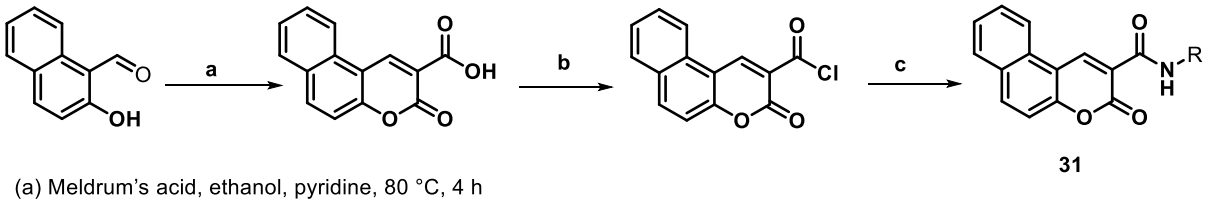

(a) Meldrum's acid, ethanol, pyridine, 80 °C, 4 h
(b) $SOCl_2$, 1,2-dichloroethane, 60–70 °C, 4 h
(c) R_1-NH_2, triethylamine, CH_2Cl_2, room temperature (r.t.), 10–30 min

Coumarin-3-carbamides are a class of compounds that have garnered significant attention in the field of medicinal chemistry due to their diverse biological activities. These compounds have been synthesized using various methods, including the Ugi-multicomponent reaction approach. Shaabani et al. has developed a novel synthesis method for coumarin-3-carbamides **32** by employing salicylaldehyde, Meldrum's acid, aromatic amine, propargyloxy aldehyde, cyclohexyl isocyanide, and azide in an ethanol medium in the presence of $Cu(OAc)_2$ catalyst. This transformation involves a domino sequence of reactions, starting with Knoevenagel condensation, which produces coumarin-3-carboxylate, followed by Ugi reaction and click reaction to produce the final compound (**Scheme 6**) (Shaabani et al., 2014). It is worth mentioning that similar types of Ugi reactions have also been reported for synthesizing coumarin-3-carbamides (Sepay et al., 2015; Balalaie et al., 2012).

Scheme 6

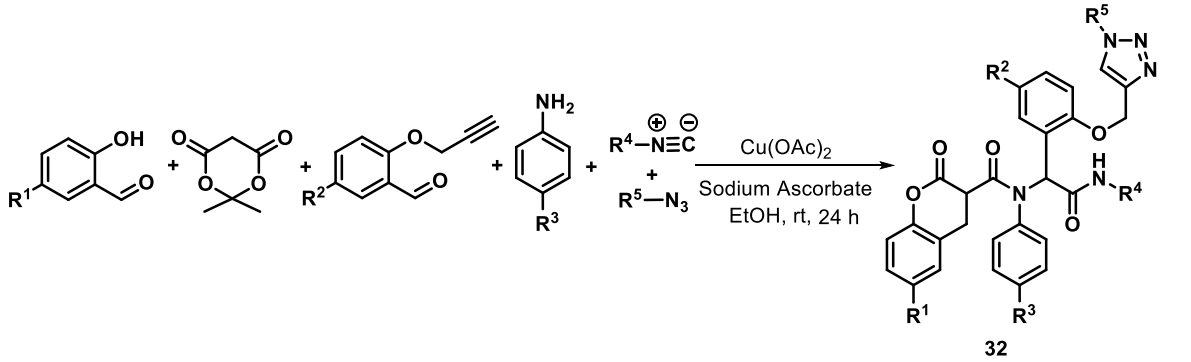

Areias et al. used an interesting route to obtain coumarin-3-carbamides. An active methylene amide 2-cyanoacetamides **33** was used for Knoevenagel condensation and cyclization to produce **34**, which was then converted into the target compound **35** through acid hydrolysis. This compound shows a binding property to the adenosine A2A receptors (**Scheme 7**) (Areias et al., 2012).

Scheme 7

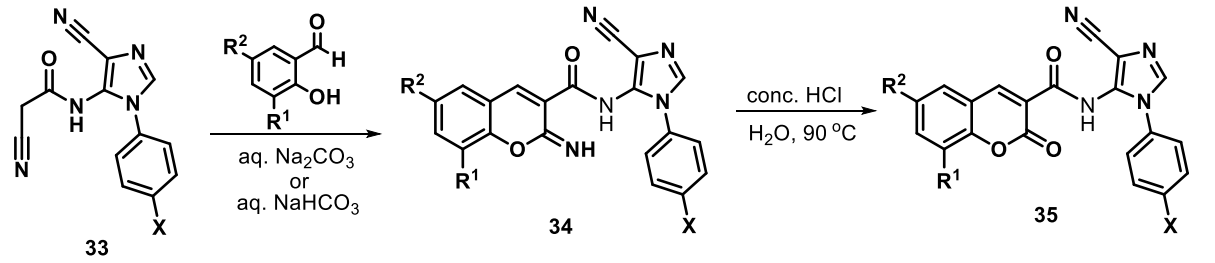

5.1.2. Recent application of coumarin-3-carbamides start from here again

The development of chemical probes to study important molecular recognition processes in chemistry and biology has been the subject of significant effort. Fluorescent probes are versatile and appealing tools for both optical imaging and analytical sensing because of their high sensitivity, fast response time, and technical ease. A common method for developing newer fluorescent probes involves modifying known fluorescent structures with commercially available building blocks through traditional synthetic procedures. This approach usually produces large libraries of such probes.

The scope of libraries encompassing fluorescent scaffolds is dictated by the diversity of building blocks that are either available or synthesized. These libraries can be tailored to exploit one or more physical or biological attributes of a fluorescent scaffold. For instance, tricarbocyanines can serve as near-infrared fluorescent dyes, while rhodamines can be utilized as mitochondria-targeting agents (as depicted in **Figure 5**). Coumarins are highly coveted for their facile synthesis, biocompatibility, and fluorescence properties. The photo-physical characteristics of coumarin-3-carbamides closely resemble those of simple coumarin. Specifically, coumarin-3-carbamides can be excited at approximately 410 nm and they emit fluorescence within the region in close proximity to 460 nm (Vendrell et al., 2012).

Figure 5

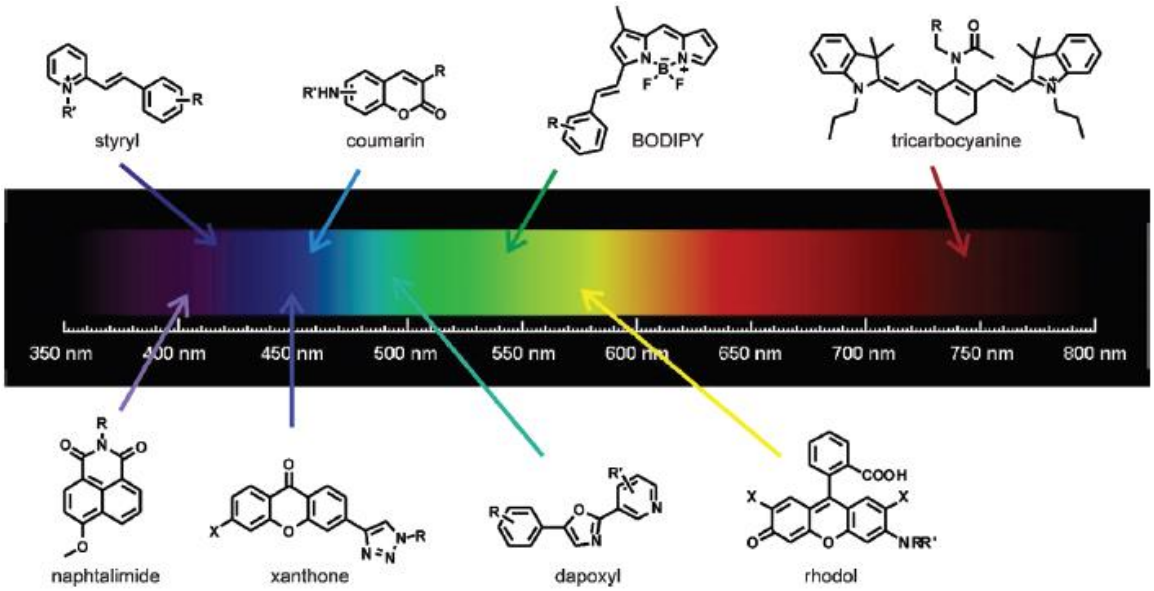

In recent years, coumarin-3-carbamides have been used as fluorescent probes for sensing metal ions, anions, and neutral molecules. They have also been utilized for labeling proteins and as part of drug delivery systems. In this section of the review, we will explore these various applications.

Chen and colleagues synthesized coumarin-3-carbamide compounds (**36**, **37**, **38**, and **39**) using different amino alcohols in acetonitrile (**Figure 6**). These compounds showed high selectivity for Fe^{3+} ions and exhibited a selective fluorescence quenching effect. It was observed that under the same conditions, other ions such as Na^{+}, K^{+}, Mg^{2+}, Ca^{2+}, Zn^{2+}, Cu^{2+}, Co^{2+}, Ni^{2+}, Fe^{3+}, Mn^{2+}, Cd^{2+}, Ag^{+}, Hg^{2+}, and Pb^{2+} were unable to effectively quench the fluorescence of coumarin-3-carbamide. Compound **39** was found to be the best probe among the synthesized compounds (Chen et al., 2013).

Figure 6

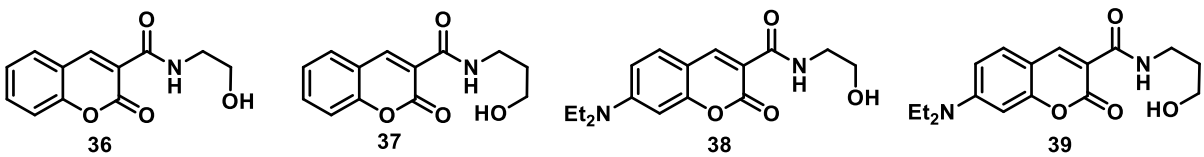

Wang and his team have developed a new coumarin-3-carbamide compound that is capable of specifically sensing Au^{3+} by fluorescent "turn-on" and colorimetric methods. In this process, Au^{3+} reacts with the alkyne moiety present in the coumarin probe **40**, resulting in the formation

of **41** (**Scheme 8**). This reaction is highly selective for Au^{3+} ions and doesn't respond to other alkynophilic metal ions like Au^{+}, Ag^{+}, Pd^{2+}, Ni^{2+}, Cu^{2+}, and Hg^{2+}. The molecule is yellowish in color when dissolved in acetonitrile-water solution, and it has no fluorescence properties. However, the color disappears and shows strong fluorescence only in the presence of Au^{3+} ion. Additionally, it has been discovered that a modified TLC plate based on **41** can be used for simple naked-eye detection of Au^{3+}. The spectroscopic detection limit of this method is 3.58 nmol/L (Wang et al., 2016).

Scheme-8

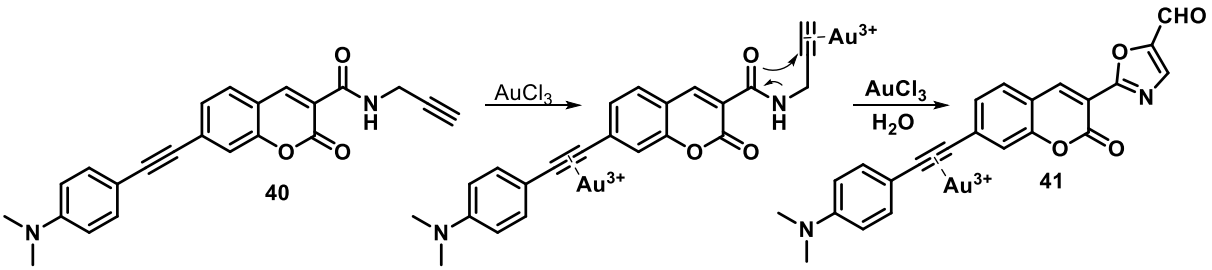

A group of researchers, including Bekhradnia et al., discovered a new type of fluorescent chemosensor that can detect Cu^{2+} in water and differentiate it from other metal ions. They used 6-nitro-coumarin-3-carbamide derivatives **42** (**Scheme 9**) for this purpose (Bekhradnia et al., 2016). Although this compound doesn't have any significant fluorescence properties, its fluorescence intensity increases when it comes into contact with Cu^{2+}. The system needs to be excited at 320 nm for this reaction to occur.

Scheme 9

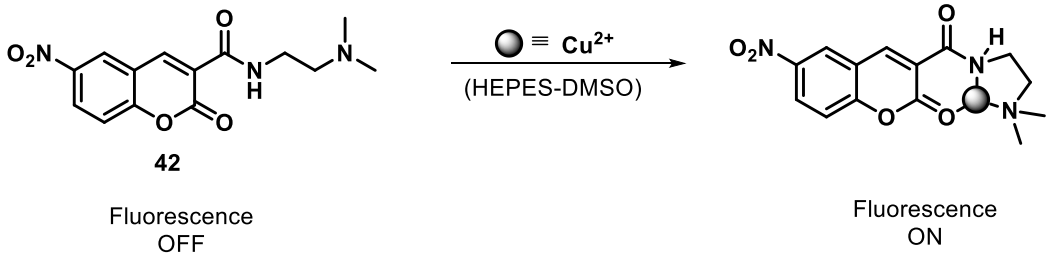

In their research, Sun et al. utilized coumarin-3-carbamide derivatives **43** and **44** of aliphatic and aromatic amines to sense CN^{-} anions. The fluorescence intensity of these derivatives was observed to decrease upon the addition of TBACN, the source of CN- anions. Interestingly, other anions such as F^{-}, Cl^{-}, Br^{-}, I^{-}, HSO_4^{-}, NO_3^{-}, $H_2PO_4^{-}$, AcO^{-}, and SCN^{-} exhibited negligible changes. These findings demonstrate a high degree of selectivity and sensitivity in the sensing of CN^{-}, as well as a remarkable colorimetric and fluorescent response. The authors

proposed a mechanism in which the CN^- sensing proceeds via a Michael addition reaction at the 4-position of coumarin, followed by an intramolecular cyclization reaction between the cyano and amido groups to yield **45** (**Scheme 10**) (Sun et al., 2012).

Scheme 10

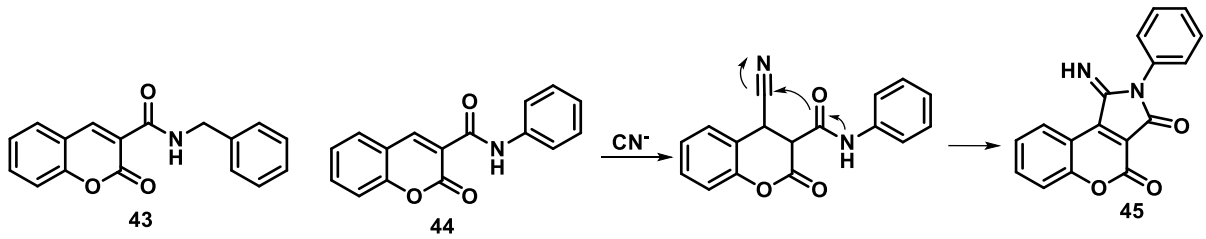

Wang et al. conducted a study where they used four derivatives of coumarin-3-carbamide benzothiazole (compounds **46**, **47**, **48,** and **49**) to detect cyanide anions in acetonitrile. The photophysical properties of these compounds were used to detect the cyanide anions. Compounds **46** and **47**, which are shown in **Figure 7**, can react with cyanide anions through Michael addition. This reaction changes color from yellow to colorless and completes quenching of green fluorescence for compound **47**, which can be observed with the naked eye. On the other hand, coumarin-3-carbamide derivative **49** can detect cyanide ions through a fluorescence turn-on response due to the displacement mechanism of the copper complex ensemble (Wang et al., 2015).

Figure 7

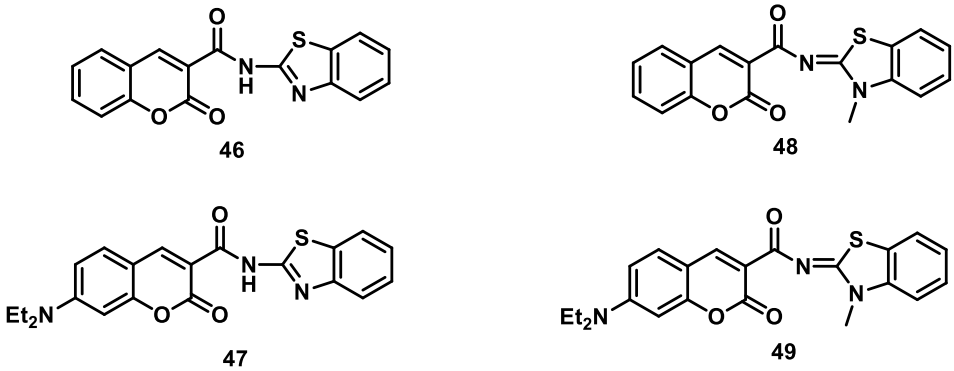

Chen and his research group have successfully synthesized a series of ring-substituted maleimide derivatives, which are labelled with coumarin-3-carbamide. These fluorogenic compounds react selectively to hydrolysis by water at the carbonyl center near the substituted carbon of the imide ring through a base-catalyzed process. They also undergo a regioselective thiol addition reaction, as shown in **Scheme 11**. The maleimide moiety effectively quenches

the fluorescence of the coumarin unit. However, after reacting with water and thiols, the maleimide part is destroyed, and the coumarin unit regains its fluorescence. This unique property of the molecules makes them excellent candidates for use as novel bioconjugation reactants or fluorogenic labeling agents (Chen et al., 2015).

Scheme 11

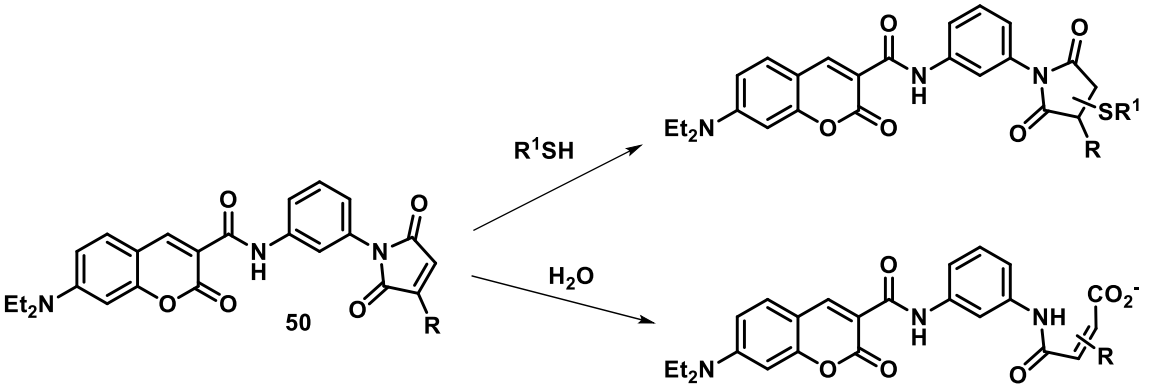

A team led by Harris et al. (2016) created an energy transfer system using coumarin-3-carbamide to investigate the stability of nanoaggregates in complex solutions and cell cultures (**Figure 8**). They used one- and two-photon fluorescence microscopy and optical imaging techniques to analyze the system. This drug delivery system is effective for adding single or multiple tumor-targeting molecules and has been successfully tested for biological imaging processes such as MRI. It has also been used to observe the behavior of folate receptors and to deliver hydrophobic drugs like doxorubicin to specific targets (Harris et al., 2016).

Figure 8

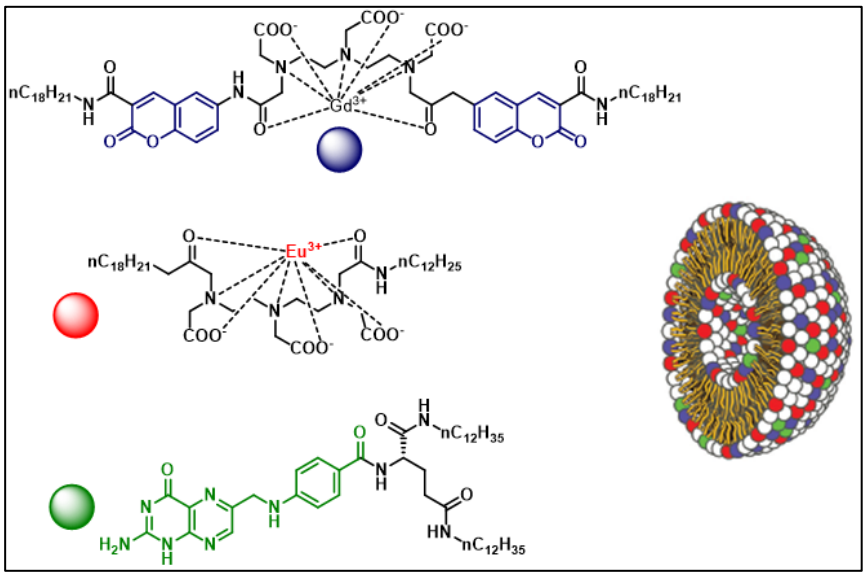

Liu et al. have presented a new fluorescent probe that can measure the hydroxyl radical (•OH) with high accuracy. The probe is made up of coumarin-3-carbamide hybrid silica nanoparticles, as shown in **Figure 9**. The nanoparticles contain a red fluorescent dye serving as the reference unit, which is unaffected by the presence of •OH. The surface of the nanoparticle is modified with coumarin-3-carboxylic acid by converting it into the corresponding amide. The blue emission of the system is stimulated only in the presence of •OH due to the conversion of coumarin to a corresponding hydroxylation product. Thus, the probe can be used for ratiometric fluorescence measurement and can detect •OH with a detection limit as low as 1.65 μM. The probe is highly selective for detecting •OH species and can differentiate them from metal ions, biological species (protein, DNA, etc.), and other reactive oxygen species. It is also biocompatible and has low cytotoxicity, making it suitable for use in living cells. This probe has also been successfully used for cellular imaging of •OH (Liu et al., 2016).

Figure 9

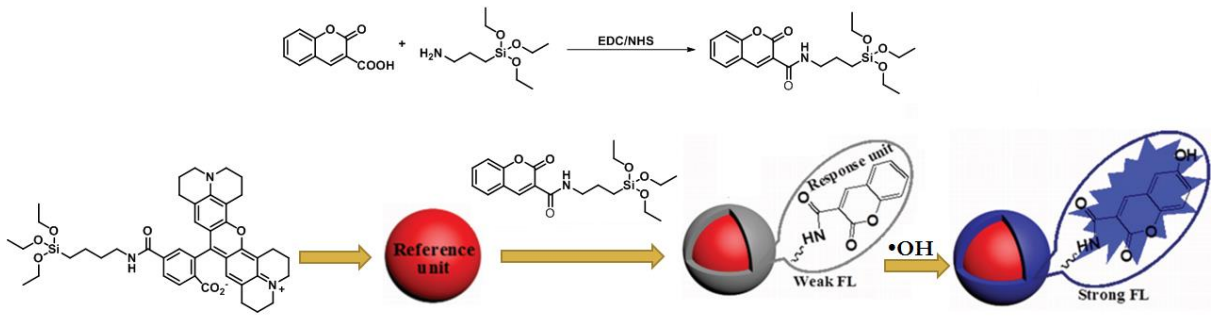

The development of inhibitors that target α-helix mediated protein-protein interactions is of great interest due to its significance in therapy. Barnard and his colleagues have devised a method for orthogonal functionalization of N-alkylated aromatic oligoamide helix mimetics to alter the binding properties of a selective series of p53/hDM2 inhibitors. A fluorescence probe, coumarin-3-carbamide, was used on the non-binding face of the helix mimetic to assess its ability to directly bind to target proteins (Barnard et al., 2014).

Figure 10

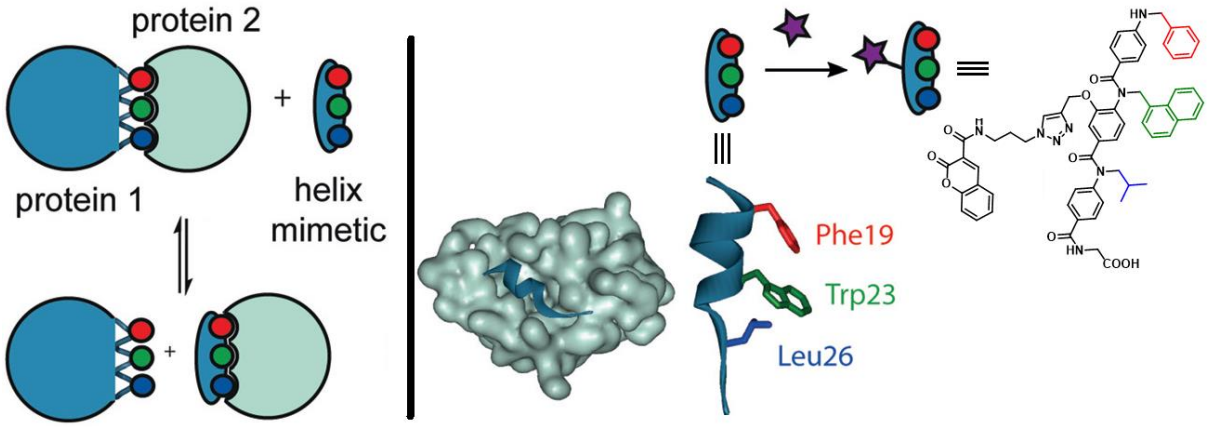

Transglutaminases (TG2) play a key role in catalyzing the transamidation reaction of glutamine residues with primary amines. To monitor TG2 transpeptidation activity, Gnaccarini et al. have developed a sensitive new assay. This assay features ligation of fluorescently labelled substrates and identification of intramolecular FRET (**Figure 11**). The fluorescence probe used for this purpose is coumarin-3-carbamide, which contains another free amine group. The assay is transpeptidation-specific, making it ideal for high-throughput applications. In fact, this coumarin-3-carbamide-containing amine has passed this assay in competition with 18 different types of amines, building a structure-activity profile for acyl-acceptor substrates of TG2 (Gnaccarini et al., 2012).

Figure 11

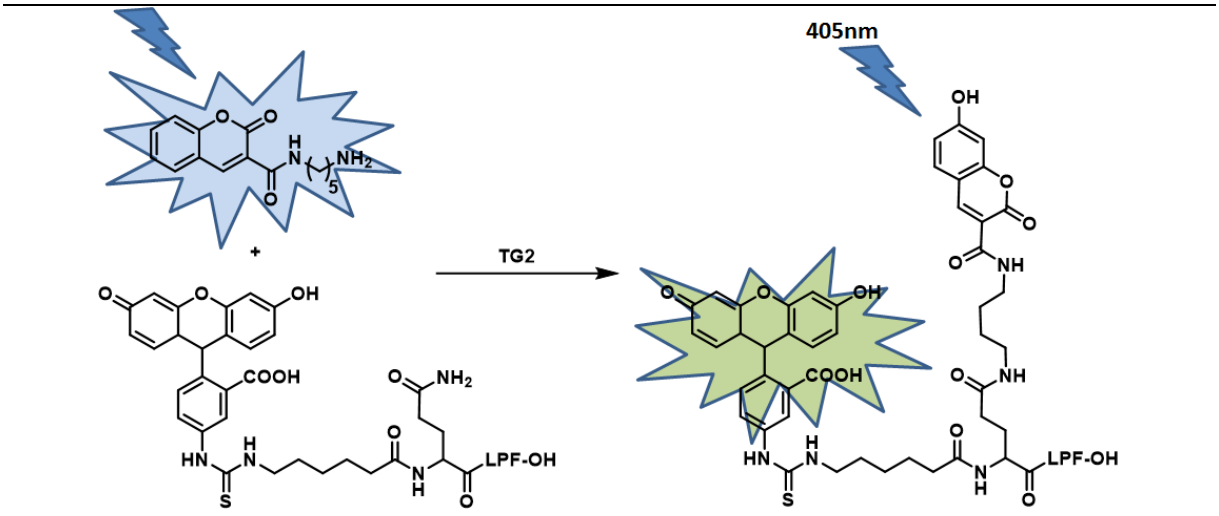

Jin et al. have developed new fluorescent ligase substrates based on coumarin-3-carbamide, which can be used for the imaging of proteins in acidic organelles and extend PRIME

technology. Coumarin-3-carbamide derivatives **51**, **52**, and **53** were used for this process and can be seen in **Figure 12**. To convert 7-aminocoumarin-3-carbamide to its corresponding hydroxyl derivative, the team used a palladium-catalyzed Buchwald–Hartwig cross-coupling reaction. Compound 51 has demonstrated site-specific binding ability with LAP fusion proteins on the surface of cells and inside living mammalian cells31 (Jin et al., 2011).

Figure 12

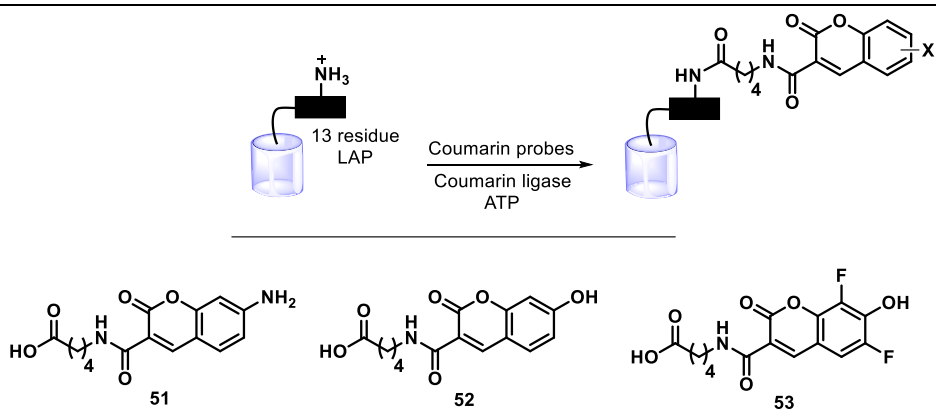

Kuru et al. used a fluorescence probe called coumarin-3-carbamide-amino acid conjugate **54** to label the bacterial growth-controlling peptidoglycan (PG) cell wall. They achieved this by taking advantage of the cells' tolerance for incorporating different non-natural D-amino acids (as shown in **Figure 13**). As a result, they were able to preferentially label active PG synthesis sites and accurately track cell-wall dynamics in various morphologically and phylogenetically different bacteria using these nontoxic D-amino acids (Kuru et al., 2012).

Figure 13

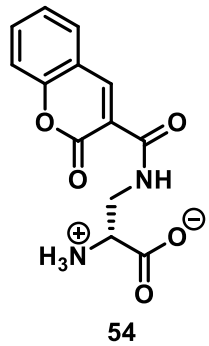

Velasco and colleagues carried out a study on a one-pot, three-component synthetic method for creating coumarin-3-carboxamides. The method involved reacting salicylaldehyde, aliphatic primary or secondary amines, and diethylmalonate using piperidine-iodine as a dual system catalyst and ethanol as a green solvent (**Figure 14**). This approach has several advantages,

including being a clean and metal-free reaction, having low catalyst loading, and requiring no tedious workup (Velasco et al., 2022).

Figure 14

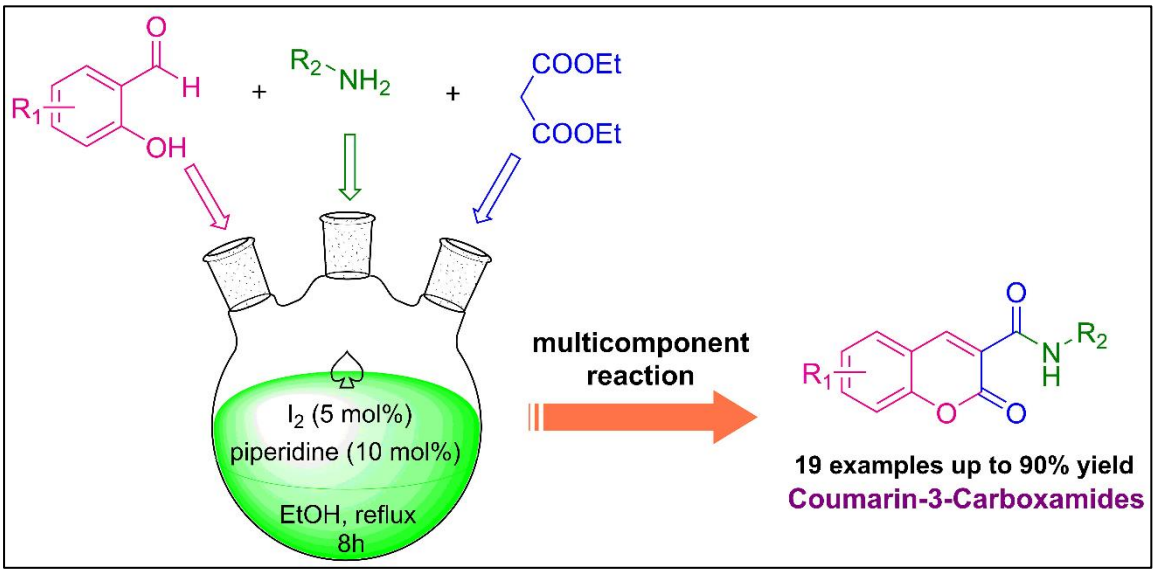

A new method has been developed by Sepay et al. for synthesizing coumarin-3-carbamides, a class of compounds that are known for their remarkable biological activities and fluorescent properties. This method involves a three-component reaction of 2-hydroxybenzaldehydes, aliphatic primary/secondary amines, and diethyl malonate. The reaction is catalyzed by Ni-NiO nanoparticles and takes place in the green solvent ethanol, making it an efficient and eco-friendly process (**Figure 15**). This method is able to accommodate various functional groups and moieties (Sepay et al., 2015).

Figure 15

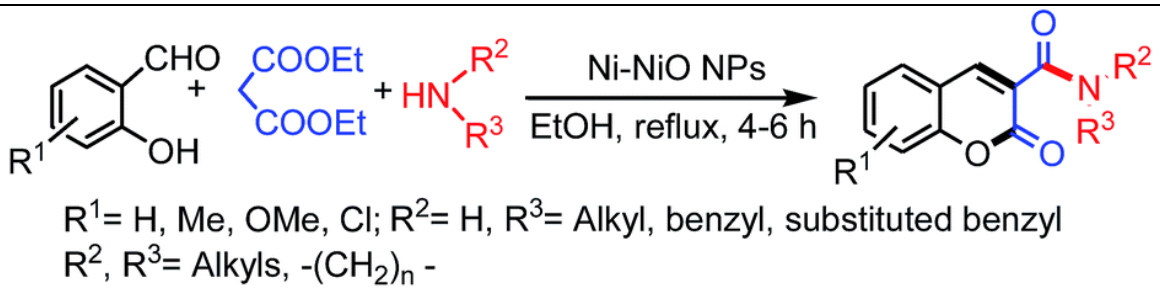

In a study conducted by Onder et al., a novel series of coumarin-3-carboxamide derivatives (**A1**, **A2**, and **B1**–**B4**) were designed and synthesized to evaluate their efficacy in inhibiting the activity of eukaryotic elongation factor-2 kinase (eEF-2K) in breast cancer cells. The study utilized homology modeling of eEF-2K and in silico analysis to determine the interaction

energies between the compounds and eEF-2K. The results revealed that compounds **A1** and **A2** displayed superior interaction energies with eEF-2K when compared to compounds **B1–B4** (**Figure 16**). The in vitro tests confirmed that **A1** and **A2** were highly effective in inhibiting eEF-2K at concentrations of 1.0 and 2.5 μM, respectively, relative to compounds **B1–B4**. These findings corroborated the in silico results and suggest that homology modeling may prove to be a valuable tool for designing eEF-2K inhibitors. A1 and A2 may have potential therapeutic applications as novel eEF-2K inhibitors (Onder et al., 2020).

Figure 16

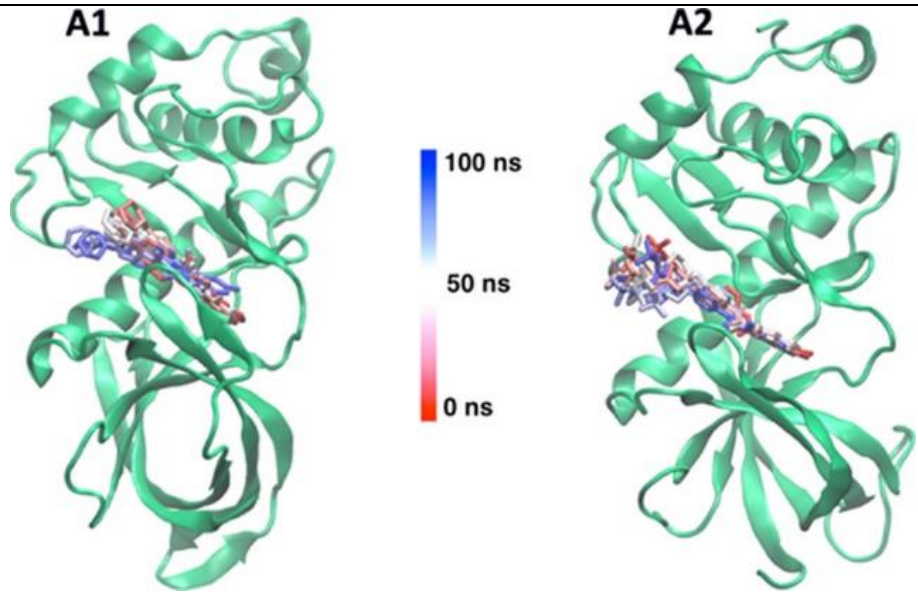

Phutdhawong et al. (2021) conducted an investigation on a series of coumarin-3-carboxamides to assess their effectiveness against bacterial and cancerous cells. The study revealed that the inclusion of carboxylic acid at the C3 position of coumarins was crucial for antibacterial activity, as evidenced by the moderate activity shown by compounds 10 and 13 against gram-positive bacteria (**Figure 17** and **Figure 18**). Furthermore, most of the tested compounds showed potent anticancer activity, with the 4-fluorophenyl coumarin-3′-carboxazine 4b being the most active. This compound exhibited similar activity to that of the widely-used anticancer drug doxorubicin, and it also displayed low levels of cytotoxicity against normal cells. The molecular docking study revealed that the compounds bind to the active site of the CK2 enzyme, therefore highlighting the importance of the phenyl carboxamide functionality for anticancer activity (Phutdhawong et al., 2021).

Figure 17

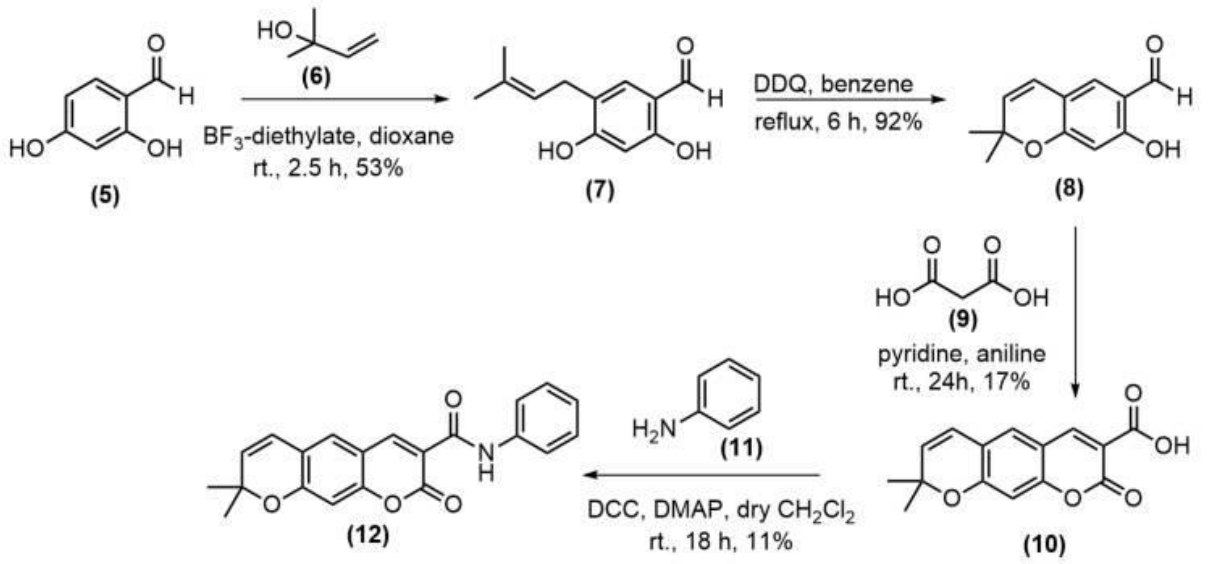

Figure 18

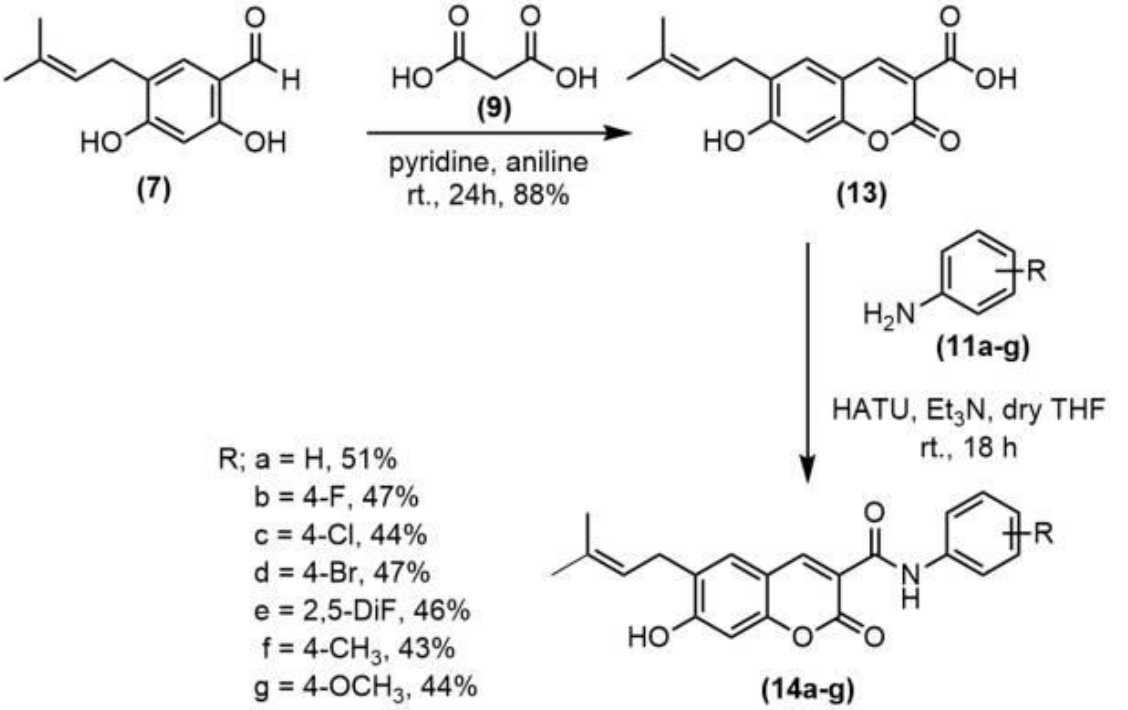

5.2. Introduction

Coumarin, a secondary metabolite of plants, is a member of the benzopyrone class of organic compounds. Coumarin is often extracted from a variety of sources, including plants like the Tonka bean and celery. It is extensively studied and developed to create new medications with improved efficacy and safety profiles. This family of organic compounds that are often used as dyes and flavouring agents in food products. They can also be used to develop sensors that can monitor chemical and biological processes, such as detecting pollutants in water or monitoring the health of a patient. They are also used in the pharmaceutical industry as active ingredients in drugs used to treat various medical conditions. It is known for its anticoagulant, anti-inflammatory, and antioxidant properties, making it a valuable ingredient in drugs used to treat conditions such as heart disease, diabetes, and liver disease. They can also be used to develop new materials, such as organic solar cells.

Protein interactions of coumarin are important because they are key to understanding its biological effects and potential applications in healthcare. By studying these interactions, insights can be gained into the mechanisms by which coumarin interacts with proteins, leading to its effects on various biological processes such as cell division, inflammation, and clotting. This knowledge can contribute to the development of targeted therapies and treatments for various diseases, as well as the identification of potential side effects and risks. This can contribute to the development of new drugs or therapeutic interventions based on the targeting of protein interactions mediated by coumarin.

Beta-lactoglobulin is the most abundant whey protein found in cow's milk and other dairy products and is the primary allergen in cow's milk that may also interact with various molecules such as lipids, vitamins, minerals, drugs, toxins, and allergens. These interactions are important for the nutrition of humans and animals. Small-molecule interactions with beta-lactoglobulin are also important to understand the stability and functionality of the protein. The binding of small-molecule ligands to beta-lactoglobulin can influence its structure, solubility, and ability to bind with other types of molecules. It can also affect the taste, texture, and other properties of the food product. Furthermore, it can be used as a carrier for the delivery of bioactive compounds. It can also help to improve the nutritional value of the protein. Finally, it can help to reduce the cost associated with the production of the protein.

Studies show that beta-lactoglobulin and small-molecule interactions include the binding of flavours, (Reiners et al., 2000; Kühn et al., 2006), doxorubicin, (Agudelo et al., 2012),

antidepressant fluoxetine, antibiotic ciprofloxacin and Kanamycin, (Mehraban et al., 2017), retinol, (Pérez and Calvo, 1995) and fatty acids (Pérez and Calvo, 1995) which have higher binding affinities compared to lactose, (Booth et al., 2016; Villaume et al., 2004) dextran, (Xiang et al., 2021) antibiotic neomycin. (Barcik et al., 2015) The binding affinity of a molecule to beta-lactoglobulin can determine its efficacy as a drug candidate and its potential for therapeutic use.

5.2.1. Choice of the compounds

A crystallography-based study to design coumarin molecules for better protein interactions shows that the coumarin-3-carbamide molecule containing chlorine group at the coumarin nucleus has the best protein interaction with beta-lactoglobulin. (Sepay et al., 2022). The electron-donating group at the coumarin nucleus also has a good binding ability to the same protein. In their study, they designed coumarin-3-carbamide with an alkyl chain attached to the amide nitrogen. (Sepay et al., 2022) This study encourages us to design our molecule. In our design, we have determined to get both electron-donating and chloride groups at coumarin-3-carbamide molecules. For this purpose, we have chosen an aromatic moiety with a chloride group at the amide nitrogen and an electron-donating (-OMe) group at the coumarin moiety.

The green method by Sepay et al. for the coumarin-3-carbamide molecules was used to synthesize the designed molecules (Sepay et al., 2015). The reaction of 2-hydroxybenzaldehydes (**1**), diethyl malonate (**2**), and (2-chlorophenyl)methanamine (**3**) gave the coumarin-3-carbamide (**C3A**) under refluxing ethanol for 4h in the presence of Ni-NiO nanoparticles (Scheme 12). In this way, two coumarin-3-carbamide (**C3A**) molecules have been synthesized. In both the molecules, the chloride group is present as it has the ability to interact with the amino acid in the protein. However, the absence and the presence of the OMe group at the 1 have produced **C3A1** and **C3A2**, respectively. The compounds have been characterized using NMR spectroscopy and verified with the reported data.

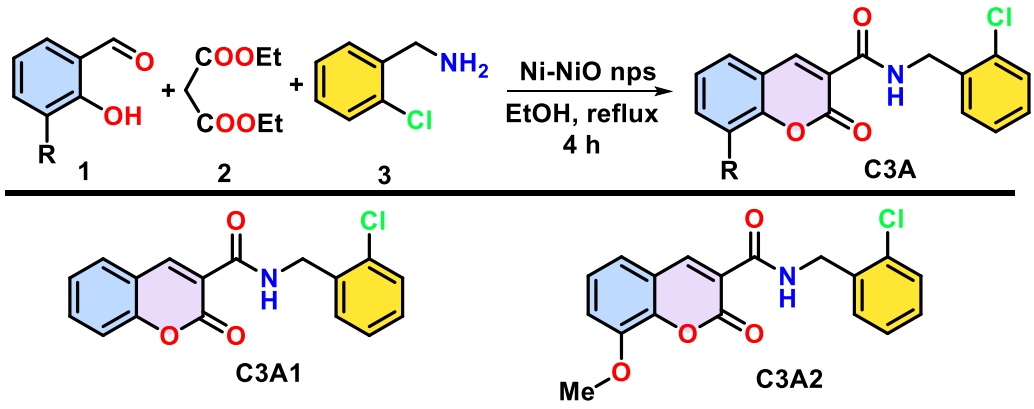

Scheme 12: Synthesis of coumarin-3-carbamide from 2-hydroxybenzaldehydes (**1**), diethyl malonate (**2**), and (2-chlorophenyl)methanamine (**3**).

5.3. Materials

2-hydroxy[1]benzaldehyde, Diethylmalonate, and Benzaldehyde were purchased from Sigma-Aldrich, USA. Na2SO4 and Dichloromethane were obtained from Merck, Germany. Fluorescent probes, namely 8- anilinonaphthalene-1-sulfonic acid ammonium salts (ANS), was purchased from Sigma Chemical (St. Louis, USA). All chemicals used were of the highest available purity.

5.4. Methodology

5.4.1. Preparation and purification of β-lactoglobulin

Bovine beta-lactoglobulin (β-lg), a major protein component of cow milk, was extracted and purified following the methods described by Aschaffenburg and Drewry. The final product was subjected to freeze-drying and stored at 4°C to maintain its structural integrity. For spectroscopic analysis, β-lg was weighed and dissolved in a solution of 0.01 M Na-phosphate buffer at pH 7.4, containing 2% ethanol. Stock solutions of the protein were prepared using phosphate buffer at pH 7.4. The extinction coefficient of β-lg at 280 nm, determined to be 0.96 mg^{-1} mL^{-1} cm^{-1}, was utilized to obtain different concentrations of protein samples by dissolving β-lg in Milli-Q water and measuring the optical density at 280 nm. These standardized procedures were employed to ensure accuracy and consistency in the characterization of β-lg samples.

5.4.2. Synthesis of coumarin-3-carbamide compounds

In a round-bottomed flask of 10 mL capacity, equipped with a condenser and a stirring bar, 3 mL of ethanol was introduced. To this, 1.0 mmol of 2-hydroxy[1]benzaldehyde (1), 1.0 mmol of diethylmalonate, 1.2 mmol of amine, and 6.5 mg mmol-1 of Ni-NiO nanoparticles were added. The color of the reaction mixture was observed to change to yellow or red, depending on the nature of the amine employed. The mixture was subjected to reflux for a duration of 4 hours with stirring, followed by cooling to room temperature. The catalyst was separated from the reaction mixture using a magnet, and 10 mL of water was added to the remaining mixture. The resulting mixture was subjected to extraction using CH_2Cl_2 (3 x 5 mL), and the combined organic layer was dried over anhydrous Na_2SO_4 and subsequently evaporated under vacuum. The amide thus obtained was purified through a process of crystallization or column chromatography followed by crystallization.

5.4.3. UV-visible spectroscopy

We employed a JASCO Spectrophotometer model no. V700 (Serial No. B184461798) at standard temperature (25°C) to precisely measure the absorbance and determine the binding affinity and binding constants. The UV titrations were carried out by progressively increasing the concentrations of **C3A1** (1-16 μM) and **C3A2** (1-16 μM) for β-lg in a 1 cm quartz cuvette that contained a constant concentration of β-lg (20 μM) in Milli-Q water. The spectra were recorded within the range of 200-600 nm.

5.4.4. Intrinsic fluorescence study of beta-lactoglobulin in the presence of coumarin molecules

A study was conducted using fluorescence quenching experiments with a HORIBA machine (Model: FLUOROMAX-4C, serial no. 1734D-4018-FM) at room temperature. The protein solutions were excited at 295 nm, and the emission was observed in the wavelength range of 310-600 nm. The excitation and emission slits were kept at 5 nm. The concentration of β-lg was maintained at 20 μM, while **C3A1** and **C3A2** were added successively with concentrations ranging from 2 to 20 μM. The aim was to understand the spectroscopic behavior of both compounds, and concentration-dependent fluorescence spectroscopy was recorded in water at the said excitation wavelength.

5.4.5. ANS assay for monitoring the hydrophobicity changes

The hydrophobicity of protein molecules is a significant characteristic that plays a critical role in protein structure and function. The determination of protein hydrophobicity can be achieved by using a fluorescence-based technique that involves the utilization of a fluorescent probe. Specifically, the 1-anilinonapthalene-8-sulfonate (ANS) probe is widely employed as a polarity-sensitive fluorescent molecule that binds to hydrophobic pockets on the protein surface. In this study, a stock solution of ANS was prepared and mixed with the protein samples to determine the hydrophobicity of monomeric insulin samples. A constant ANS concentration of 30 mM was maintained in each sample aliquot. The protein samples were then treated with **C3A1** and **C3A2** molecules at varying doses ranging from 2 to 16 µM. The Shimadzu Spectrofluorometer (Shimadzu 5301 PC) was employed to acquire the emission spectra from 390 to 600 nm upon excitation at 350 nm. The length of the path was set at 1 cm while both the excitation and emission slits were adjusted to 5 nm. This study provides insights

into the hydrophobicity of protein molecules and establishes the ANS probe as a reliable tool for the characterization of protein hydrophobicity.

5.4.6. Circular dichroism (CD) spectroscopy

Our study analyzed the response of β-lg protein to the presence of **C3A1** and **C3A2** coumarin molecules using a Jasco spectropolarimeter (Model: J-815). The measurements were carried out under a nitrogen atmosphere, using a quartz cell of path length 0.2 cm in the far-UV region (200–260 nm). We kept the concentration of β-lg constant at 10 µM while we varied the concentrations of **C3A1** and **C3A2** derivatives from 1 to 8 µM. Our data collection involved scanning each nm from 260 to 200 nm at a scan speed of 50 nm per minute. To maintain a constant temperature of 25°C, we used a Neslab RTE-111 circulating water bath connected to water-jacketed quartz cuvettes. To calculate the secondary structures of insulin, we utilized CDNN 2.1 software attached to the instrument.

5.5. Results and discussion

5.5.1. NMR spectroscopic data of the synthesized compounds (C3A1 and C3A2)

N-(2-Chlorobenzyl)-2-oxo-2H-chromene-3-carboxamide (C3A1).

Yield –79%, colorless crystalline solid, M.P. 196–198 C; IR (KBr pellet): 3055, 1712, 1664, 1525, 1454, 1255, 1035, 917, 802, 761, 632 cm^{-1}; ^{1}H NMR (300 MHz, $CDCl_3$): d 4.75 (d, J ¼

5.8 Hz, 2H, –NH–CH_2–), 7.22–7.26 (m, 2H, ArH), 7.36–7.46 (m, 4H, ArH), 7.65–7.70 (2H, m, ArH), 8.93 (s, 1H, H-4), 9.29 (br s, 1H, NH); ^{13}C NMR (100 MHz, $CDCl_3$): d 41.8, 116.7, 118.4, 118.6, 125.3, 127.0, 128.9, 129.6, 129.8, 133.7, 134.1, 135.3, 148.6, 154.5, 161.4, 161.7; HRMS: m/z calculated for $C_{17}H_{12}ClNO_3$ $[M + H]^+$: 314.0584, found 314.0536.

N-(2-Chlorobenzyl)-8-methoxy-2-oxo-2H-chromene-3-carboxamide (C3A2). Yield – 72%, colorless crystalline solid, M.P. 218– 220 °C; ^{1}H NMR (500 MHz, $CDCl_3$):: δ 4.00 (s, 3H, OCH_3), 4.77 (d, J ¼ 6.0 Hz, 2H, –NH–CH_2–), 7.20–7.39 (m, 5H, ArH), 7.40 (d, J ¼ 6.5 Hz, 1H, ArH), 7.45 (d, J ¼ 6.5 Hz, 1H, ArH), 8.91(s, 1H, H-4), 9.31 (s, 1H, NH); ^{13}C NMR (125 MHz, $CDCl_3$): d 41.9, 56.5, 115.8, 118.7, 119.4, 121.1, 125.3, 127.1, 129.0, 129.7, 129.9, 133.8, 135.5, 144.3, 147.2, 148.9, 161.0, 161.8; HRMS: m/z calculated for $C_{18}H_{14}ClNO_4$ $[M + H]^+$: 344.0690, found 344.0656.

5.5.2. Absorption spectroscopic studies

UV−visible absorption spectroscopy is a widely used tool for investigating ligand−protein interactions, and it has been used for a long time to monitor the binding of small molecules to proteins. The UV−visible absorption spectra of **C3A1** and **C3A2** without (Figure 19) and with β-lg are presented in Figure 20. The absorption peak of **C3A1** was observed at 289, 353, and 422 nm, whereas **C3A2** shows peaks at 254 and 321 nm. The β-lg absorbs light at 279 nm, which rises with the addition of **C3A1** and **C3A2**. Along with this, a shoulder peak at 331 and 317 nm for **C3A1** and **C3A2**, respectively, provides a clear indication of the ground-state complexation between the compounds and β-lg.

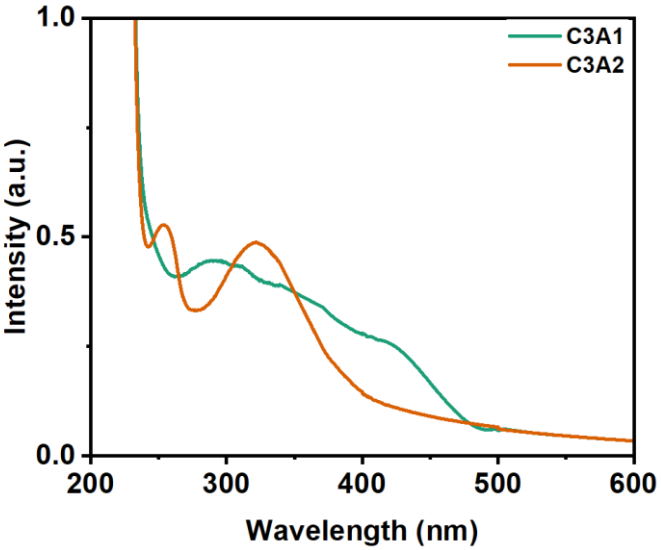

Figure 19: The UV−visible absorption spectra of **C3A1** and **C3A2** without β-lactoglobulin.

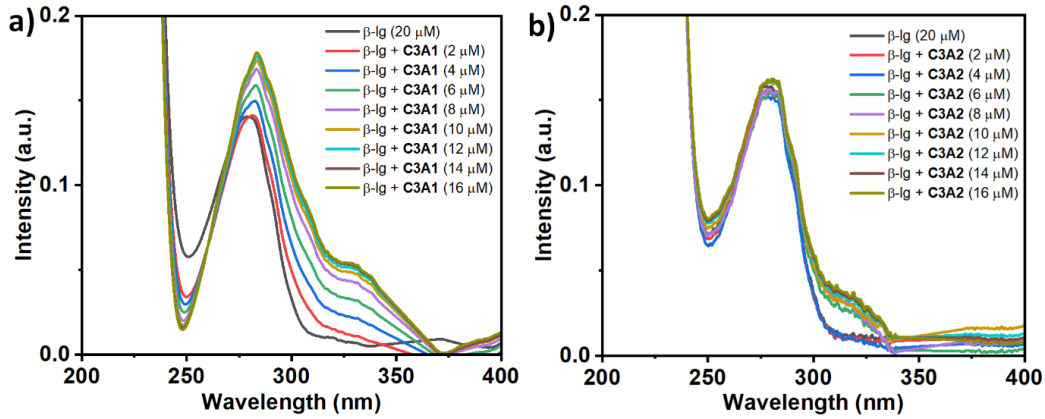

Figure 20: UV-vis spectra of beta-lactoglobulin in the absence and presence of (a) **C3A1** and (b) **C3A2**.

5.5.3. Fluorescence quenching studies

There are many ways to investigate changes in the conformation of proteins when bound with ligands, but one of the most sensitive tools is fluorescence spectroscopy. As Phe is a low quantum yield amino acid, tryptophan (Trp 19 and Trp 61) and tyrosine (Tyr) amino acids are more commonly responsible for the emission intensity of β-lg. We excited the protein sample at 295 nm to monitor Trp fluorescence. The emission intensity of β-lg centered at 340 nm progressively decreases (shown in Figure 21) with the successive addition of **C3A1** and **C3A2**. For **C3A2**, a 3 nm red shift of the band was observed (Figure 21b). It is also interesting to note that, for **C3A1** and **C3A2**, another peak was developed at 412 and 452 nm, respectively. For both cases, an iso-emissive point was identified. Therefore, this indicates that **C3A1** and **C3A2** interact with the β-lg. A similar type of observation was reported by Sepay and co-workers during the binding interactions of said coumarin-3-carbamide and β-lg.

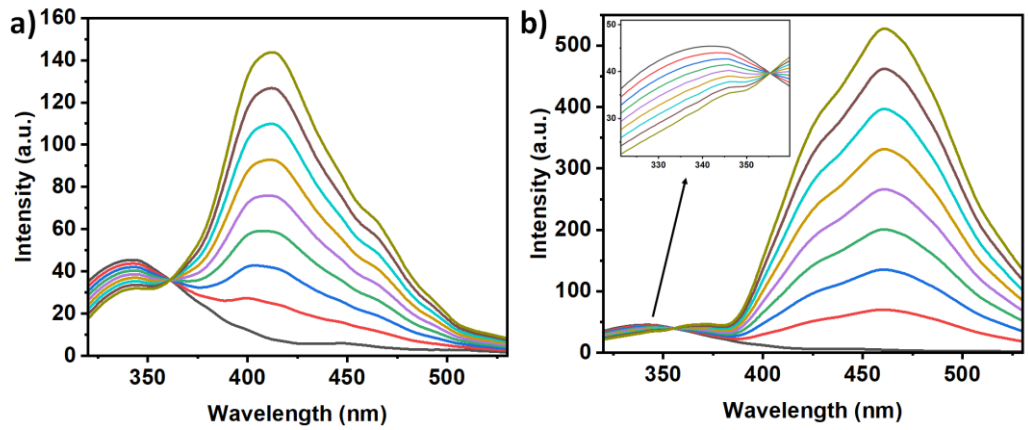

Figure 21: The emission spectral change of β-lg (20 μM) in the presence and absence of (a) **C3A1** and (b) **C3A2**.

The basic mechanism used for quenching fluorophores and how it occurs can proceed through three ways. It is usually attributed to the ground-state complexation of the fluorophore (static quenching), collisional quenching (dynamic quenching), and the inner filter effect. The decrease of β-lg emission was also observed even after considering the inner filter effects corrections. It is, therefore, possible to induce quenching of β-lg emission via collision (static) or ground-state complexation (dynamic). Based on data obtained from steady-state emission measurements, the Stern-Volmer equation has been applied to analyze the data obtained from those measurements.

$$I^o/I = 1 + K_{sv}\,[Comp] \qquad (1)$$

Here, I0 and I stand for the emission intensities of β-lg in the absence and presence of compounds, respectively. K_{SV} is used to demonstrate the Stern-Volmer constant. The binding of **C3A1** or **C3A2** with β-lg (Figures 22a and 22c) has only involved one type of quenching process (static or dynamic), which describes a linear Stern−Volmer plot (Figure 22). At 298 K, the K_{SV} value is found to be $2.27 \times 10^4\ M^{-1}$ and $2.57 \times 10^4\ M^{-1}$ for **C3A1** or **C3A2**, respectively (Table 1). Therefore, the compound **C3A2** has a higher efficiency to quench the emission than that of **C3A1**. The same experiments for both compounds were performed at three different temperatures. It is interesting to note that the K_{SV} values increase with both compounds as temperature increases. Therefore, the quenching of emission intensity of the protein due to the protein binding of compounds increases with rising temperature.

The constant known as the Stern-Volmer constant (K_{SV}) can also be calculated by multiplying the quencher rate coefficient (k_q) with the average fluorescence lifetime ($\langle\tau\rangle^0$) of β-lg, without the presence of the quencher (1.57 ns). At a temperature of 298 K, the kq value has been determined to be $1.44 \times 10^{13}\ M^{-1}\ s^{-1}$ for **C3A1**. This value is significant as it exceeds the maximum diffusion collision quenching rate constant of $2.0 \times 10^{10}\ M^{-1}\ s^{-1}$. It is suggested that the higher k_q value for the maximum diffusion collision rate could be the result of specific interactions between the protein and **C3A**. in their ground states, which may cause a conformational change in the protein. Hence, a conformational change in the protein is not initiated through dynamic collision, which is also evident from UV−visible absorption spectroscopy.

Table 1: The Stern–Volmer (Ksv) and binding (K_b) constant of **C3A1** and **C3A2** at different temperatures.

Compounds	Temperature (K)	K_{SV} M^{-1}	k_q $M^{-1}s^{-1}$	K_b	n
C3A1	298	2.27×10^4	1.44×10^{13}	0.883×10^4	1.32
	308	3.42×10^4	2.18×10^{13}	1.133×10^4	1.37
	318	4.45×10^4	2.83×10^{13}	1.657×10^4	1.32
C3A2	298	2.57×10^4	1.64×10^{13}	1.906×10^4	1.08
	308	3.64×10^4	2.32×10^{13}	2.328×10^4	1.14
	318	4.74×10^4	3.02×10^{13}	2.738×10^4	1.17

5.5.4. Determination of binding parameters

A quantitative evaluation of the ligand-protein interactions requires the determination of binding parameters. Hence, in order to determine the quantitative assessment binding constant (K) in the static quenching process, the binding equilibrium between **C3A** and β-lg can be written as

$$\beta - \text{lg} + n\ (\mathbf{C3A}) \leftrightharpoons (\mathbf{C3A})_n\ \beta\text{-lg} \tag{2}$$

The equilibrium binding constant (K) is defined as

$$K = \frac{[(\mathbf{C3A})_n\ \beta\text{-LG}]^n}{[\mathbf{C3A}]^n \times [\beta\text{-LG}]} \tag{3}$$

Here, the concentrations at equilibrium of the protein not bound with the **C3A** are denoted by [β-lg]. If the total quantity of β-lg (bound and not bound) is presented as $[\beta\text{-lg}]^0$, then $[\beta\text{-lg}]^0 = [(\mathbf{C3A})_n\ \beta\text{-lg}] + [\beta\text{-lg}]$. The fluorescence intensity ratio of the not bound and total β-lg can be replaced with $[\beta\text{-lg}]/[\beta\text{-lg}]^0 = I/I^0$. Therefore, the equation 3 becomes

$$\ln((I^0\text{-}I)/I) = \ln K + n \ln\{[\mathbf{C3A}]^0\} \tag{4}$$

Here, the binding sites are denoted as n. The binding parameters obtained from the quenching data are usually elucidated by equation 1. The values of K and n have been calculated from the plot of $\ln[(I^0 - I)/I]$ versus $\ln\{[\mathbf{C3A}]^0\}$, and all the results are shown in Table 1. The analysis of $\ln[(I^0 - I)/I]$ versus $\ln\{[\ \mathbf{C3A}]^0\}$ (Figure 22b and d) reveals a linear reversion with an n value close to unity. This indicates that the interaction between (**C3A**) and β-lg involves a single binding site and 1:1 binding stoichiometry. If the quenching is purely static, then one would expect the binding constant to decrease as the temperature rises, due to the weakening of the ligand−protein complex in the ground state. However, it is observed that the K_{SV} and K of both compounds increase with a rise in temperature, as demonstrated in Table 1. Although the values

of the K_{SV} and K plots are comparable, the trend of K_{SV} and K with increasing temperature is parallel.

A decrease in fluorescence quenching is likely caused by a conformational change of the fluorophore in β-lg, which is initiated by various types of interactions (i.e., hydrophobic, van der Waals, H-bonding, and Coulombic/ionic) associated with the quencher (**C3A**) molecules, leading to an increase in K_{SV} value (Table 1) with a rise in temperature. Nonetheless, the Le Chatelier principle provides a good explanation for the peculiar disordered results of K with temperature that are frequently observed in the static quenching mechanism. According to the Le Chatelier principle, if the system's temperature rises, the reaction equilibrium (represented in equation 3) for both **C3A1** and **C3A2** can be moved forward since the reaction's ΔH° value is positive, indicating the endothermic nature of the binding process. Therefore, when the temperature rises, the value of K rises as well. The stability of the **C3A**−β-lg ground-state complex at a certain temperature is indicated by the K values at that temperature (see Table 1). Therefore, the current work indicates that the stability of the **C3A**−β-lg ground-state complex with a rise in temperature is responsible for the influence of the increment of K with a rise in temperature.

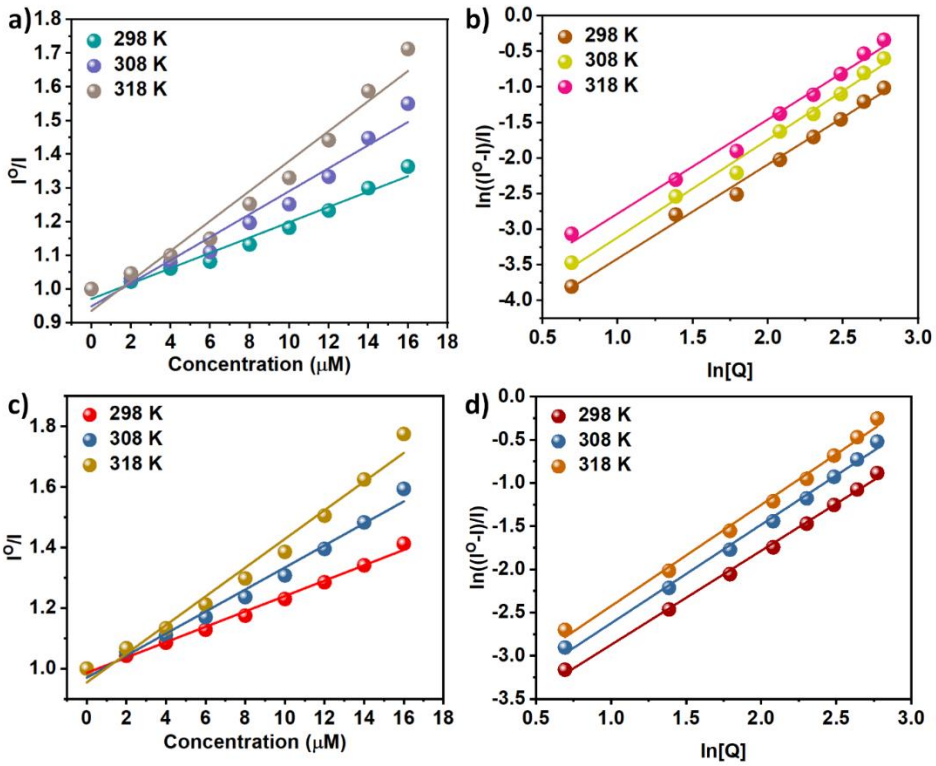

Figure 22: Stern–Volmer plots (a and c) and ln((I 0 − I)/I) versus ln[Q] plots (b and d) of beta-lactoglobulin at 298, 308, and 318 K in the presence of two coumarin molecules **C3A1** and **C3A2** in solution.

5.5.5. Thermodynamics and nature of binding forces.

The actual force involved in the interaction process can be determined by thermodynamics. In order to understand the mechanistic aspects of the ligand-protein interaction, the Van't Hoff equation is utilized to calculate both the enthalpy change (ΔH°) and entropy change (ΔS°).

$$lnK = -\frac{\Delta H^\circ}{R} \times \frac{1}{T} + \frac{\Delta S^\circ}{R} \quad (5)$$

The universal gas constant and absolute temperature are represented as R and T (in K), respectively. By assuming that both the enthalpy change (ΔH°) and the entropy change (ΔS°) remain constant within the experimental temperature range, Equation 5 is employed. The Gibbs free energy changes (ΔG°) associated with the binding interactions are estimated using the following equation:

$$\Delta G^\circ = \Delta H^\circ - T \Delta S^\circ \quad (6)$$

Ross and Subramanian have comprehensively interpreted the detailed characterizations of different types of interactions with thermodynamic parameters related to the ligand-protein association process. Hydrophobic forces are referred to as $\Delta H^\circ > 0$, $\Delta S^\circ > 0$, van der Waals and hydrogen bonding forces are referred to as $\Delta H^\circ < 0$, $\Delta S^\circ < 0$, and Coulombic/ionic interaction is referred to as $\Delta H^\circ < 0$, $\Delta S^\circ > 0$.

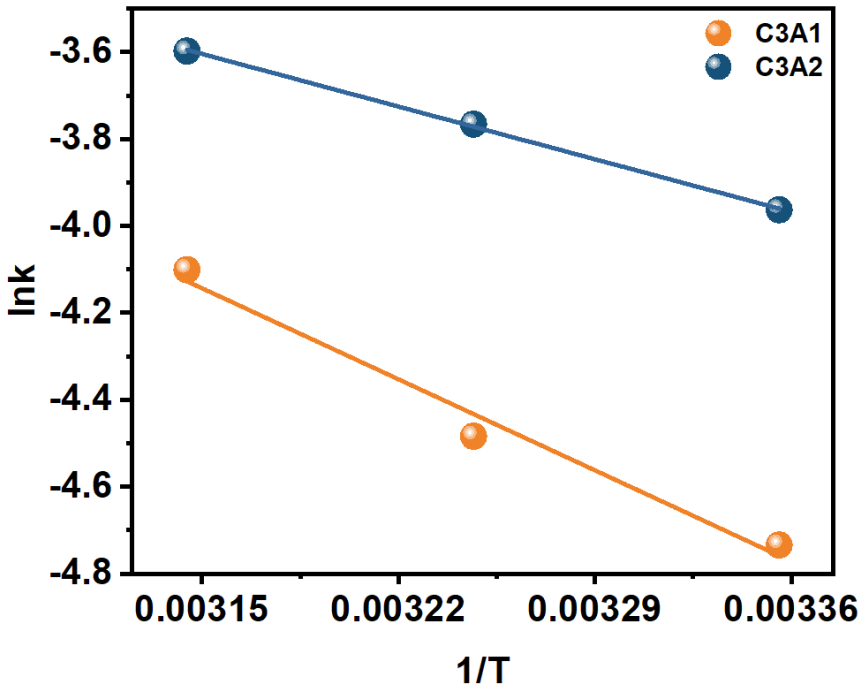

Figure 23: ln K vs. 1/T plot at 298, 308, and 318 K of two coumarin molecules **C3A1** and **C3A2.**

The thermodynamic parameters obtained from the Van't Hoff plot (ln K vs 1/T) presented in Figure 23 are demonstrated in Table 2. The negative values of ΔG° at the experimental condition indicate the spontaneity of **C3A**-β-lg binding for both **C3A1** and **C3A2**. In an aqueous medium, β-lg holds negative surface charges, and **C3A** is somewhat hydrated because of its amide and ester groups at physiological pH. During β-lg-**C3A** interactions, β-lg accommodates **C3A**, which can change the solvent environment of the ligand by releasing solvent molecules, resulting in a positive value of entropy. Electrostatic and hydrophobic interactions become a competitive factor whenever the dye binds inside β-lg. The present study implies that, for **C3A1**, both the positive enthalpy (35.97 kJ mol^{-1}) and entropy (213.14 J K^{-1} mol^{-1}) and, for **C3A2**, both the positive enthalpy (20.87 kJ mol^{-1}) and entropy (174.23 J K^{-1} mol^{-1}) indicate that interaction processes are enthalpically disfavored but entropically favoured. Table 2 shows that a large magnitude of positive ΔS° value outweighs the poor positive ΔH° value, indicating that the overall Gibbs free energy change (ΔG°) is negative. This explains the significance of entropy-driven binding with remarkable interactions of such type of amphoteric dye with the hydrophobic part of the protein.

Table 2: Thermodynamic parameters involved in the β-lg and **C3A1**/**C3A2** interactions

Compound	Temperature (K)	ΔG° (kJ mol^{-1})	ΔH° (kJ mol^{-1})	ΔS° (J $K^{-1}mol^{-1}$)
C3A1	298	-27.54		
	308	-29.68	35.97	213.14
	318	-31.80		
C3A2	298	-31.05		
	308	-32.79	20.87	174.23
	318	-34.53		

5.5.6. Surface hydrophobicity ANS binding displacement assay

The use of a hydrophobic probe like 8-anilino-1-naphthalenesulfonic acid (ANS) has become very common in the study of ligand location within proteins. ANS binds with β-lg on the hydrophobic binding surface of the protein and provides precise information regarding the location of the ligand around β-lg's hydrophobic portion.

In this regard, the binding between **C3A** and β-lg has been studied with and without ANS under similar conditions to identify the probable location of the compounds within β-lg. The results

indicate that **C3A1** significantly displaces ANS, already bound to β-lg's hydrophobic portion, and shifts it to a polar environment (Figure 24a). The location of the ligand around the hydrophobic surface of β-lg was further verified, and it was found that ANS-bound β-lg gets excited at 380 nm with the subsequent addition of **C3A1**. The decrease in emission intensity, combined with a 6 nm red shift of emission maxima, suggests that ANS has been moved from the hydrophobic part of β-lg to a polar environment (Figure 24a). The gradual addition of **C3A** causes a decrease in emission intensity and red shift of emission maximum of ANS, which may be due to the displacement of ANS from the protein surface and simultaneous alteration in the molecular microenvironment of Trp 19. This shift is caused by the displacement of ANS from the protein surface and simultaneous alteration in the molecular microenvironment of Trp 19, which affects the global conformational change of β-lg. Hence, the result indicates an increase in hydrophobicity adjacent to Trp 19.

It can be concluded that **C3A** displaces ANS, which is already bound to the hydrophobic part of β-lg. However, in the case of **C3A2**, such a change in ANS fluorescence intensity is very low (Figure 24b). The results indicate that the **C3A2** cannot bind at the protein surface, whereas the compound **C3A1** binds at the protein surface.

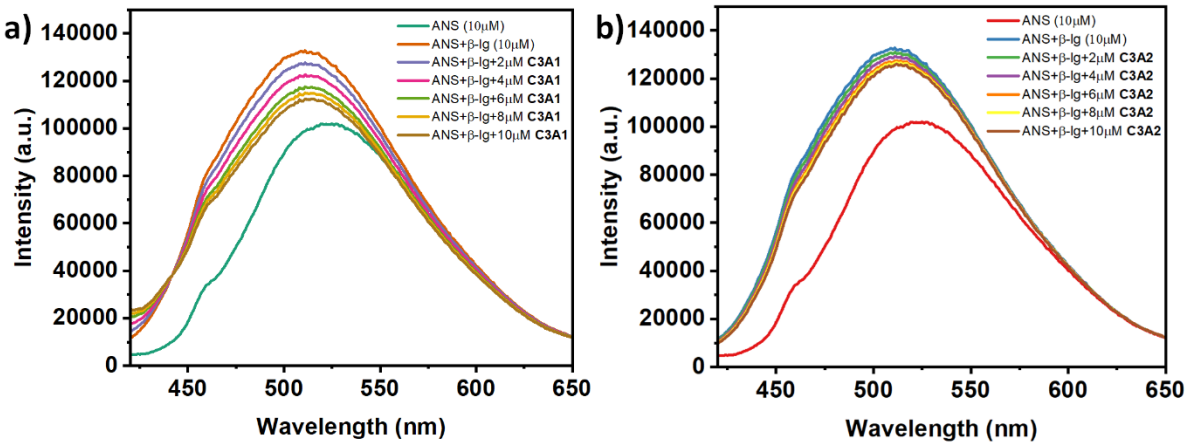

Figure 24: ANS-fluorescence emission spectra of β-lg incubated separately at 25 °C in the absence and presence of coumarin molecule **C3A1** (a) and in the absence and presence of coumarin molecule **C3A2** (b). Beta-lactoglobulin concentrations throughout all the experiments were kept at 10 µM. The results were the average of three different experiments.

5.5.7. Circular dichroism spectroscopy

CD spectroscopy is a widely used analytical tool in biochemistry, especially for the determination of proteins in the secondary structure. The β-lg protein, in its native form,

exhibits a characteristic shape of negative minimum at 216 nm, indicating a high proportion of β-sheet content. However, Figure 25a shows that the negative band ellipticity of β-lg shifted to 210 nm as the β-sheet content of the protein decreased. UV-visible and fluorescence studies have revealed that there is a ground-state complexation between **C3A1** and β-lg, which can cause a structural change in the protein structure, mainly in its tertiary structure. A very similar observation was also observed for **C3A2** (Figure 25b). This **C3A**-β-lg complexation displaces the solvent molecules around **C3A** and the binding site of β-lg, promoting complexation entropically. As a result, the ground-state complexation may cause structural deformation, such as additional water removal, by bending and twisting the β-sheet of the protein. This is also reflected in the change in the population of β-sheet content, which is calculated using CDNN software (Table 3). Therefore, it can be concluded that the peptide strand of the native β-lg undergoes an unfolding upon binding with **C3A**.

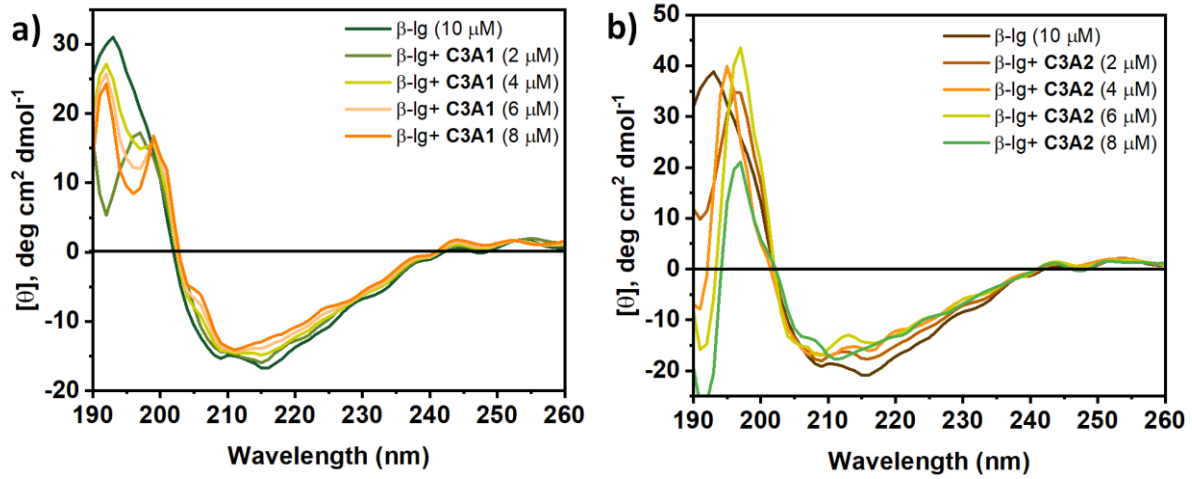

Figure 25: Far-UV CD spectra (190–260 nm) of β-lactoglobulin in the absence and presence of two small molecules (coumarin-3-carbamide compounds) **C3A1** and **C3A2** at 25 °C, showing the secondary structural changes of insulin.

Table 3: Structural integrity of beta-lactoglobulin in the absence and presence of **C3A1** and **C3A2** as determined by calculations. (calculated by CDNN 2.1 Software)

Samples	% of α-Helix	% of β-Sheet	% of β-Turn	% of Random coil
Native β-lactoglobulin	29.65	20.06	17.12	33.17
Native β-lactoglobulin+**C3A1** 2μM	20.37	29.20	16.70	33.74

Samples	% of α-Helix	% of β-Sheet	% of β-Turn	% of Random coil
Native β-lactoglobulin+**C3A1** 4μM	22.25	26.67	16.85	34.32
Native β-lactoglobulin+**C3A1** 6μM	20.94	28.09	16.70	34.36
Native β-lactoglobulin+**C3A2** 8μM	19.64	29.41	16.52	34.43
Native β-lactoglobulin+**C3A2** 2μM	25.56	23.41	17.13	33.80
Native β-lactoglobulin+**C3A2** 4μM	23.36	26.92	17.34	32.39
Native β-lactoglobulin+**C3A2** 6μM	21.99	27.07	17.01	33.84
Native β-lactoglobulin+**C3A1** 8μM	17.36	34.57	16.54	31.52

5.6. Summary of the work

In summary, in this work, we have designed two coumarin-3-carbamide derivatives containing both chloride and electron-donating groups (in one molecule **C3A2**) as Sepay et al. shown that the chloride groups at coumarin moiety show high binding affinity to the β-lg. In this case, in two molecules, one has the OMe and Cl groups (**C3A2**), and the other has only the Cl group. For both the molecules, the Cl groups are attached to the aromatic ring at amide nitrogen. We have synthesized these molecules and investigated the protein interactions with the β-lg. We have found that **C3A2** has greater binding ability than **C3A1**. Both compounds bind with the β-lg through an entropy-driven endo-thermic process. During this binding, the **C3A1** prefers the hydrophobic surface of the protein, whereas **C3A2** interacts at the calyx of the protein. Such binding of the compounds changes the protein conformations. Therefore, the presence of Cl and OMe groups at coumarin-3-carbamide introduces a polar nature in the molecule, which enhances the β-lg binding process.

5.7. References

Agudelo, D., Beauregard, M., Bérubé, G. and Tajmir-Riahi, H.A., 2012. Antibiotic doxorubicin and its derivative bind milk β-lactoglobulin. Journal of Photochemistry and Photobiology B: Biology, 117, pp.185-192.

Andrés-Lacueva, C., Medina-Remon, A., Llorach, R., Urpi-Sarda, M., Khan, N., Chiva-Blanch, G., Zamora-Ros, R., Rotches-Ribalta, M. and Lamuela-Raventós, R.M., 2009. Phenolic compounds: chemistry and occurrence in fruits and vegetables. Fruit and vegetable phytochemicals: chemistry, nutritional value, and stability, pp.53-88.

Annunziata, F., Pinna, C., Dallavalle, S., Tamborini, L. and Pinto, A., 2020. An overview of coumarin as a versatile and readily accessible scaffold with broad-ranging biological activities. International Journal of Molecular Sciences, 21(13), p.4618.

Areias, F., Costa, M., Castro, M., Brea, J., Gregori-Puigjané, E., Proença, M.F., Mestres, J. and Loza, M.I., 2012. New chromene scaffolds for adenosine A2A receptors: Synthesis, pharmacology and structure–activity relationships. European journal of medicinal chemistry, 54, pp.303-310.

Asadipour, A., Alipour, M., Jafari, M., Khoobi, M., Emami, S., Nadri, H., Sakhteman, A., Moradi, A., Sheibani, V., Moghadam, F.H. and Shafiee, A., 2013. Novel coumarin-3-carboxamides bearing N-benzylpiperidine moiety as potent acetylcholinesterase inhibitors. European journal of medicinal chemistry, 70, pp.623-630.

Balalaie, S., Bigdeli, M.A., Sheikhhosseini, E., Habibi, A., Moghadam, H.P. and Naderi, M., 2012. Efficient Synthesis of Novel Coumarin-3-carboxamides (= 2-Oxo-2H-1-benzopyran-3-carboxamides) Containing Lipophilic Spacers. Helvetica Chimica Acta, 95(3), pp.528-535.

Barcik, W., Untersmayr, E., Pali-Schöll, I., O'Mahony, L. and Frei, R., 2015. Influence of microbiome and diet on immune responses in food allergy models. Drug Discovery Today: Disease Models, 17, pp.71-80.

Bekhradnia, A., Domehri, E. and Khosravi, M., 2016. Novel coumarin-based fluorescent probe for selective detection of Cu (II). Spectrochimica Acta Part A: Molecular and Biomolecular Spectroscopy, 152, pp.18-22.

Booth, M.A., Karaosmanoglu, H., Wu, Y. and Partridge, A., 2016. Biosensor platforms for detecting target species in milk samples.

Bruneton, J., 1999. Pharmacognosy, phytochemistry, medicinal plants (No. Ed. 2). Intercept Limited.

Chen, G.F., Jia, H.M., Zhang, L.Y., Hu, J., Chen, B.H., Song, Y.L., Li, J.T. and Bai, G.Y., 2013. A highly selective fluorescent sensor for Fe 3+ ion based on coumarin derivatives. Research on Chemical Intermediates, 39, pp.4081-4090.

Chen, H. and Walsh, C.T., 2001. Coumarin formation in novobiocin biosynthesis: β-hydroxylation of the aminoacyl enzyme tyrosyl-S-NovH by a cytochrome P450 NovI. Chemistry & biology, 8(4), pp.301-312.

Chen, Y., Tsao, K., De Francesco, E. and Keillor, J.W., 2015. Ring substituent effects on the thiol addition and hydrolysis reactions of N-arylmaleimides. The Journal of Organic Chemistry, 80(24), pp.12182-12192.

Comert Onder, F., Durdagi, S., Sahin, K., Ozpolat, B. and Ay, M., 2020. Design, synthesis, and molecular modeling studies of novel coumarin carboxamide derivatives as eEF-2K inhibitors. Journal of Chemical Information and Modeling, 60(3), pp.1766-1778.

Fu, X.B., Wang, X.F., Chen, J.N., Wu, D.W., Li, T., Shen, X.C. and Qin, J.K., 2015. Synthesis, Fluorescence Properties, and Antiproliferative Potential of Several 3-Oxo-3 H-benzo [f] chromene-2-carboxylic Acid Derivatives. Molecules, 20(10), pp.18565-18584.

Ghanei-Nasab, S., Khoobi, M., Hadizadeh, F., Marjani, A., Moradi, A., Nadri, H., Emami, S., Foroumadi, A. and Shafiee, A., 2016. Synthesis and anticholinesterase activity of coumarin-3-carboxamides bearing tryptamine moiety. European journal of medicinal chemistry, 121, pp.40-46.

Gnaccarini, C., Ben-Tahar, W., Mulani, A., Roy, I., Lubell, W.D., Pelletier, J.N. and Keillor, J.W., 2012. Site-specific protein propargylation using tissue transglutaminase. Organic & Biomolecular Chemistry, 10(27), pp.5258-5265.

Harris, M., De Keersmaecker, H., Vander Elst, L., Debroye, E., Fujita, Y., Mizuno, H. and Parac-Vogt, T.N., 2016. Following the stability of amphiphilic nanoaggregates by using intermolecular energy transfer. Chemical communications, 52(91), pp.13385-13388.

He, X., Chen, Y.Y., Shi, J.B., Tang, W.J., Pan, Z.X., Dong, Z.Q., Song, B.A., Li, J. and Liu, X.H., 2014. New coumarin derivatives: Design, synthesis and use as inhibitors of hMAO. Bioorganic & Medicinal Chemistry, 22(14), pp.3732-3738.

Jin, X., Uttamapinant, C. and Ting, A.Y., 2011. Synthesis of 7-aminocoumarin by Buchwald–Hartwig cross coupling for specific protein labeling in living cells. Chembiochem: a European journal of chemical biology, 12(1), p.65.

Kühn, J., Considine, T. and Singh, H., 2006. Interactions of milk proteins and volatile flavor compounds: implications in the development of protein foods. Journal of Food Science, 71(5), pp.R72-R82.

Kuru, E., Hughes, H.V., Brown, P.J., Hall, E., Tekkam, S., Cava, F., de Pedro, M.A., Brun, Y.V. and VanNieuwenhze, M.S., 2012. In situ probing of newly synthesized peptidoglycan in live bacteria with fluorescent D-amino acids. Angewandte Chemie, 124(50), pp.12687-12691.

Lacy, A. and O'kennedy, R., 2004. Studies on coumarins and coumarin-related compounds to determine their therapeutic role in the treatment of cancer. Current pharmaceutical design, 10(30), pp.3797-3811.

Liu, S., Zhao, J., Zhang, K., Yang, L., Sun, M., Yu, H., Yan, Y., Zhang, Y., Wu, L. and Wang, S., 2016. Dual-emissive fluorescence measurements of hydroxyl radicals using a coumarin-activated silica nanohybrid probe. Analyst, 141(7), pp.2296-2302.

Lončar, M., Jakovljević, M., Šubarić, D., Pavlić, M., Buzjak Služek, V., Cindrić, I. and Molnar, M., 2020. Coumarins in food and methods of their determination. Foods, 9(5), p.645.

Mehraban, M.H., Odooli, S., Yousefi, R., Roghanian, R., Motovali-Bashi, M., Moosavi-Movahedi, A.A. and Ghasemi, Y., 2017. The interaction of beta-lactoglobulin with ciprofloxacin and kanamycin; a spectroscopic and molecular modeling approach. Journal of Biomolecular Structure and Dynamics, 35(9), pp.1968-1978.

Pérez, M.D. and Calvo, M., 1995. Interaction of β-lactoglobulin with retinol and fatty acids and its role as a possible biological function for this protein: a review. Journal of dairy science, 78(5), pp.978-988.

Phutdhawong, W., Chuenchid, A., Taechowisan, T., Sirirak, J. and Phutdhawong, W.S., 2021. Synthesis and biological activity evaluation of coumarin-3-carboxamide derivatives. Molecules, 26(6), p.1653.

Pratap, R. and Ram, V.J., 2014. Natural and synthetic chromenes, fused chromenes, and versatility of dihydrobenzo [h] chromenes in organic synthesis. Chemical reviews, 114(20), pp.10476-10526.

Reiners, J., Nicklaus, S. and Guichard, E., 2000. Interactions between beta-lactoglobulin and flavour compounds of different chemical classes. Impact of the protein on the odour perception of vanillin and eugenol. Le Lait, 80(3), pp.347-360.

Sashidhara, K.V., Kumar, A., Kumar, M., Singh, S., Jain, M. and Dikshit, M., 2011. Synthesis of novel 3-carboxamide-benzocoumarin derivatives as orally active antithrombotic agents. Bioorganic & medicinal chemistry letters, 21(23), pp.7034-7040.

Sepay, N., Banerjee, M., Islam, R., Dey, S.P. and Halder, U.C., 2022. Crystallography-based exploration of non-covalent interactions for the design and synthesis of coumarin for stronger protein binding. Physical Chemistry Chemical Physics, 24(11), pp.6605-6615.

Sepay, N., Guha, C., Kool, A. and Mallik, A.K., 2015. An efficient three-component synthesis of coumarin-3-carbamides by use of Ni–NiO nanoparticles as magnetically separable catalyst. RSC advances, 5(87), pp.70718-70725.

Shaabani, S., Shaabani, A. and Ng, S.W., 2014. One-pot synthesis of coumarin-3-carboxamides containing a triazole ring via an isocyanide-based six-component reaction. ACS Combinatorial Science, 16(4), pp.176-183.

Sun, Y., Wang, Y., Cao, D., Chen, H., Liu, Z. and Fang, Q., 2012. 3-Amidocoumarins as chemodosimeters to trap cyanide through both Michael and intramolecular cyclization reaction. Sensors and Actuators B: Chemical, 174, pp.500-505.

Tandon, S. and Rastogi, R.P., 1979. Recent advances in naturally occurring coumarins. Journal of scientific and Industrial Research, 38, pp.428-441.

Tiwari, A.D., Panda, S.S., Asiri, A.M., Hall, C.D. and Katritzky, A.R., 2014. Fluorescent-Labeled Amino Acid–Antibiotic Conjugates. Synthesis, 46(18), pp.2430-2435.

Velasco, M., Romero-Ceronio, N., Torralba, R., Hernández Abreu, O., Vilchis-Reyes, M.A., Alarcón-Matus, E., Ramos-Rivera, E.M., Aparicio, D.M., Jiménez, J., Aguilar García, E. and Cruz Cruz, D., 2022. Piperidine-iodine as efficient dual catalyst for the one-pot, three-component synthesis of coumarin-3-carboxamides. Molecules, 27(14), p.4659.

Vendrell, M., Zhai, D., Er, J.C. and Chang, Y.T., 2012. Combinatorial strategies in fluorescent probe development. Chemical reviews, 112(8), pp.4391-4420.

Villaume, C., Sanchez, C. and Méjean, L., 2004. β-Lactoglobulin/polysaccharide interactions during in vitro gastric and pancreatic hydrolysis assessed in dialysis bags of different molecular weight cut-offs. Biochimica et Biophysica Acta (BBA)-General Subjects, 1670(2), pp.105-112.

Wang, K., Liu, Z., Guan, R., Cao, D., Chen, H., Shan, Y., Wu, Q. and Xu, Y., 2015. Coumarin benzothiazole derivatives as chemosensors for cyanide anions. Spectrochimica Acta Part A: Molecular and Biomolecular Spectroscopy, 144, pp.235-242.

Xiang, J., Liu, F., Wang, B., Chen, L., Liu, W. and Tan, S., 2021. A literature review on maillard reaction based on milk proteins and carbohydrates in food and pharmaceutical products: advantages, disadvantages, and avoidance strategies. Foods, 10(9), p.1998.

Yang, Y., Liu, Q.W., Shi, Y., Song, Z.G., Jin, Y.H. and Liu, Z.Q., 2014. Design and synthesis of coumarin-3-acylamino derivatives to scavenge radicals and to protect DNA. European Journal of Medicinal Chemistry, 84, pp.1-7.

ANNEXURE

Tel: 26588204-26588662 26589620

तार / GRAM : विज्ञानी / SCIENTIFIC
Web-site : www.icmr.nic.in
E-mail : icmrhqds@sansad.nic.in

भारतीय आयुर्विज्ञान अनुसंधान परिषद
INDIAN COUNCIL OF MEDICAL RESEARCH

वी. रामलिंगस्वामी भवन, अन्सारी नगर, पोस्ट बॉक्स 4911, नई दिल्ली - 110 029
V. RAMALINGASWAMI BHAWAN, ANSARI NAGAR, POST BOX 4911, NEW DELHI - 110 029

No. 45/32/2019 –BIO/BMS **Date: 08.07.2019**

To,

Dr. Umesh Chandra Halder,
Professor,
Department of Chemistry,
Jadavpur University, Kolkata,
West Bengal-700032

Subject:- Award of Research Fellowship to **Miss Shahnaz Begum, SRF** on the Research project entitled "**Investigation of the anti-amyloidogenic activity of different physical and chemical modulators against the fibrillation of bovineβ-lactoglobulin and human insulin.**".

Dear Sir/Madam

The Director General, ICMR sanctions Research Fellowship to **Miss Shahnaz Begum, SRF** on a stipend of **Rs. 35,000/-** p.m. to carry out research on the project mentioned above, under your guidance. H.R.A. and Medical reimbursement will be paid as per rules of your University.

The award of Fellowship will be subject to the following terms and condition:

TENURE: It will be tenable for one year only from the date of joining duty and will be on yearly basis subject to maximum of **three years.**

Its continuance will, however, depend on the satisfactory progress of work and can be terminated at any time on a one month's notice, if the progress is not satisfactory, or on receiving adverse report from the Guide. The Fellow will be required to work on the project for a period at least one year.

The event of his/her leaving before completing one year on the fellowship, he/she may be required to refund the stipend drawn by him/her from the date of joining to the date of leaving the fellowship.

PRIVATE PRACTICE: Private practice of any kind, or taking up any appointment even in an honorary capacity during the fellowship is not permitted.
ADMINISTRATIVE CONTROL: The candidate will be under the administrative control of the Institution where he/she works, and will also be subject to the rules and regulations of the Institute.
LEAVE: Leave will be admissible according to the rules of the Institution, however in the case of female research fellows leave with stipend upto 6 months (in lieu of maternity leave) may be granted. No other kind of leave (such as sick leave) etc. will be admissible. Awardees are not entitled to vacation normally admissible to the staff of an Institution.
HRA: HRA will only be paid, if the fellow is not availing any hostel facility. A certificate to this effect should be sent along with joining report for payment of HRA.
REPORTS: The awardee shall submit six hard copies of 1st annual reports along with original proposal for the first 10 months on the prescribed standard proforma.

The first annual report should be submitted after 10 months from the date of commencement of the fellowship giving complete factual details of the research work done through the Guide alongwith his/her appraisal. Subsequent annual report should be submitted through the Guide two months before the completion of fellowship tenure. Failure to submit reports in time may lead to termination of the award. Six copies of the final report in the prescribed form clearly shall be submitted one month before the date of termination of the award.

A list of the papers published or presented at Scientific Conferences during the tenure of the fellowship should also be furnished with the annual and final reports.

PUBLICATION OF PAPERS: Prior permission for publication of papers based on the research work done during the tenure of the award should be obtained from the Council. The paper should be sent to the Council through the Guide with his/her recommendations. Due acknowledgement to the Council should be made in these papers.

PAYMENT OF FUNDS: The stipend and the funds for contingencies shall be paid as per procedure laid down in the enclosed an annexure.

CONTINGENT EXPENDITURE: An annual contingent grant of Rs. 20000/- p.a. will be admissible. The contingent grant is given to meet petty expenditure for purchase of chemicals, reagents etc. No non-expenditure article or equipment can be purchased out of the grant.

TRAVEL:-

Traveling allowance will not be admissible for joining duty or on termination of the award.

The Council may approve tours of research fellows/associate for:-

1. **Attending symposium/seminar/conference provided the fellow/associate is presenting a paper which has been accepted by the organizers of the symposium/seminar/conference.**
2. **Field work connected with research**
3. **TA/DA would be admissible as per the rules applicable to Central Government Officers with basic pay equivalent to the amount of the fellowship stipend.**

NOTE:- The expenditure on this account will be met

POST FELOWSHIP CARRIER:-

1. The Research Fellow can register himself/herself for postgraduate qualification and to utilize in his/her the work done by him/her during his/her fellowship tenure. A copy of these submitted for postgraduate degree will have to be sent to the Council for information and record **from the contingent grant sanctioned to the fellow**. Due acknowledgement to the ICMR should be made in the thesis by the research fellows.
2. The Research Fellow should also send to the Council for information a brief report on the post/job taken by him/her after the expiry of the fellowship.

The date indication forenoon/afternoon on which he/she the fellowship may please be intimated to this office. He/she may be asked to report for duty within a month from the date of issue of this letter failing which the award will be treated as cancelled.

Yours faithfully,

(G.S. Sandhu)
Administrative Officer
For Director-General

1. Copy to :- (Head of the Institution) The Registrar, Jadavpur University, Kolkata, West Bengal-700032
2. **Miss Shahnaz Begum, SRF,** Department of Chemistry, Jadavpur University, Kolkata, West Bengal-700032
3. Accounts Section – V, ICMR
4. IRIS ID: 2019-5056

Administrative Officer
For Director General

যাদবপুর বিশ্ববিদ্যালয়
কলকাতা-৭০০০৩২, ভারত

*JADAVPUR UNIVERSITY
KOLKATA-700 032, INDIA

Ref. No.: R-II/190/2019
Dated : 05/03/2019

To
Smt. Shahnaz Begum,
C/o – Prof. Umesh Chandra Halder,
Organic Chemistry Section,
Department of Chemistry,
Jadavpur University.

Sir / Madam,

I am pleased to inform you that you have been selected Research Fellow at Doctoral level to work in the Department of Chemistry of this University under JU-RUSA 2.0 Doctoral Scholarship Scheme.

You will be paid a fellowship of Rs. 30,000/- (consolidated) per month. The tenure of your Fellowship is for 14 (fourteen) months i.e. from 1st February 2019 to 31st March 2020.

Your service will be governed by the same terms and conditions of the University Service Rules as may be applicable to the temporary staff of the University and you will be under the administrative control of the undersigned.

You are requested to join the post within ten days from the date of receipt of this letter and submit your joining report in prescribed format through proper channel to the undersigned with a declaration stating that you are not a recipient of any emoluments from any other source from the date of your joining the Fellowship. Otherwise, your fellowship will be offered to the next candidate according to the waiting list.

University is not responsible for any matter of continuity of Non-Net Fellowship after the completion of JU-RUSA 2.0 Doctoral Research Fellowship.

Yours faithfully

27.02.19

Registrar

PUBLICATIONS

RSC Advances

PAPER

Cite this: *RSC Adv.*, 2023, **13**, 34097

Structural modulation of insulin by hydrophobic and hydrophilic molecules†

Shahnaz Begum,[a] Hasan Parvej,[a] Ramkrishna Dalui,[a] Swarnali Paul,[a] Sanhita Maity,[a] Nayim Sepay,[b] Mohd Afzal[c] and Umesh Chandra Halder *[a]

Received 29th September 2023
Accepted 13th November 2023

DOI: 10.1039/d3ra06647a

rsc.li/rsc-advances

In the bloodstream, insulin interacts with various kinds of molecules, which can alter its structure and modulate its function. In this work, we have synthesized two molecules having extremely hydrophilic and hydrophobic side chains. The effects of hydrophilic and hydrophobic molecules on the binding with insulin have been investigated through a multi-spectroscopic approach. We found that hydrophilic molecules have a slightly higher binding affinity towards insulin. Insulin can bind with the hydrophilic molecules as it binds glucose. The high insulin binding affinity of a hydrophobic molecule indicates its dual nature. The hydrophobic molecule binds at the hydrophobic pocket of the insulin surface, where hydrophilic molecules interact at the polar surface of the insulin. Such binding with the hydrophobic molecule perturbs strongly the secondary structure of the insulin much more in comparison to hydrophilic molecules. Therefore, the stability of insulin decreases in the presence of hydrophobic molecules.

Introduction

Protein structure is very sensitive to their microenvironments.[1] Structural alteration of proteins is often observed due to several factors (modulators) like pH,[2] temperature,[2] salt concentration,[3] and different types of small molecules.[4,5] This change in the presence of physical and chemical modulators is significant because it may change the function of the proteins.[6,7] The study of the modulators' interactions with proteins has drawn attention from the scientific community.[8,9]

Human insulin is a protein hormone in the blood that regulates blood sugar levels.[10,11] Depending upon the exposure and availability of it in the body, several medical conditions like hypertension,[12] coronary heart disease,[13] stroke,[14] cancer,[15] and type II diabetes[16] are widespread nowadays. The small monomeric insulin contains fifty-one amino acids and is divided into two α-helical structures, joined together by three disulfide bonds (intra-chain and inter-chain).[17] This small monomeric form of insulin is highly unstable.[18,19] Again, insulin is one of the serum proteins that commonly interact with the polar poly-hydroxyl group containing molecules like glucose. However, in the serum, many hydrophobic molecules can affect the structure and function of the insulin. Thus, the structure of insulin may change in the presence of diverse molecules in the blood and these compound can initiate insulin-related diseases. Therefore, an investigation of the effect of molecules with hydroxyl groups and hydrophobic groups on the insulin's structure is highly essential.

Protein-small molecule interaction studies are used to investigate the structural effect on proteins in the presence of different microenvironments.[20,21] The tuning of the microenvironment is possible through the proper choice of small molecules.[22,23] Hydrophilic to hydrophobic molecules can be synthesized from simple organic reactions. The reaction of an aldehyde with primary amine is one of the simple organic reactions used to join two fragments through imine bond formation.[24] The products of the reaction are known as Schiff's base.[24] With the proper choice of the substituent attached to the amine and aldehyde part, the hydrophilicity and hydrophobicity of the molecule can be tunable. For this reason, Schiff's base is used in very diverse fields of science like coordination chemistry,[25,26] hydrogels,[27,28] sensing,[29] analytical chemistry, electronics, optics[25] *etc.*

In this study, we have synthesized one hydrophobic Schiff's base (*E*)-2-((*tert*-butylimino) methyl)-6-methoxyphenol and one hydrophilic Schiff's base (*E*)-2-((2-hydroxy-3-methoxybenzylidene) amino)-2-(hydroxymethyl)propane-1,3-diol. The interactions of these two molecules with insulin have been investigated here. Therefore, it will provide a scope to monitor the structure of insulin in two opposite microenvironments.

Results and discussion

Synthesis of Schiff's base and choice of compounds

Insulin binds with glucose, which is a polar poly-hydroxy compound. For this reason, a poly-hydroxy compound is

[a]*Department of Chemistry, Jadavpur University, Kolkata-700032, India. E-mail: juumesh.halder@gmail.com*

[b]*Department of Chemistry, Lady Brabourne College, Kolkata-700017, India*

[c]*Department of Chemistry, College of Science, King Saud University, Riyadh 11451, Saudi Arabia*

† Electronic supplementary information (ESI) available. See DOI: https://doi.org/10.1039/d3ra06647a

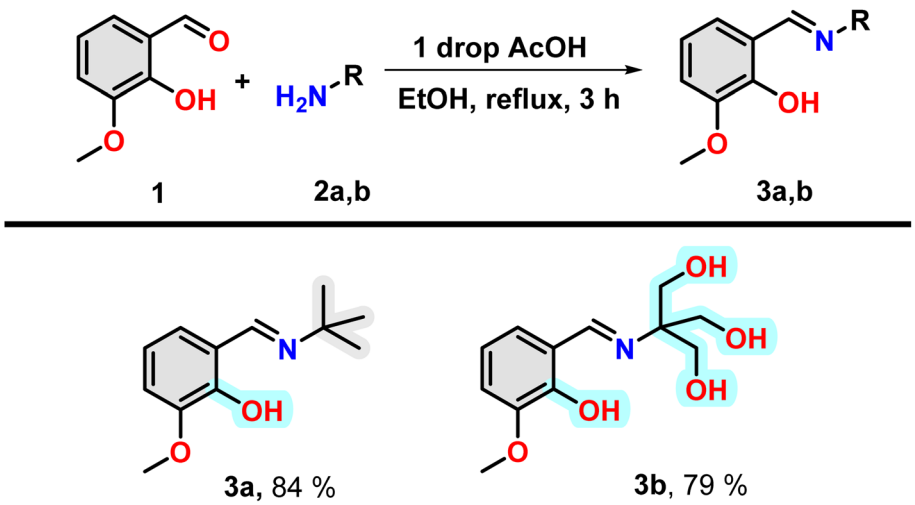

Scheme 1 Synthesis of Schiff base compounds **3a** and **3b**.

required to be designed in our study as one of the compounds. To understand the effect of binding a hydrophobic molecule to insulin, a similar molecule without the hydroxyl group has been designed. It is found that electron-rich aromatic molecules have unique protein binding ability. For this reason, the attachment of said poly-hydroxyl group containing and hydrophobic moiety with an aromatic moiety having a hydroxyl group separately will be one of the choices for the fulfilment of the target of investigation. For the easy joining of these two moieties, Schiff bases formation reaction is a convenient choice. Thus, two amine compounds 2-amino-2-(hydroxymethyl)propane-1,3-diol and 2-methylpropan-2-amine were selected for a poly-hydroxyl and hydrophobic moiety, respectively. Now, one electron-rich aldehyde is required for Schiff base formation. In this case, *ortho*-vanillin is the best because it contains one *ortho*-hydroxy and *meta*-methoxy group along with aldehyde at the benzene ring.

Under refluxing conditions in dry ethanol, the reaction between *ortho*-vanillin (**1**) and aliphatic amine (**2**) yielded corresponding Schiff bases. With the addition of one drop of glacial acetic acid, this reaction proceeded for three hours. When *tert*-butyl amine (**2a**) and 2-amino-2-(hydroxymethyl) propane-1,3-diol (**2b**) were employed in the reaction, high-yield production of compound **3a** and **3b** was achieved respectively (Scheme 1). The compounds were characterized through the use of ^{1}H NMR.

It is to be noted that the compound **3a** have one hydrogen bond forming group, *i.e.* hydroxyl group and have hydrophobic *t*-Bu group and an aromatic ring (grey highlighted). Therefore, the molecule is hydrophobic in nature. However, in the case of **3b**, the presence of three OH group in the nitrogen containing part instead of *t*-Bu group, make this region hydrophilic (cyan highlighted). Therefore, compound **3a** and **3b** will offer purely hydrophobic and largely hydrophilic environment in the vicinity of insulin.

Spectroscopic study of the Schiff base compounds

UV-vis spectroscopy study. The small molecule under investigation (**3a** and **3b**) show response in the UV-vis spectroscopy and give peaks at 402, 285, and 232 nm for compound **3a** and 412, 292 and 237 nm for **3b** (Fig. S1†). To check the stability of the compounds in this solvent system, the compounds (**3a** and **3b**) were separately mixed into the solvent system, and UV-vis spectra were recorded with time. The results indicate that the compounds are stable in these conditions, as slight changes were observed during 3.5 h (Fig. S2†).

Fluorescence study. The investigating compounds also have fluorescence properties. Both compounds **3a** and **3b** produce three hump emission spectra with peaks at 322, 333, and 347 nm on excitation at 276 nm (Fig. S3†). The hydrophobic nature of **3a** can influence its aggregation-caused quenching (ACQ) or aggregation-induced emission (AIE) in water. To check this effect, we set an experiment where the compound was gradually added to the experimental conditions without insulin. The results show that the **3a** has ACQ (Fig. S4A and B†) at high concentration. However, at lower concentrations of the **3a** (insulin-compound interaction was observed in this concentration range), any type of self-aggregation of the compound is absent, which is evident from the linear relation between concentration and fluorescence intensity. This linear behavior breaks after 25 μM and follows a polynomial curve, which indicates their self-aggregation in the experimental solvent system.

The **3b** is a hydrophilic molecule, and it shows self-aggregation in the experimental conditions at high concentrations. In this case, the compound shows aggregation-induced emission as the fluorescence intensity increases slowly with **3b** concentration (Fig. S4C and D†). However, at low concentrations (2–25 μM), there is also a linear relation between concentration and **3b** fluorescence intensity. Therefore, at lower concentrations of both compounds, the self-aggregation of them cannot proceed rapidly.

Study of interactions of the Schiff bases with human insulin

UV-vis spectroscopy study. The ultraviolet-visible spectroscopic can be employed to understand the environment of the chromophore of the protein or small molecules during their

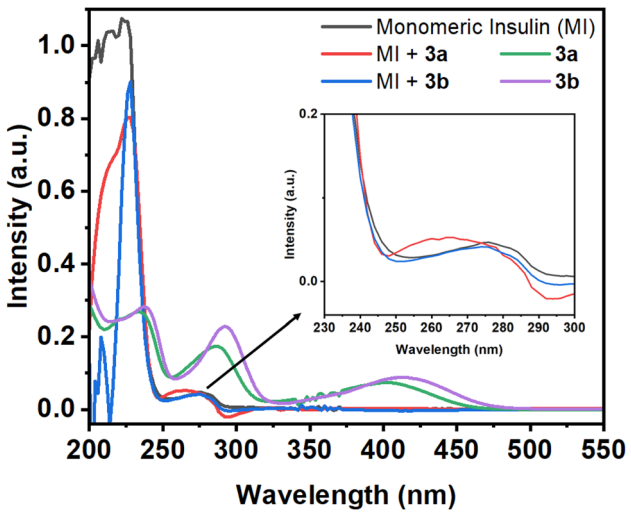

Fig. 1 Absorption spectra of monomeric insulin (10 μM in pH 2.0) in the absence and presence of Schiff base compounds **3a** and **3b**. Absorption spectra of **3a** and **3b** (50 μM in pH 2.0).

interaction. In this work, we have chosen the insulin as a model protein where *p*-hydroxyphenyl group in the Tyr residue acts as a chromophore. Monomeric insulin contains four Tyr residues and shows a peak at $\lambda_{max} = 276$ nm (Fig. 1).

If the environment of the Tyr residues of protein changes during the interactions with small molecules, then the nature of this peak may changes. In the presence of the compound **3a**, the 276 nm peak of the protein show a blue shift of 11 nm with the enhancement of the intensity. However, in the case of compound **3b**, the protein peak shows slight blue shift of 2 nm. Although, the compounds have peak at 286 and 289 nm for **3a** and **3b**, respectively, but the protein peak (276 nm) shows blue shift upon addition of compounds. From this initial study, it may be assumed that the compounds can have capability to interact with the protein.

Intrinsic fluorescence study of insulin in presence of Schiff base compounds

The Tyr residues of the monomeric insulin also show an emission response and give an emission peak at 304 nm on excitation at 276 nm. Upon addition to the **3a** in the monomeric insulin solution (25 μM) at 283 K, the peak intensity of insulin (304 nm) decreases rapidly with a 7 nm red shift (Panel A, Fig. 2). The appearance of the peak at 312 nm with the addition of the compound is the characteristic of the compound **3a**. In the case of compound **3b**, a similar type of observation was found at the same temperature (Panel B, Fig. 2). The intensity of the said protein peak was decreased with the gradual addition of the compound.

Table 1 The Stern–Volmer (K_{sv}) and binding (K_b) constant of **3a** and **3b** at different temperature

	K_{sv}, 10^4 (M^{-1})			K_b, 10^4 (M^{-1})		
Compound	283 K	293 K	303 K	283 K	293 K	303 K
3a	4.99	3.94	3.65	2.83	2.18	1.65
3b	6.64	7.47	8.64	16.08	17.09	18.57

Stern–Volmer equation can be used to determine the affinity of compounds to bind to proteins.

$$I^0/I = 1 + K_{sv}[C] \quad (1)$$

Here, initial protein fluorescence intensity (I^0) and intensity (I) after the addition of compounds **3a** and **3b**. This quenching constant (K_{sv}) is a measurement of the strength of the interaction between the compound and the protein. The slope of the plot of I^0/I *vs.* C is related to the quenching constant and can be used to calculate the quenching constant. In order to analyze fluorescence quenching, the Stern–Volmer eqn (1) was used, and Table 1 provides the quenching constants for different temperatures (Fig. 3). As can be seen in Table 1, the results indicate that the K_{sv} for **3a** is inversely proportional to the temperature, while for **3b**, it has been found to have a direct correlation with the temperature. Consequently, it implies that these compounds bind to proteins in different ways depending on the binding mechanism that they use.

Binding parameters

By evaluating the binding constant (K) and the change in free energy (ΔG) of the synthesized compounds–insulin interaction,

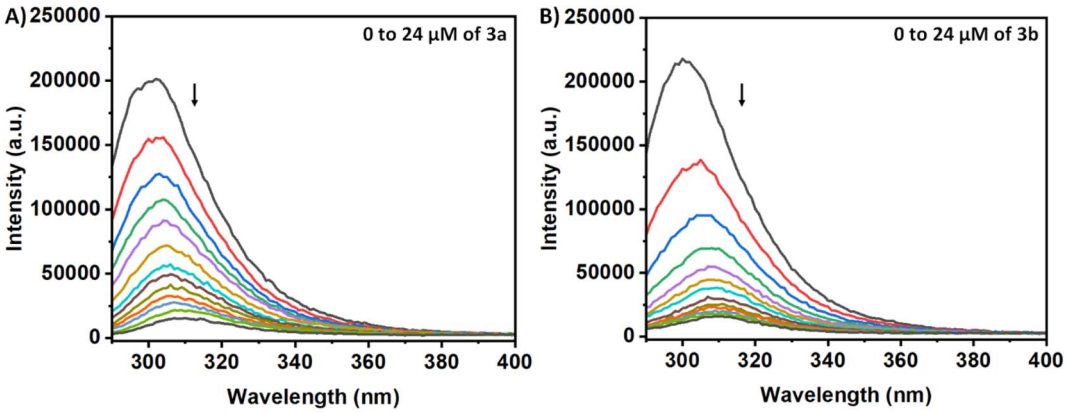

Fig. 2 Fluorescence spectral change of insulin on gradual addition of (A) **3a** and (B) **3b**.

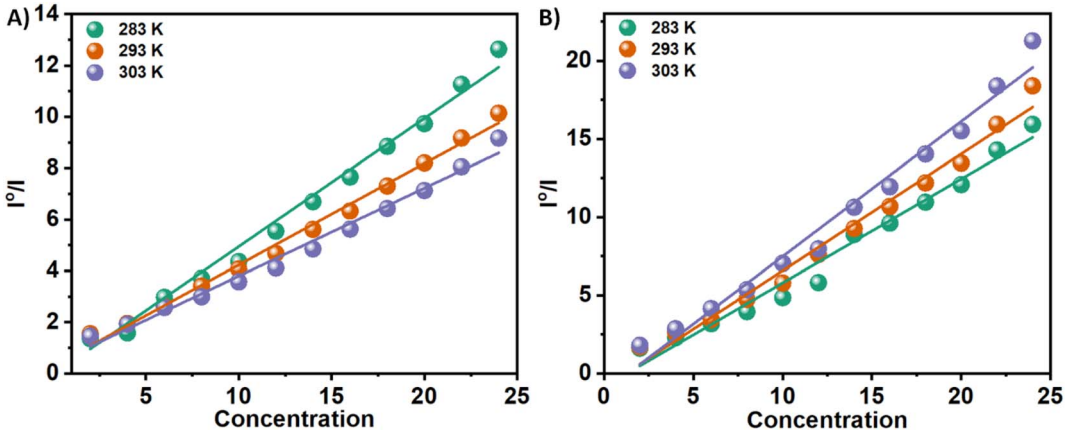

Fig. 3 Stern–Volmer plots for the quenching of Tyr-fluorescence of insulin at 283, 293, and 303 K in the presence of two Schiff base **3a** (Panel A) and **3b** (Panel B) in solution.

we can quantify the interaction between small molecules (**3a** and **3b**) and protein. A fundamental aspect of the efficacy of small molecules lies in their ability to bind to the target protein, as well as their subsequent effect on its stability. This significantly affects binding efficacy. In order to determine the quantitative assessment of K and ΔG, the following equation is used to analyze the fluorescence quenching data. When a pair of complimentary species bind independently to equal sites in a macromolecule, this equation describes the equilibrium between the free and bound species.

$$\ln((I^0 - I)/I) = \ln K_b + n \ln[C] \quad (2)$$

n is the number of binding sites, and K_b is the binding constant. There have been extensive studies in the literature utilizing the above eqn (2) to elucidate binding parameters from fluorescence quenching data as a method for predicting binding parameters. Table 1 summarizes the results of this study, conducted at various temperatures. Fig. 4 shows representative plots of $\ln((I^0 - I)/I)$ *versus* $\ln[C]$, which is a measure of how protein–compound interactions were affected by temperature. The results also indicate that the binding of **3a** is weaker than that of **3b**. Therefore, insulin has more preference to bind with the polar molecules in contrast with the hydrophobic molecules. The binding of the **3a** to the insulin decreases with increasing temperature. However, reverse phenomenon was found in the case of **3b**.

Binding forces and thermodynamic parameters

In a broader sense, the interactions between small molecules and biomolecules can be summed up as having many different types of forces. A variety of forces interact within an interacting site, including electrostatic forces, hydrogen bonds, van der Waals interactions, and hydrophobic and steric contacts. Traditionally, to account for the principal forces of binding between small molecules and proteins, the signs and magnitudes of thermodynamic parameters have been invoked. By taking into account the assumption that there is no significant change in the enthalpy change (H) over a particular temperature range, the enthalpy change (H) and the entropy change (S) can both be calculated from the following van't Hoff equation:

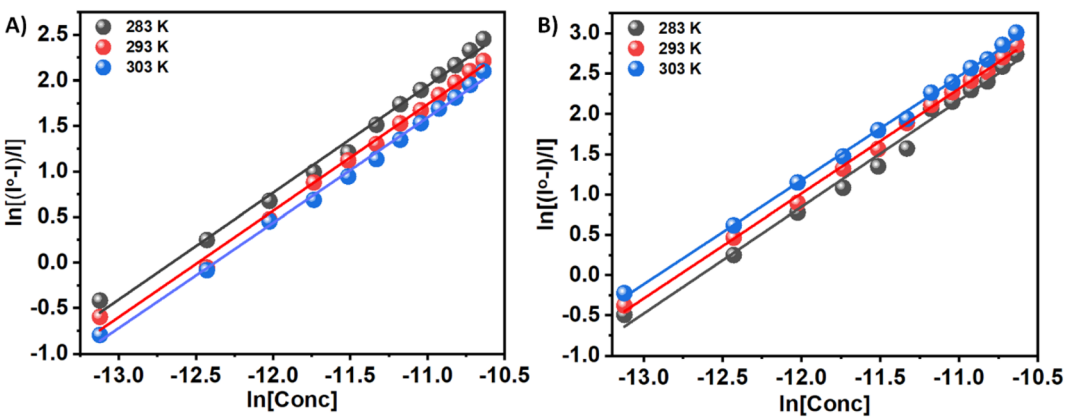

Fig. 4 $\ln((I^0 - I)/I)$ *versus* $\ln[C]$ plots for the quenching of Tyr-fluorescence of insulin at 283, 293, and 303 K in the presence of two Schiff base **3a** (Panel A) and **3b** (Panel B) in solution.

Table 2 Thermodynamic parameters involved in the insulin–3a/3b interactions

Compounds	Temperature (K)	$\Delta G°$ kJ mol^{-1}	$\Delta H°$ kJ mol^{-1}	$\Delta S°$ kJ mol^{-1}
3a	283	−5.41		
	293	−5.98	+10.72	+0.057
	303	−6.55		
3b	283	−12.16		
	293	−11.33	−35.65	−0.083
	303	−10.50		

$$\ln K = \Delta H/RT + \Delta S/R \quad (3)$$

In this case, R represents the universal gas constant and T represents the Kelvin temperature. The free energy change (ΔG) resulting from the process in this case is then estimated by using the relationship given below:

$$\Delta G = \Delta H - T\Delta S \quad (4)$$

There are several thermodynamic parameters that can be calculated and listed in Table 2, and a representation of the van't Hoff plot ($\ln K$ *vs.* $1/T$) can be found in Fig. 5.

Several kinds of interaction occur during protein–small molecule interaction. There is a link between these interactions and the thermodynamic parameters previously documented by Ross and Subramanian. These parameters have provided insights into the mechanisms by which each interaction occurs. According to the thermodynamic data, the following can be summarized as the model of interaction on the basis of the data related to the interaction:

(i) $\Delta H > 0$, $\Delta S > 0$ correspond to hydrophobic forces.

(ii) $\Delta H < 0$, $\Delta S < 0$ correspond to hydrogen bond formation and van der Waals interaction.

(iii) $\Delta H < 0$, $\Delta S > 0$ correspond to electrostatic/ionic interactions.

It has been demonstrated that the enthalpically unfavorable and entropically favorable thermodynamic parameters for the interaction between **3a** and insulin are presented in Table 2, with a negative Gibbs free energy change, suggesting that the interaction may occur spontaneously. However, with a negative Gibbs free energy change, the **3b**–insulin interaction is enthalpically favorable and entropically unfavorable. It should be noted that the positive enthalpy and entropy change demonstrate that the interaction process between **3a** and insulin is dominated by hydrophobic forces. Again, **3b** and insulin interact through hydrogen bond formation and van der Waals interaction, as demonstrated by the negative enthalpy and entropy changes.

Monitoring the hydrophobicity changes in the microenvironment of insulin: ANS assay

8-Anilinonaphthalene-1-sulfonic acid is a fluorescent probes having higher fluorescence intensity when binds at the hydrophobic pocket of the protein surface (also for insulin)[30–33] with

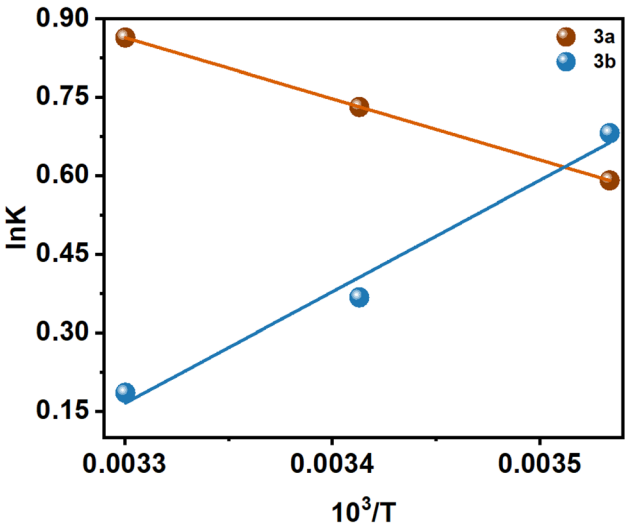

Fig. 5 ln K *vs.* $1/T$ plot at 283, 293, and 303 K of two Schiff base **3a** and **3b**.

respect to its unbound state. Therefore, if one compounds able to displace ANS from the binding site of the protein, then the intensity of the ANS bound insulin will decrease. The results will indicate the said compound can bind at the hydrophobic site of the protein surface. In the case of the compound **3a**, the intensity of the ANS-insulin system decrease with the gradual addition of it (Panel A, Fig. 6). However, for **3b**, the decrease of fluorescence intensity is low with addition of the compound (Panel B, Fig. 6). Due to the presence of four hydroxyl groups in the compound, the compound is polar and unable to bind at hydrophobic protein surface. Again, **3a** is sufficiently hydrophobic because it contains only one OH group and hydrophobic *tert*-butyl group. For this reason, the molecule has low solubility in the buffer medium.

In the presence of insulin, having few hydrophobic pocket on the protein surface, become a host for both ANS and **3a**. Due to lower solubility and higher binding ability of **3a** with respect to the ANS, the molecule will move from polar aqueous medium to hydrophobic protein sites which will replace ANS from their binding site on insulin. It is evident from the decrease of ANS intensity. However, for the presence of four hydroxyl group in **3b**, it is sufficiently hydrophilic and has lesser tendency to replace ANS from their binding sites. Therefore, **3b** have different binding site than **3a** which is polar in nature. The slight decrease in the ANS fluorescence intensity may be due to the ANS displacement from their binding sites for the conformational change of the protein during **3b** binding to the protein. To confirm the results obtained in different studies, the circular dichroism (CD) spectroscopy was employed for monitoring the secondary structural changes.

Circular dichroism (CD) spectroscopy

Circular dichroism (CD) of a protein gives indications of the secondary and tertiary structural change of the investigating protein. Insulin is an α-helix enriched protein which shows peak at 208 nm in far-UV CD spectral regions for its α-helical

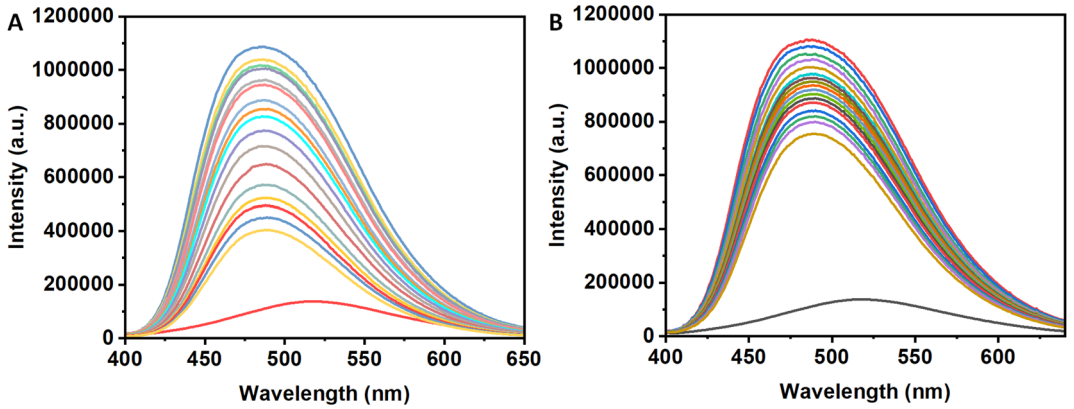

Fig. 6 ANS-fluorescence emission spectra of monomeric insulin incubated separately at 25 °C and at pH 2.0 in the absence and presence of Schiff base **3a** (Panel A) and in the absence and presence of Schiff base **3b** (Panel B). Insulin concentrations throughout all the experiments were kept at 25 μM. Results were the average of three different experiments.

structure. If a small molecule such as a Schiff base interacts with the protein and is able to perturb the secondary structure of the insulin, then there will be a change or shift of these peaks. The purified monomeric insulin (6 μM) shows peaks at 208 nm and 221 nm which are the characteristic peaks of an alpha helix containing protein like insulin along with the presence of beta sheet structure. For a solution containing insulin and the compound **3a** (1 μM), a significant change of far-UV CD spectrum was observed in the above-mentioned peak indicating that the binding of the compound to the protein unable to cause a major change of the secondary structure of the protein (Fig. 7). But addition of higher concentration of **3a** (2 and 6 μM) changes the CD spectral pattern of insulin giving higher percent of random structure (Table S1†). Thus the hydrophobic compound **3a** interacts with insulin and perturbs strongly its secondary structure. However, the compound **3b** at its lower concentration (1 and 2 μM) interacts with insulin shows red-shift of these peaks with greater negative ellipticity value compared to monomeric insulin. CD structural analysis shows the formation of slight higher content of β-structure. The difference in MRE value can be related to the structure of the two molecules **3a** and **3b**. At higher concentration of the **3b**, structural transition of insulin was observed. It showed lesser MRE value at 215 nm and increased MRE at 207 nm compared to insulin alone. Thus the hydrophilic compound **3b** has influences in the secondary structure as well as the tertiary structure of the insulin.

Protein function is very much related to the structure of the protein. The results indicate that hydrophobic molecule **3a** has a high potential for the destruction of the secondary structure of insulin in comparison with hydrophilic molecule **3b**. Therefore, the study shows that the stability of insulin is highly dependent on the hydrophilic and hydrophobic environment.

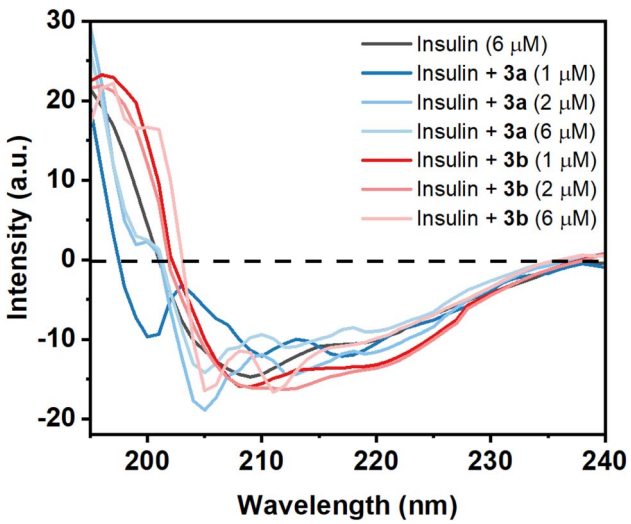

Fig. 7 Far-UV CD spectra (190–250 nm) of monomeric insulin in the absence and presence two small molecules (Schiff bases) **3a** and **3b** at 25 °C and at pH 2.0, showing the secondary structural changes of insulin.

Theoretical studies

Structural investigation of the Schiff bases will provide significant insight into the nature of the molecule and the contribution of the functional groups to the properties. The molecular electrostatic potential map (MEP) of the energy-minimized structure (using density functional theory (DFT)) of the Schiff bases can provide its electronic distribution around the molecular backbone. Color-coding of the map indicates electron-rich (red), neutral (green), and electron-poor (blue) regions. The **3a** molecule has methoxy and phenolic oxygen and imine nitrogen as polar atoms, whereas **3b** has three additional hydroxyl groups (Fig. 8). All these groups can form an H-bond with protein through either H-bond donation or acceptance depending upon the group. The MEP of both compounds shows a red color on oxygen atoms. It is interesting to notice that the nitrogen atoms are buried in the neutral region. Therefore, imine nitrogen is less capable of H-bond formation.

The polar surface area of **3a** was calculated to be 41.82 $Å^2$, whereas the value was 102.51 $Å^2$ for **3b**. Therefore, **3b** has more than double the polar surface area than that of **3a**. For this

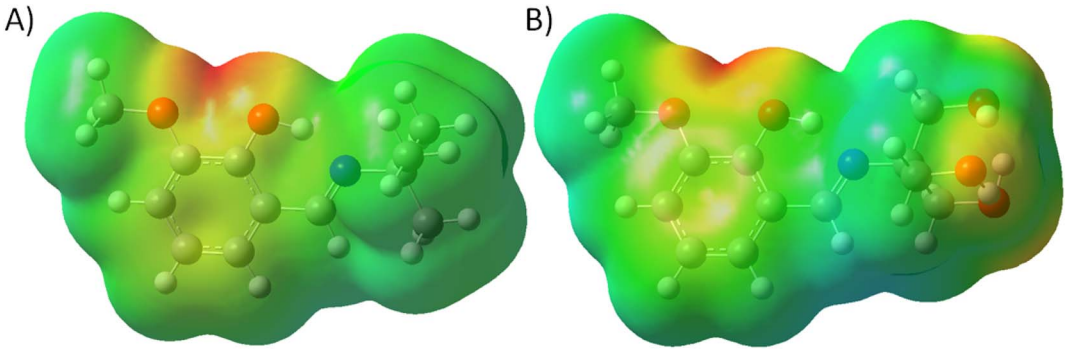

Fig. 8 Molecular electrostatic map of (A) **3a** and (B) **3b**.

reason, the lipophilicity of **3a** ($\log P_o/w = 2.83$) is higher than ($\log P_o/w = 1.73$). Again, both the compounds are somewhat water soluble and the $\log S$ of **3a** and **3b** were calculated to be -2.41 and -0.48, respectively. For such small molecules, these parameters indicate that they have the potential to form H-bonds with molecules and enough polar.

Molecular docking is one of the most fascinating computational techniques which is used to predict the binding site of a small molecule to a protein, mechanism of protein binding, and weak forces involved in such binding process.[34–36] Here, this method has been used to predict the binding mode of **3a** and **3b** in the human insulin. The structure of the molecules was energy minimized with the help of density functional theory (DFT). The molecular docking of these compounds to the human insulin showed that the compound **3b** have higher binding affinity with respect to the **3a**. The change of free energy for this binding process is -6.83 and -5.74 kcal mol^{-1} for **3b** and **3a**, respectively. It indicates that the compound **3b** have more binding affinity to the human insulin than **3a** which was also observed experimentally.

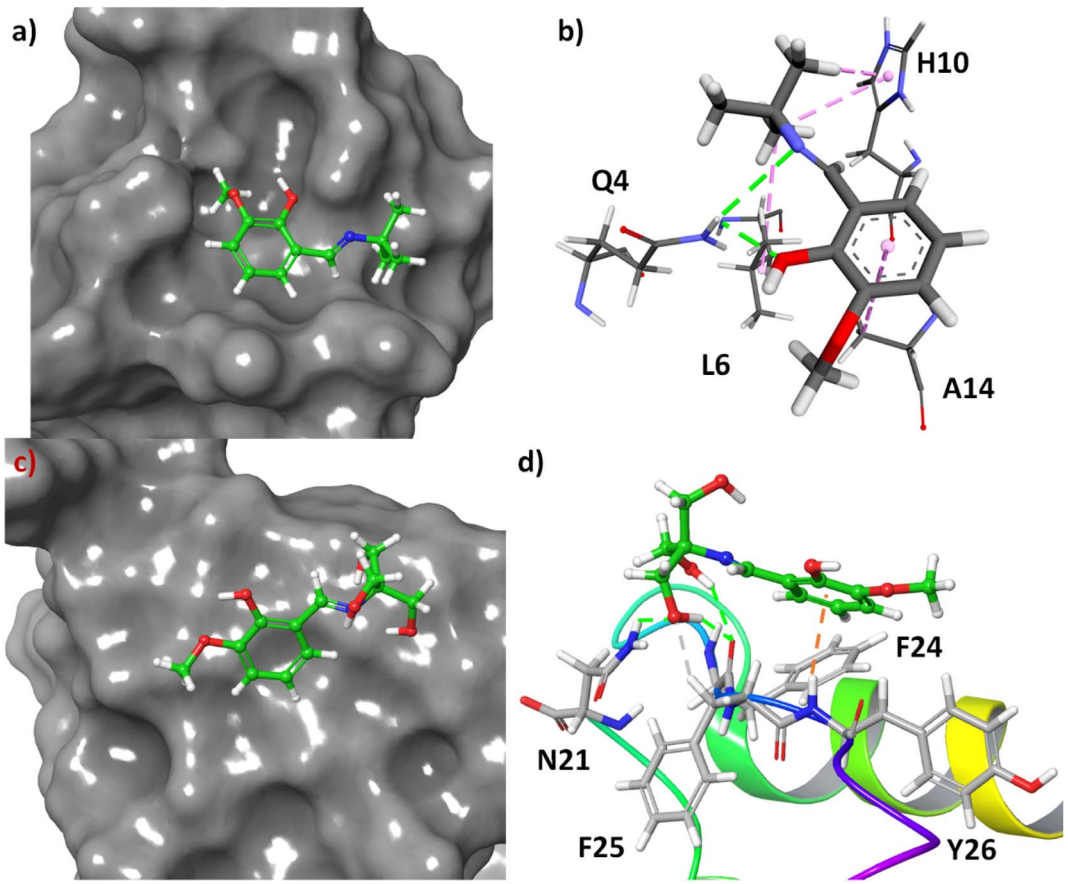

Fig. 9 (a) Docking pose of **3a** in the hydrophobic pocket of the insulin, (b) different non-covalent interactions between **3a** and active site amino acids, (c) docking pose of **3b** on the surface of insulin, (d) different non-covalent interactions in the binding site of the protein with **3b**.

The molecular docking showed that the compound **3a** has been bound at the hydrophobic cavity on the protein surface whereas the **3b** attached at the surface of the protein (Fig. 9, Panel A and Panel B). In the binding process of the **3a**, the amino acid residues Q4, L6, H10, and A14 are involved (Fig. 9C). In the case of **3b**, the binder amino acids are Q21, F24, F25, and Y26 (Fig. 9D). In the binding sites, the N–H of amide group have hydrogen bond with the imine and hydroxyl group of **3a**, imidazole ring of H10 shows C–H$\cdots\pi$ interactions with *t*-butyl group of **3a**, the methyl group of A14 interact with C–H$\cdots\pi$ to the benzene ring of **3a**, and L6 interact through hydrophobic interaction with *tert*-butyl group of **3a**. However, hydrogen bonding is the main driving forces for the binding of **3b** to the insulin. Amide C=O of F25 involved in hydrogen bonding with two hydroxyl groups at the side-chain of **3b**. Another hydrogen bonding was found to be between amide N–H of N21 and the side-chain OH. The aliphatic C–H of F25 involved in non-conventional H-bonding interactions with the said OH group. Amide N–H of Y26 showed N–H$\cdots\pi$ interactions with benzene ring of **3b**.

Experimental

Materials

Human insulin, marketed by Eli Lilly, India under the trade name 'Huminsulin' was purchased from medicine shop. Few chemicals such as *o*-vanillin, tris(hydroxymethyl)aminomethane, *tert*-butyl amine were procured from Sigma-Aldrich, USA; acetic acid and HCl were purchased from Merck, Germany. Different fluorescent probes, namely 8-anilinonaphthalene-1-sulfonic acid ammonium salts (ANS), thioflavin T (ThT) were purchased from Sigma Chemical (St. Louis, USA). All the other reagents used in our experiments were of analytical grade or of high purity reagent available.

Preparation and purification of monomeric state of insulin

The hexameric state of insulin marketed as 100 IU mL^{-1} equivalent to 2 mg mL^{-1} contains the preservative *m*-cresol, tonicity modifier glycerin and pH adjusting substances HCl/NaOH. However, through extensive dialysis with water, these substances were successfully removed. In the next step, 80% acetic acid was added to convert it to a monomer state with a final concentration of 20%. To ensure the formation of amyloid-like fibrils, the solution was filtered through a 0.22 μm (Millipore) filter membrane to remove traces of hexameric molecules. The filtrate was then kept at 37 °C overnight, resulting in a homogeneous solution serving as the monomeric state of insulin (1.5 mg mL^{-1}). An optical value of ε (276 nm) = 10.0 was considered in this process.

Synthesis of 3a and 3b

In a 10 mL round-bottomed flask equipped with a condenser and stirring bar, a mixture of ethanol (3 mL), *ortho*-vanillin (1.0 mmol), amine (1.2 mmol) and one drop of acetic acid was prepared. Upon addition of the components, the reaction mixture turned yellow in color. The mixture was then refluxed for three hours with stirring and subsequently allowed to cool to room temperature. To the cooled mixture, 10 mL of water was added and the resulting mixture was extracted with CH_2Cl_2 (3 × 5 mL). The combined organic layer was dried over anhydrous Na_2SO_4 and evaporated in vacuum. Finally, the compounds obtained were purified by either crystallization or column chromatography, followed by crystallization. The ^1H and ^{13}C NMR of the products (observed in DMSO-d_6) can be found in ESI File (Fig S5–S8).†

UV-visible spectroscopy

We utilized a JASCO Spectrophotometer model no. V700 (Serial No. B184461798) at room temperature (25 °C) to measure precisely the absorbance and determined the binding affinity and binding constants. UV titrations were conducted by gradually increasing the concentrations of insulin (1–20 μM) for **3a** and (1–20 μM) for **3b** in a 1 cm quartz cuvette that contained a constant concentration of **3a** and **3b** (20 μM) in Milli-Q water. The spectra were recorded between 200–600 nm. To check the stability of the compounds, they were subject to under investigation through UV-vis spectroscopy in water at 20 μM separately with respect to time.

Intrinsic fluorescence study of insulin in presence of Schiff base compounds

The study conducted fluorescence quenching experiments using HORIBA (Model: FLUOROMAX-4C, serial no. 1734D-4018-FM) at room temperature after exciting the solutions at 276 nm and following the emission in the wavelength range 290–400 nm and keeping the excitation and emission slits at 5 nm. The concentration of insulin was kept constant at 25 μM while **3a** and **3b** were added successively from 2 to 24 μM and 2 to 24 μM, respectively. The excitation wavelength for **3a** and **3b** derivative was 335 nm and 325 nm, respectively, and emission was recorded between 350–550 nm. To understand the spectroscopic behaviour of both the compounds, concentration dependent fluorescence spectroscopy was recorded in water at the said excitation wavelength.

ANS assay for monitoring the hydrophobicity changes

The hydrophobicity of protein molecules was determined by employing a fluorescent probe that binds to the hydrophobic pockets on the protein 1-anilinonapthalene-8-sulfonate (ANS) is a well-known polarity sensitive probe that shows specific binding with the hydrophobic pockets. A stock solution of ANS was prepared and mixed to 2 mL monomeric insulin samples to determine hydrophobicity. The final ANS concentration in each sample aliquot was kept constant at 30 μM. The protein samples were then treated with **3a** and **3b** chemicals at doses ranging from 2 to 60 μM and 2 to 60 μM, respectively. Shimadzu Spectrofluorometer (Shimadzu 5301 PC) was used to record the emission spectra from 390 to 600 nm after excitation at 350 nm. The length of the path was 1 cm. Both the excitation and emission slits were set at 5 nm.

Circular dichroism (CD) spectroscopy

We recorded far-UV CD spectra of insulin in the presence of the Schiff bases **3a** and **3b** using a Jasco spectropolarimeter (Model: J-815). The measurements were done in a nitrogen atmosphere, with a quartz cell of path length 0.2 cm in the far-UV region (200–260 nm). We maintained a constant concentration of insulin at 6 μM, while the concentrations of **3a** and **3b** derivatives were varied (1–6 μM). We collected data for each nm from 260 to 200 nm at a scan speed of 50 nm per minute. The sample temperature was kept at 25 °C using a Neslab RTE-111 circulating water bath connected to water-jacketed quartz cuvettes. To calculate the secondary structures of insulin, we utilized CDNN 2.1 software attached with the instrument.

Molecular docking

The RCSB Protein Data Bank website (PDB ID: 3I40) provided us with the crystal structure of human insulin. We thoroughly analyzed this biopolymer's structure and prepared it for a docking experiment. Our team optimized the structures of **3a** and **3b** using the Density Functional Theory (DFT) B3LYP/6-31G level of theory to minimized energy. For MEP, a same functional and basis sets have been utilized. These optimized structures were then used for docking with insulin protein to identify the most probable site and mode of binding using the grid-based docking program Auto Dock 4.2. To ensure accuracy, we removed the ligand present in the protein and water molecules from the protein and assigned Atom Kollman charges after adding polar hydrogen for the protein. We utilized the default parameters of Auto Dock and the generic algorithm to conduct this calculation. The visualization effects were expertly prepared using Discovery Studio 4.1 Client. We are confident in the accuracy and validity of our findings. The polar surface area, lipophilicity, and water solubility was predicted using SwissADMET.[37]

Conclusions

In conclusion, the effects of hydrophilic and hydrophobic molecules on the insulin binding process have been investigated through a multi-spectroscopic approach. We have synthesized two Schiff base molecules with hydrophilic and hydrophobic side chains. The findings of our investigation show that glucose (hydrophilic) binding protein insulin has also a sufficient affinity to bind with the hydrophobic molecules. The binding constant of hydrophobic and hydrophilic molecules was found to be 4.99×10^4 M^{-1} and 6.64×10^4 M^{-1}, respectively, at 283 K. The binding of hydrophobic molecules at the hydrophobic pocket of insulin perturbs greatly the secondary structure of the monomeric insulin whereas the hydrophilic molecule causes small alterations in the secondary structural contents on binding with insulin. Thus, stability of insulin is diminished in the presence of hydrophobic molecules.

Conflicts of interest

The authors declare no competing financial interest.

Acknowledgements

Financial support of Indian Council of Medical Research (ICMR), Govt. of India, is greatly acknowledged. Shahnaz Begum is the recipient of ICMR-SRF fellowship. Financial support of University Grants Commission UGC-CAS-II and DST-PURSE-II (Govt. of India) Program of Department of Chemistry, Jadavpur University, Kolkata are also acknowledged. Dr Mohd Afzal extends his appreciation to Researchers Supporting Project Number (RSPD2023R979), King Saud University, Riyadh, Saudi Arabia, for financial assistance.

References

1 S. C. Bagley and R. B. Altman, *Protein Sci.*, 2008, **4**, 622–635.
2 V. H. Nguyen and B.-J. Lee, *Int. J. Nanomed.*, 2017, **12**, 3137–3151.
3 R. Sinha and S. K. Khare, *Front. Microbiol.*, 2014, **5**, 165.
4 H.-X. Zhou and X. Pang, *Chem. Rev.*, 2018, **118**, 1691–1741.
5 L. Mabonga and A. P. Kappo, *Biophys. Rev.*, 2019, **11**, 559–581.
6 D. K. Ghosh and A. Ranjan, *Protein Sci.*, 2020, **29**, 1559–1568.
7 L. M. Stevers, E. Sijbesma, M. Botta, C. MacKintosh, T. Obsil, I. Landrieu, Y. Cau, A. J. Wilson, A. Karawajczyk, J. Eickhoff, J. Davis, M. Hann, G. O'Mahony, R. G. Doveston, L. Brunsveld and C. Ottmann, *J. Med. Chem.*, 2018, **61**, 3755–3778.
8 V. Corradi, B. I. Sejdiu, H. Mesa-Galloso, H. Abdizadeh, S. Y. Noskov, S. J. Marrink and D. P. Tieleman, *Chem. Rev.*, 2019, **119**, 5775–5848.
9 E. Hallacli, C. Kayatekin, S. Nazeen, X. H. Wang, Z. Sheinkopf, S. Sathyakumar, S. Sarkar, X. Jiang, X. Dong, R. Di Maio, W. Wang, M. T. Keeney, D. Felsky, J. Sandoe, A. Vahdatshoar, N. D. Udeshi, D. R. Mani, S. A. Carr, S. Lindquist, P. L. De Jager, D. P. Bartel, C. L. Myers, J. T. Greenamyre, M. B. Feany, S. R. Sunyaev, C. Y. Chung and V. Khurana, *Cell*, 2022, **185**, 2035–2056.
10 G. Wilcox, *Clin. Biochem. Rev.*, 2005, **26**, 19–39.
11 M. S. Rahman, K. S. Hossain, S. Das, S. Kundu, E. O. Adegoke, M. A. Rahman, M. A. Hannan, M. J. Uddin and M.-G. Pang, *Int. J. Mol. Sci.*, 2021, **22**, 6403.
12 B. M. Y. Cheung and C. Li, *Curr. Atheroscler. Rep.*, 2012, **14**, 160–166.
13 W. Fan, *Cardiovasc. Endocrinol.*, 2017, **6**, 8–16.
14 R. Chen, B. Ovbiagele and W. Feng, *Am. J. Med. Sci.*, 2016, **351**, 380–386.
15 E. Giovannucci, D. M. Harlan, M. C. Archer, R. M. Bergenstal, S. M. Gapstur, L. A. Habel, M. Pollak, J. G. Regensteiner and D. Yee, *Diabetes Care*, 2010, **33**, 1674–1685.
16 I. Martín-Timón, *World J. Diabetes*, 2014, **5**, 444.
17 T. N. Vinther, M. Norrman, U. Ribel, K. Huus, M. Schlein, D. B. Steensgaard, T. Å. Pedersen, I. Pettersson, S. Ludvigsen, T. Kjeldsen, K. J. Jensen and F. Hubálek, *Protein Sci.*, 2013, **22**, 296–305.
18 N. Nagel, M. A. Graewert, M. Gao, W. Heyse, C. M. Jeffries, D. Svergun and H. Berchtold, *Biophys. Chem.*, 2019, **253**, 106226.

19 C. L. Maikawa, A. A. A. Smith, L. Zou, C. M. Meis, J. L. Mann, M. J. Webber and E. A. Appel, *Adv. Ther.*, 2020, **3**, 1900094.
20 A. D. G. Lawson, M. MacCoss and J. P. Heer, *J. Med. Chem.*, 2018, **61**, 4283–4289.
21 R. R. Thangudu, S. H. Bryant, A. R. Panchenko and T. Madej, *J. Mol. Biol.*, 2012, **415**, 443–453.
22 S. Chaturvedi, P. P. Hazari, A. Kaul, Anju and A. K. Mishra, *ACS Omega*, 2020, **5**, 26297–26306.
23 S. Zhong, J.-H. Jeong, Z. Chen, Z. Chen and J.-L. Luo, *Transl. Oncol.*, 2020, **13**, 57–69.
24 H. Schiff, *Ann. Chem. Pharm.*, 1864, **131**, 118–119.
25 M. G. Humphrey, T. Schwich, P. J. West, M. P. Cifuentes and M. Samoc, in *Comprehensive Inorganic Chemistry II*, Elsevier, 2013, pp. 781–835.
26 C. J. Burns, M. P. Neu, H. Boukhalfa, K. E. Gutowski, N. J. Bridges and R. D. Rogers, in *Comprehensive Coordination Chemistry II*, Elsevier, 2003, pp. 189–345.
27 W. Wang, R. Narain and H. Zeng, in *Polymer Science and Nanotechnology*, Elsevier, 2020, pp. 203–244.
28 Y. Dong and W. Wang, in *Wound Healing Biomaterials*, Elsevier, 2016, pp. 289–307.
29 H. Liu, S. Ding, Q. Lu, Y. Jian, G. Wei and Z. Yuan, *ACS Omega*, 2022, **7**, 7585–7594.
30 P. Patel, K. Parmar and M. Das, *Int. J. Biol. Macromol.*, 2018, **108**, 225–239.
31 P. Alam, A. Z. Beg, M. K. Siddiqi, S. K. Chaturvedi, R. K. Rajpoot, M. R. Ajmal, M. Zaman, A. S. Abdelhameed and R. H. Khan, *Arch. Biochem. Biophys.*, 2017, **621**, 54–62.
32 A. Das, Y. M. Gangarde, V. Tomar, O. Shinde, T. Upadhyay, S. Alam, S. Ghosh, V. Chaudhary and I. Saraogi, *Mol. Pharm.*, 2020, **17**, 1827–1834.
33 S. Das and D. Bhattacharyya, *J. Cell. Biochem.*, 2017, **118**, 4881–4896.
34 N. Sepay, P. C. Saha, Z. Shahzadi, A. Chakraborty and U. C. Halder, *Phys. Chem. Chem. Phys.*, 2021, **23**, 7261–7270.
35 N. Sepay, N. Sepay, A. Al Hoque, R. Mondal, U. C. Halder and M. Muddassir, *Struct. Chem.*, 2020, **31**, 1831–1840.
36 N. Sepay, S. Chakrabarti, M. Afzal, A. Alarifi and D. Mal, *RSC Adv.*, 2022, **12**, 24178–24186.
37 A. Daina, O. Michielin and V. Zoete, *Sci. Rep.*, 2017, **7**, 42717.

ChemistrySelect

Research Article
doi.org/10.1002/slct.202303699

Chemistry Europe
European Chemical Societies Publishing

www.chemistryselect.org

Anion–Induced Amyloid Fibrillation of Human Insulin *In vitro*

Shahnaz Begum,[a] Swarnali Paul,[a] Hasan Parvej,[a] Falguni Mondal,[a] Ramkrishna Dalui,[a] Anirban Pradhan,[b] Nayim Sepay,[c] and Umesh Chandra Halder*[a]

In the present study, we have focused on the effect of three biologically important salt anions on insulin aggregation. The result of the present study reveals that salts differing in their anions (NaI, NaOAc, and $NaNO_3$) induce the self–assembly formation of insulin even at low physiological (in the micromolar range) salt concentration with efficacy that follows the order $I^- > CH_3COO^- > NO_3^-$. Here, the anion–driven aggregation of insulin does not follow either the Hofmeister series or electroselectivity series at very low salt concentrations; instead, the binding of anions at low pH to the positively charged residues of insulin is determined by a mechanism where the salt anions promote the fibrillation of insulin and modify the morphology of the monomeric precursor molecule. Both the nucleation and fibril elongation are controlled by the electrostatic forces and hydrophobic interactions. Aggregation mechanism and aggregate morphology were investigated employing a combination of Thioflavin T (ThT) and ANS fluorescence, circular dichroism (CD), dynamic light scattering (DLS), and transmission electron microscopy (TEM). Overall, the present data will enhance the idea to rationalize the anion effects on the aggregation of amyloid-prone protein and to understand the influence of charged biomolecules in cellular compartments.

Introduction

Many proteins and peptides can form the stable self–assembly termed amyloid fibrils under stress due to misfolding.[1,2] Morphologies of these fibrils are independent of the nature of the proteins, albeit they consist of common cross-β sheet structure.[3] Efforts have been made to understand the formation of oligomeric intermediates of amyloid fibrils playing key roles in the pathology of amyloid diseases.[4] More than twenty diseases are associated with the phenomenon 'amyloidosis' in human. They include Alzheimer's disease, Parkinson's disease, cataracts, systemic amyloidosis, type 2 diabetes mellitus, and cardiovascular diseases.[5] Researchers devoted their time to investigate the fibril-forming events and the structural intermediates triggering the protein oligomerization process. Nucleation and subsequent growth of these oligomers induces to form worm-like protofibrillar assembly having less organized structures than the resultant fibrillar aggregates.[6]

Two factors generally can control the oligomerization rate and morphology of the aggregates arising from unfolded peptides and proteins. These are the amino acid sequence (intrinsic parameter) of the involved peptides or proteins and the surrounding physicochemical or environmental factors. The intrinsic parameter is thus related to the primary structure, types and distribution of the amino acid residues, the charge on the residues, and their beta-sheet propensity to adapt the crossed β-structure. Conversely, physicochemical or environmental factors are related to pH, temperature, salt ions, small additives, cosolvents, or solutes.[7–10]

Salts are abundantly present in our physiological system of cellular compartments at smaller concentrations (nanomolar to micromolar concentration range), acting as micronutrients. The ions of these salts can act as an essential environmental determinant during amyloid formation and have been observed to play a specific role in the aggregation of the α-synuclein,[7] Aβ peptide,[11] prion protein,[12] HypF–N[13] and bovine serum albumin.[9] The protein aggregation ability of various ions is generally related to the electroselectivity principle or the Hofmeister series, a ranking of the ions commonly employed to explain various chemical and biological science phenomena. The historic 'Hofmeister effect' is brought into play at moderate to high (> 0.3 M) concentrations of salts, wherein the 'kosmotropic' ions are assumed to make water structure and decrease protein solubility by increasing the conformational stability. On the contrary, the 'chaotropic' ions are assumed to break the water structure to increase protein solubility by decreasing the conformational stability.[14] However, the effects are considered negligible at lower and physiological salt concentrations. Below 0.1 M salt concentrations, the nonspecific electrostatic interactions mainly control protein–ion interactions and screen the charges on protein surfaces.[15] Still, literature shows many examples where ion–specific influences play important role in solubility[16] and stability of protein[17] and amyloid fibrillation[7] in this concentration range. Although some anions, like sulfates, precipitate the native protein solution, their action on non-native protein solution is complex, and fewer are reported. Again, some anions can stabilize the structure of the protein in nonnative conditions, thus decreasing the possibility of forming aggregation–prone structures. Ions of varying charges can

[a] S. Begum, S. Paul, H. Parvej, F. Mondal, R. Dalui, U. Chandra Halder
Department of Chemistry, Jadavpur University, Kolkata 700 032, India
E-mail: uhalder2002@yahoo.com

[b] A. Pradhan
Department of Chemistry, Birla Institute of Technology (BIT) Mesra, Jharkhand, 835215, India

[c] N. Sepay
Department of Chemistry, Lady Brabourne College, Kolkata 700017, India

influence the electrostatic fields and ionic medium of the proteins. Differential electrostatic effects imposed by anions of varying charges can either inhibit[18] or promote[13,19] the protein aggregation propensity. Again, the binding of anions to the positively charged residues of protein at low pH not only modulates the rate of oligomerization but also the morphology of the aggregates. The effectiveness of various ions in controlling the protein fibrillation phenomenon depends strongly on the anion concerned, its concentration, pH and temperature of the medium and also on the particular protein under investigation. In the present study we have selected some biologically important monovalent salt anions and have focused our studies on the influence these anions at their physiologically relevant concentrations on the fibrillation mechanism and fibril morphology of human insulin under acidic environment.

Insulin, a 51-residue peptide hormone having two peptide chains, chain A and chain B, regulates blood–glucose levels and has a predominantly α-helical structure in its native state.[20] In the physiological environment, insulin primarily exists in the Zn^{2+}-stabilized hexameric form and as a monomer at low pH.[21] Under altered environmental conditions, the insulin fibrillation process involves a rate-limiting dissociation of its hexameric form into its monomeric state with the exposure of the hydrophobic residues those are normally buried in the native hexamer.[22] The residues from B11 to B18 and B24 to B26 of the insulin B chain play a key role during its fibrillation pathway.[23] Under stress-induced conditions, it shows a strong tendency to undergo structural changes leading to different oligomeric forms, including the amyloid structures, and it has received our attention as a model system for amyloid fibril formation but also raised an issue regarding the efficacy of the insulin in the treatment type II diabetes.[25] Deposition of insulin amyloid occurs both in patients with type II diabetes as well as after repeated injection and subcutaneous insulin infusion. It has been observed that insulin forms fibrillar network having greater β-structure under stress at high temperature and low pH.[26] Moreover, previous reports show that strong acids can also induce the formation of the molten globule of insulin.[27] It has been assumed the intermediacy of molten globule state in protein folding as well as in amyloid formation. We have chosen three important salt anions, acetate, iodide and nitrate, as they are present in our cellular components in very small concentrations (in the micromolar range). The chosen salt anions occupy different positions in the Hofmeister and electroselectivity series. Again, the selected salt anions were studied with very low concentrations (1 μM and 50 μM) so that the specific ion binding with charged side chains and Debye–Huckel charge screening become important. At the same time, the Hofmeister effect is negligible at these very low concentration ranges. We employed the salts sodium acetate (NaOAc), sodium iodide (NaI), and sodium nitrate ($NaNO_3$) to investigate the aggregation kinetics and morphology changes of insulin at pH 1.6 and 60 °C. At low pH, protein surfaces are dominated mainly by the positive charges, and thus, the particular effect imparted by the cations is negligible compared to the effect of the anions. Previous works on anion-induced fibrillation of insulin demonstrated the involvement of higher salt concentrations (mM range). Still, in our present study, we maintained the anion concentrations relevant to our physiological conditions (μM range).

In this paper, we investigated the fibrillation mechanism and morphology of the insulin amyloid aggregates employing the multi–spectroscopic approaches involving ANS-fluorescence, Thioflavin T (ThT) assay, dynamic light scattering (DLS), circular dichroism (CD) spectroscopy and transmission electron microscopy (TEM).

Materials and Methods

Materials

Human insulin was procured from Eli Lilly, India, under the trade name of 'Huminsulin' from the local medicine shop. Other chemicals,such as sodium acetate, sodium iodide, sodium nitrate, acetic acid, and hydrochloric acid were purchased from Merck, India.

Different fluorescent probes, like Thioflavin T (Th T) and 8-anilinonaphthalene-1-sulfonic acid ammonium salt (ANS), were purchased from Sigma Chemical Co. (USA). The other chemicals used were of the highest purity available. All buffer solutions were filtered using a 0.22 μMMicro Syringe filter (Millipore, USA).

Sample Preparation

Monomeric Insulin Preparation

The procured insulin solution having concentration 100 IU/mL Insulin Human I. P. (r-DNA origin) (equivalent to 2 mg/mL) exists mostly in the hexameric state.[28] Firstly we dialyzed exhaustively the insulin solution against water to eliminate glycerine (tonicity modifier) and the preservative m-cresol. Then HCl/NaOH was added to adjust the pH. Next we converted it to the monomeric state with the addition of 80 % acetic acid to a final concentration of 20 %.[26] The resulting solution was then allowed to pass into Millex-G 0.22 mm (Millipore) membrane filter to discard the small traces of hexameric insulin if exists and thus preventing the amyloid–like fibril formation. Next the filtrate was kept overnight at 37 °C in a temperature control ovento form a homogeneous solution containingmonomeric insulin having concentration 1.5 mg/mL.[26,29] The extinction co–efficient of insulin was considered as $\varepsilon^{1\%}_{276nm} = 10.0$.[30]

Preparation of Insulin Oligomers

The 20 % acetic acid solution of monomeric insulin (MI) was taken and was diluted to 1.0 g/L with 1(N) HCl. The solution was then heated at 65 °C, pH 1.6 for 4 h to initiate the amyloid fibrillation of insulin.[31] To study with salt anions, monomeric insulin at pH 1.6 was incubated separately with 1 μM and 50 μM NaOAc, NaI and $NaNO_3$ solutions at 65 °C for 4 h. The aggregation process was investigated through the measurements of ThT and ANS fluorescence, dynamic light scattering (DLS) and transmission electron microscopy (TEM).

Methods

Intrinsic Fluorescence measurements

Tyrosine intrinsic fluorescence of monomeric insulin (20 μM), heat treated insulin (65 °C for 4 h) were measured at 20 °C, pH 1.6 in absence and presence and of 1 μM and 50 μM NaOAc, NaI and $NaNO_3$ salt solutions. The excitation wavelength was set at 276 nm and spectra were recorded in the wavelength range of 280–400 nm. Slit width were kept at 5 nm for both excitation and emission.

ANS Fluorescence Measurements

Hydrophobic patches of insulin were opened up during its aggregation process and it was monitored using polarity sensitive fluorescent probe ANS. A stock solution of ANS was added to each of the insulin samples (20 μM) with or without NaOAc, NaI and $NaNO_3$ solutions of two different strengths at pH 1.6. ANS concentration in each aliquot was 30 mM using a 50 fold molar excess of insulin concentration. After keeping the mixture in the dark for 15 min, ANS–fluorescence intensities were measured after excitation at 380 nm. The emission spectra were recorded between 400 and 600 nm in a fluorescence spectrophotometer (Horiba, Fluoro Max FM-4). Blank corrections were done with ANS as control for all sets. Excitation and emission slit width were kept at 3 and 5 nm respectively. Data points are the mean of three consecutive measurements.

ThT Fluorescence Measurements

ThT is a commonly used dye for identifying amyloid fibrils as it binds with the crossed beta-sheet structure of amyloid fibrils.[31] The ThT fluorescence assay was carried out using a Horiba fluorescence spectrophotometer (FluoroMax FM-4). The stock solution of ThT was prepared with miliQ water, and its concentration was calculated from the absorbance value at 412 nm using the molar extinction coefficient of 36,000 $M^{-1}cm^{-1}$.[17] Insulin samples thermally incubated separately with or without 1 μM and 50 μM OAc^-, I^- and NO_3^- solutions having pH 1.6 were withdrawn from each sample set and added to ThT to detect the amyloid fibrils, keeping the final protein and dye concentrations 20 μM. The ThT was excited at 440 nm, and emission intensity was measured by recording the spectra from 450 to 600 nm keeping the excitation and emission slit widths at 3 and 5 nm, respectively. The sample spectrum was corrected from the respective blank. Data points are the mean of three consecutive measurements.

Measurement of HydrodynamicRadius (RH) of Insulin Oligomers by DLS

Dynamic light scattering (DLS) measurements were done to determine the size of proteins, its aggregate and other macromolecules in solution. Diffusion of any of nano–sized small particle can alter the intensity of the scattered light. It monitors these fluctuations on the basis of an auto correlation and analyze the distribution of the particles and fibrillar aggregates due to its sensitivity towards the size of the particle.[32] DLS measurements were carried out separately with heat incubated insulin (65 °C for 4 h) in the absence and in the presence of OAc^-, I^- and NO_3^-anions employing Zetasizer Nanos (Malvern Instrument, U. K.) equipped with 633 nm laser. Measurements were done in a 2 mL rectangular cuvette of path length 10 mm.All measurements were carried out at 20 °C and the solutions were filtered through the syringe filter of 0.22 μM pore size. The time-dependent auto–correlation function was achieved with twelve acquisitions for each run.

Monitoring the Secondary Structural Changes of Insulin by Circular Dichroism (CD) Spectroscopy

To monitor the conformational changes of insulin in the absence and presence of the anions OAc^-, I^- and NO_3^- of two different concentrations, the far–UV CD spectra were recorded at 20 °C in the 195–255 nm wavelength range on a JASCO-815 Spectropolarimeter (Jasco, Japan) with a rectangular cuvette of path length 1 mm. In a temperature–controlled water bath, insulin solutions (pH 1.6) were incubated at 75 °C for 4 h in the absence and presence of the anions. Aliquots of different insulin solutions were taken and diluted to 0.2 mg mL^{-1} to monitor the secondary structural change of insulin with the CD spectropolarimeter. The final spectra of the protein samples were recorded only after subtracting the corresponding buffer spectrum. Each spectrum is the average of three consecutive scans. The secondary structural contents of different insulin samples were calculated from a curve-fitting program CDNN2.1.

High–Resolution Transmission Electron Microscopy (HR–TEM)

To characterize and differentiate the fibrils of insulin samples in different anionic environments, TEM images were taken on a high–resolution transmission electron microscopy (JEOL-HRTEM-2011, Japan) operating with an accelerating voltage of 80–85 kV in different magnifications. A droplet of the diluted insulin solutions (15 μL) in the absence and presence of OAc^-, I^- and NO_3^- ions were placed on a carbon–coated copper grid of mesh size 300 C (ProSci Tech). Excess liquid was removed from the grid after 20 s followed by the addition of two drops of 2% uranyl acetate (Sigma, Steinheim, Germany) for staining and removed after 15 second, dried in air and the specimens were utilized for imaging. All specimens were left for 6 h prior to get the images.

Results and Discussion

Effect of Salt Anions on the Intrinsic Fluorescence of Insulin

The intrinsic fluorescence of tyrosine (Tyr) residues in insulin has been measured in this study as the monomeric insulin (MI) contains tyrosine residues (at the position of 14, 19 of chain A and 16, 26 of chain B) only as fluorophore as it is devoid of any tryptophan residue and thus it shows emission at $\lambda_{max} = 306$ nm (Figure 1). Results suggest no influence of the microenvironment around the excited fluorophore of insulin to alter its normal fluorescence characteristics. The heat–incubated insulin exhibited lower fluorescence intensities in absence of any salt anions due thermal unfolding of the native structure leading to the change of the conformation and microenvironment around the excited fluorophore. The quenching of the intrinsic tyrosine fluorescence of insulin were also observed when it was incubated with the anions OAc^-, I^- and NO_3^-separately at 65 °C for 4 h. The lowering of emission intensity indicates that the anions interact with insulin molecule and the Tyr residues of the protein are exposed in anionic environment. The decreases of emission intensities in the presence of salt anions are smaller than monomeric heat treated insulin in absence any anion. This

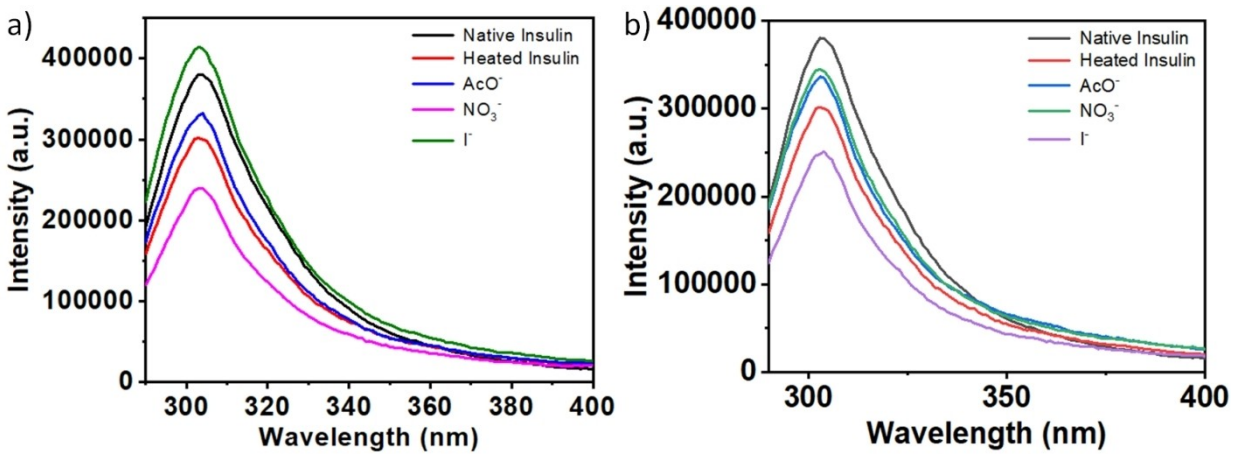

Figure 1. Intrinsic fluorescence emission spectra of monomeric insulin and thermally incubated insulin (65 °C for 4 h) in the absence and presence of salt anions OAc^-, I^- and $NO_3^-$of varying concentrations (a) 1 μM and (b) 50 μM. Excitation was done at the wavelength 276 nm keeping both the excitation and emission slits width at 5 nm.

clearly indicates lesser change of insulin structure in the anionic environment compared to heat treated (HT) insulin alone as the positively charged residues on insulin backbone in acidic medium are stabilized by the anions. Iodide ions show a greater lowering of intrinsic fluorescence intensity than the acetate and nitrate ions when salt concentrations were kept at 50 μM (physiological concentration) due to greater negative charge density and greater quenching ability of iodide ions than acetate and nitrate ions.

Monitoring the Change of the Microenvironment of Insulin in the Presence of Salt Anions

Hydrophobic collapse results in the formation of fibrillar protein aggregates in the nucleation state. Thermal incubation of insulin in acidic medium leads to the exposure of patches formed by the hydrophobic residues. We have investigated the influence of the selected salt anions on the exposure of the clusters formed by the hydrophobic residues through the monitoring of the interactions of 8-anilinonaphthalene-1-sulfonate (ANS), a hydrophobic fluorescent probe with the protein samples. But the interactions of ANS with the exposed hydrophobic clusters of heat treated (65 °C for 4 h, pH 1.6) insulin in the absence and presence of salt anions OAc^-, I^- and $NO_3^-$of two different concentrations (1 μM and 50 μM) increased the fluorescence emissions of the ANS and a blue–shift of its emission maxima. In the acidic environment when ANS was added to the insulin in absence of any salt, emission maximum was centered near 515 nm. Native insulin showed low ANS binding as it has little exposed hydrophobic residues. In contrary, ANS binds strongly to the newly exposed hydrophobic sites due to partial or complete unfolding in acidic environment during thermal incubation of insulin in absence of salt anions and shows a blue shift in the emission maxima to 490 nm. ANS emission intensity was also significantly increased due to its binding with insulin in the presence of anions during thermal incubation with the similar blue shifts of emission maxima from 515 nm to 490 nm (Figure 2). All the selected anions at their lower salt concentrations (10 μM)showed similar ANS fluorescence intensity like heat–treated insulin alone indicating little interactions with the heat–induced insulin at low salt anion concentration. Addition of 50 μM salt solutions to the thermally incubated insulin increased the ANS–fluorescence emission with the blue shifts in each case, focusing the modulation of electrostatic forces during the interactions of the anions with the positively charged residues of insulin. ANS–fluorescence intensity was enhanced noticeably when insulin was treated with 50 μM iodide ions (I^-) compared to the similar treatment with acetate (CH_3COO^-) and nitrate (NO_3^-) ions of same strength. Thus I^- interact strongly with the positively charged residues at the acidic pH and modulate the electrostatic forces leading to the exposure of hydrophobic clusters in acid and heat induced insulin molecules. The greater interaction of I^-compared to CH_3COO^- and NO_3^- ions with the positively charged residues of insulin at acidic pH is owing to the greater charge density on the I^- ions. The efficacy of the anions to modulate the electrostatic forces in the acid-induced insulin follows the order $I^- > CH_2COO^- > NO_3^-$ at this low salt concentrations (physiological concentration range). Our findings support the observations in the study of aggregation kinetics, secondary structural changes and electron microscopic studies. It is noteworthy, that in acidic medium ANS can also influence to form the partially unfolded structure.[33] Thus spectral data acquisition was done when the addition of the ANS was completed at a protein concentration lower than that required during study of the aggregation kinetics to eliminate the possibility of formation of the oligomers.

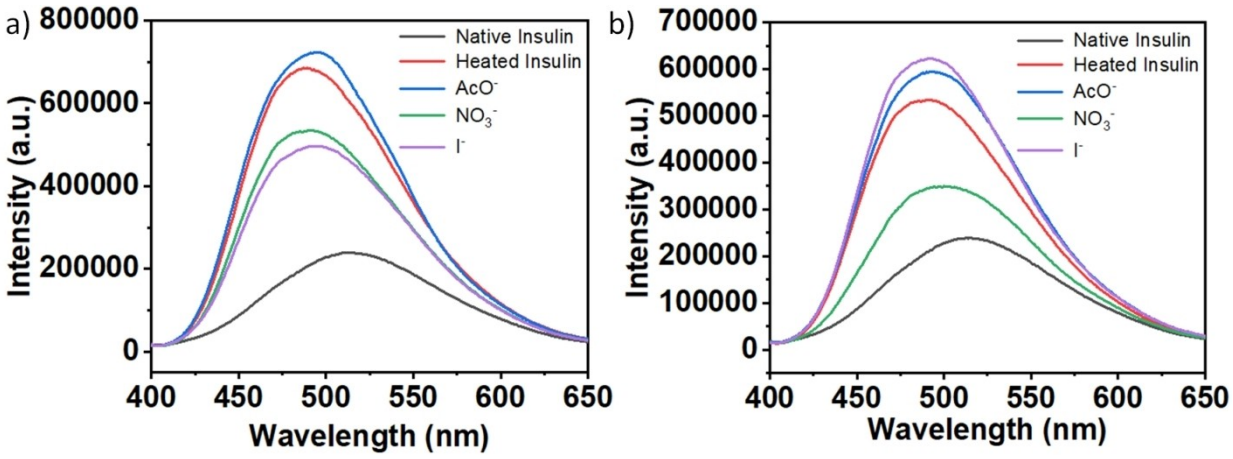

Figure 2. ANS-fluorescence of monomeric insulin and thermally incubated insulin (65 °C for 4 h) without or with the salt anions OAc^-, I^- and NO_3^-at pH 1.6:(a) 1 μM and (b) 50 μM concentration. Insulin concentrations maintained 20 μM keeping the excitation and emission slits width at 3 and 5 nm, respectively. Each spectrum was the average of three scans.

Effect of Salt Anions on the Propensity of Fibrillation of Insulin

To investigate the influence of the selected salt anions on the propensity and rate of insulin amyloid fibril formation, ThT–fluorescence measurements were done. The benzothiazole dye, ThT binds specifically with the amyloid aggregates and causes an enhancement of ThT fluorescence intensity. It is routinely used to identify the cross beta-structure of the protein aggregates and also to measure the extent ofamyloid formation.[34] ThT emission spectra of insulin in the absence and presence of OAc^-, I^- and NO_3^-ions at low physiological salt concentrations in the stressed conditions at pH 1.6, and temperature 65 °C were monitored and represented in the Figure 3a. The result demonstrates that the monomeric insulin showed weak interaction with ThT probe and thus showing lowest Th T intensity. Upon thermal incubation at 65 °C, the monomeric insulin without any salt anion showed enhanced Th T fluorescence intensity and thus indicating the cross β-sheet structures formation during amyloid fibrillation of the protein. All other insulin samples when coincubated with the OAc^-, I^- and NO_3^- ions having two different concentrations at pH 1.6 for 4 h produced different ThT emission intensities which are proportional to amount of fibrillar aggregates formed in the solution. From the comparative analysis of the ThT–fluorescence emission spectra, it is obvious that the selected salt anions of biological relevant promote the aggregation propensity of insulin at the acidic pH differently depending on their concentrations used. At their lowest concentration range (ca. 1 μM) the anions OAc^-, I^- and NO_3^- showed ThT–fluorescence intensity similar to heat–incubated monomeric insulin alone indicating that the anions are unable to interact with the positively charged residues of insulin at this very low salt concentration and have little influence on thermal aggregation of insulin.

All the three anions interact strongly with acid denatured insulin at their higher (also relevant to physiological concentration) salt concentrations (50 μM) and showed enhanced ThT emission intensities compared to heat- treated insulin alone. The results indicate the increased cross β-sheet structures formation when insulin was incubated with 50 μM $NaNO_3$, NaOAc and NaI separately. Thus all the three anions OAc^-, I^- and NO_3^-promote the fibrillation of insulin with greater efficiancy. Significantly I^-showed highest ThT fluorescence emission intensity at 50 μM concentration. The other two anions NO_3^- and OAc^- also enhanced the fluorescence signals compared to heat–treated insulin alone.

Hence the anionic environments brought about by OAc^-, I^- and NO_3^- ions have enhanced ThT emission intensities of insulin. Significantly maximum ThT fluorescence emission intensity was noted with 50 μM NaI. The other two salts NaOAC and $NaNO_3$ also enhanced the fluorescence signals compared to heat–treated insulin alone (2–3 times signal enhancement).The results indicate the increased crossed β-sheet structures formation occur when insulin was incubated with salt anions. Efficiency of beta–amyloidogenesis of the anions increases in the order $I^- > CH_3COO^- > NO_3^-$. It also indicates that anions producing higher ionic strength interact more efficiently with positively charged side chain residues in acid denatured insulin and thus modulating the electrostatic forces resulting the aromatic and other hydrophobic amino acid residues to come closer during the beta–amyloids formation.

Figure 3b represents the plot of comparative Th T-fluorescence curve of insulin with incubation time in presence of selected anions. Results shown in the figure clearly demonstrate the formation of a typical two–phase sigmoidal growth–curve with a lag phase initially and then following a sharp increases of the intensity value and finally reaches a constant curve. In this study we monitored the ThT kinetic assay up to 4 h and the final reading was taken after 24 h. ThT intensity did not change any further after reaching the plateau. The growth of amyloid fibrils can clearly be represented by the middle phase where ThT-fluorescence increases rapidly, while the plateau or the last phase shows the completion of the

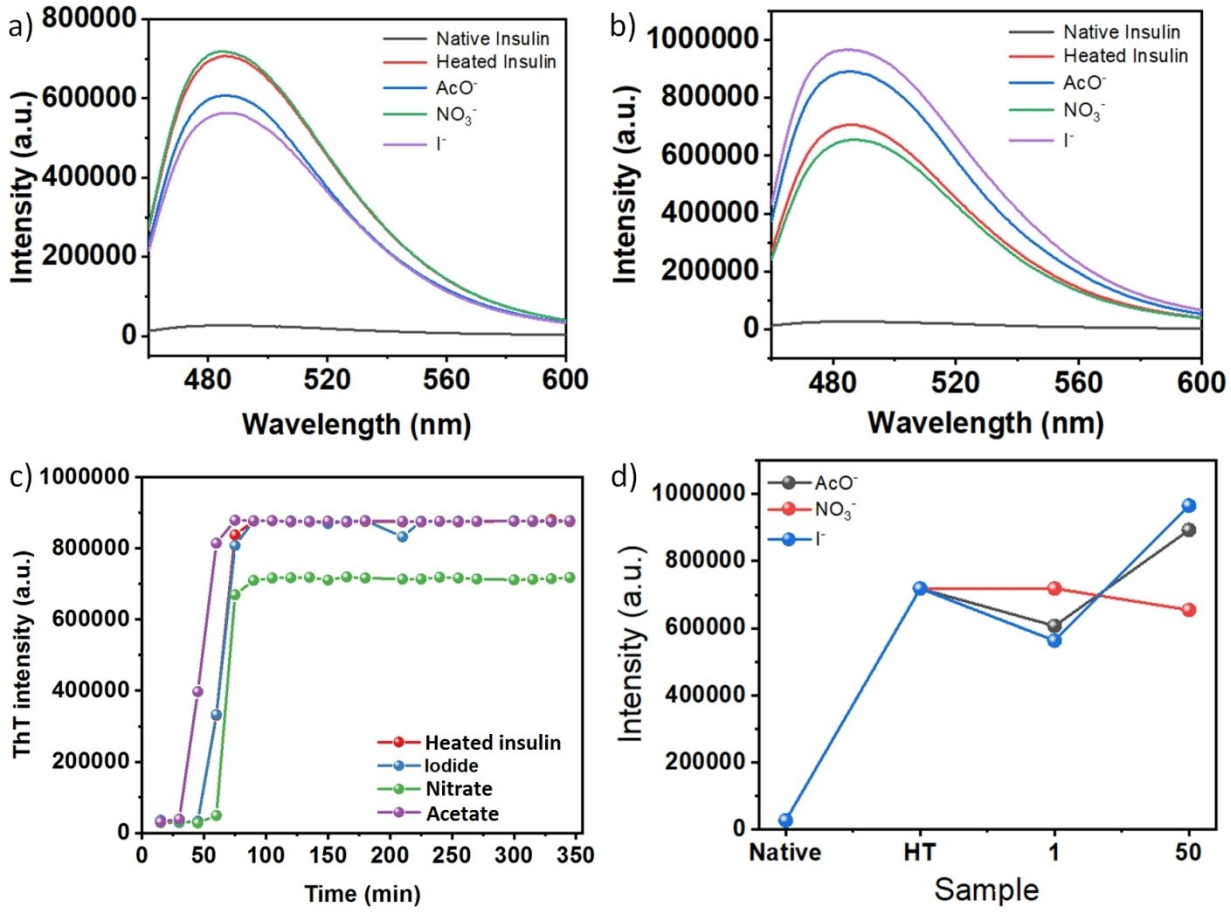

Figure 3. ThT-fluorescence profile of monomeric insulin and thermally incubated insulin(65 °C for 4 h) with or without different salt anions at pH 1.6: (a) 1 μM and (b) 50 μM concentration. The excitation wavelength was set at 440 nm, and fluorescence emissions were monitored from 450 to 600 nm. Slit widths were set at 3 nm (excitation) and 5 nm (emission). Each spectrum was the average of three scans within a 5% error limit. (c) The ThT fluorescence kinetics have been shown with the salt anions (50 μM) at pH 1.6; (d) Relative ThT fluorescence intensity curves (at 485 nm) of insulin in the presence of different salts anions at two different concentrations (1 and 50 μM).

nucleation leading to the maturation of the fibrils. Such ThT kinetic curves are quite commonly observed in protein aggregation phenomenon and many workers have reported them.[16,45] With $I^-$and CH_3COO^-ions, insulin exhibits smaller lag time while longer lag phase was observed with nitrate anions. Thus NO_3^-ion delays the aggregation of insulin whereas $I^-$and CH_3COO^- accelerate the fibrillation.

Earlier report on anion–induced oligomerization of insulin, shows that both at low (< 5 mM) and high chloride salt concentrations nucleation-polymerization mechanism operates leading to the generation of amyloid fibrillar state of insulin. Conversely at low sulfate concentration (< 5 mM), insulin forms fibrillar aggregates similar to monovalent chloride ions but at > 5 mM concentration, sulfate salt firstly leads the formation of amorphous aggregates which subsequently changed to both amorphous and fibrillar type of aggregates and ultimately slows down the insulin fibrillation.[18]

Dynamic Light Scattering (DLS) Study To measure R_h of the Insulin Oligomers in the Presence of Salt Anions

Insulin was thermally incubated for aggregate formation without or with the sodium salt of iodide, acetate and nitrate (1 μM and 50 μM) at 65 °C for 4 h.The propensity of aggregate formation of insulin in the absence and presence of salt solutions was monitored using DLS. DLS profiles (Figure 4) show the size distribution of insulin aggregates and qualitatively estimate the size of the protein and its aggregates. The monomeric insulin (MI) has hydrodynamic radii (R_h) around 32–60 nm. This hydrodynamic radius increases to ~200 nm after incubation of insulin solution at 65 °C for 4 h, and these R_h value corresponds to the hydrodynamic radii of insulin aggregate (IA). The $R_h$values of the insulin aggregates increased significantly when insulin was co-incubated with the salt anions. The largest aggregates with an R_h value of around 750 nm were observed with iodide ions. In contrast, the other monovalent acetate and nitrate ions induced the formation of relatively smaller aggregates with $R_h$values around 450 nm and 225 nm, respec-

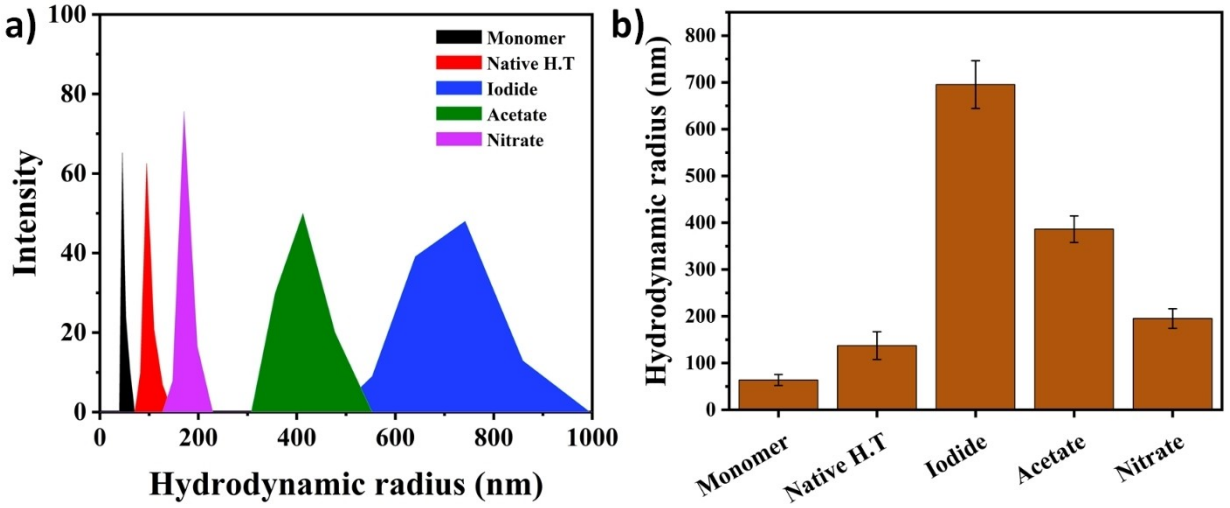

Figure 4. Intensity vs. particle size distribution in DLS studies of monomeric insulin and different insulin aggregates obtained after incubation at 65 °C for 4 h with or without the salt anions OAc^-, I^- and NO_3^-(50 μM) at pH 1.6.

tively. Sample solutions (0.1 mg/mL) were prepared with a total volume of 1 mL during the experiment.

The net positive charge of insulin is reduced upon binding with the anions, thus enhancing the hydrophobic interactions. Due to preferential exclusion, the net attractive forces between insulin molecules promote the protein-protein interactions, particularly nucleation of aggregates, to the fibrillar morphology, as revealed later by TEM. The increasing trend of the size of insulin aggregates (IA) can be explained by the charge density and shape of the anions employed. Therefore, considering the size and morphology of fibrils, the aggregation efficiency of the selected anions follows the order $I^- > CH_3COO^- > NO_3^-$.

Zeta potential Measurement

Insulin shows 22.86 mV zeta–potential whereas heat incubated insulin (form fibrillar aggregates as can be evidenced from Th–T, DLS, CD, TEM studies) have higher value (27.87 mV). Therefore, protein aggregate formation can be interpreted from increasing zeta–potential values. In the case of acetate ion, at both the ion concentration (1 μM and 50 μM), we have found higher values (29.4 and 35.36 mV, respectively) when they are incubated with insulin (Figure 5). It is interesting to note that the zeta–potential values of heat incubated insulin with iodide ions appear at the highest value. However, in the case of nitrate ions, the zeta–potential value was found to be the lowest among other anions under the same experimental conditions. They have shown positive zeta–potential values in all the cases. The increasing order of the zeta–potential of the ions are nitrate > acetate > iodide. This order also observed in above–mentioned experiments.

The Secondary Structural Changes in Insulin During Fibril Formation are Monitored by Circular Dichroism (CD) Spectroscopy

CD is a very useful spectroscopic technique for the determination of different secondary structures of peptides and proteins in solution.[38] Far-UV CD (190–260) is employed to investigate the interconversion of various secondary structures (alpha–helix to beta–sheet or random coil to beta–sheet, etc.) in the nucleation process during insulin amyloid fibril formation. The appearance of a characteristic negative CD signal at 218 nm confirms the crossed β-sheet structure formation during aggregation.[25] Here, we have examined the influence of the salt anions (I^-, CH_3COO^- and NO_3^-) on the conformation of insulin after thermal incubation at 65 °C for 4 h to analyze whether these anions can perturb the secondary structures of the protein in the nonnative condition. Figure 6 shows the corresponding far-UV CD spectra of insulin with or without 50 μM $NaNO_3$, NaOAc and NaI separately. In the absence of any salt anion, the CD spectrum of the native insulin displays two negative ellipticities around 207 nmand 222–224 nm respectively and a positive maximum at 196 nm, as expected, which clearly indicates the existence of a predominantly α-helical structure-rich protein as previously reported. The far UV CD spectrum of insulin after incubation at 65 °C for 4 h in the absence of any anion, showed significant structural transitions resulting from the appearance of a single minima at 217 nm with the disappearance of two negative ellipticities for α-helices and thus confirming the formation of β-sheet rich structure during amyloid fibrillation. Insulin solutions coincubated similarly with I^-, CH_3COO^- and NO_3^- ions, exhibiting similar secondary structural transitions and showing negative tough at 217 nm, having greater negative ellipticity values than heat–treated insulin alone. The thermal exposure of insulin in the presence of iodide, acetate and nitrate ions thus displayed significant changes in the intensity and band position, similar to

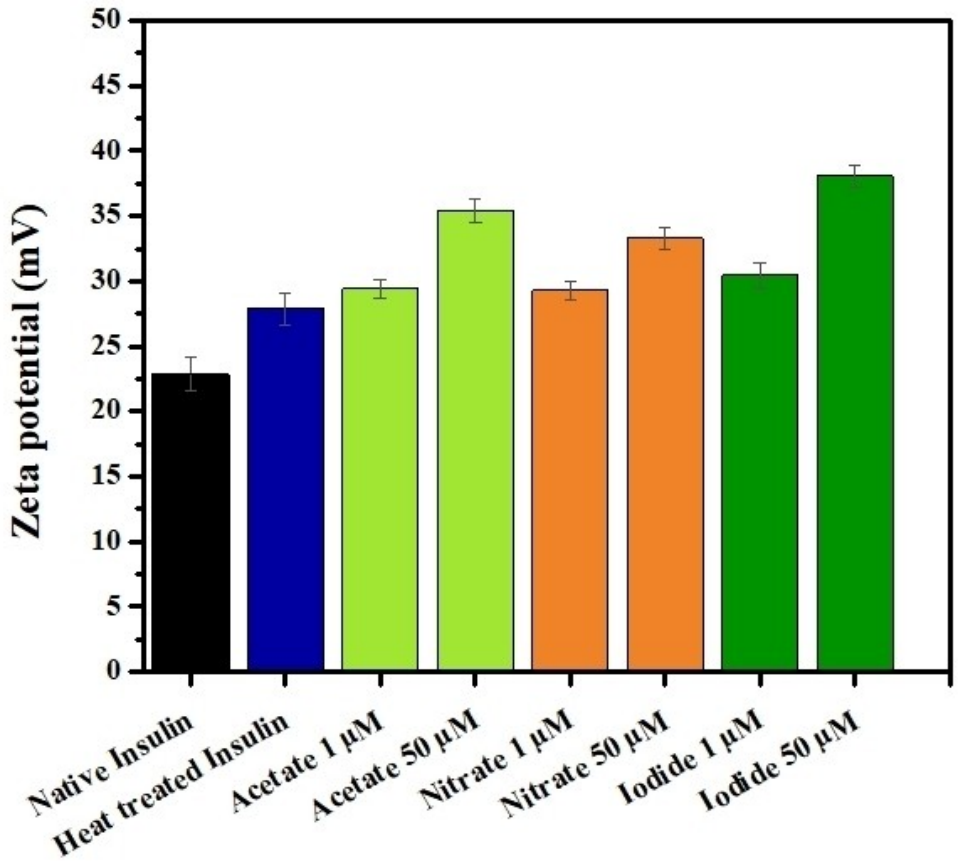

Figure 5. Zeta potential of insulin and different insulin aggregates obtained after incubation at 65 °C for 4 h with or without the salt anions OAc^-, $I^-$and NO_3^- (50 μM) at pH 1.6.

the heat–treated insulin. The single negative minima around 217–218 nm were also observed with all three anions, indicating the presence of crossed β-structure. The results thus support the formation of insulin amyloid fibrils at our chosen condition, and the selected anions perturb the secondary structure of the insulin even at their low physiological concentrations. Iodide interacts more strongly than acetate and nitrate ions with the positively charged residues of the insulin backbone. Thus, maximum negative ellipticity was observed for iodide anions, while nitrate showed minimum negative ellipticity at 217 nm. This result confirms that all our selected anions I^-, CH_3COO^- and NO_3^-having common cationic counterpart, Na^+, accelerate the insulin amyloid fibril formation even at their low physiological salt concentrations and the order of their effectiveness follows the series $I^- > CH_3COO^- > NO_3^-$. The changes in secondary structural contents of different insulin samples with or without the salt anions were calculated using CDNN 2.1 software available in the instrument and shown in Table S1 of the supporting information file. The calculation clearly shows the formation of increased β-structure (β sheet + β-turn) of insulin in presence of the selected anions I^-, CH_3COO^- and NO_3^- compared to native or heat-treated insulin in absence of salt anions.

Morphological Study of the Aggregates with Transmission Electron Microscopy (TEM)

To confirm the results obtained from the other experiments, the morphology of the insulin aggregates formed under various experimental conditions was examined by using TEM imaging with better accuracy. The microscopic images of insulin fibrils after thermal incubation at 65 °C for 4 h with and without the selected salt anions (I^-, CH_3COO^- and NO_3^-) are shown in Figure 7. No fibrillar aggregate was observed with insulin monomer at pH 1.6 in the room temperature (Figure 7a). We then analyzed the TEM image of insulin samples incubated at 65 °C for 4 h without any salt anion. The result displayed in Figure 7b shows the formation of matured, straight long and branched fibrils, a characteristic feature of amyloids. After incubation of insulin solutions with 50 μM iodide, 50 μM acetate and 50 μM nitrate salts, the final aggregated forms are shown in the TEM images (Figure 7c–e). Under acidic conditions, when insulin coincubated with I^-ions at 65 °C for 4 h, larger numbers of mature, straight long and branched fibrils (Figure 7c.) are formed by the nucleated polymerization mechanism in the presence of monovalent I^-anion. Thus, the iodide ion accelerates and modulates the amyloid fibrillation of insulin.

With the same concentration (50 μM) of NaOAc, insulin forms a lesser number of fibrils, which are thinner, shorter and

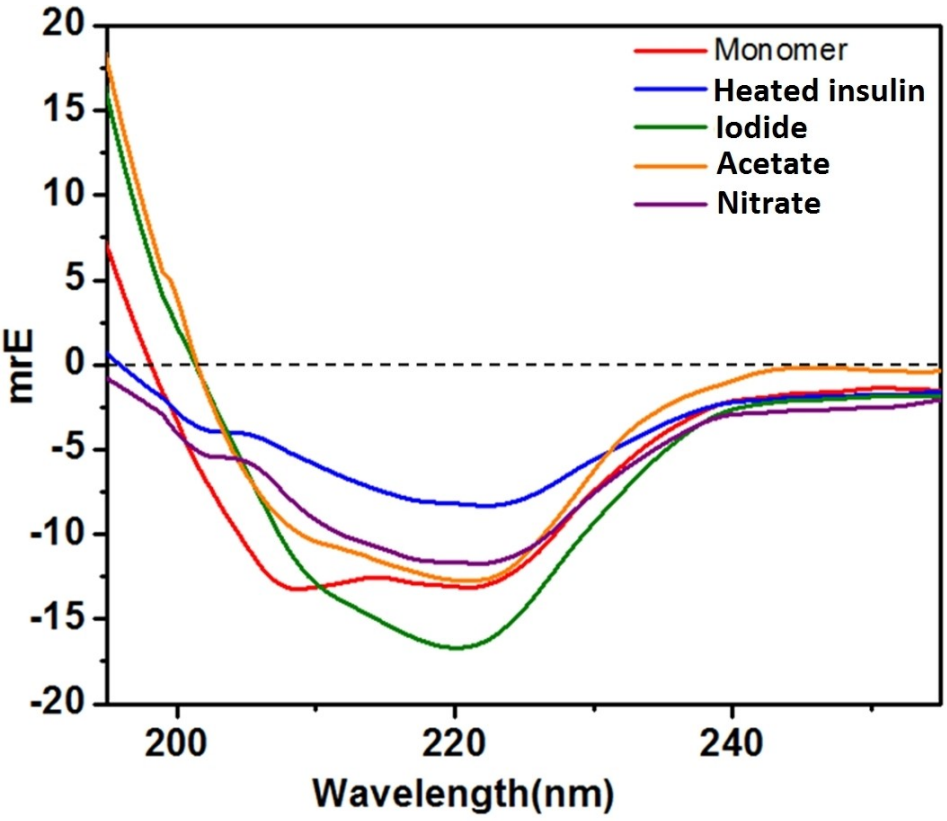

Figure 6. Far–UV CD curves of monomeric insulin (20 μM) and insulin incubated at 65 °C for 4 h in the presence and absence of I^-, CH_3COO^- and NO_3^- anions (50 μM) at 25 °C.

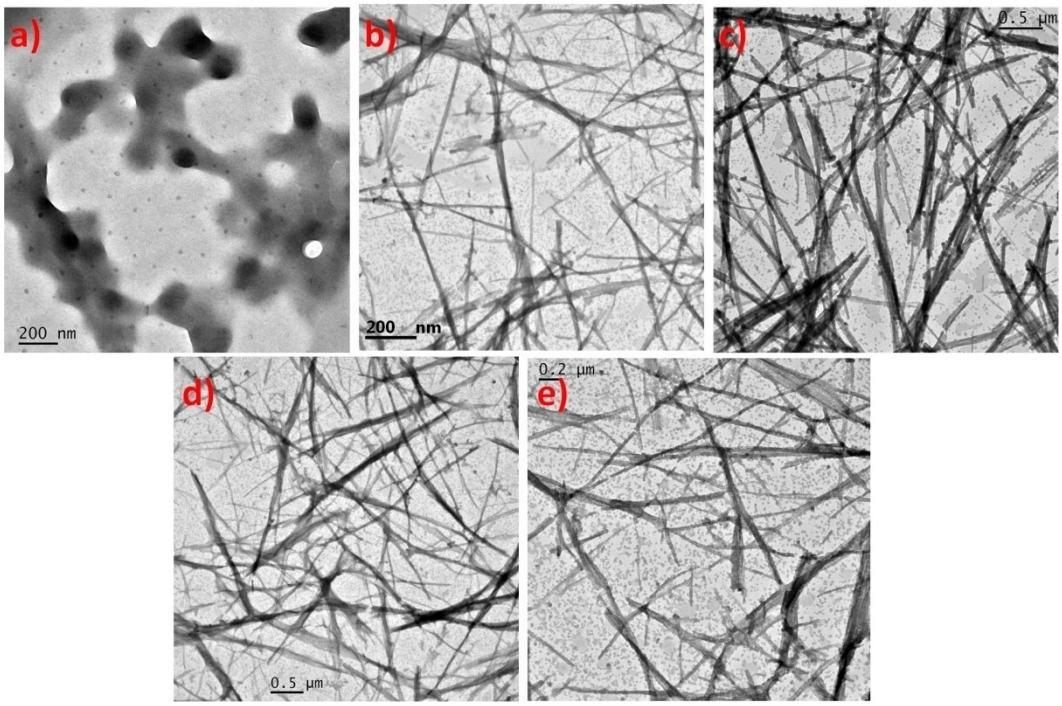

Figure 7. Selected images in transmission electron microscopyof monomeric insulin (a), insulin incubatedat 65 °C for 4 h (b), insulin incubated at 65 °C for 4 h in the presence of iodide (c), acetate (d), and nitrate (e) anions.

more branched as compared to those formed with I^- ions (Figure 7d.). In contrast, 50 μM $NaNO_3$ induces to form shorter and lesser fibrillar aggregates as compared to both NaI and NaOAc of the same strength. Thus, NO_3^- ions are less effective in inducing amyloid fibrillation of insulin due to lesser charge density and greater size in comparison with other monovalent ions I^- and OAc^- (CH_3COO^-). Thus, the morphology changes of the insulin aggregates in the presence of I^-, CH_3COO^- and NO_3^-ions were observed, yet they follow similar kinetics for amyloid fibrillation as revealed from Th T kinetics and CD studies. Considering the results of all the studies, we may conclude these selected anions accelerate amyloid fibril formation of insulin under stress—inducing conditions at their very low physiological salt concentrations.

Discussion

Mechanism of Anion–Induced Amyloid Fibrillation of Insulin

Our experimental results clearly demonstrate that insulin aggregation in acidic environment is accelerated by the salt anions having Na^+ as counter cations with different efficacy at their low physiological concentrations. This leads to the decision, the salt can promote insulin aggregation through their anions at acidic pH rather than the cationic counterpart where insulin bears a net positive charge of six units. On the other hand, cations may control the process of oligomerization at basic pH in different experimental set–up for example, aggregation of lysozyme is largely influenced by the cations where the anions have negligible role. The findings of the investigations in this present study are helpful in providing the correct mechanism of interaction between the anions and heat incubated insulin at acidic pH. Salts can modulate the electrostatic and hydrophobic interactions between anion and protein in a number of ways. Indeed, if the Debye–Hückel electrostatic effect solely determines the insulin fibrillation in acidic environment by screening its positive charges and thereby reducing the repulsive electrostatic forces among insulin chains, then the same concentrations of monovalent anions (I^-, CH_3COO^- and NO_3^-) should induce the oligomerization to similar extents. Actually it is contrary to our observations. All the selected anions accelerate the insulin fibrillation at a faster rate than the incubated insulin alone. Both I^- and CH_3COO^- induce nucleation and growth of the fibril at a faster rate than the nitrate ion of identical concentration. But our ThT kinetics study show that nitrate ion delays the aggregation pathway and induces to form smaller and lesser aggregates compared to I^- and CH_3COO^- ion. Therefore the aggregation mechanism of heat induced insulin is not directly related with the solution ionic strength which may influence largely insulin fibril formation. The ionic strength provided by the anions not only induces the nucleation mechanism but also stabilizes the intermediates and it can be evidenced from the results of intrinsic fluorescence of insulin in presence of anions (Figure 1). Again if the hydration shell of insulin is perturbed by the salt anions, then the efficiency order of the selected anions should be equal as all the three ions carry single negative charge. In accordance with Hofmeister series should be $CH_3COO^- > NO_3^- > I^-$, as iodide and nitrate are chaotropic ion while acetate ion fall in the category of kosmotropic ion.[39] But the order does not support our experimental observations. The result demonstrates actual order is $I^- > CH_3COO^- > NO_3^-$. Thus here the anion induced aggregation of insulin does not follow either the Hofmeister series or electroselectivity series at very low salt concentrations. The electrostatic effect and electroselectivity series are considered as important factors only in dilute salt concentrations where as the Hofmeister effect plays crucial role at higher salt concentrations (>100 mM). But our investigation procedure directed us to explore the ion–protein interactions even at very low salt concentration in the micromolar range similar to those present in the biological system.

Here the experimental result depicts that iodide and acetate ions have greater efficiency in accelerating the fibrillation of insulin and thereby producing larger and greater number of fibrillar structure of insulin than nitrate ion. Not only have the two anions (iodide and acetate) induced to form the final aggregate with different morphology but they also showed different ThT signal intensities as compared with the nitrate ions. In case of iodide ion, long and greater numbers of fibrils are formed whereas in nitrate ions shorter, lesser and branched fibrils are observed (Figure 7c and e).

Previous reports show that salt anions can promote the amyloid fibril formation of many peptides and proteins including insulin,[40] β2-microglobulin (β2-m),[41] α-synuclein,[7] glucagon,[19] an immunoglobulin light chain,[42] the amyloid-β peptide (Aβ1-40),[11] HypF–N,[13] the mouse prion protein[43] and bovine serum albumin.[9] It's important to note that HypF–N and the later proteins bear an excess of positive charges at this pH. In contrast, net charge on α-synuclein is close to zero at acidic pH due to the presence of large number of acidic residues in this protein. It has also been observed prion fibril growth is favored by 10 mM Na_2SO_4[43] while fibrillation of insulin is accelerated only in 5 mM NaCl.[18]

The three anions I^-, CH_3COO^- and NO_3^- chosen for this study differ clearly in their charge density, shape and size. Iodide ion is spherical, smallest and having largest negative charge density can move at faster rate to the positively charged side chain of insulin. Nitrate anion carrying smallest charge density and having larger size and planar geometry than iodide (spherical shape) approaches slowly to insulin positively charged residues and thus take longer lag time for insulin fibril formation than iodide and acetate ions.

Along with the electrostatic interactions, hydrophobic interactions need to be addressed because a balance between the two forces appears to be an important factor for self–association and amyloid fibrillation. The hydrophobic interactions are not to be significantly affected by the very low salt concentrations used in this study.[39] Added chloride, sulfate, and iodide anions screened the positive charges on the insulin and thus enhanced hydrophobic interactions which in turn favored the self–association and nucleation. So it is obvious from this study that both electrostatic and hydrophobic interactions control the nucleation of insulin. It has been observed that in the initial aggregation step electrostatic forces between calcitonin monomers play a crucial role.[44] Again, in amyloid-β peptide, both the electrostatic and hydrophobic interactions were involved during the fibril formation.[45] In this study, the existence of hydrophobic interactions can be evidenced for the formation of a partially folded intermediate of insulin in the

fibrillation pathway comes from the ANS binding study (Figure 2a) and far UV-CD experiment (Figure 6). ANS biding clearly shows the formation of populated states/intermediates having greater tendency to bind with the hydrophobic probe ANS. Thus thermal incubation at low pH in the presence of salt anions, both tertiary and secondary structures of insulin have been observed leading to the formation of partially unfolded (conformationally changed) intermediates triggering the insulin fibrillation. The low pH and higher temperature will favor the shifting the equilibrium between native form of insulin toan increased population of the partially unfolded intermediate (Scheme 1).

Once formed, the partially unfolded intermediate has a strong tendency to oligomerize into insulin amyloid fibrils. Here, our observation is that the nucleation of the monomer and elongation of fibril do not necessarily work in the same direction. Nucleation and fibril elongation both are controlled by electrostatic and hydrophobic interactions. The fibril elongation step is also dependent on the electronic structure of the concerned anionic species. Considering the overall experimental data, the ability of the selected salts anions to promote the propensity for the formation of fibrillar aggregates of insulin at low pH does not, however, follow the Hofmeister series, but the order of anions in their ability to promote the insulin fibrillation is $I^- > CH_3COO^- > NO_3^-$ at very low salt concentration range (micromolar range) having physiological relevance.

Conclusions

Formation of ordered irreversible protein aggregates due to its misfolding is the etiology of several human diseases. It becomes a challenging task to evaluate the forces between different cellular components and proteins molecules at the molecular level. Protein aggregation in the presence of salt solution encounters the serious problems during its separation, storage and therapeutic applications. In this work, we emphasized to evaluate the mechanism of fibrillation of human insulin, a peptide hormone playing the key role in the metabolism of glucose in the presence of three biologically relevant important salt anions iodide, acetate and nitrate in very low (physiological range) salt concentrations under acidic environment. We have elucidated the fibrillation mechanism and the fibril morphology employing multispectroscopic and microscopic approaches like ANS and Thioflavin T (ThT) fluorescence, circular dichroism (CD), dynamic light scattering (DLS) and transmission electron microscopy (TEM). Combining the result of investigations it revealed that at acidic environment the preferential binding of anions to the positively charged residues on insulin and subsequent perturbation of its structure by the anions are the major causes of its salt-induced aggregation and amyloid–like oligomeric product formation. Nitrate anion carrying smallest charge density and having larger size and planar geometry than iodide (spherical shape) approaches slowly to insulin positively charged residues and thus take longer lag time for insulin fibril formation than iodide and acetate ions. Our results clearly demonstrate that both the nucleation of heat incubated insulin and its fibril elongation at

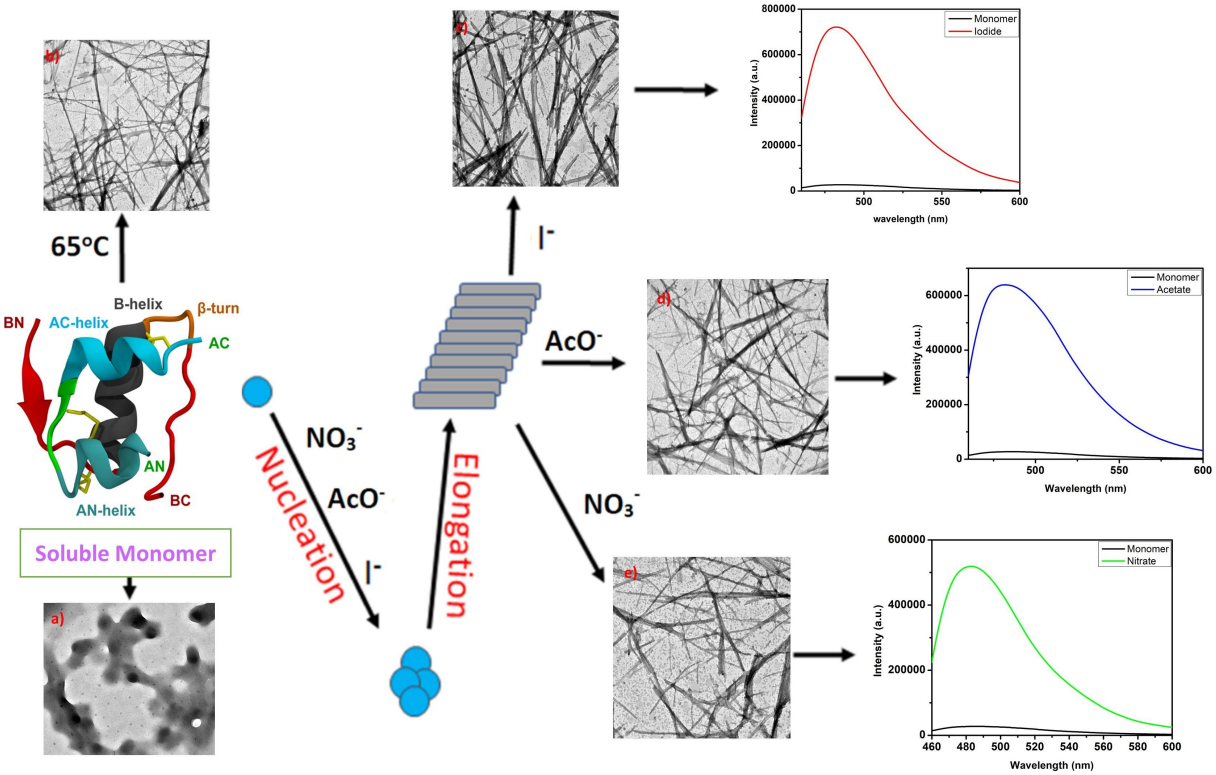

Scheme 1. Scheme for insulin fibrillation.

acidic environment are controlled by electrostatic and hydrophobic interactions.

Acknowledgements

Financial support of Indian Council of Medical Research (ICMR), Govt. of India, is greatly acknowledged. Shahnaz Begum is the recipient of the ICMR-SRF fellowship. Financial support of University Grants CommissionUGC-CAS-II and DST-PURSE-II (Govt. of India) Program of Department of Chemistry, Jadavpur University, Kolkata are also acknowledged.

Conflict of Interests

The authors declare no competing financial interest.

Data Availability Statement

The data that support the findings of this study are available from the corresponding author upon reasonable request.

Keywords: Insulin · Fibrill · Self-assembly · iodide · acetate · and nitrate

[1] D. J. Selkoe, *Nature* **2003**, *426*, 900–904 https://doi.org/10.1038/nature02264.
[2] F. Chiti, C. M. Dobson, *Annu. Rev. Biochem.* **2006**, *75*, 333–66 https://doi.org/10.1146/annurev.biochem.75.101304.123901.
[3] D. S. Eisenberg, M. R. Sawaya, *Annu. Rev. Biochem.* **2017**, *86*, 69–95https://doi.org/10.1146/annurev-biochem-061516-045104.
[4] D. Eisenberg, M. Jucker, *Cell* **2012**,*148*, 1188–203https://doi.org/10.1016/j.cell.2012.02.022.
[5] P. C. Ke, M.-A. Sani, F. Ding, A. Kakinen, I. Javed, F. Separovic, T. P. Davis, R. Mezzenga, *Chem. Soc. Rev.* **2017**, *46*, 6492–6531 https://doi.org/10.1039/C7CS00372B.
[6] C. S. Goldsbury, G. J. Cooper, K. N. Goldie, S. A. Müller, E. L. Saafi, W. T. Gruijters, M. P. Misur, A. Engel, U. Aebi, J. Kistler, *J. Struct. Biol.* **1997**, *119*, 17–27 https://doi.org/10.1006/jsbi.1997.3858.
[7] L. A. Munishkina, J. Henriques, V. N. Uversky, A. L. Fink, *Biochemistry* **2004**, *43*, 3289–3300 https://doi.org/10.1021/bi034938r.
[8] S. Sardar, S. Maity, S. Pal, H. Parvej, N. Das, N. Sepay, M. Sarkar, U. C. Halder, *RSC Adv.* **2016**, *6*, 85340–85346 https://doi.org/10.1039/c6ra14162e.
[9] P. P. Madeira, I. L. D. Rocha, M. E. Rosa, M. G. Freire, J. A. P. Coutinho, *J. Mol. Liq.* **2022**, *349*, 118183 https://doi.org/10.1016/j.molliq.2021.118183.
[10] V. Banerjee, K. P. Das, *Colloids Surf. B* **2012**,*92*, 142–150https://doi.org/10.1016/j.colsurfb.2011.11.036.
[11] K. Klement, K. Wieligmann, J. Meinhardt, P. Hortschansky, W. Richter, M. Fändrich, *J. Mol. Biol.* **2007**, *373*, 1321–1333 https://doi.org/10.1016/j.jmb.2007.08.068.
[12] V. Yeh, J. M. Broering, A. Romanyuk, B. Chen, Y. O. Chernoff, A. S. Bommarius, *Protein Sci.* **2010**, *19*, 47–56 https://doi.org/10.1002/pro.281.
[13] S. Campioni, B. Mannini, J. P. López-Alonso, I. N. Shalova, A. Penco, E. Mulvihill, D. V. Laurents, A. Relini, F. Chiti, *J. Mol. Biol.* **2012**, *424*, 132–149 https://doi.org/10.1016/j.jmb.2012.09.023.
[14] A. Salis, B. W. Ninham, *Chem. Soc. Rev.* **2014**, *43*, 7358–7377 https://doi.org/10.1039/C4CS00144C.
[15] W. Kunz, *Curr. Opin. Colloid Interface Sci.* **2010**, *15*, 34–39 https://doi.org/10.1016/j.cocis.2009.11.008.
[16] Y. Zhang, P. S. Cremer, *Proc. Nat. Acad. Sci.* **2009**, *106*, 15249–15253https://doi.org/10.1073/pnas.0907616106.
[17] W. Yao, K. Wang, A. Wu, W. F. Reed, B. C. Gibb, *Chem. Sci.* **2021**, *12*, 320–330 https://doi.org/10.1039/D0SC04245E.
[18] M. Owczarz, P. Arosio, *Biophys. J.* **2014**, *107*, 197–207 https://doi.org/10.1016/j.bpj.2014.05.030.
[19] J. S. Pedersen, J. M. Flink, D. Dikov, D. E. Otzen, *Biophys. J.* **2006**, *90*, 4181–4194 https://doi.org/10.1529/biophysj.105.070912.
[20] S.-G. Chang, K.-D. Choi, S.-H. Jang, H.-C. Shin, *Mol. Cells.* **2003**, *16*, 323–30 http://www.ncbi.nlm.nih.gov/pubmed/14744022.
[21] S. Li, R. M. Leblanc, *J. Phys. Chem. B.* **2014**, *118*, 1181–1188 https://doi.org/10.1021/jp4101202.
[22] M. I. Ivanova, S. A. Sievers, M. R. Sawaya, J. S. Wall, D. Eisenberg, *Proc. Nat. Acad. Sci.* **2009**, *106*, 18990–18995 https://doi.org/10.1073/pnas.0910080106.
[23] L. Nielsen, S. Frokjaer, J. Brange, V. N. Uversky, A. L. Fink, *Biochemistry* **2001**, *40*, 8397–8409 https://doi.org/10.1021/bi0105983.
[24] Q. Hua, M. A. Weiss, *J. Biol. Chem.* **2004**, *279*, 21449–21460 https://doi.org/10.1074/jbc.M314141200.
[25] A. Ahmad, V. N. Uversky, D. Hong, A. L. Fink, *J. Biol. Chem.* **2005**, *280*, 42669–42675 https://doi.org/10.1074/jbc.M504298200.
[26] J. L. Whittingham, D. J. Scott, K. Chance, A. Wilson, J. Finch, J. Brange, G. Guy Dodson, *J. Mol. Biol.* **2002**, *318*, 479–490 https://doi.org/10.1016/S0022-2836(02)00021–9.
[27] Y. Goto, L. J. Calciano, A. L. Fink, *Proc. Nat. Acad. Sci.* **1990**, *87*, 573–577 https://doi.org/10.1073/pnas.87.2.573.
[28] D. L. Bakaysa, J. Radziuk, H. A. Havel, M. L. Brader, S. Li, S. W. Dodd, J. M. Beals, A. H. Pekar, D. N. Brems, *Protein Sci.* **1996**, *5*, 2521–2531 https://doi.org/10.1002/pro.5560051215.
[29] A. Ahmad, I. S. Millett, S. Doniach, V. N. Uversky, A. L. Fink, *Biochemistry* **2003**, *42*, 11404–11416 https://doi.org/10.1021/bi034868o.
[30] L. Nielsen, R. Khurana, A. Coats, S. Frokjaer, J. Brange, S. Vyas, V. N. Uversky, A. L. Fink, *Biochemistry* **2001**, *40*, 6036–6046 https://doi.org/10.1021/bi002555c.
[31] M. Nilsson, *Methods* **2004**, *34*, 151–160 https://doi.org/10.1016/j.ymeth.2004.03.012.
[32] W. W. Yu, E. Chang, J. C. Falkner, J. Zhang, A. M. Al-Somali, C. M. Sayes, J. Johns, R. Drezek, V. L. Colvin, *J. Am. Chem. Soc.* **2007**, *129*, 2871–2879 https://doi.org/10.1021/ja067184n.
[33] D. E. Kamen, R. W. Woody, *Protein Sci.* **2001**, *10*, 2123–2130https://doi.org/10.1110/ps.19801.
[34] M. Biancalana, S. Koide, *Acta-Proteins Proteomics* **2010**, *1804*, 1405–1412 https://doi.org/10.1016/j.bbapap.2010.04.001.
[35] W. Dzwolak, R. Ravindra, J. Lendermann, R. Winter, *Biochemistry* **2003**,*42*, 11347–11355 https://doi.org/10.1021/bi034879 h.
[36] S. Krimm, J. Bandekar, *Polypeptides and Proteinsin*: **1986**, pp. 181–364 https://doi.org/10.1016/S0065-3233(08)60528–8.
[37] W. K. Surewicz, H. H. Mantsch, D. Chapman, *Biochemistry* **1993**, *32*, 389–394 https://doi.org/10.1021/bi00053a001.
[38] N. J. Greenfield, *Nat. Protoc.* **2006**, *1*, 2876–2890 https://doi.org/10.1038/nprot.2006.202.
[39] K. D. Collins, M. W. Washabaugh, *Q. Rev. Biophys.* **1985**,*18*, 323–422 https://doi.org/10.1017/S0033583500005369.
[40] V. Babenko, W. Surmacz-Chwedoruk, W. Dzwolak, *Langmuir* **2015**,*31*, 2180–2186 https://doi.org/10.1021/la5048694.
[41] B. Raman, E. Chatani, M. Kihara, T. Ban, M. Sakai, K. Hasegawa, H. Naiki, C. M. Rao, Y. Goto, *Biochemistry* **2005**, *44*, 1288–1299 https://doi.org/10.1021/bi048029t.
[42] L. A. Sikkink, M. Ramirez-Alvarado, *Biophys. Chem.* **2008**, *135*, 25–31 https://doi.org/10.1016/j.bpc.2008.02.019.
[43] S. Jain, J. B. Udgaonkar, *Biochemistry* **2010**, *49*, 7615–7624 https://doi.org/10.1021/bi100745j.
[44] T. Arvinte, A. Cudd, A. F. Drake, *J. Biol. Chem.* **1993**, *268*, 6415–22 http://www.ncbi.nlm.nih.gov/pubmed/8454614.
[45] P. E. Fraser, J. T. Nguyen, W. K. Surewicz, D. A. Kirschner, *Biophys. J.* **1991**, *60*, 1190–1201 https://doi.org/10.1016/S0006-3495(91)82154–3.

Manuscript received: September 15, 2023

NJC

ROYAL SOCIETY OF CHEMISTRY

PAPER

View Article Online
View Journal | View Issue

Cite this: *New J. Chem.*, 2024, **48**, 3120

In vitro retardation and modulation of human insulin amyloid fibrillation by Fe^{3+} and Cu^{2+} ions

Swarnali Paul,[a] Shahnaz Begum,[a] Hasan Parvej,[a] Ramkrishna Dalui,[a] Subrata Sardar,[a] Falguni Mondal,[a] Nayim Sepay[b] and Umesh Chandra Halder *[a]

Metal ions of the later part of the first-row transition series (Fe, Co, Ni, Cu, and Zn) can form bonds through the carboxylate, hydroxyl, thiol, and imidazole side chains of proteins and those bonds are significantly more stable than those formed by non-transition metals. Their adventitious binding to protein surfaces provides a great platform for maintaining the native structure of many biologically significant proteins and thus inhibiting the self-aggregation phenomenon of proteins. Aggregation followed by deposition of proteins used for therapeutic purposes either at the site of administration *in vivo* or during storage conditions *in vitro* is a major concern. In this work, human insulin is induced to form 'amyloid fibrils' at acidic pH and elevated temperature and then the inhibitory activities of two transition metal ions Fe^{3+} and Cu^{2+} towards insulin amyloid fibrillation were investigated. The results show that the formation of β-sheet-rich fibrillar structures was inhibited more with Fe^{3+} than Cu^{2+}-treated insulin. Dynamic light scattering and circular dichroism proved that Cu^{2+} was effective at lowering the interaction ratios with insulin, yet Fe^{3+} was effective in maintaining the size as well as the alpha-helical conformation of monomeric insulin. This metal complex (insulin-Fe^{3+} or insulin-Cu^{2+}) delayed the nucleation step of aggregation and Fe^{3+} is far better than Cu^{2+} in this endeavor. However, both of the metal ions proved their effectiveness in preventing amyloid fibrillation *in vitro* and can modulate the morphology of the aggregates as revealed by TEM studies. Overall the two transition metal ions Fe^{3+} and Cu^{2+} employed in this investigation are essential micronutrients too and are required in minute concentrations. The present study will encourage the applications of transition metal ions Fe^{3+} and Cu^{2+} as effective interrupters of amyloidogenesis in aggregation-prone proteins showing pathogenic amyloid deposition.

Received 21st September 2023,
Accepted 4th January 2024

DOI: 10.1039/d3nj04431a

rsc.li/njc

1. Introduction

There are many known human etiopathogeneses associated with the generation of oligomers and mature fibrils[1] by aggregation of therapeutic proteins at the sites of application or other places. To carry out their functions, proteins must remain in their folded conformation, which usually corresponds to the thermodynamically most stable state.[2] But secondary structures having marginal stability may act as nucleation sites for protein misfolding or aggregation due to deviation from its optimal physical state (called the native state) or under stress-inducing conditions.[3] The deviations include the conversion of the native protein into cross-β-sheet rich structures under different non-optimal conditions and causing the loss of their functional properties. This leads to the process of protein oligomerization resulting in the formation of amyloid-like fibrils.[4] Amyloid formation at the site of repeated injections in patients administered with insulin having diabetes mellitus is a common example of such protein aggregation.[5] Besides this, long term storage or keeping under improper conditions may lead to the generation of such clumps of many important therapeutic proteins/enzymes due to their unfolding followed by the misfolding phenomenon.[6,7] The functional properties of such cytotoxic[8] fibrillar forms are lost and deposited in various parts of the body like the shoulders,[9] arms,[10] thighs,[11] and abdominal walls[12] after injection, and thus can induce inflammation. The close relationship of neurodegenerative diseases and amyloidosis has been established.[13] Human insulin is a widely used model protein[14] for the investigation of the mechanism of amyloid formation as its fibrillar structure resembles the other amyloid prone proteins, like amyloid precursor protein (Aβ peptides causing Alzheimer's disease), atrial natriuretic factor (amyloid ANF causing atrial amyloidosis), and prion protein (causing spongiform encephalopathies), *etc.* Even during the

[a] *Department of Chemistry, Jadavpur University, Kolkata-700032, India. E-mail: uhalder2002@yahoo.com*
[b] *Department of Chemistry, Lady Brabourne College, Kolkata-700017, India*

RSC Advances

PAPER

View Article Online
View Journal | View Issue

Cite this: *RSC Adv.*, 2022, **12**, 17020

Coumarin derivatives inhibit the aggregation of β-lactoglobulin †

Hasan Parvej,[a] Shahnaz Begum,[a] Ramkrishna Dalui,[a] Swarnali Paul,[a] Barun Mondal,[a] Subrata Sardar,[a] Nayim Sepay,[b] Gourhari Maiti[a] and Umesh Chandra Halder *[a]

Received 16th February 2022
Accepted 15th May 2022

DOI: 10.1039/d2ra01029a

rsc.li/rsc-advances

The binding of a small molecule to a protein through non-covalent interactions mainly depends on its size and electronic environment. Such binding can change the stability of the three dimensional protein structure which sometimes may destabilize it to accelerate or to inhibit protein aggregation. Coumarin is a widely used fluorescent dye with several biological applications. Different substituents (electron-donating and electron-withdrawing) at different positions of the coumarin moiety can influence its molecular volume, physical and chemical properties. Here we investigate the effect of such substituents of coumarin on the aggregation of a model protein, beta-lactoglobulin (β-lg) through a multi spectroscopic approach. It was observed that coumarin methyl ester with an 8-hydroxyl group can inhibit the β-lg aggregation. This compound can bind the hydrophobic site of beta-lactoglobulin and stabilize a particular protein conformation through the formation of hydrogen bond and hydrophobic interactions. Thus a properly designed compound can inhibit protein–protein interactions through protein–small molecule interactions. Other coumarinoid compounds also are effective in the prevention of thermal aggregation of β-lg.

Introduction

The formation of insoluble amyloid fibrils from normal soluble proteins is well known. Amyloid fibrils are impervious to degradation.[1] Proteins can form amyloid fibrils and each case brings a different characteristic disease. Aggregation of Aβ, α-synuclein, or prion proteins causes neurodegenerative brain disorders Alzheimer's disease, Parkinson's disease, or mad cow disease, respectively. It is also found that diseases like diabetes type 2 are disorders due to amyloid fibril formation of insulin.[1] Since amyloid fibrils are insoluble in physiological conditions, they can deposit around the cell and tissues and cause a pathogenic effect.[2] Aggregation of such proteins gives very stable systems and facilitates the process. Structurally, fibrillar assemblies are predominantly cross-β conformation of the proteins. Interestingly, the formation of fibrils is independent of protein size, shape, and sources. Recently, hydrophobins, curli, and melanosomes are identified as the expression of functional amyloidogenesis.[1]

To prevent the amyloid fibrils formation, a number of therapeutic strategies have been developed. Site-specific glycosylation of protein[3] and protein engineering[4] are of some example of prevention techniques. Most of the proteins have a very stable conformational structure in fibrillar form because it is in a global free-energy minimum.[5–7] Therefore, once a protein starts partial degradation to form a fibril, it is very hard to stop the process. Stabilization of the native conformer of a protein can slow down the partial degradation of protein and can deem fibrillation.[8] It is the most acceptable therapeutic strategy to prevent fibrils formation now. Therefore, the design of new anti-fibrillating molecules is in demand.

Coumarin, an aromatic heterocyclic lactone compound, is an important natural product found in many plants. Coumarin derivatives or coumarinoids have a large family containing thousands of compounds. They have very interesting photophysical,[9] biological, and medicinal[10] properties. Coumarin absorbs light at ~280 nm wavelength and shows fluorescence property by the emission at 410 to 470 nm. This photophysical property is very much tunable with the substituents attached to the moiety.[11] For this reason, these compounds are widely used as dyes. Some coumarinoids were designed for blue-green tunable organic laser dyes.[11]

Whey contains an important lipocalin protein, *i.e.* β-lactoglobulin (β-lg), which is of immense interest due to its nutritional and small molecule carrier properties.[12] Structurally, the protein is β-sheet enriched (eight anti-parallel β-sheets forms a barrel-like structure) and forms self-assembly upon thermal exposure. The protein can be isolated and purified in high yield

[a]*Department of Chemistry, Jadavpur University, Kolkata 700 032, India. E-mail: uhalder2002@yahoo.com*

[b]*Department of Chemistry, Lady Brabourne College, Kolkata 700017, India*

† Electronic supplementary information (ESI) available. See https://doi.org/10.1039/d2ra01029a

J. Chem. Sci. (2020) 132:103
https://doi.org/10.1007/s12039-020-01796-z

REGULAR ARTICLE

Antioxidant ferulic acid prevents the aggregation of bovine β-lactoglobulin *in vitro*

SAMPA PAL[a], SANHITA MAITY[a], SUBRATA SARDAR[a], SHAHNAZ BEGUM[a], RAMKRISHNA DALUI[a], HASAN PARVEJ[a], KAUSHIK BERA[b], ANIRBAN PRADHAN[c], NAYIM SEPAY[a], SWARNALI PAUL[a] and UMESH CHANDRA HALDER[a,*]

[a]Organic Chemistry Section, Department of Chemistry, Jadavpur University, Kolkata 700 032, India
[b]Natural Products Laboratory, Department of Chemistry, The University of Burdwan, Burdwan 713 104, India
[c]Director's Research Unit (DRU), Indian Association for the Cultivation of Science, Kolkata 700 032, India
E-mail: uhalder2002@yahoo.com

MS received 20 November 2019; revised 27 April 2020; accepted 4 May 2020; published online 11 August 2020

Abstract. Amyloids, a well-ordered β-sheet-enriched structural network, can be broadly defined as insoluble protein aggregates that are linked to a wide variety of diseases including systemic amyloidosis and some neurodegenerative disorders. Ferulic acid (FA), a phenolic acid, abundant in antioxidant and efficient pharmaceutical has beneficial effects against several ailments. Based on this, we have investigated the protective role of FA on amyloid formation of bovine β-lactoglobulin (β-lg), a model globular protein. Using a set of *in vitro* biophysical methods, such as UV-Vis spectroscopy, fluorescence, circular dichroism, transmission electron microscopy, etc., our research group has concluded that FA significantly inhibits the heat-induced amyloid formation of β-lg and this inhibitory effect is dose-dependent. Exposed surface hydrophobicity of β-lg amyloid fibrils decreased significantly in the presence of FA. Docking study revealed that ionic and hydrogen bonding interactions between FA and β-lg prevented protein conformational changes leading to fibrillation. We anticipate that our finding would give an insight into the protein aggregation inhibited by the antioxidant compound, FA and pave the way for finding and developing other new small molecules (protein misfolding inhibitors) that give similar result against amyloid fibril formation and its allied neurodegenerative disorders.

Keywords. Antioxidant; ferulic acid; β-lactoglobulin; aggregation.

1. Introduction

In the present area of research, a very interesting topic is the alteration of native (often soluble) proteins into non-native folded fibrillar structures; these are often not soluble in various solvents as well as in water. These protein fibrils are usually called amyloid fibrils and are the hallmark for numerous ailments, including Alzheimer's, Huntington's, type II diabetes, Parkinson's, prion-associated encephalopathy diseases and others.[1–6] Amyloid fibrils are highly organised polypeptide aggregates and are rich in β-sheet secondary conformation.[7] These fibrils are stable against temperature,[8] hydrolytic pressure,[9] proteolytic enzymes[10] and denaturants.[11] Several proteins and peptides, e.g. amyloid β-peptide (Aβ), β-lactoglobulin (β-lg) islet amyloid polypeptide (IAPP), insulin, α-synuclein, and transthyretin have been identified as amyloidogenics,[12–16] but it has been observed that there is no similarity in primary structure among them.[17] The aggregation pattern of such peptides and proteins differs owing to their differential forms.[18–20]

In recent research work, a number of endeavours have been applied to find or design the compounds which can prevent the formation of these toxic oligomeric species or break up the pre-formed fibrils. Several working parameters, e.g. concentration of protein, pH of experimental solution, ionic strength of the reaction medium, reaction temperature, existence of co-solvents, etc., can be altered to modulate the aggregation process of β-lg into the oligomers or fibrils.[21–23]

Small organic molecules (either from natural origin or synthetically derived) play a significant role in

*For correspondence

International Journal of Biological Macromolecules 125 (2019) 596–604

Contents lists available at ScienceDirect

International Journal of Biological Macromolecules

journal homepage: http://www.elsevier.com/locate/ijbiomac

Silver nanoparticle modulates the aggregation of beta-lactoglobulin and induces to form rod-like aggregates

Subrata Sardar, Md. Anas, Sanhita Maity, Sampa Pal, Hasan Parvej, Shahnaz Begum, Ramkrishna Dalui, Nayim Sepay, Umesh Chandra Halder *

Organic Chemistry Section, Department of Chemistry, Jadavpur University, Kolkata 700032, India

ARTICLE INFO

Article history:
Received 10 September 2018
Received in revised form 23 November 2018
Accepted 2 December 2018
Available online 7 December 2018

Keywords:
Silver nanoparticle (SNP)
β-Lactoglobulin (β-lg)
Amyloid fibrillar aggregates
Rod-shaped aggregates
Scanning electron microscopy (SEM)
Transmission electron microscopy (TEM)
Docking

ABSTRACT

Silver nanoparticles (SNPs) have been increasingly used in medicines and biomaterials as a drug carriers and diagnostic or therapeutic material due to their smaller size, large surface area and cell penetration ability. Here we report the preparation of SNPs of diameter 10 ± 3 nm by using silver nitrate and sodium borohydride and the interaction of synthesized SNPs with our model protein β-lactoglobulin (β-lg) in 10 mM phosphate buffer at pH 7.5 after thermal exposure at 75 °C. Heat exposed β-lg forms amyloidal fibrillar aggregates whereas this protein aggregates adopt rod-like shape instead of fibrillar structure in presence of SNP under the same conditions. Size of the synthesized SNPs is confirmed by UV–Visible spectroscopy, SEM and TEM. Interactions and subsequent formation of molecular assembly of heat stressed β-lg with SNP were investigated using Th-T assay and ANS binding assay, DLS, RLS, CD, FT-IR, SEM, TEM. Docking study parallely also support the experimental findings.

1. Introduction

Silver nanoparticles (SNPs) play a significant role in catalytic reaction, wound dressing, optical property, electrical property, antimicrobial activity, purification of ground water, removal of some chemical hazards, medical implants, prevention in infection, drug delivery, cancer treatment, antifungal activity, molecular linkers, pharmacological application, etc. [1–4]. Silver nanocrystals encapsulated in mesoporous silica nanoparticles displayed antimicrobial activity against both Gram-positive and Gram-negative bacteria [5]. Some researchers applied silver nanoparticles in purification of ground water in a convenient way. This nanoparticle is suitably used to detect some chemical hazards like Hg^{2+}, Cu^{2+} and S^{2-} [6–7]. It is also increasingly used in cosmetics and it has also been proposed in medical implants and instruments for the prevention of infection [8–10]. The silver nanocrystals encapsulated with silica nanoparticles are now used for imaging and drug delivery purpose [11]. Very low concentrations of silver nanoparticles are effective in induction of apoptosis in cancer cells [12]. Recent study demonstrates the antitumor activity of green-synthesized SNPs against lung cancer in vitro and in vivo [13]. The interactions between SNPs and various DNA bases (adenine, guanine, cytosine, and thymine) are also used as molecular linkers because of their biological significance [14]. The interaction of silver nanoparticles with proteins like SNPs-BSA and SNPs-BSA-emodin, interactions over the protein structure as well in the protein-drug binding show that silver nanoparticles may play a good role in biomedical and pharmacological applications [15].

Several diseases are known to occur due to the misfolding and aggregation of the proteins that are naturally present for normal the functioning of our body. Protein misfolding and aggregation are associated with many neurodegenerative diseases like Alzheimer's (AD), Parkinson's (PD), amyotrophic lateral sclerosis (ALS), frontotemporal dementia (FTD), diabetes type II and Huntington's diseases are the notorious examples for this kind [16–20]. The pathologic characteristics of AD are the formation of amyloid-beta (Aβ) fibrils enriched with cross β-sheet structures caused by the misfolding of Aβ peptide [21,22]. The mechanism of the formation of the fibrils is formed based on the nucleation and growth mechanism [23]. In the progression, the monomers are transformed into oligomers and the oligomers act as nuclei for the formation of fibril followed by the elongation of the fibrils through the addition of the monomers [24]. In our previous study, we have shown that gold nanoparticles (GNP) inhibit the amyloid fibril formation of β-lg [25]. β-Lg has been extensively utilized in the study of protein folding and aggregation.

β-Lg is a predominantly β-sheet protein having 162 amino acid residues and molecular weight 18.4 kDa. Basically it is a well-known globular whey protein of pI 5.2. In its β-barrel structure there are 8 strands (A to H) which are succeeded by three turn α-helix and a final β-strand (strand I) [26]. At pH 7.0 the protein exists as a reversible dimer and extent of dimerization depends on pH, temperature, protein

* Corresponding author.
E-mail address: uhalder2002@yahoo.com (U.C. Halder).

https://doi.org/10.1016/j.ijbiomac.2018.12.039
0141-8130/

NJC

PAPER

View Article Online
View Journal | View Issue

Cite this: *New J. Chem.*, 2018, **42**, 19260

Inhibition of amyloid fibril formation of β-lactoglobulin by natural and synthetic curcuminoids†

Sanhita Maity,[a] Sampa Pal,[a] Subrata Sardar,[a] Nayim Sepay,[a] Hasan Parvej,[a] Shahnaz Begum,[a] Ramkrishna Dalui,[a] Niloy Das,[b] Anirban Pradhan[c] and Umesh Chandra Halder*[a]

The aggregation of proteins has been associated with several aspects of daily life, including food processing, blood coagulation and many neurodegenerative infections. However, the actual mechanisms responsible for amyloidosis, the irreversible fibril formation of various proteins, which is linked to disorders such as Alzheimer's disease, Creutzfeldt–Jakob disease and Huntington's disease, have not yet been fully elucidated. Curcumin, a potent anti-oxidant, exhibits anti-amyloid activity; however, its activity is limited due to its instability. Therefore, chemical modifications of curcumin have been performed to obtain molecules with enhanced stability and superior anti-amyloid activity. Herein, the main objective of this study is related to the inhibitory effects of three stable analogs of curcumin against bovine β-lactoglobulin (β-lg) fibrillization. We inferred that a pyrazole derivative of curcumin showed remarkable potency in arresting the fibrillization of β-lg, as revealed by biophysical techniques. Molecular docking demonstrated that pyrazole-mediated inhibition of β-lg fibrillogenesis may be initiated by interacting with aggregation-prone regions of the protein and preventing interactions between monomers, leading to suppression of the overall aggregation process. This work alludes to a possible broader scope for discovery of other small molecules that may exert similar effects against amyloid formation and its associated neurodegenerative diseases.

Received 27th June 2018,
Accepted 13th October 2018

DOI: 10.1039/c8nj03194k

rsc.li/njc

Introduction

The anomalous self-assembly and accumulation of misfolded proteins is known to have common cellular and molecular mechanisms, including protein aggregation, which is the known leading causative agent of a number of conformational diseases, such as Alzheimer's disease (AD), Parkinson's disease (PD), Huntington's disease (HD) and prion disease.[1,2] The aggregates consist of fibers with cross β-sheet structures, termed harmful 'amyloids', and their morphological features are not associated with behaviors of specific proteins. Although the proper aetiology of AD remains controversial, diverse factors appear to play vital roles in the pathophysiology of the disease; these include abnormal β-amyloid (Aβ) deposits in extracellular amyloid plaques, which lead to progressive neuronal death, tau protein hyperphosphorylation, metal ion dyshomeostasis, oxidative stress, and neurotransmitter system dysfunction.[3–7] Different peptides and proteins generate morphologically similar or different amyloid fibrils through dimer and oligomer formation; this has been hypothesized to occur in a stepwise fashion, with a slow phase of nucleation of the precursors of the amyloid fibrils followed by a relatively fast elongation phase.[8] Moreover, in the formation of amyloid fibrils, the incentive to assemble arises from favorable solvation energies and side-chain interactions accompanying the formation of β-sheet structures.[9] Currently, numerous clinical and experimental studies are revealing that soluble oligomeric and protofibrillar forms of proteins are potentially neurotoxic.[10,11]

Recently, the most challenging research task has focused on the inhibition of fibril formation[12–14] by the employment of small molecules. These potent modulators are believed to stabilize monomers by blocking the formation of toxic oligomers and to divert the monomeric proteins to off-pathway non-toxic intermediates. Small molecules are being developed to inhibit aggregation of Aβ,[15] α-synuclein[16] and prions.[17]

Much evidence has shown that polyphenols, which have structural constraints, are effective in the inhibition of amyloid fibrillation.[18,19] Curcumin, a classical active yellow lipid-soluble β-diketone dietary polyphenolic component, has been

[a] *Organic Chemistry Section, Department of Chemistry, Jadavpur University, Kolkata 700032, India. E-mail: uhalder2002@yahoo.com*
[b] *Department of Chemistry, Durgapur Govt. College, Durgapur, West Bengal 713214, India*
[c] *Director's Research Unit (DRU), Indian Association for the Cultivation of Science, Kolkata-700032, India*

† Electronic supplementary information (ESI) available. See DOI: 10.1039/c8nj03194k

PRESENTATION IN NATIONAL/INTERNATIONAL CONFERENCES

International Conference on Chemistry for Human Development (ICCHD-2018)

January 8–10th, 2018

Certificate

This is to Certify that Prof/Dr./Mr./Mrs. Shahnaz Begum

of Jadavpur University

has participated and presented a Paper (Oral/Poster) ~~Delivered Talk~~ in the International Conference on Chemistry for Human Development (ICCHD-2018) held at Heritage Institute of Technology, Kolkata

Jt. Convenor

Convenor

National Seminar on

Emerging Trends in Chemical Sciences
(January 07, 2020)

under

Centre for Advanced Studies II Program

Organized by

Department of Chemistry, Jadavpur University, Kolkata 700 032

Certificate of Participation

This is to certify that Shahnaz Begum

of Jadavpur University *has ~~taken part~~/presented a poster in the seminar organized by the Department of Chemistry, Jadavpur University, Kolkata 700 032 on January 07, 2020.*

Date: 07-01-2020
Place: Kolkata

KAJAL KRISHNA RAJAK
Convener

SAMIT GUHA
Co-Convener

National Seminar on

CHEMICAL SCIENCES: TODAY AND TOMORROW (CSTT-2019)

(Thursday, March 14, 2019)

under

Centre for Advanced Studies II Program

Organized by

Department of Chemistry, Jadavpur University, Kolkata 700 032

This is to certify that SHAHNAZ BEGUM *of* Dept. of Chemistry JADAVPUR UNIVERSITY *has delivered an invited talk /participated/ presented* ✓ *a poster in the seminar organized by the Department of Chemistry, Jadavpur University, Kolkata 700 032 on Thursday, March 14, 2019.*

Date: 14-03-2019
Place: Kolkata

Partha Roy
Co-Convener

Bhattacharya
Swapan Kumar Bhattacharya
Convener

RAC 2019

Organized by
Department of Chemistry

NATIONAL INSTITUTE OF TECHNOLOGY MEGHALAYA

Supported By

CSIR | SERB | NEC | NIT Meghalaya | TEQIP

CERTIFICATE OF PARTICIPATION

This is to certify that

Ms. Shahnaz Begum, Jadavpur University

participated and presented a poster

at **the National Conference**

on

Recent Advances in Chemistry (RAC 2019)

held in the **Department of Chemistry, NIT Meghalaya**

during **October 14-15, 2019**

Dr. Atanu Singha Roy
(Convener)

Dr. Amit Kumar Paul
(Convener)

Prof. Ayon Bhattacharjee
(Dean R & C, NIT Meghalaya)

National Seminar on

CURRENT DEVELOPMENTS IN CHEMICAL SCIENCES (CDCS-2018)

(Wednesday, March 7, 2018)

under

Centre for Advanced Studies II Program

Organized by

Department of Chemistry, Jadavpur University, Kolkata 700 032

This is to certify that Shahnaz Begam *of* Jadavpur University *has participated/presented a poster in the seminar organized by the Department of Chemistry, Jadavpur University, Kolkata 700 032 on Wednesday, March 7, 2018.*

Date: 07-03-2018
Place: Kolkata

SAUBHIK HALDAR P. Mahata **PARTHA MAHATA**

Conveners

National Workshop on
Electron Microscopy and Its Applications in Material Science and Biological Science

January 29 - 30, 2018

Organized by
DEPARTMENT OF INSTRUMENTATION SCIENCE
JADAVPUR UNIVERSITY, KOLKATA – 700032

Certified that *Shahnaz Begum of Jadavpur University* **has actively participated and successfully completed the National Workshop on 'Electron Microscopy and Its Applications in Material Science and Biological Science' held during January 29- 30, 2018, in the Department of Instrumentation Science, Jadavpur University.**

(Dr P.P.Lahiri)	**(Dr Sankar Narayan Patra)**	**(Prof. R. Bhar)**
Registrar	*Head*	*Convener*
Jadavpur University	*Dept. of Instrumentation Science, JU*	*Dept. of Instrumentation Science, JU*

Date: 30.01.2018